ACTA PHARMACEUTICA SCIENCIA

International Journal in Pharmaceutical Sciences, Published Quarterly

ISSN: 2636-8552
e-ISSN: 1307-2080,
Volume: 63, No: 1, 2025
Formerly: Eczacılık Bülteni / Acta Pharmaceutica Turcica
Founded in 1953 by Kasım Cemal GÜVEN

ACTA PHARMACEUTICA SCIENCIA

International Journal in Pharmaceutical Sciences
is Published Quarterly
ISSN: 2636-8552
e-ISSN: 1307-2080,
Volume: 63, No: 1, 2025
Formerly: Eczacılık Bülteni/Acta Pharmaceutica Turcica
Founded in 1953 by Kasım Cemal Güven

Address
İstanbul Medipol Üniversitesi
Kavacık Güney Kampüsü
Göztepe Mah. Atatürk Cad.
No: 40 34810 Beykoz/İSTANBUL
Tel: 0216 681 51 00

E-mail
editor@actapharmsci.com
secretary@actapharmsci.com

Web site
http://www.actapharmsci.com

Contents

Aims and Scope of Acta Pharmaceutica Sciencia

Acta Pharmaceutica Sciencia is a continuation of the former "Eczacılık Bülteni" which was first published in 1953 by Prof. Dr. Kasım Cemal GÜVEN's editorship. At that time, "Eczacılık Bülteni" hosted scientific papers from the School of Medicine-Pharmacy at İstanbul University, Türkiye.

In 1984, the name of the journal was changed to "Acta Pharmaceutica Turcica" and it became a journal for national and international manuscripts, in all fields of pharmaceutical sciences in both English and Turkish. (1984-1995, edited by Prof. Dr. Kasım Cemal GÜVEN, 1995-2001, edited by Prof. Dr. Erden GÜLER, 2002-2011, edited by Prof. Dr. Kasım Cemal GÜVEN)

Since 2006, the journal has been published only in English with the name, "Acta Pharmaceutica Sciencia" which represents internationally accepted high-level scientific standards. The journal has been published quarterly except for an interval from 2002 to 2009 in which its issues were released at intervals of four months. The publication was also temporarily discontinued at the end of 2011 but since 2016, Acta Pharmaceutica Sciencia has continued publication with the reestablished Editorial Board and also with the support of you as precious scientists.

Yours Faithfully

Prof. Dr. Gülden Zehra OMURTAG
Editor

INSTRUCTIONS FOR AUTHORS

Manuscripts must be prepared using the manuscript template.

Manuscripts should contain the following elements in the following order:

Title Page

Abstract

Keywords

Introduction (without author names and affiliations)

Methodology

Results and Discussion

Statement of Ethics

Conflict of Interest Statement

Author Contributions

Funding Sources (optional)

Acknowledgments (optional)

References

It is best to use the Times New Roman font, 11 font size, and all kinds of articles must be 1.5 spaced including text, references, tables, and legends.

The title should be concise and informative. Avoid abbreviations and formulae, where possible. The title page should include full title, author names and affiliations, present addresses, corresponding author, and ORCID numbers for every author. Also, the full manuscript should include a full title page.

Abstracts should not be separated into categories; it should be written in a paragraph format.

Keywords: Max. 5

Graphics may be included with both in the text and uploaded as separate files.

Sections: (Capital letters should be used in) Introduction, Methodology, Results and Discussion, Statement of Ethics, Conflict of Interest Statement, Author Contributions, Funding Sources (optional), Acknowledgments (optional).

Table and figure titles should not be abbreviated exp. fig. is not acceptable. It should be written as; Table 1. .... Figure 1. .....

Figure captions: A caption should comprise a brief title (not on the figure itself) and a description of the illustration. Keep text in the illustrations themselves to a minimum but explain all symbols and abbreviations used. Figure captions should be written on the bottom.

Titles: Number tables consecutively by their appearance in the text and place any table notes below the table body. Table captions should be written on the top.

References in the text should be identified using Arabic numerals. Years of the references should not be written boldly. More than one reference from the same author(s) in the same year must be identified by the letters “a”, “b”, “c”, etc., placed after the year of publication. References should conform to Vancouver style and be numbered consecutively in the order in which they are cited in the text.

*Obligatory files are manuscript main document, title page and copyright form for submission. If exist, supplementary files should also be added.

1. Scope and Editorial Policy

1.1 Scope of the Journal

Acta Pharmaceutica Sciencia (Acta Pharm. Sci.), formerly known as Bulletin of Pharmacy and Acta Pharmaceutica Turcica is a peer-reviewed scientific journal publishing current research and reviews covering all fields of pharmaceutical sciences since 1953.

The original studies accepted for publication must be unpublished work and should contain data that have not been published elsewhere as a whole or a part. The reviews must provide critical evaluation of the state of knowledge related with the subject.

All manuscripts have to be written in clear and concise English.

Including the October 2023 issue, the journal has started to be published online only. It will also publish special issues for national or international scientific meetings and activities in the interested field.

1.2 Manuscript Categories

Manuscripts can be submitted as Research Articles.

Research Articles are definitive accounts of significant, original studies. They are expected to present important new data or provide a fresh approach to an established subject.

1.3 Prior Publication

Authors should submit only original work that has not been previously published and is not under consideration for publication elsewhere. Academic theses, including those on the Web or at a college Web site, are not considered to be prior publication.

1.4 Patents and Intellectual Property

Authors need to resolve all patent and intellectual property issues. Acceptance and publication will not be delayed for pending or unresolved issues of this type. Note that Accepted manuscripts and online manuscripts are considered published documents.

1.5 Professional Ethics

Editors, reviewers, and authors are expected to adhere to internationally accepted criteria for scientific publishing. Helsinki declaration is applied and accepted for the ethical standards of the journal.

World Medical Association. (2001). World Medical Association Declaration of Helsinki. Ethical principles for medical research involving human subjects. Bulletin of the World Health Organization, 79(4),373-374.

1.5.1 Author Consent

Submitting authors are reminded that consent of all coauthors must be obtained prior to submission of manuscripts. If an author is removed after submission, the submitting author must have the removed author consent to the change by e-mail or faxed letter to the assigned editor.

1.5.2 Plagiarism

Manuscripts must be original with respect to concept, content, and writing. It is not appropriate for an author to reuse wording from other publications, including one's own previous publications, whether or not that publication is cited. Suspected plagiarism should be reported immediately to the editorial office. Report should specifically indicate the plagiarized material within the manuscripts. Acta Pharmaceutica Sciencia uses iThenticate or Turnitin software to screen submitted manuscripts for similarity to published material. Note that your manuscript may be screened during the submission process.

1.5.3 Use of Human or Animal Subjects

For research involving biological samples obtained from animals or human subjects, editors reserve the right to request additional information from au-

thors. Studies submitted for publication approval must present evidence that the described experimental activities have undergone local institutional review assessing safety and humane usage of study subject animals. In the case of human subjects, authors must also provide a statement that study samples were obtained through the informed consent of the donors, or in lieu of that evidence, by the authority of the institutional board that licensed the use of such material. Authors are requested to declare the identification or case number of institution approval as well as the name of the licensing committee in a statement placed in the section describing the Material and Methods utilized in the studies.

World Medical Association. (2001). World Medical Association Declaration of Helsinki. Ethical principles for medical research involving human subjects. Bulletin of the World Health Organization, 79(4),373-374.

1.6 Issue Frequency

The Journal publishes 4 issues per year.

2. Preparing the Manuscript

2.1 General Considerations

Manuscripts should be kept to a minimum length. Authors should write in clear, concise English, employing an editing service if necessary. For professional assistance with improving English and/or the figures, or formatting in the manuscript before submission please contact to editorial office by e-mail for suggestions.

The responsibility for all aspects of manuscript preparation rests with the authors. Applying extensive changes or rewriting of the manuscript will not be undertaken by the editors. A standard list of Abbreviations, Acronyms, and Symbols is in section 5.

It is best to use the font “Times New Roman”. Other fonts, particularly those that do not come bundled with the system software, may not translate properly. Ensure that all special characters (e.g., Greek characters, math symbols) are present in the body of the text as characters and not as graphic representations. Be sure that all characters are correctly represented throughout the manuscript—e.g., 1 (one) and l (letter l), 0 (zero) and O (letter o).

All text (including the title page, abstract, all sections of the body of the paper, figure captions, scheme or chart titles, and footnotes and references) and tables should be in one file. Graphics may be included with the text or uploaded as separate files. Manuscripts that do not adhere to the guidelines may be returned to authors for correction.

2.1.1 Articles of All Kind

Use page size A4. Vertically orient all pages. Articles of all kind must be double-spaced including text, references, tables, and legends. This applies to figures, schemes, and tables as well as text. They do not have page limitations but should be kept to a minimum length. The experimental procedures for all experimental steps must be clearly and fully included in the experimental section of the manuscripts.

2.1.2 Nomenclature

It is the responsibility of the authors to provide correct nomenclature. It is acceptable to use semisynthetic or generic names for certain specialized classes of compounds, such as steroids, peptides, carbohydrates, etc. In such a case, the name should conform to the generally accepted nomenclature conventions for the compound class. Chemical names for drugs are preferred. If these are not practical, generic names, or names approved by the World Health Organization, may be used.

Authors may find the following sources useful for recommended nomenclature:

- The ACS Style Guide; Coghill, A. M., Garson, L. R., Eds.; American Chemical Society: Washington DC, 2006.
- Enzyme Nomenclature; Webb, E. C., Ed.; Academic Press: Orlando, 1992.
- IUPHAR database of receptors and ion channels (http://www.guidetopharmacology.org/).

2.1.3 Compound Code Numbers

Code numbers (including peptides) assigned to a compound may be used as follows:

- Once in the manuscript title, when placed in parentheses AFTER the chemical or descriptive name.
- Once in the abstract.
- Once in the text (includes legends) and once to label a structure. Code numbers in the text must correspond to structures or, if used only once, the chemical name must be provided before the parenthesized code number, e.g., “chemical name (JEM-398).” If appearing a second time in the text, a bold Arabic number must be assigned on first usage, followed by the parenthesized code number, e.g., “1 (JEM-398).” Subsequently, only the bold Ara-

bic number may be used. All code numbers in the text must have a citation to a publication or a patent on first appearance.

Compounds widely employed as research tools and recognized primarily by code numbers may be designated in the manuscript by code numbers without the above restrictions. Their chemical name or structure should be provided as above. Editors have the discretion of determining which code numbers are considered widely employed.

2.1.4 Trademark Names

Trademark names for reagents or drugs must be used only in the experimental section. Do not use trademark or service mark symbols.

2.1.5 Interference Compounds

Active compounds from any source must be examined for known classes of assay interference compounds and this analysis must be provided in the General Experimental section. Many of these compounds have been classified as Pan Assay Interference Compounds (PAINS; see Baell & Holloway, J. Med. Chem. 2010, 53, 2719-2740). These compounds shown to display misleading assay readouts by a variety of mechanisms by forming reactive compounds. Provide firm experimental evidence in at least two different assays that reported compounds with potential PAINS liability are specifically active and their apparent activity is not an artifact.

2.2 Manuscript Organization

2.2.1 Title Page

The title of the manuscript should reflect the purposes and findings of the work in order to provide maximum information in a computerized title search. Minimal use of nonfunctional words is encouraged. Only commonly employed abbreviations (e.g., DNA, RNA, ATP) are acceptable. Code numbers for compounds may be used in a manuscript title when placed in parentheses AFTER the chemical or descriptive name.

Authors' Names and Affiliations: The authors' full first names, middle initials, last names (with capital letters for only last names), and affiliations with addresses at time of work completion should be listed below the title. The name of the corresponding author should be marked with an asterisk (*).

2.2.2 Abstract and Keywords

Articles of all types must have an abstract following the title page. The maximum length of the Abstract should be 200 words, organized in a findings-oriented format in which the most important results and conclusions are sum-

marized. Code numbers may be used once in the abstract. After the abstract, a section of Keywords not more than five has to be given. Be aware that the keywords, chosen according to the general concept, are very significant during searching and indexing of the manuscripts.

Keywords: instructions for authors, template, journal

2.2.3 Introduction

The Introduction should argue the case for the study, outlining only essential background, and should not include the findings or the conclusions. It should not be a review of the subject area but should finish with a clear statement of the question being addressed. Authors should use this template when preparing a manuscript for submission to the ACTA Pharmaceutica Sciencia.

2.2.4 Methodology

Materials, synthetic, biological, demographic, statistical or experimental methods of the research should be given detailed in this section. The authors are free to subdivide this section in the logical flow of the study. For the experimental sections, authors should be as concise as possible in experimental descriptions. General reaction, isolation, preparation conditions should be given only once. The title of an experiment should include the chemical name and a bold Arabic identifier number; subsequently, only the bold Arabic number should be used. Experiments should be listed in numerical order. Molar equivalents of all reactants and percentage yields of products should be included. A general introductory section should include general procedures, standard techniques, and instruments employed (e.g., determination of purity, chromatography, NMR spectra, mass spectra, names of equipment) in the synthesis and characterization of compounds, isolates and preparations described subsequently in this section. Special attention should be called to hazardous reactions or toxic compounds. Provide analysis for known classes of assay interference compounds.

The preferred forms for some of the more commonly used abbrevations are mp, bp, ^{o}C, K, min, h, mL, μL, g, mg, μg, cm, mm, nm, mol, mmol, μmol, ppm, TLC, GC, NMR, UV, and IR. Units are abbreviated in table column heads and when used with numbers, not otherwise. (See section 4 for more abbreviations)

2.2.5 Results and Discussion

This section could include preparation, isolation, synthetic schemes and tables of biological and statistical data. The discussions should be descriptive. Authors should discuss the analysis of the data together with the significance of results and conclusions. An optional conclusions section is not required.

2.2.6 Ancillary Information

Include pertinent information in the order listed immediately before the references.

PDB ID Codes: Include the PDB ID codes with assigned compound Arabic number. Include the statement "Authors will release the atomic coordinates and experimental data upon article publication."

Homology Models: Include the PDB ID codes with assigned compound Arabic number. Include the statement "Authors will release the atomic coordinates upon article publication."

Corresponding Author Information: Provide telephone numbers and email addresses for each of the designated corresponding authors.

Present/Current Author Addresses: Provide information for authors whose affiliations or addresses have changed.

Author Contributions: Include statement such as "These authors contributed equally."

Acknowledgments: Authors may acknowledge people, organizations, and financial supporters in this section.

Abbreviations Used: Provide a list of nonstandard abbreviations and acronyms used in the paper, e.g., YFP, yellow fluorescent protein. Do not include compound code numbers in this list. It is not necessary to include abbreviations and acronyms from the Standard Abbreviations and Acronyms listed in section 4.

2.2.7 References and Notes

Vancouver style is used in the reference list and citations. List manuscripts as "in press" only accepted for publication. Manuscripts available on Web with a DOI number are considered published. For manuscripts not accepted, use "unpublished work" after the names of authors. Incorporate notes in the correct numerical sequence with the references. Footnotes are not used. List submitted manuscripts as "in press" only if formally accepted for publication. Manuscripts available on the Web with a DOI number are considered published. For manuscripts not accepted, use "unpublished results" after the names of authors. Incorporate notes in the correct numerical sequence with the references. Footnotes are not used. In-text citations should be given superscript numbers (see examples) according to order in the manuscript.

References

Please check with your faculty for any specific referencing or formatting requirements.

- References are listed in numerical order, and in the same order in which they are cited in text. The reference list appears at the end of the paper.
- Begin your reference list on a new page and title it 'References'.
- The reference list should include all and only those references you have cited in the text. (However, do not include unpublished items such as correspondence.)
- Use Arabic numerals (1, 2, 3, 4, 5, 6, 7, 8, 9) as a superscripts.
- Abbreviate journal titles in the style used in the NLM Catalog.
- Check the reference details against the actual source – you are indicating that you have read a source when you cite it.
- Use of DOI URL at the end of reference is strongly advised.

Examples

For printed articles

• Article with 1-6 authors:

Author AA, Author BB, Author CC, Author DD. Title of article. Abbreviated title of journal, Date of publication YYYY;volume number(issue number):page numbers.

Sahin Z, Ertas M, Berk B, Biltekin SN, Yurttas L, Demirayak S. Studies on non-steroidal inhibitors of aromatase enzyme; 4-(aryl/heteroaryl)-2-(pyrimidin-2-yl)thiazole derivatives. Bioorg Med Chem, 2018; 26(8): 1986–1995. https://doi.org/10.1016/j.bmc.2018.02.048.

• Article with more than 6 authors:

Author AA, Author BB, Author CC, Author DD, Author EE, Author FF, et al. Title of article. Abbreviated title of journal, Date of publication YYYY Mon DD;volume number(issue number):page numbers.

For electronic journal articles

Author AA, Author BB, Author CC, Author DD, Author EE, Author FF. Title of article. Abbreviated title of Journal [Internet], Year of publication [cited YYYY Mon DD];volume number(issue number):page numbers. Available from: URL DOI

For books and book chapters

Book: a.) Print book OR b.) Electronic book

a.) Author AA. Title of book. # edition [if not first]. Place of Publication: Publisher; Year of publication. Pagination.

b.) Author AA. Title of web page [Internet]. Place of Publication: Sponsor of Website/Publisher; Year published [cited YYYY Mon DD]. Number of pages. Available from: URL DOI: (if available)

2.2.8 Tables

Tabulation of experimental results is encouraged when this leads to more effective presentation or to more economical use of space. Tables should be numbered consecutively in order of citation in the text with Arabic numerals. Footnotes in tables should be given italic lowercase letter designations and cited in the tables as superscripts. The sequence of letters should proceed by row rather than by column. If a reference is cited in both table and text, insert a lettered footnote in the table to refer to the numbered reference in the text. Each table must be provided with a descriptive title that, together with column headings, should make the table self-explanatory. Titles and footnotes should be on the same page as the table. Tables may be created using a word processor's text mode or table format feature. The table format feature is preferred. Ensure each data entry is in its own table cell. If the text mode is used, separate columns with a single tab and use a return at the end of each row. Tables may be inserted in the text where first mentioned or may be grouped after the references.

2.2.9 Figures, Schemes/Structures, and Charts

The use of illustrations to convey or clarify information is encouraged. Structures should be produced with the use of a drawing program such as ChemDraw. Authors using other drawing packages should, in as far as possible, modify their program's parameters so that they conform to ChemDraw preferences. Remove all color from illustrations, except for those you would like published in color. Illustrations may be inserted into the text where mentioned or may be consolidated at the end of the manuscript. If consolidated, legends should be grouped on a separate page(s). Include as part of the manuscript file.

To facilitate the publication process, please submit manuscript graphics using the following guidelines:

1. The preferred submission procedure is to embed graphic files in a Word document. It may help to print the manuscript on a laser printer to ensure all artwork is clear and legible.

2. Additional acceptable file formats are: TIFF, PDF, EPS (vector artwork) or CDX (ChemDraw file). If submitting individual graphic files in addition to them being embedded in a Word document, ensure the files are named based on graphic function (i.e., Scheme 1, Figure 2, Chart 3), not the scientific name. Labeling of all figure parts should be present and the parts should be assembled into a single graphic.

EPS files: Ensure that all fonts are converted to outlines or embedded in the graphic file. The document settings should be in RGB mode. NOTE: While EPS files are accepted, the vector-based graphics will be rasterized for production. Please see below for TIFF file production resolutions.

3. TIFF files (either embedded in a Word doc or submitted as individual files) should have the following resolution requirements:

- Black & White line art: 1200 dpi
- Grayscale art (a monochromatic image containing shades of gray): 600 dpi
- Color art (RGB color mode): 300 dpi
- The RGB and resolution requirements are essential for producing high-quality graphics within the published manuscript. Graphics submitted in CMYK or at lower resolutions may be used; however, the colors may not be consistent and graphics of poor quality may not be able to be improved.
- Most graphic programs provide an option for changing the resolution when you are saving the image. Best practice is to save the graphic file at the final resolution and size using the program used to create the graphic.

4. Graphics should be sized at the final production size when possible. Single column graphics are preferred and can be sized up to 240 points wide (8.38 cm.). Double column graphics must be sized between 300 and 504 points (10.584 and 17.78 cm's). All graphics have a maximum depth of 660 points (23.28 cm.) including the caption (please allow 12 points for each line of caption text).

Consistently sizing letters and labels in graphics throughout your manuscript will help ensure consistent graphic presentation for publication.

2.2.10 Image Manipulation

Images should be free from misleading manipulation. Images included in an account of research performed or in the data collection as part of the research require an accurate description of how the images were generated and produced. Apply digital processing uniformly to images, with both samples and

controls. Cropping must be reported in the figure legend. For gels and blots, use of positive and negative controls is highly recommended. Avoid high contrast settings to avoid overexposure of gels and blots. For microscopy, apply color adjustment to entire image and note in the legend. When necessary, authors should include a section on equipment and settings to describe all image acquisition tools, techniques and settings, and software used. All final images must have resolutions of 300 dpi or higher. Authors should retain unprocessed data in the event that the editors request them.

2.3 Specialized Data

2.3.1 Biological Data

Quantitative biological data are required for all tested compounds. Biological test methods must be referenced or described in sufficient detail to permit the experiments to be repeated by others. Detailed descriptions of biological methods should be placed in the experimental section. Standard compounds or established drugs should be tested in the same system for comparison. Data may be presented as numerical expressions or in graphical form; biological data for extensive series of compounds should be presented in tabular form.

Active compounds obtained from combinatorial syntheses should be resynthesized and retested to verify that the biology conforms to the initial observation. Statistical limits (statistical significance) for the biological data are usually required. If statistical limits cannot be provided, the number of determinations and some indication of the variability and reliability of the results should be given. References to statistical methods of calculation should be included.

Doses and concentrations should be expressed as molar quantities (e.g., mol/kg, μmol/kg, M, mM). The routes of administration of test compounds and vehicles used should be indicated, and any salt forms used (hydrochlorides, sulfates, etc.) should be noted. The physical state of the compound dosed (crystalline, amorphous; solution, suspension) and the formulation for dosing (micronized, jet-milled, nanoparticles) should be indicated. For those compounds found to be inactive, the highest concentration (*in vitro*) or dose level (in vivo) tested should be indicated.

If human cell lines are used, authors are strongly encouraged to include the following information in their manuscript:

· the cell line source, including when and from where it was obtained;

· whether the cell line has recently been authenticated and by what method;

· whether the cell line has recently been tested for mycoplasma contamination.

2.3.2 Purity of Tested Compounds

Methods: All scientifically established methods of establishing purity are acceptable. If the target compounds are solvated, the quantity of solvent should be included in the compound formulas. No documentation is required unless asked by the editors.

Purity Percentage: All tested compounds, whether synthesized or purchased, should possess a purity of at least 95%. Target compounds must have a purity of at least 95%. In exceptional cases, authors can request a waiver when compounds are less than 95% pure. For solids, the melting point or melting point range should be reported as an indicator of purity.

Elemental Analysis: Found values for carbon, hydrogen, and nitrogen (if present) should be within 0.4% of the calculated values for the proposed formula.

2.3.3 Confirmation of Structure

Adequate evidence to establish structural identity must accompany all new compounds that appear in the experimental section. Sufficient spectral data should be presented in the experimental section to allow for the identification of the same compound by comparison. Generally, a listing of 1H or 13C NMR peaks is sufficient. However, when the NMR data are used as a basis of structural identification, the peaks must be assigned.

List only infrared absorptions that are diagnostic for key functional groups. If a series contains very closely related compounds, it may be appropriate merely to list the spectral data for a single representative member when they share a common major structural component that has identical or very similar spectral features.

3. Submitting the Manuscript

3.1 Communication and Log in to Author's Module

All submissions to Acta Pharmaceutica Sciencia should be made by using e-Collittera (Online Article Acceptance and Evaluation) system on the journal main page (www. actapharmsci.com).

3.2 Registration to System

It is required to register into the e-Collittera system for the first time while entering by clicking "Create Account" button on the registration screen and the fill the opening form with real information. Some of the information required in form is absolutely necessary and the registration will not work if these fields are not completely filled.

After the registration, a "Welcome" mail is sent to the user by the system automatically reminding user name and password. Authors are expected to return to the entry screen and log on with their user name and password for the submission. Please use only English characters while determining your username and password.

If you already registered into the e-Collittera system and forget your password, you should click on "Forgot My Password" button and your user name and password will be mailed to your e-mail in a short while.

3.3 Submitting a New Article

The main page of author module consists of various parts showing the situation of manuscripts in process. By clicking the New Manuscript button, authors create the beginning of new submission, a process with a total of 9 consecutive levels. In first 7 levels, information such as the article's kind, institutions, authors, title, summary, keywords etc. are asked respectively as entered. Authors can move back and forth while the information is saved automatically. If the is transaction is discontinued, the system move the new submission to "Partially Submitted Manuscripts" part and the transaction can be continued from here.

3.3.1 Sort of Article Authors should first select the type of article from the drop-down menu.

Warning. If "Return to Main Page" button is clicked after this level, the article automatically assigned as "Partially Submitted Manuscripts".

3.3.2 Institutions Authors should give their institutional information during submission.

3.3.3 Authors The authors' surnames, names, institutional information appear as entered order in the previous page. Filling all e-mail addresses are required. Institutional information is available in Manuscript Details table at the top of the screen. After filling all required fields, you may click the Continue button.

3.3.4 Title should be English, explaining the significance of the study. If the title includes some special characters such as alpha, beta, pi or gamma, they can easily be added by using the Title window. You may add the character by clicking the relevant button and the system will automatically add the required character to the text.

Warning. No additions to cornered parenthesis are allowed. Otherwise, the system will not be able to show the special characters.

3.3.5 Abstract The summary of the article should be entered to Abstract window at this level. There must be an English summary for all articles and the quantity of words must be not more than 200. If special characters such as alpha, beta, pi or gamma are used in summary, they can be added by Abstract window. You may add the character by clicking the relevant button and the system will automatically add the required character to the text. The abstract of the articles is accessible for arbitrators; so, you should not add any information related to the institutions and authors in this summary part. Otherwise, the article will be returned without evaluation. Authors will be required to comply with the rules.

Warning. No additions to cornered parenthesis are allowed. Otherwise, the system will not be able to show the special characters.

3.3.6 Keywords There must be five words to define the article at the keywords window, which will be diverged with commas. Authors should pay attention to use words, which are appropriate for "Medical Subjects Headings" list by National Library of Medicine (NLM).

3.3.7 Cover Letter If the submitting article was published as thesis and/or presented in a congress or elsewhere, all information of thesis, presented congress or elsewhere should be delivered to the editor and must be mentioned by the "Cover Letter" field.

3.4 Adding Article

This process consists of four different steps beginning with the loading of the article in to system. Browse button is used to reach the article file, under the Choose a file to upload tab. After finding the article you may click to Choose File and file will be attached.

Second step is to select the file category. Options are: Main Document, Black and White Figure, Color Figure and Video.

The explanation of the files (e.g., Figure 1, Full Text Word File, supplements etc.) should be added on third step and the last step is submitting the prepared article into the system. Therefore, Download button under the Send your file by clicking on download button tab is clicked.

Reminder. If the prepared article includes more than one file (such as main document, black and white figure, video), the transaction will be continued by starting from the first step. The image files must be in previously defined format. After all required files were added, Continue button should be clicked. All details and features of the article might be reached from the Article Information page.

This page is the last step of the transaction which ensures that entered information is controlled.

3.4.1 Your Files After adding the article you may find all information related to article under Your Files window.

File Information This window includes file names, sizes, forming dates, categories, order numbers and explanations of files. The details about the files can be reached by clicking on Information button.

If you click on Name of File, the file download window will be opened to reach the copy of the file in system.

File Download This window submits two alternatives, one of them is to ensure the file to be opened in valid site and the second one is to ensure to download submitted file into the computer.

Opening the Category part on fourth column can change the category of the file.

Opening the Order column on fifth column can change the order of file.

The file can be deleted by clicking on Delete button on the last column. Before deleting, system will ask the user again if it is appropriate or not.

3.4.2 Sending Article Last level is submitting the article and the files into the system. Before continuing the transaction, Article Information window must be controlled where it is possible to return back; by using Previous button and required corrections can be made. If not, clicking the Send the Article button completes transaction.

3.4.3 Page to Follow the Article The Main Page of Author ensures possibility to follow the article. This page consists of three different parts; some information and bridges related to the sent articles, revision required articles and the articles that are not completed to be sent.

3.4.3.1 Articles Not Completed to be Sent After the sending transaction was started, if article is not able to continue until the ninth step or could not be sent due to technical problems shown at this part. Here you can find the information such as the article's number which is assigned by system, title and formation date. You may delete the articles by using Delete button on the right column, if the article is not considered to send into the system.

3.4.3.2 Articles that Require Revision Articles, which were evaluated by the referee and accepted by the editor with revision, continues to Waiting for Revision table.

The required revisions can be seen in "Notes" part by clicking the articles title. In order to send any revision, Submit Revision button on the last column should be clicked. This connection will take the author to the first level of Adding Article and the author can complete the revision transaction by carrying out the steps one by one. All changes must be made in the registered file, and this changed file must be resent. Author's most efficacious replies relating to the changes must be typed in "Cover Letter" part.

If the is transaction is discontinued, the system move the revised article to Submitted Manuscripts part and the transaction can be continued from here.

After the transaction was completed, the system moves the revised article to "Submitted Manuscripts" part.

3.4.4 Submitted Manuscripts Information related to articles can be followed through the Submitted Manuscripts line. Here you can find the information such as the article's number assigned by system, title, sending date and transaction situation. The Manuscript Details and summary files can be reached by clicking the title of the article and the Processing Status part makes it possible to follow the evaluation process of the article.

3.5 Article Review Process

Articles uploaded to the Manuscript submission system are checked by the journal administration for format consistency and similarity rate which is required to be less than 20%. Then sent to the chief editor if found appropriate.

Articles that are not suitable are sent back to the author for correction and resubmit (sent back to the author). Studies that have not been prepared using the draft for submitting to Acta Pharmaceutica Sciencia "acta_msc_tmp" and that have not been adapted in terms of format, will be directed to the editor-in-chief, after the 3rd time, by giving the information that "the consistency requirements have not been met".

The manuscripts sent to the chief editor will be evaluated and sent to the "language and statistics editor" if deemed appropriate.

Studies found appropriate after language-statistics editor will be sent to field editors. If the field editor does not deem it appropriate after evaluating the article scientifically, he/she will inform the editor-in-chief of its negative comments, otherwise, at least two independent referee comments will be asked.

Authors should consider that this time may take time because of the reviewer assignments and acceptance for review may take time for some cases.

Our review system is double-blind. The editor, who evaluates according to the comments of the referees, submits his/her comment and suggestion to the editor-in-chief. In this way, the article takes one of the acceptance, rejection, or revision decisions. In the case of revision, after the author revises, the editor submits his/her final opinion to the editor-in-chief. The editor-in-chief conveys his or her final decision to the author. After the accepted articles are subjected to the final control by the journal and the corresponding author, the article starts to be included in the "accepted papers" section by giving the inactive DOI number. When the article is placed in one of the following issues, the DOI number will be activated and displayed in the "current issue" section on the journal homepage.

EDITORIAL

Superdrugs & Supertherapies: High prices to pay for miracles…

Editorial Article

Yusuf ÖZTÜRK*

Istanbul Aydın University, Faculty of Pharmacy, Department of Pharmacology, Istanbul, Türkiye

Today, in Istanbul and other parts of our country, at bus stops, metro stations and on various street corners, we can hear the heartbreaking cries of parents of children with SMA (Spinal Muscular Atrophy) Type-1 seeking financial resources for exorbitantly priced treatment. In fact, this is a gene-based life-saving treatment that is effective in pediatric patients under two years of age with just one dose. This miraculous treatment costs patients approximately $2.1 million. This miraculous treatment costs patients around $2.1 million. But that is not all, and it is not the most expensive either, there are others worth mentioning.

After a rocky start, gene therapy is on fire and drawing intense interest from the biopharmaceutical industry—and it's still evolving and improving. In fact, the journey of fundamental developments in gene therapy begins with the discovery of the DNA structure by Watson and Crick in the year of 1953. The concept of gene therapies first emerged in the 1960s, when the feasibility of adding new genetic functions to mammalian cells began to be studied. Several methods for this purpose were tested, including injecting genes directly into a living mammalian cell via a micropipette and exposing the cells to a DNA precipitate containing the desired genes. Later, scientists developed theories that viruses could also be used as a vehicle or vector to deliver new genes to cells. Among the avenues of biomedical sciences, humanity's fast lane, but hard journey to gene therapies began in the 1990s. There are various versions of gene therapies forming different highways to arrive final destination of therapy. But unfortunately, some of these highways of gene therapies have turned into dead-end streets:

*Corresponding author: Yusuf ÖZTÜRK
E-mail: yusufozturk10@aydin.edu.tr
ORCID: 0000-0002-9488-0891

- Gene therapy ver. 1.0 - First introduction of corrected genes
- Gene therapy ver. 2.0 - Improved viral vectors
- Gene therapy ver. 3.0 - Gene editing and base editing
- Miscellaneous genetic therapies

Gene therapy ver. 1.0 - First introduction of corrected genes: Seemingly, the first successful example of gene therapy was obtained with a 4-year-old girl in 1989. The girl, Ashanthi de Silva, who was the hero of the first successful gene therapy was born with severe combined immunodeficiency (SCID), a disease caused by a deficiency of the enzyme adenosine deaminase (ADA). Without ADA, T cells were dying and not be able to fight invading infections. Injections of a synthetic ADA enzyme were being helpful only temporarily. This application, which seemed like a success at first glance, encouraged scientists on the subject and they applied gene treatments for various genetic diseases. After a few years of gene therapies using this methodology have been reported to cause very severe side effects, including leukemia, fatal immune responses, which were mainly due to activation of some oncogenes by viral vector used. Gene therapies which use this technique have been stopped.

Gene therapy ver. 2.0 - Improved viral vectors: In the early 2010s, gene therapy was in a renaissance age. Scientists discovered improved viral vectors to deliver genetic therapies. They also added some regulatory elements called promoters and enhancers to direct the activity of genes. These elements were defining where, when, and at what level the genes should be turned on. Popular viruses for gene therapy include adenoviruses, adeno-associated virus, and lentiviruses. Agustín, born in 2010, had suffered from X chromosome-linked severe combined immunodeficiency syndrome (SCID-X1) and had spent the first few months of his life in isolation. He became the first patient to receive gene therapy with improved viral vector at Boston Children's and today is an active fifth-grade soccer and tennis player.

Gene therapy ver. 3.0 - Gene editing and base editing: While traditional gene therapy uses viruses to transfer healthy genes into cells, compensating for a faulty or missing gene, this newer generation of gene therapy employs various fine-tune molecular tools and divided into two methodologies: a) Gene editing b) Base editing. Gene editing precisely target troublesome genes and create a cut or break in their DNA. It can knock out a defective gene, place a new DNA sequence, or both in a "cut and paste" operation. The common gene editing systems of today are CRISPR/Cas 9, zinc-finger nucleases (ZFNs), and transcription activator-like effector nucleases (TALENs). Base editing is even more

fine-tuned, specifically replacing DNA bases found in defective genes. It takes advantage of CRISPR's targeting capabilities but relies on specific enzymes to chemically alter a gene's code one by one—changing a C to a T or an A to a G, for example. In contrast to gene editing, base editing has not yet been tested in clinical trials, but it offers the promise of more precision, efficiency, and safety.

Miscellaneous genetic therapies: Some other new techniques are blurring the line between gene therapy and conventional drug treatment. For instance, antisense oligonucleotides (ASOs) are new type of drugs consist of short, synthetic pieces of DNA or RNA that aim at the messenger RNA made by the defective gene. As another approach, RNA interference, uses small RNAs for silencing a targeted gene by neutralizing the gene's mRNA. The messenger RNAs (mRNA) and the microRNA (miRNA) used for some COVID-19 vaccines are regarded as a form of gene therapy too. This RNAs introduce genetic code that cells then use to make the coronavirus spike protein, stimulating people to produce antibodies to the virus.

Today, there are approximately 400 gene therapy studies worldwide on ClinicalTrials.gov and more than a dozen approved gene therapy drugs on the market. It is only a matter of time before newer ones enter the pharmaceutical market. These products related to this issue, which will shape the future of pharmacy and medicine, are called "super drugs". These drugs, which are the products of advanced biotechnology, have been developed for the treatment of diseases that are currently fatal, and some of them offer a definitive solution to diseases with a single dose of miraculous treatments. However, these are not only miraculous ones but also the most expensive therapies known in medical/pharmaceutical market. Here is a summarized list of most expensive drugs in US, and most probably in the world:

1. Lenmeldy®: Cost: $4.25 million per one-time treatment, Use: Metachromatic leukodystrophy (MLD), FDA Approval Date: March 18, 2024 (Gene editing therapy)

2. Hemgenix®: Cost: $3.5 million per one-time dose, Use: Hemophilia B, FDA Approval Date: November 22, 2022 (Improved virus vector-based gene therapy)

3. Elevidys®: Cost: $3.2 million per one-time dose, Use: Duchenne Muscular Dystrophy (DMD), FDA Approval Date: June 22, 2023 (Gene editing therapy)

4. Skysona®: Cost: $3 million per one-time dose, Use: Cerebral Adrenoleukodystrophy (CALD), FDA Approval Date: September 16, 2022 (Improved virus vector-based gene therapy)

5. Zynteglo®: Cost: $2.8 million per one-time dose, Use: Beta-thalassemia, FDA Approval Date: September 16, 2022 (Improved virus vector-based gene therapy)

6. Zolgensma®: Cost: $2.1 million per one-time dose, Use: Spinal Muscular Atrophy (SMA) Type 1, FDA Approval Date: May 24, 2019 (Improved virus vector-based gene therapy)

7. Myalept®: Cost: $1.3 million annually, Use: Lipodystrophy / Leptin deficiency, FDA Approval Date: February 24, 2014 (Leptin replacement therapy)

8. Danyelza®: Cost: $1.2 million annually, Use: Neuroblastoma, FDA Approval Date: November 25, 2020 (Monoclonal antibody therapy)

9. Zokinvy®: Cost: $1.2 million annually, Use: Progeria and Progeroid Laminopathies, FDA Approval Date: November 20, 2020 (Enzyme inhibitor)

10. Kimmtrak®: Cost: $ 1.1 million annually, Use: Uveal Melanoma, FDA Approval Date: January 25, 2022 (Immunotherapy).

The first six drugs on the list of the most expensive drugs are gene-based therapies. Another feature of some of these therapies is that they are specifically designed for each individual. This situation also causes the prices of some gene-based treatments to become uncertain. Whatever it is, these drugs are game changer in their characters and promise better management of certain fatal diseases. That is not all, there are also engineered cell therapies approved for certain indications, mainly CAR-T cells.

It is anticipated that gene and cell-based treatments will diversify and increase in the future, and even cloned organs will be used for treatment purposes. It is said that these future drugs and treatments could extend human lifespan to 150 years. However, it is also obvious that these will create very important socio-economic and scientific problems. First, how will access be made to medicines that are economically difficult to access even today? Experts on the subject suggest that prices may fall over time as technology becomes more widespread and advanced. However, there is no glimmer of hope in this regard yet. What if more advanced treatments emerge that cost more than what we have today? Moreover, it is known that many countries in the world have reduced or even eliminated drug/treatment reimbursements in order to reduce healthcare expenses. Fearing that in the future, the world will be one where only the rich can live longer and more quality lives. Second, this situation will also lead to striking demographic changes in the world population. How will these demographic changes in the world population affect today's environmental and

climate problems? Third, what will happen with these treatments in terms of side effects and unexpected effects in the longer term? Finally, it is obvious that developments in this field will cause radical scientific changes in the fields of pharmacy and medicine.

ORIGINAL ARTICLES

Acta Pharm. Sci. Vol 63:(1), 2025
Original article
DOI: 10.23893/1307-2080.APS6301

Development and evaluation of propolis loaded mixed micellar gel: Formulation, optimization and anticancer potential

Harshad KAPARE[1*], Shubham GADGE[1], Nagesh PATIL[1], Vinita PATOLE[1]
Sadhana RAUT[2]

1 Dr. D. Y. Patil Institute of Pharmaceutical Sciences and Research, Department of Pharmaceutics, Pimpri, Pune, Maharashtra, India

2 Sinhgad College of Pharmacy, Department of Pharmaceutical Chemistry, Pune, Maharashtra, India

ABSTRACT

To increase the effectiveness of the anticancer natural product propolis extract (PE), mixed micellar gel formulation composed of Pluronic F127 and Tween 80 was investigated. Cold technique was used to formulate mixed micellar gel loaded with propolis extract (PE-MMG). 3^2 factorial design was employed to optimize formulation. PE-MMG was characterized for micellar size, surface morphology, surface charge, drug loading, entrapment, release study and *in vitro* cytotoxicity. Developed optimized formulation showed desirable formulation characteristics Optimized formulation showed desirable characteristics for improved therapeutic performance. Enhanced cytotoxicity potential revealed through MTT Assay by PE-MMG as compared with PE showed enhanced permeability and chemosensitization. In overall developed formulation further studied as a promising carrier for cancer therapy.

Keywords: mixed micellar gel, propolis, Pluronic F127, Tween 80, MCF 7

*Corresponding author: Harshad KAPARE
E-mail: hskapare@yahoo.in
ORCIDs:
Harshad KAPARE: 0000-0003-2991-7413
Shubham GADGE: 0009-0004-7201-8354
Nagesh PATIL: 0009-0009-0244-5736
Vinita PATOLE: 0000-0001-9544-4074
Sadhana RAUT: 0000-0002-2076-6439
(Received 27 Dec 2023, Accepted 27 Sep 2024)

INTRODUCTION

The sticky resinous bee product well known as propolis masticated from a combination of beeswax and resin that is gathered by Indian stingless bees from plant parts. Propolis is composed of different chemical constituents including flavonoids, polyphenols, amino acids, minerals etc., due to which it shows various biological activities. Because of the anti-inflammatory, immunomodulatory, and antiviral properties of propolis, it is widely used in traditional medicine[1]. Propolis is investigated for its antiproliferative impact on cancer cells in addition to these benefits. Its anticancer activity of propolis is also well proven through several investigations[2-5]. Propolis is thought to have an anticancer impact by causing apoptosis and cell cycle arrest. Propolis and its active ingredients, primarily CAPE, blocks cell cycle progression and trigger apoptosis in a variety of cancer types[6-9]. The region (where propolis was gathered) and dose, which both affect the chemical composition of propolis, are the primary determinants of its antiproliferative effects. The chemical compositions of propolis changes based on the bee species, area, and types of plants etc.[10–14]. Previous studies[6,15-19] have demonstrated the impact of propolis on breast cancer cell lines, prostate cancer cell lines, and leukemia cell lines. Propolis, however, may have distinct impacts on various cancer cells[4,20]. Apoptosis induction is shown to be substantially dependent on the concentration of propolis extract consist of phenolic acids and flavonoids[21-23] as well as the cytotoxic components of propolis that causes anticancer effects[23-25].

Propolis from different geographical locations are well proven for anticancer potential with apoptosis and some other mechanisms[25]. CAPE a propolis constituent also plays a role in the modulation of breast cancer through an epigenetically mediated pathway[26]. Propolis nanoparticles have antibacterial and anticancer properties *in vitro,* and cancer cells internalize the nanoparticles. Nanoparticle formulation of propolis demonstrated excellent anticancer potential with safety and biocompatibility[26-27]. However, their clinical application is limited by their low bioavailability, poor targeting, and low aqueous solubility. To increase therapeutic efficacy, safety, and patient acceptability for a variety of natural bioactives, nanomedicine-based drug delivery systems have been created[24-27]. Solubility of poorly soluble drugs can be enhanced encapsulation in inner hydrophobic core of mixed micelles due to their distinctive self-assembled core-shell structure, which improves solubility, stability, and bioavailability. The pharmacokinetic and biodistribution behavior of the micelles is significantly influenced by the outside hydrophilic shell[28]. In addition, the improved permeability and retention (EPR) effect of mixed micellar

nanostructures enables passive targeting into solid tumors[28]. Literature study reports that Pluronic® F127 micelles have the limitation in terms of physical stability, drug release and loading of lipophilic moieties. Mixed micelles composed of Pluronic F127 (PF127) and Tween 80 overcame these issues and shows improved stabilities and biopharmaceutical properties of dosage form[29]. Additionally, Pluronic F127 and Tween 80 in a fixed combination so as to provide the desired thermos reversibility for the skin application[30]. These systems have been used in conjunction with a number of anticancer medications, including doxorubicin, propofol, docetaxel, and gambogic acid[31-36]. This study aims for design, development and evaluation of mixed micellar gel formulation of propolis extract PE-MMG to improve drug loading, drug solubilization, stability, better release profile and enhanced cytotoxicity and cancer therapy.

METHODOLOGY

Material

Authenticated Indian propolis was procured from CBRTI, Pune. Tween 80 (Polysorbate 80, Mw=1309) and Pluronic F127 (Mw=12,600, PEO99-PPO67-PEO99) were bought from Sigma-Aldrich Bangalore, India. Analytical Reagent (AR) grade was used for all other reagents and solvents in the investigation.

Methods

Extraction and characterization of propolis

Authenticated crude propolis was purchased from CBRTI, Pune and extracted by following the previously developed method from removal of wax, debris matter etc. by giving hexane pretreatment. Further ethanolic extract of propolis was prepared by maceration technique to obtain enriched ethanolic extract of Indian propolis which was characterized for physical appearance, color, odor, melting point, UV absorbance, total balsam content etc.[20,28].

Preparation of propolis mixed micellar gel

Propolis mixed micellar gels was formulated using “cold” technique, followed by method previously described with slight modifications[29]. PF127 (20%, w/w) and Tween 80 were added to doubled distilled water. The liquid mixture was gently stirred with the magnetic stirrers to dissolve all the PF127 granules overnight at 4°C. The transparent mixed micelle solution at 4°C obtained. Further drug was added at 4°C and mixed until a clear solution was obtained.

The procedure and the process variables that affected the properties and usefulness of the mixed micelles were better understood with preliminary trials. Pluronic F127 concentration (X1) and Tween 80 concentration (X2) were

shown to be important variables in defining the characteristics of the micelles. In order to explore the impact of X1 and X2 (independent variables) on micelle size and EE (dependent variables) a 3^2 factorial design was used as shown in Table 1. This allowed for the creation of a response surface plot[28].

Table 1. Details of formulation batches 3^2 factorial design

Batches	X1 Amt. of PF127	X2 Amt. of Tween 80	X1 Amt. of PF127 (mg)	X2 Amt. of Tween 80 (ml)
F1	-1	-1	100	2
F2	-1	0	100	1.5
F3	-1	1	100	1
F4	0	-1	75	2
F5	0	0	75	1.5
F6	0	1	75	1
F7	1	-1	50	2
F8	1	0	50	1.5
F9	1	1	50	1

Micelles size & surface charge

Size of PE-loaded mixed micelles was assessed on Horiba SZ 100, at 90° scattering angle, measurements of particle size were made. The samples' average particle size was calculated in nanometer after being dispersed in distilled water. Electrophoretic mobility was also determined at a temperature of 25°C.

Drug Loading (DL) & Entrapment Efficiancy (EE)

UV-VIS spectrophotometer was used to measure PE's absorbance at 314 nm, the concentration of PE in the mixed micelles was discovered. Prior to measurement, the micellar solution was suitably diluted with alcohol and by following procedures as described by Bothiraja C et al. drug loading and entrapment efficiancy was evaluated[28].

$$DL\ (\%) = \frac{\text{Weight of the drug in micelles}}{\text{Weight of the feeding phospholipid and drug}} \text{ X } 100$$

$$EE\ (\%) = \frac{\text{Weight of the drug in micelles}}{\text{Weight of the feeding drug}} \text{ X } 100$$

Surface morphology

Transmission electron microscopy technique was used to examine the morphology of the mixed micelles that were loaded with PR. Zeiss EM 109 TEM was used at 80 kV accelerating voltage was to inspect and take pictures of the sample after any surplus solution had beendrained[27].

In vitro release of PE from mixed micelles

in vitro dialysis bag technique was used to study release of PE from mixed micelles using phosphate-buffer saline (pH 6.8) as release medium. Dialysis bag MW cut-off 12,000 Da was used for formulation (1 mg equivalent) as well pure drug as control. Study was carried out under continuous magnetic stirring at 100 rpm/min and 37°C + 0.5°C. UV-VIS spectrophotometer was used to measure the absorbance of PR[26].

In vitro cytotoxicity studies

In vitro cytotoxicity study for propolis extract and developed formulation was carried out by MTT assay as with 96 well plate technique as shown in schematic presentation in Figure 1. ELISA plate reader was used to record the intensity at 540 nm[20]. Schematic presentation of assay format has been given in Figure 1.

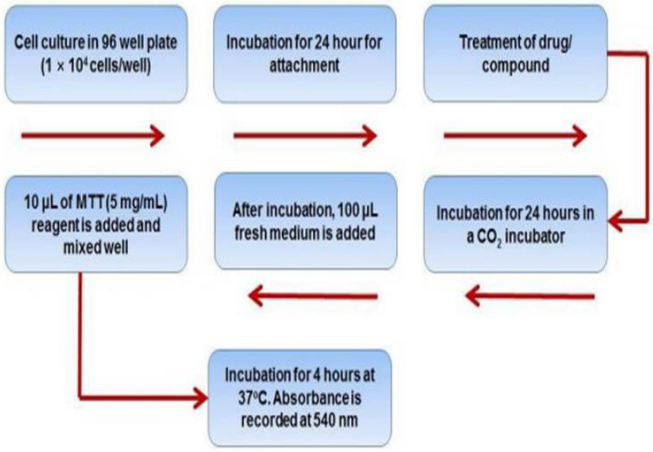

Figure 1. Schematic diagram of MTT assay

RESULTS and DISCUSSION

Attempt has been made to formulate Propolis-loaded Mixed Micelle Gel (PE-MMG). Over the past few decades, it has been well demonstrated that drug delivery methods based on micellar nanotechnology can increase the solubility, effectiveness, and safety of a variety of active ingredients. In order to increase its solubility and ensure prolonged release, PE-MMG has been formulated and explored as a nano-carrier. Design of Experiments (DoE) methodology was used to investigate the impact of the Propolis loaded Mixed Micelle Gel composition on particle size and encapsulation effectiveness.

Preliminary evaluation and characterization of Propolis

At room temperature propolis extract was sticky and yellow to brownish red in color. Propolis was found to have a melting point of 70-71°C.

Propolis extract UV absorbance maxima was observed at 314 nm. Propolis calibration curves was plotted in phosphate buffer saline pH 6.8 was found to follow Beer-Lambert's law over this range. Propolis was found to exhibit high linearity (r2=0.998) over the concentration range of 10-80 micro gram/mL.

Formulation development and optimization

Cold technique method was employed for formulation of Mixed Micelle Gels (MMG). Impact of formulation variables are studied on the particle size and encapsulation as crucial evaluation parameters.

Initial trial batches studied to understand effect of formulation variable subsequently based on results obtained detailed 3^2 factorial design was used for optimization of material attributes. Drug concentration was kept constant, and nine batches were formulated using a 3^2 factorial design. Using Design Expert® Version 12.0, multiple regression analysis was performed. The equation obtained from multiple regression analysis are as below;

Equation 1 Particle Size = +165.00-11.67*A+18.17*B+2.25*AB+8.00A2-15.50*B2

Equation 2 Encapsulation Efficiency = +82.83+1.83*A-4.17*B-1.25*AB-0.40*A2+2.60*B2

Study results revealed that as shown in Figure 1, and Table 1; PF127 and Tween 80 had a favorable effect on the particle size and encapsulation efficiency was shown by the positive coefficients of the major terms X1 and X2. According to the surface plot, the effects of PF127 and Tween 80 on encapsulation efficiency and particle size were curvilinear as shown in Figure 2. The results obtained

from data analysis taken for the determination of optimized batch. From the Design Expert® Version 12.0 software the optimized batch was determined at level of PF127 as (0) and that of Tween 80 as (+1). These values were best fitted with F5 batch of mixed micelle formulation. So F5 batch was considered as an optimized batch based on data in Table 2 and Table 3.

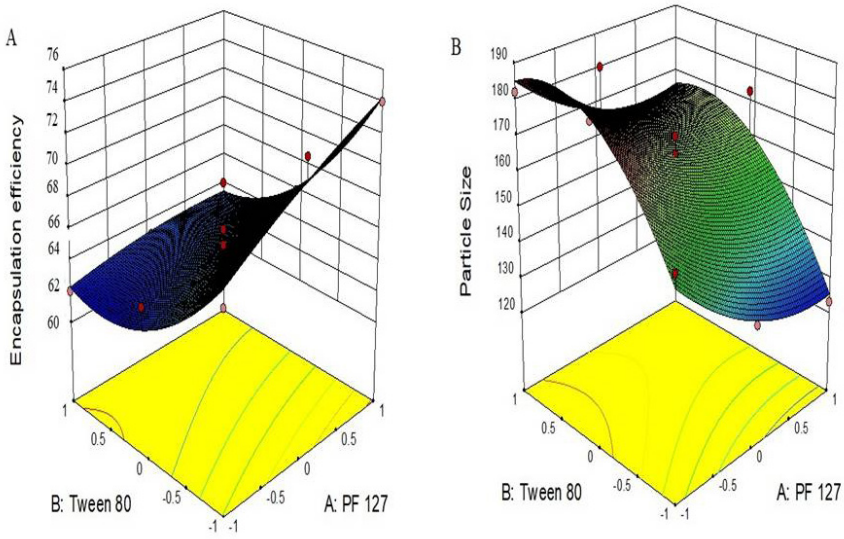

Figure 2. Response surface plots, (A) Encapsulation efficiency (B) Particle size

Table 2. Formulation characterization of PE-MMG

Batch	Particle Size (nm)	Zeta Potential (mV)	Entrapment Efficiency (%)
F1	123 ± 0.85	5.04 ± 1.02	62.52 ± 0.75
F2	130 ± 0.73	5.56 ± 1.13	61.33 ± 0.83
F3	157 ± 1.01	5.88 ± 1.06	65.22 ± 0.76
F4	157 ± 0.96	5.01 ± 1.24	70.65 ± 0.73
F5	162 ± 0.94	5.37 ± 1.04	76.45 ± 0.96
F6	170 ± 1.02	5.09 ± 0.85	71.69 ± 1.22
F7	173 ± 0.71	5.05 ± 0.98	73.75 ± 1.01
F8	180 ± 0.80	5.92 ± 0.70	72.31 ± 1.13
F9	182 ± 0.83	5.89 ± 0.90	62.52 ± 0.96

Table 3. Optimized batch solution

Sr. No	PF127 mg	Tween 80 Ml	Particle Size nm	Encapsulation Efficiency %	Desirability (R2)	Remark
01	72	1.5	160	75%	0.9924	Selected

Characterization of formulation

Particle size

As shown in Table 2 increase in particle size was seen as the concentration of PF127 and Tween 80 was raised. The optimum particle size 162 + 0.5 nm as shown in Figure 3 with single peak of size distribution observed. Micellar size was strongly affected by concentration of selected variables.

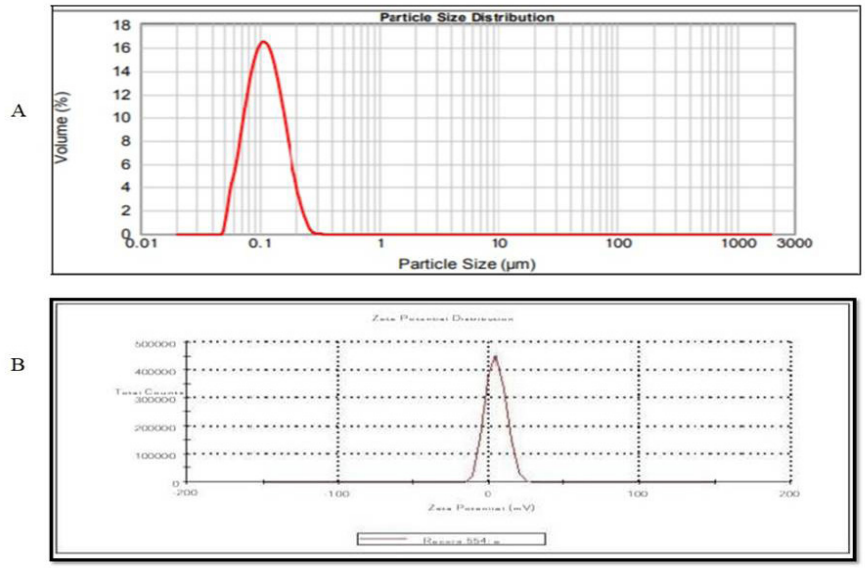

Figure 3. Particle size (A) and zeta potential analysis (B) of F5 formulation of mixed micelle

Zeta potential

Zeta potential is a crucial metric that provides data on surface charges, which directly affect colloidal stability and interaction with bodily cells. The mixed micelle formulation was evaluated for zeta potential from the value it is observed that slight positive values as shown in Table 2 which may be due to presence of PF127 on surface. The values are within acceptable limit and ensure stability. The optimized formulation showed positive zeta potential 5.37 + 1.04 mV as shown in Figure 3.

Encapsulation efficiency

The percent encapsulation efficiency in mixed micelle formulation was observed as shown in Table 2. The F5 batch showed 76.45 + 0.96 % the higher amount of encapsulation efficiency in formulation, with optimal concentration of PF127 and Tween 80.

Surface morphology

The typical spherical core-shell architecture of mixed micelles, which were spherical in shape and homogenous in size, was seen in TEM image (Figure 4). Into the dark core area Propolis is forming the micellar core which is hydrophobic in nature whereas hydrophilic PF127 shows their presence in outer corona shell structure.

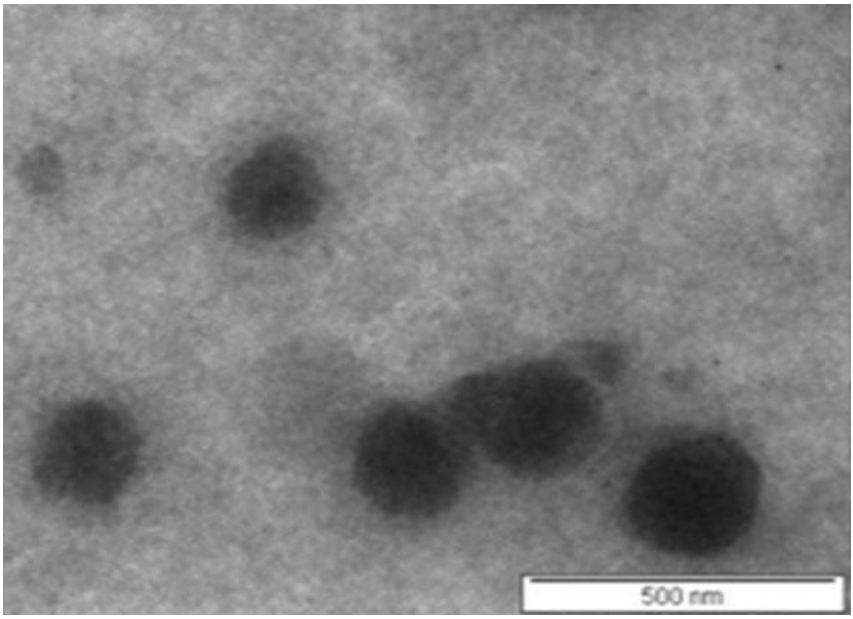

Figure 4.TEM image of Mixed Micelles

***In-vitro* drug release study**

Release pattern of propolis from a mixed micellar gel formulation is observed as shown in Figure 5. Result pattern shows that propolis diffuses freely in solution at about 97.12 + 0.55% in 8 hours. However, the Propolis release from formulation burst release of 46.20 + 0.48% at initial phase in first 2 hrs and sustained release 97.12 + 0.55% up to 8 hours. Three fundamental mechanisms erosion, diffusion, and degradation help a loaded medication release from a mixed mi-

celle. Any one of the three mechanisms or all three can contribute to drug release in a mature system. The first burst release observed during the *in vitro* release may be due to adsorbed drug on micelles, whereas a sustained release may have been brought on by the drug's diffusion. The sustained release of entrapped drug from mixed micelles is a crucial factor in the production of the desired formulation because it keeps a steady level of drug at the site of action over time.

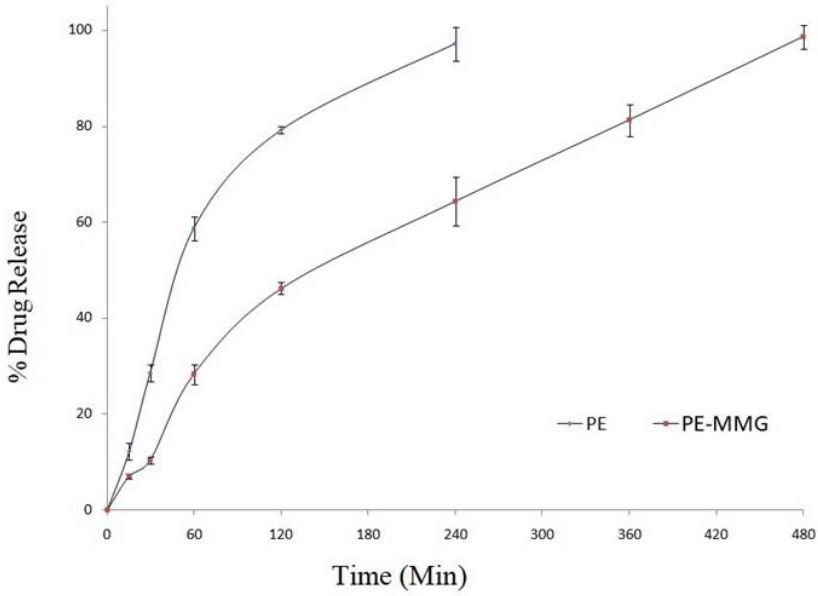

Figure 5. *In vitro* drug release study

Cytotoxicity study

The cytotoxicity study is performed by the MTT Assay method. In this study different concentration of formulation was used to carried cytotoxicity 10, 20, 40 and 80 ug/ml. The *in vitro* anticancer activity of drug and formulation was investigated against MCF-7 cells. The results illustrated in Figure 6 (a–d), Table 4 indicated that PE-MMG showed comparatively better GI50 and TGI as cell growth inhibition parameters to propolis extract.

The TGI value of mixed micellar formulation and propolis extract was found to be 19.2 ± 0.12 µg/mL and 30.10 ± 0.49 µg/mL, respectively. Whereas GI50 value of mixed micellar formulation and propolis extract were obtained less than 10µg/mL. Improved cytotoxicity of formulation as compared to pure drug form may be due to increased cellular uptake through phagocytosis or micellar solubilization.

Table 4. *In vitro* cytotoxicity study

Samples	MCF-7cell line TGI (µg/mL)	MCF-7cell line GI50 (µg/mL)
PE	30.10 ± 0.49	<10
PE-MMG	19.2 ± 0.12	<10
ADR	<10	<10
Blank MMG	74.8 ± 0.11	27.2 ± 0.05

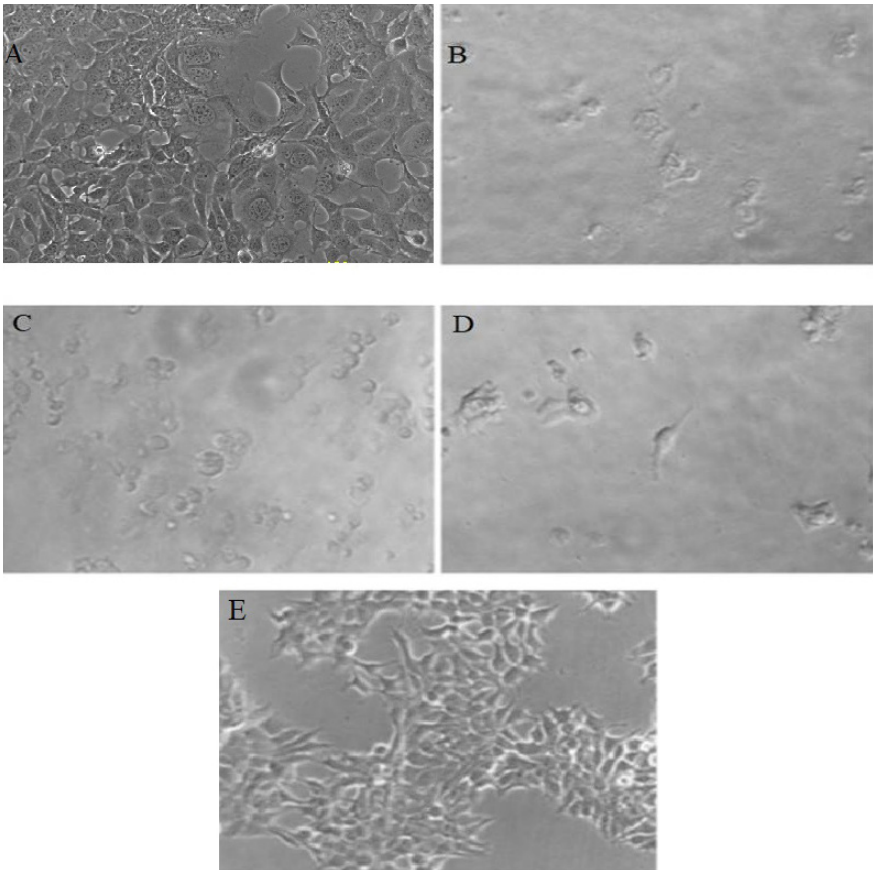

Figure 6. *In vitro* cytotoxicity study (A- MCF 7 Breast cancer cells-Control, B- Treatment of standard, C- Treatment with ethanolic extract of propolis, D- Treatment with Formulation PE-MMG, E- Treatment with blank MMG without drug)

Overall, developed propolis mixed micellar gel formulation displayed desirable formulation characteristics. Optimized formulation showed micellar size 134 nm, spherical shape, 5.04 mV zeta potential, 91.21 + 0.56 % drug loading and encapsulation efficiency was obtained 74 + 0.42 %. The developed formulation showed 46.20 + 0.48% burst release in first 2 hr followed by sustained release 97.12 + 0.55% up to 8 hrs. In overall PE-MMG also showed high encapsulation efficiency which may also give good physical as well chemical stability at various physiological pH. Desirable drug release pattern and improved cytotoxicity potential on MCF-7 cells as compared with propolis extract may improve biopharmaceutical performance. In overall present formulations strategy may be a promising for the delivery of propolis in cancer therapy.

STATEMENT OF ETHICS

Not applicable as no human or animal subjects were involved in the study.

CONFLICT OF INTEREST STATEMENT

The authors declare that there is no conflict of interest associated with this study.

AUTHOR CONTRIBUTIONS

Concept – H.K, S.R; Design – H.K, S.R,V.P; Supervision – H.K, S.R; Resources – H.K, N.P; Materials – H.K, S.R, N.P.; Data Collection and/or Processing – H.K, S.G, S.R, N.P, V.P.; Analysis and/or Interpretation – H.K, S.G, S.R, N.P, V.P.; Literature Search – H.K, S.G, N.P.; Writing – H.K, N.P; Critical Reviews – H.K, S.G, N.P, V.P, S.R.

FUNDING SOURCES

No funding or other financial support was received for this study.

ACKNOWLEDGMENTS

Not applicable.

REFERENCES

1. Marcucci MC. Propolis: chemical composition, biological properties and therapeutic activity. Apidologie, 1995;26(2):83-99. Doi: 10.1051/apido:19950202

2. Sawicka D, Car H, Borawska MH, Niklinski J. The anticancer activity of propolis. Folia Histochem Cytobiol, 2012;50(1):25-37. Doi: 10.2478/18693

3. Aso K, Kanno S, Tadano T, Satoh S, Ishikawa M. Inhibitory effect of propolis on the growth of human leukemic U937. Biol Pharm Bull, 2004;27:727-730. Doi: 10.1248/bpb.27.727

4. Orsolic N, Basic I. Immunomodulation by water-soluble derivative of propolis: a factor of antitumor reactivity. J Ethnopharmacol, 2003;84:265-273. Doi: 10.1016/s0378-8741(02)00329-x

5. Orsolic N, Knezevic AH, Sver L, Terzic S, Basic I. Immunomodulatory and antimetastatic action of propolis and related polyphenolic compounds. J Ethnopharmacol, 2004;94:307-315. Doi: 10.1016/j.jep.2004.06.006

6. Vatansever SH, Sorkun K, Deliloğlu Gurhan SI, Ozdal-Kurt F, Turkoz E, Gencay O, et al. Propolis from Turkey induces apoptosis through activating caspases in human breast carcinoma cell lines. Acta Histochem, 2010;112:546-556. Doi: 10.1016/j.acthis.2009.06.001

7. Eom HS, Lee EJ, Yoon BS, Yoo BS. Propolis inhibits the proliferation of human leukaemia HL-60 cells by inducing apoptosis through the mitochondrial pathway. Nat Prod Res, 2010;24:375-386. Doi: 10.1080/14786410903370908

8. Szliszka E, Czuba ZP, Domino M, Mazur B, Zydowicz G, Krol W. Ethanolic extract of propolis (EEP) enhances the apoptosis-inducing potential of TRAIL in cancer cells. Molecules, 2009;14:738-754. Doi: 10.3390/molecules14020738

9. Jin UH, Song KH, Motomura M, Suzuki I, Gu YH, Kang YJ, et al. Caffeic acid phenethyl ester induces mitochondria-mediated apoptosis in human myeloid leukemia U937 cells. Mol Cell Biochem, 2008;310:43-48. Doi: 10.1007/s11010-007-9663-7

10. Watabe M, Hishikawa K, Takayanagi A, Shimizu N, Nakaki T. Caffeic acid phenethyl ester induces apoptosis by inhibition of NF kappaB and activation of Fas in human breast cancer MCF-7 cells. J Biol Chem, 2004;279:6017-6026. Doi: 10.1074/jbc.M306040200

11. Chen MJ, Chang WH, Lin CC, Liu CY, Wang TE, Chu CH, et al. Caffeic acid phenethyl ester induces apoptosis of human pancreatic cancer cells involving caspase and mitochondrial dysfunction. Pancreatology, 2008;8:566-576. Doi: 10.1159/00015984

12. Daugsch A, Moraes CS, Fort P, Park YK. Brazilian red propolis-chemical composition and botanical origin. Evid Based Complement Alternat Med, 2008;5:435-441. Doi: 10.1159/000159843

13. Nieva MMI, Isla MI, Cudmani NG, Vattuone MA, Sampietro AR. Screening of antibacterial activity of Amaicha del Valle (Tucuman, Argentina) propolis. J Ethnopharmacol, 1999;68:97-102. Doi: 10.1016/s0378-8741(99)00051-3

14. Sibel S, Semiramis K. Chemical composition and antibacterial activity of propolis collected by three different races of honeybees in the same region. J Ethnopharmacol, 2005;99:69-73. Doi: 10.1016/j.jep.2005.01.046

15. Uzel A, Sorkun K, Oncag O, Cogulu D, Gencay O, Salih B. Chemical compositions and antimicrobial activities of four different Anatolian propolis samples. Microbiol Res, 2005;160:189-195. Doi: 10.1016/j.micres.2005.01.002

16. Gunduz C, Biray C, Kosova B, Yilmaz B, Eroglu Z, Sahin F, et al. Evaluation of Manisa propolis effect on leukemia cell line by telomerase activity. LeukRes, 2005;29:1343-1346. Doi: 10.1016/j.leukres.2005.04.010

17. Barlak Y, Deger O, Colak M, Karataylı SC, Bozdayı M, Yücesan F. Effect of Turkish propolis extracts on proteome of prostate cancer cell line. Proteome Sci, 2011;9:74. Doi: 10.1186/1477-5956-9-74

18. Kapare HS, Rele H, Bhosale MK, Bhole RP, Kulkarni D, Neve V, et al. Development and optimization of Indian propolis formulation for enhanced immunomodulatory potential. Immuno, 2024; 4(4):426-443. Doi: 10.3390/immuno4040027

19. Pecere T, Gazzola MV, Mucignat C, Parolin C, Vecchia FD, Cavaggioni A, et al. Aloe-emodin is a new type of anticancer agent with selective activity against neuroectodermal tumors. Cancer Res, 2000;60(11):2800-2804.

20. Kapare H, Lohidasan S, Sinnathambi A, Mahadik K. Standardization, anti-carcinogenic potential and biosafety of Indian propolis. J Ayurveda Integr Med, 2019;10(2):81-87. Doi: 10.1016/j.jaim.2017.06.003

21. Kapare H, Raut S, Sathiyanarayanan L. Propolis and its key chemical constituents: a promising natural product in therapeutic applications. Frontiers in Natural Product Chemistry, 2022;9:1-27. Doi: 10.2174/9789815040586122090003

22. Kapare H, Sathiyanarayanan L. Nutritional and therapeutic potential of propolis: a review. Research J Pharmand Tech, 2020;13(7):3545-3549. Doi: 10.5958/0974-360X.2020.00627.7

23. Kapare H, Nagaraj S, Wakalkar S, Rathi K. Caffeic acid phenethyl ester: a potential anticancer bioactive constituent of propolis. Curr Cancer Ther Rev, 2022;18(3):181-192. Doi: 10.2174/1573394718666220603103458

24. Kapare H, Sathiyanarayanan L, Arulmozhi S, Mahadik K. Design and development of Indian propolis loadedpoly (ε-caprolactone) nanoparticles for improved anticancer efficacy. Int J Pharm Res, 2017;9(3),73-80.

25. Kapare HS, Sathiyanarayanan L, Sinnathambi A, Mahadik K. Indian propolis loaded folic acid conjugated PLGA nanoparticles: formulation development, characterization. J Pharm Drug Deliv Res, 2017;6(1):1-7. Doi: 10.4172/2325-9604.1000164

26. Kapare HS, Sathiyanarayanan L, Sinnathambi A, Mahadik K. Formulation development of folic acid conjugated PLGA nanoparticles for improved cytotoxicity of caffeic acid phenethyl ester. Pharm Nanotechnol, 2021;9(1):111-119. Doi: 10.2174/2211738509666210111160528

27. Kapare HS, Sathiyanarayanan L, Sinnathambi A, Mahadik K. Caffeic acid phenethyl ester loaded poly (ε-caprolactone) nanoparticles for improved anticancer efficacy: formulation development, characterization and *in vitro* cytotoxicity study. Nanomed Res J, 2020;5(4):324-333. Doi: 10.22034/nmrj.2020.04.003

28. Bothiraja C, Kapare H, Pawar A, Shaikh K. Development of plumbagin-loaded phospholipid–Tween® 80 mixed micelles: formulation, optimization, effect on breast cancer cells and human blood/serum compatibility testing. Ther Deliv, 2013;4(10):1247-1259. Doi: 10.4155/tde.13.92

29. Sharma G, Kamboj S, Thakur K, Negi P, Raza K, Katare OP. (2017). Delivery of thermoresponsive-tailored mixed micellar nano gel of lidocaine and prilocaine with improved dermatokinetic profile and therapeutic efficacy in topical anaesthesia. AAPS Pharm Sci Tech, 18(3), 790-802. Doi: 10.1208/s12249-016-0561-8

30. Yang Y, Wang J, Zhang X, Lu W, Zhang Q. A novel mixed micelle gel with thermo-sensitive property for the local delivery of docetaxel. J Control Release, 2009;135(2):175-182. Doi: 10.1016/j.jconrel.2009.01.007

31. Gao H, Cao S, Chen C, Cao S, Yang Z, Pang Z, et al. Incorporation of lapatinib into lipoprotein-like nanoparticles with enhanced water solubility and anti-tumor effect in breast cancer. Nanomedicine (Lond), 2013;8(9):1429-1442. Doi: 10.2217/nnm.12.180

32. Bothiraja C, Pawar AP, Shaikh KS, Sher P. Eudragit® EPO based nanoparticle suspension of andrographolide: *in vitro* and *in vivo*. Nanosci Nanotechnol Lett, 2009;1(3):156-164. Doi: 10.1166/nnl.2009.1029

33. Schütz CA, Juillerat-Jeanneret L, Mueller H, Lynch I, Riediker M. Therapeutic nanoparticles in clinics and under clinical evaluation. Nanomedicine (Lond), 2013;8(3):449-467. Doi:10.2217/nnm.13.8

34. Sun M, Su X, Ding B, He X, Liu X, Yu A, et al. Advances in nanotechnology-based delivery systems for curcumin. Nanomedicine (Lond), 2012;7(7):1085-1100. Doi: 10.2217/nnm.12.80

35. Deepagan VG, Sarmento B, Menon D, Nascimento A, Jayasree A, Sreeranganathan M, et al. *In vitro* targeted imaging and delivery of camptothecin using cetuximab-conjugated multifunctional PLGA-ZnS nanoparticles. Nanomedicine (Lond), 2012;7(4):507-519. Doi: 10.2217/nnm.11.139

36. Yoncheva K, Calleja P, Agüeros M, Petrov P, Miladinova I, Tsvetanov C, et al. Stabilized micelles as delivery vehicles for paclitaxel. Int J Pharm, 2012;436(1-2):258-264. Doi: 10.1016/j.ijpharm.2012.06.030

Acta Pharm. Sci. Vol 63:(1), 2025
Original article
DOI: 10.23893/1307-2080.APS6302

Mitragyna inermis (Willd.) O. Kuntze ethnopharmacology and metabolic disorders: An update review and in *silico* study

Relwende Justin OUEDRAOGO[1*], Nadeem AHMAD[2], Lassina OUATTARA[1,3]
Zaheer UL-HAQ[2,4], Georges Anicet OUEDRAOGO[1]

1 Nazi BONI University, Laboratory of Research and Teaching in Animal Health and Biotechnologies, Bobo-Dioulasso, Burkina Faso

2 Karachi University, H.E.J. Research Institute of Chemistry, International Center for Chemical and Biological Sciences, Karachi, Pakistan

3 Nazi BONI University, Department of Biochemistry-Microbiology, Life and Earth Sciences Training and Research Unit, Bobo-Dioulasso, Burkina Faso

4 Karachi University, International Center for Chemical and Biological Sciences, Dr. Panjwani Center for Molecular Medicine and Drug Research, Karachi, Pakistan

ABSTRACT

Mitragyna inermis is a wild plant whose parts are traditionally used. However, there is no particular report on the compounds bioactivity evidence against metabolic disorders. We carried out a literature review of this plant uses and compounds mostly isolated in diabetic and hypertensive states. Following the review, we carried out an *in silico* study on major targets for research into antidiabetic and antihypertensive candidates. From this study, it emerged that the plant is used in the treatment of diabetes and hypertension. The main compounds isolated from this plant were terpenoids and alkaloids. The *in silico* study revealed that these compounds could inhibit α-amylase, α-glucosidase and sodium glucose co-transporter 2 in diabetic status, as well as angiotensin converting enzyme in hypertensive status. Most of these compounds could be absorbed and metabolized on the basis of ADME (Adsorption, Distribution, Metabolism and Excretion) pharmacokinetic prediction. Further studies are

*Corresponding author: Relwendé Justin OUEDRAOGO
E-mail: rjustino14@yahoo.com
ORCIDs:
Relwende Justin OUEDRAOGO: 0000-0002-5036-2144
Nadeem AHMA0: 0009-0002-0503-5280
Lassina OUATTARA: 0000-0001-5537-5246
Zaheer UL-HAQ: 0000-0002-8530-8711
Georges Anicet OUEDRAOGO: 0000-0002-1588-1379
(Received 10 Sep 2023, Accepted 30 Dec 2023)

needed to optimize its activities and conduct *in vitro* trials.

Keywords: *Mitragyna inermis,* metabolic disorders, *in silico* study, diabetes, hypertension

INTRODUCTION

Mitragyna inermis (Willd.) O. Kuntze leaf, fruit, wood, stalk, bark, root and whole plant are used for a variety purposes. Leaves and roots are used in traditional medicine[1]. Several ethnopharmacological studies have been carried out to reveal extracts and some compounds derived from *M. inermis* various parts pharmacological properties in relation to communicable and metabolic disorders.

Indeed, ethnobotanical studies have shown leaf and bark use in the treatment of body pain and diarrhea[2]. In infection cases, leaf or bundles in decoctions are used to treat urinary tract infection[3]. The aqueous extract of the roots stimulates immune defense[4]. Studies have shown that leaf, root stem bark and alkaloids extracts possess antimicrobial properties[5-8]. Also, bark and leaf in decoction are recommended for recovering human immunodeficiency virus patients, herpes simplex virus-1, poliomyelitis and smallpox[9-11]. That plant finds most application especially in malaria disease. For instance, leaves bundles, leaves, stems, roots and compounds as well as ursolic acid, speciophylline and isorhyncophylline isolated from this plant are used to treat malaria fever and against *Plasmodium falciparum*[12,13]. Furthermore, *M. inermis* parts are used in the management of neuronal failure. Indeed, aqueous, ethanolic and ethyl acetate extracts of *M. inermis* stem bark showed significant anti-seizure effects. Extracts flavonoids and alkaloids have these anticonvulsant properties[14].

Today, non-communicable diseases have overtaken infectious diseases as the world's leading cause of death[15]. Among metabolic disorders, special attention is devoted to cardiovascular disease and diabetes[16]. To the best of our knowledge, there are neither potential compounds isolated from *M. inermis* against these diseases, nor synthetic data bringing attention to this plant use in these diseases' treatment. However, the lower adverse effects of *M. inermis* parts and isolated compounds has been reported[17-19]. Furthermore, α-amylase and α-glucosidase through carbohydrate breakdown are involved in diabetes happening[20,21]. Also, kidney sodium glucose co-transporter 2 is involved in diabetes complications[22]. So, these enzymes inhibitors are required for diabetes treatment. Among hypertension management, Angiotensin Converting Enzyme (ACE) inhibitors are mostly required[23]. The implementation of virtual screening of small molecules can be valuable in the search for novel lead compound with potential for further

exploration in new drug discovery studies[22]. So, the present study aims to review the ethnopharmacological and phytochemical studies relating to diabetes and hypertension on the one hand. Then, to carry out an *in silico* study of alkaloids and terpenoids this plant main compounds on these diabetes and hypertension potential targets in order to orient future research and its rational use.

METHODOLOGY

Data sources and research strategy

Two authors (R.J.O. and L.O.) independently searched electronic databases such as Google, Google Scholar, EMBASE, PubMed, PubChem, Scopus and Science Direct. Relevant articles were searched from inception to May 2023. The search strategic term was "*Mitragyna inermis*" or "*Mitragyna africana*". No restrictions were placed on language or study design. Our exclusion criteria were *Mitragyna speciosa*, *Mitragyna africanus*, *Mitragyna parvifolia*, *Mitragyna rotundifolia*, *Mitragyna rubrostipulata*, *Mitragyna ciliata*, *Mitragyna stipulosa*, *Mitragyna tubulosa*, *Mitragyna hirsuta*, *Mitragyna diversifolia*, *Mitragyna ledermannii*, and *Mitragyna savanica*.

Furthermore, in this systematic review after searching for articles, we removed duplicates, examined titles and abstracts and obtained the full text of each article. We included research classified as *M. inermis* ethnobotanical studies[1], phytochemistry studies[2], antihypertensive properties[3], and antidiabetic properties[4]. Review articles were excluded. Accepted articles and articles in press were included in this mini review. Evaluations were carried out by two independent investigators.

In silico study

The *in silico* study focused on potential targets for diabetes namely α-amylase, Sodium-Glucose co-Transporter 2 (SGLT2) and α-glucosidase, and hypertension namely Angiotensin Converting Enzyme (ACE). Studies relating to the various major compounds of *M. inermis* (alkaloids and terpenoids) were diagnosed on PubChem to avoid any duplication in relation to the chosen metabolic disorder's targets.

Molecular docking

The molecular docking studies were conducted to investigate the *in silico* interactions of alkaloids and terpenoids extract from *M. inermis* against the enzyme's α-amylase, α-glucosidase, SGLT2 and ACE. The purpose of the study was to identify potential inhibitors for these four specific enzymes using compounds extracted from the aforementioned. Finally, for comparison we docked

a typical molecule acarbose against α-amylase and α-glucosidase, captopril against ACE and empagliflozin against SGLT2. All molecular docking analyses were performed using the Molecular Operating Environment (MOE).

Ligand dataset preparation

A library consisting of various compounds was created for molecular studies including all alkaloids and all terpenoids. The ligands were draw by using ChemDraw software and saved in MOL file format. Furthermore, the three-dimensional (3D) structure of the ligands was refined through energy minimization using MMFF94x force field implemented in the MOE software.

Receptors preparation

The 3D structures of the receptors including α-amylase, α-glucosidase, angiotensin converting enzyme and kidney Sodium Glucose co-Transporter 2 (SGLT2) were retrieved from the RCSB Protein Data Bank using the PDB IDs: 4W93[20], 5NN5[21], 1O8A[23] and 2XQ2[22], respectively. Prior to molecular docking studies, the receptors underwent preparation using a previously described protocol[24]. In case of α-amylase, SGLT2 and α-glucosidase, the binding site for docking was determined by extracting the coordinates of the co-crystallized ligand. On the other hand, for angiotensin converting enzyme, the reported catalytic site was selected as the binding site for docking study[25]. The alkaloids and terpenoids were docked into the proposed binding site of the receptors using triangular matcher as a placement method in combination with an induced-fit docking protocol. For post docking analysis, Chimera software was utilized. The 2D interactions occurring among the specific amino acid residues inherent in the proteins under investigation, which are manifested in 3D interactions and the docked ligands were meticulously illustrated using the computational framework provided by Discovery Studio software.

ADME profile prediction

Gastrointestinal absorption and brain access are two pharmacokinetic behaviors crucial to estimate at various stages of the drug discovery processes[26]. The most scoring compounds Adsorption, Distribution, Metabolism and Excretion (ADME) profile were predicted using the SwissADME web server[27].

RESULTS AND DISCUSSION

Botanical aspects

M. inermis (Wild.) O. Kuntze is a medium-sized tree or bushy shrub with smooth or scaly gray bark (Figure 1 a,d)[28].

The species is distinguished by its elliptical, acuminate, wedge-shaped leaves, solitary and terminal cream flowers (Figure 1 b,c,e)[28,29]. This plant produces spherical and dark-brown fruits (Figure 1f)[29,30].

Figure 1. *M. inermis* different parts (a: young plant; b: leaf arrangement on twigs; c: whole leaf in acuminate form; d: stem bark; e: flowers; f: dry fruit)

M. inermis is common of savannah, forest, marsh banks, temporarily flooded sites and on heavy, clayey and poorly drained soils[31]. It grows in temporarily flooded lowlands, ponds and riverbanks in the Sahelo-Sudanian to Guinean zones as well as from Senegal, Mauritania to Cameroon, the Central African Republic, Chad, the Democratic Republic of Congo and Sudan (Figure 2)[30,32]. In Burkina Faso, the species is found in all regions and sometimes in pure stands[30]. Floristic diversity study has shown that the plant appears as a grouping with monospecific development[33]. It develops in groups associating a variety of biological types such as phanerophytes, lianas, therophytes and hemicryptophytes[34]. The plant is reputed to support carbon and nitrogen stor-

age[35-38]. *M. inermis* is one of the top 20 plant species used in Burkina Faso[39]. That plant is among the woody plants with high ethnobotanical use value and would require large-scale reforestation to improve its availability[40]. There are not currently IUCN (International Union for the Conservation of Nature) data on the species vulnerability[41].

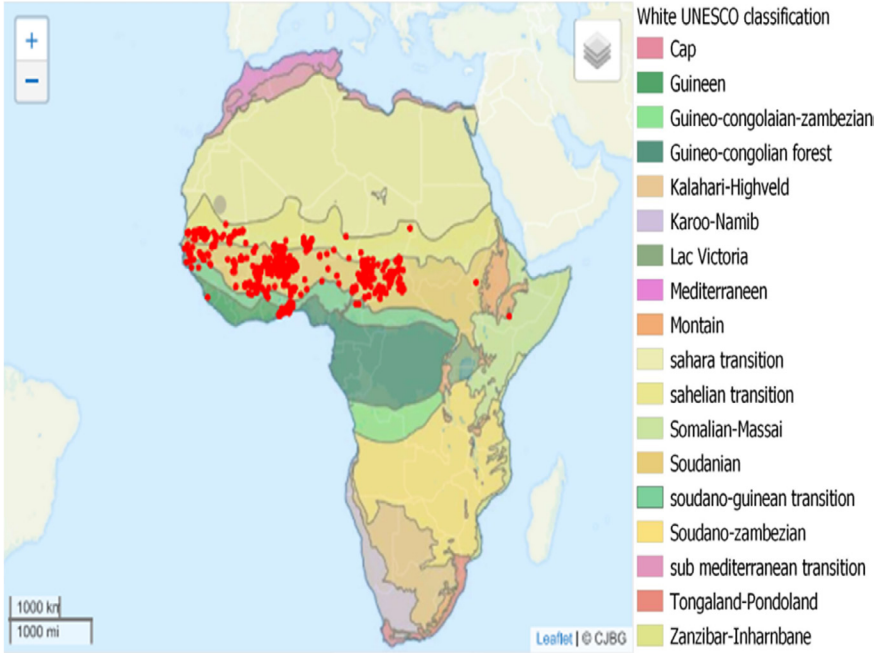

Figure 2. Phytogeography of *M. inermis:* The red dots show the distribution of *M. inermis* plants based on survey data[42].

Phytochemistry

Like other species of Rubiaceae family, *M. inermis* has biochemical potential. However, studies carried out on *M. inermis* have enabled potential compounds or groups of compounds to be identified and highlighted. Their presence is linked to their solvent affinity and the extraction method. Thus, the presence of sterols, triterpenes, polyphenols, flavonoids, catechic tannins, saponosides, quinones and alkaloids has been noted with aqueous leaf decoction[17,43,44]. Also, the presence of tannins, cardiac glycosides, alkaloids, reducing sugars, carbohydrate and flavonoids was reported in leaf methanolic extract[45]. Condensed and gallic tannins, saponin, alkaloids, flavonoids, anthraquinones, glycosides, terpenes and reducing compounds were found in the leaves methanolic and acetone decoction[46,47]. Root and stem bark chloroformic, ethanolic and aque-

ous extracts screening revealed the presence of tannins, reducing compounds, alkaloids, emedols, carotenoids, steroidal and triterpenic saponosides, flavonoids, anthracenosides, leuco-anthocyanins, anthocyanosides, coumarins, phlabotannins and steroids[48-50]. Anthraquinones, mucilage and gums, resin, terpenoids, lignins, steroids, carbohydrates, glycosides, saponins, tannins, alkaloids, flavonoids were screened in the leaves, roots and stem bark[7,51,52]. It has been reported that aqueous leaf decoction total phenolic and flavonoid content are 24.42 mg GAE (Gallic Acid Equivalent)/100 mg, and 0.95 mg QE (Quercetin Equivalent)/100 mg extract, respectively[53]. Total phenolic contents of extracts varying from acetone, ethyl acetate and water of roots, stem bark and leaves ranged from 47.05 to 112.31 mg GAE/g dry matter[54]. *M. inermis* stem bark quantitative phytochemical analysis showed that flavonoids (120 mg/g) was the highest phytochemical detected following alkaloids (62.00 ± 0.33 mg/g), tannins (48.00 ± 0.33 mg/g) and phenols (55.00 ± 0.88 mg/g) while the lowest was saponins (5.0 mg/g)[7]. These results also show solvents leading in bark compounds extraction. In depth, some studies have proceeded to these compounds' isolation and structural elucidation.

Saponosides generally take two forms, depending on whether the aglycone fragment is a triterpene or a steroid[55]. Condensation of an aglycone triterpene with one or more monosaccharides leads to saponosides. Bonding of the saccharide chain to the C-3 of the aglycone leads to monodesmoside-type saponosides; a second bond at position C-28 or C-27 leads to bidesmoside-type saponosides. A rare third bond at any position of the aglycone leads to tridesmoside saponosides. Monodesmosidic and bidesmosidic saponosides with ursane and oleanane-type aglycones are found in *M. inermis* (Figure 3)[18,56-59].

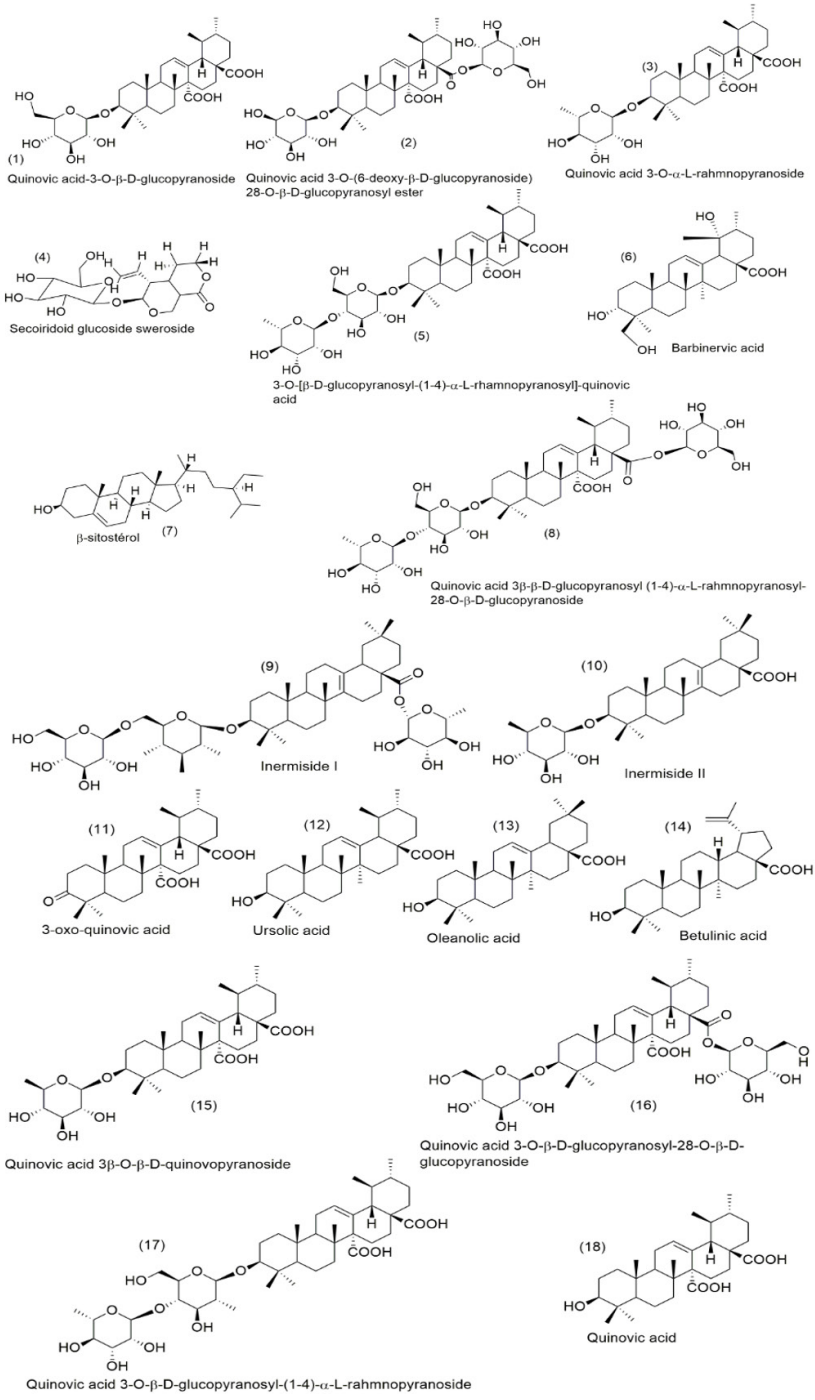

Figure 3. *M. inermis* terpenoids

On the other hand, oxindole alkaloids seem to derive from yohimbine of which secoiridoids are precursors[55]. Tetracyclic oxindoles have four asymmetric centers (C-3, C-7, C-15, and C-20) and pentacyclic oxindoles have five asymmetric centers (C-3, C-7, C-15, C-19, and C-20). Tetracyclic and pentacyclic oxindole and indole alkaloids are found in *M. inermis* (Figure 4)[59-61]. Leaves and barks phytochemistry exhibited these kinds of alkaloids as well as one of their precursors[18]. In addition to alkaloids and saponosides, *M. inermis* leaves, stem bark and roots contain chlorogenic acid and quercetin mono and diglycosides[5]. These data show *M. inermis* various parts may be rich in potentially bioactive compounds.

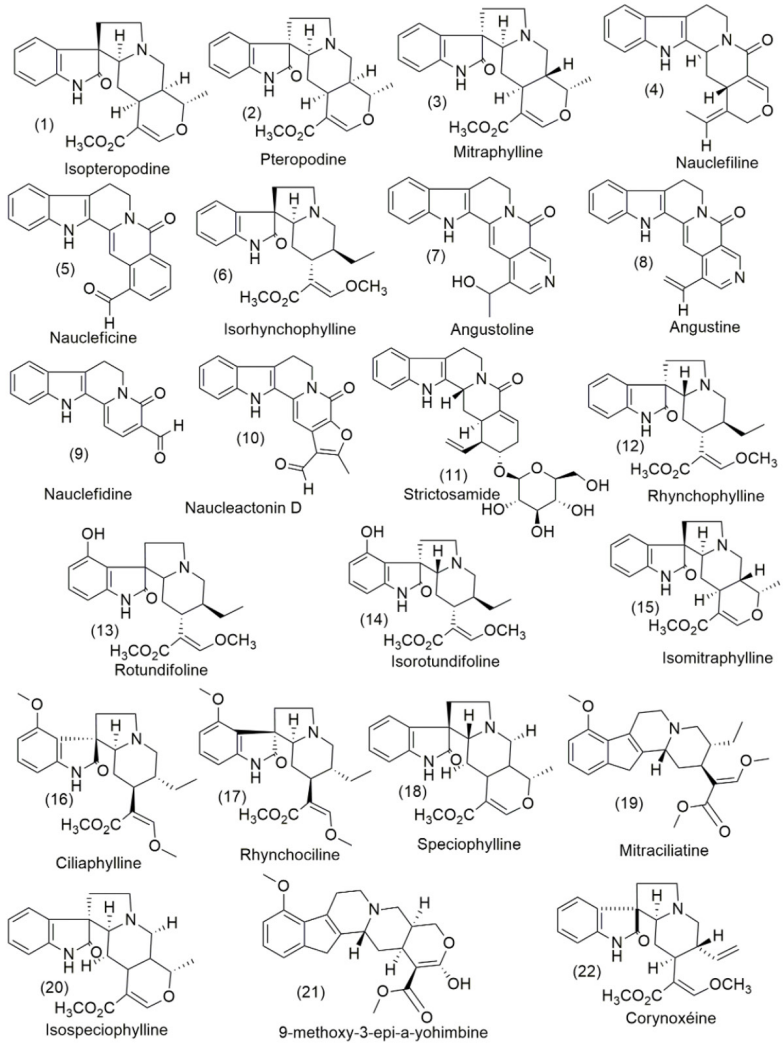

Figure 4. *M. inermis* alkaloids

Ethnobotanical study related to metabolic disorders

Various surveys have been carried out on *M. inermis* traditional knowledge. Leaves and roots are used in liver disease management[62]. Bark decoction and leaves in beverages are used to treat obesity[63]. Leaves and stem barks in decoction or infusion are used in traditional medicine for the treatment of diabetes[64]. In view of this ethnobotanical wealth, a number of studies have reported evidence of its parts use in traditional medicine, both *in vivo* and *in vitro*. Biological properties including, antihypertensive and antidiabetic properties have been reported[44,50,65-67].

M. inermis ingredients antihypertensive capacity

The aqueous extract of *M. inermis* stem bark has hypotensive, cardiotropic and vasodilatory properties. Evidence was provided that aqueous extract from *M. inermis* possess cardiac inotropic effect and induces an increase in coronary flow without inducing tachycardia in isolated heart[68].

M. inermis ingredients antidiabetic capacity

M. inermis parts extracts are reported for their potential to prevent or even treat chronic hyperglycemia and failures leading to diabetes. Thus, Alamin et al.[69] reported *M. inermis* fruits aqueous extract extensive antidiabetic potential. From this study, they showed chronic antihyperglycemic activity at a dose of 400 mg/kg b.w. in streptozotocin-induced diabetic rats orally (p.o.). An improvement in lipid metabolism was also observed suggesting regulation of the NAD+/NADH ratio. However, the aqueous extract of these fruits had no effect on the oral glucose tolerance test. Adoum et al.[58] showed that the anti-diabetic effect of ethanolic stem bark extract *in vivo* at 350 mg/kg b.w. was comparable to that of glibenclamide in diabetic rats induced with intraperitoneal (i.p.) alloxane. These results suggest an increase in insulin production by β–cells, or reduction of glucose absorption in the gastrointestinal tract. In addition, the PBS-buffered extract and aqueous maceration of the leaves resulted in up to 75% inhibition of α-amylase *in vitro*[53,70]. Fruits, stem bark and leaves could be used in the management of diabetes. A recent study reported that plant's properties on diabetes complications. Fractions varying from ethyl acetate, acetone, water and butanol significantly inhibited the formation of glycation end products (AGEs) with IC_{50}s low at the 250 µg/mL. Although, the isolated and individually tested compounds did not show inhibitory activity in AGEs formation[18].

In silico results

Docking analysis of α-amylase inhibitors

Total compound including alkaloids and terpenoids were docked into the active site of α-amylase receptor. Interestingly, the terpenoids exhibited better docking score compared to alkaloids when interacting with the α-amylase receptor. Table 1 displays the five terpenoids and alkaloids that demonstrated best docking scores. Terpenoids 8 and 9 and alkaloids 11 and 19 exhibited docking score -9.66, -9.45, -7.99, and -7.44 kcal/mol, respectively. Notably, terpenoids exhibited superior docking scores in comparison to acarbose, a standard compound with a docking score of -8.49 kcal/mol as shown in Table 1.

Table 1. Docking score of the alkaloids and terpenoids compounds targeting α-amylase receptor

Terpenoids	Docking Score (kcal/mol)	Alkaloids	Docking Score (kcal/mol)
Compound: 1	-8.14214	Compound: 1	-6.44666
Compound: 2	-9.27166	Compound: 2	-6.76994
Compound: 3	-8.14667	Compound: 3	-6.79497
Compound: 4	-6.86704	Compound: 4	-6.62143
Compound: 5	-8.55486	Compound: 5	-6.29868
Compound: 6	-7.81493	Compound: 6	-7.0353
Compound: 7	-7.95475	Compound: 7	-6.21035
Compound: 8	-9.45146	Compound: 8	-6.32868
Compound: 9	-9.66477	Compound: 9	-5.59693
Compound: 10	-7.29294	Compound: 10	-6.30043
Compound: 11	-7.00118	Compound: 11	-7.99939
Compound: 12	-6.92443	Compound: 12	-7.29308
Compound: 13	-6.81734	Compound: 13	-7.2743
Compound: 14	-7.05732	Compound: 14	-7.22914
Compound: 15	-7.73642	Compound: 15	-6.85529
Compound: 16	-8.88075	Compound: 16	-7.09234
Compound: 17	-8.82677	Compound: 17	-7.14176
Compound: 18	-7.53447	Compound: 18	-6.77523
		Compound: 19	-7.44077
		Compound: 20	-6.60598
		Compound: 21	-6.64555
		Compound: 22	-6.94727
Acarbose	-6.89	Acarbose	-6.89

Further analyses were conducted on the protein-ligand interaction. Figure 5 depicts the interaction pattern analysis of two terpenoids that exhibited good docking score with α-amylase receptor. In case of compound 8, it established hydrogen bonds with Asp-197, Glu-233, Glu-240, Asp-300 and His-305 of the protein. The distance for these hydrogen bonds is 2.29, 3.04, 2.55, 1.98, and 2.12 Å, respectively. For compound 9, it formed hydrogen bonds with Tyr-62, Asp-197, Glu-233, and Glu0-240 residues of the protein. The distance for these hydrogen bonds is 2.20, 2.22, 1.89, and 1.88 Å, respectively. Additionally, hydrophobic interactions are observed between compound and Tyr 151, Leu 162 and Ile 235 residues of the protein. According to the findings, these terpenoids appear to have a greater affinity with target receptor in the docking simulation making them potentially effective candidates for more research in drug development investigations. The molecular interaction analysis of alkaloids 11 and 19 with α-amylase receptor revealed that they fit well within the protein binding site as shown in Figure 5. Compound 11 established hydrogen bonds with Gln-63, Tyr-62, Glu-233, and His-305 amino acids of the corresponding protein with a bond distance of 2.96, 3.20, 2.21, and 3.19 Å, respectively. Additionally, this compound formed hydrophobic interaction with Ile-234. Compound 19 formed two hydrogen bonds with Asp-300, and Ala-307 at a distance of 2.61 and 3.21 Å, respectively. Furthermore, compound 19 engaged in hydrophobic contact with Trp-58, Trp-59, Tyr-62, Leu-162, and Ile-235 amino acid of the protein. 2D interaction shows that these compounds exhibited both hydrogen bonding and hydrophobic interaction with α-amylase receptor (Figure 5). These findings support the plausible inhibitory activity of the high scoring compounds.

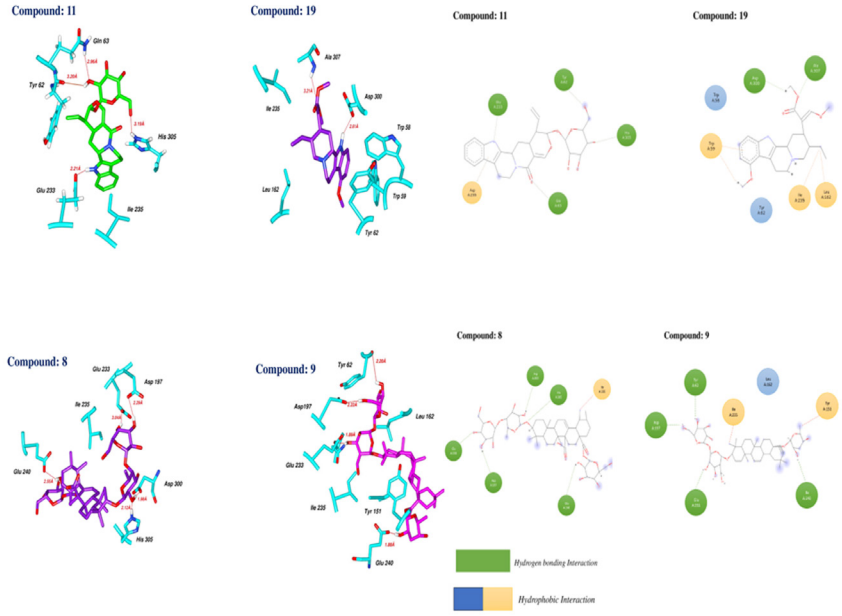

Figure 5. Molecular docking interactions between terpenoids 8 and 9 and alkaloids 11 and 19 with α-amylase (PDB: 4W93). 3D interaction in the right and 2D interactions in the left.

Docking analysis of α-glucosidase

The docking result of the compounds with α-glucosidase disclosed consistent pattern similar to that observed with α-amylase, terpenoids exhibited better docking score than alkaloids. Table 2 displays five compounds, both from terpenoids and alkaloids that demonstrated best docking scores. Additionally, both terpenoids and alkaloids shown higher docking scores than the standard compound acarbose when interacting with α-glucosidase receptor.

Table 2. Docking score of the alkaloids and terpenoids compounds targeting α-glucosidase receptor

Terpenoids	Docking Score (kcal/mol)	Alkaloids	Docking Score (kcal/mol)
Compound: 1	-8.07279	Compound: 1	-6.17872
Compound: 2	-9.19672	Compound: 2	-6.51711
Compound: 3	-8.27856	Compound: 3	-6.19423
Compound: 4	-6.85605	Compound: 4	-5.93376
Compound: 5	-8.93499	Compound: 5	-5.65457
Compound: 6	-5.89858	Compound: 6	-7.15106
Compound: 7	-6.87061	Compound: 7	-5.63317
Compound: 8	-7.35026	Compound: 8	-5.20298
Compound: 9	-8.24143	Compound: 9	-4.97044
Compound: 10	-8.22088	Compound: 10	-5.32063
Compound: 11	-5.75146	Compound: 11	-6.95613
Compound: 12	-5.7025	Compound: 12	-6.30647
Compound: 13	-5.65344	Compound: 13	-5.98386
Compound: 14	-5.13998	Compound: 14	-6.47681
Compound: 15	-7.30929	Compound: 15	-6.62774
Compound: 16	-8.45873	Compound: 16	-6.7234
Compound: 17	-8.78129	Compound: 17	-6.18068
Compound: 18	-5.52423	Compound: 18	-6.78912
		Compound: 19	-6.68291
		Compound: 20	-5.93218
		Compound: 21	-6.5742
		Compound: 22	-6.49402
Acarbose	-6.89	Acarbose	-6.89

Figure 6 displays interaction analysis. Herein, compound 2 which pertains to the terpenoids family, displayed significant interactions, established four hydrogen bonds with Arg-281, Asp-404, Asp-616, and His-674 amino acid of the protein having distances of 2.94, 2.63, 2.63, and 2.72 Å. Compound 5 also formed four hydrogen bonds with distinct residues namely Asp 282, Asp 518, Arg 600, and His 674. The distance for these hydrogen bonds is 2.45, 2.00, 1.96, and 2.12 Å. Both compounds displayed important hydrophobic interac-

tions. Furthermore, alkaloid 6 formed hydrogen bond with Asp-616 amino acid of the protein, with a distance of 2.16 Å. Additionally, Trp-386, Phe-649, and Trp-381 amino acid of the protein formed hydrophobic interaction with compound 6. Alkaloid 11 engaged hydrophobic contact with Asp 282, Ala 555, and leu 650. It established three hydrogen bonds with protein Asp-404, Asp-518 and Arg-600 residues, each having a distance 2.07, 1.95, and 2.16 Å, respectively. 2D interaction shows that these compounds exhibited both hydrogen bonding and hydrophobic interaction with α-glucosidase receptor Figure 6. These findings support the plausible inhibitory activity of the high scoring compounds.

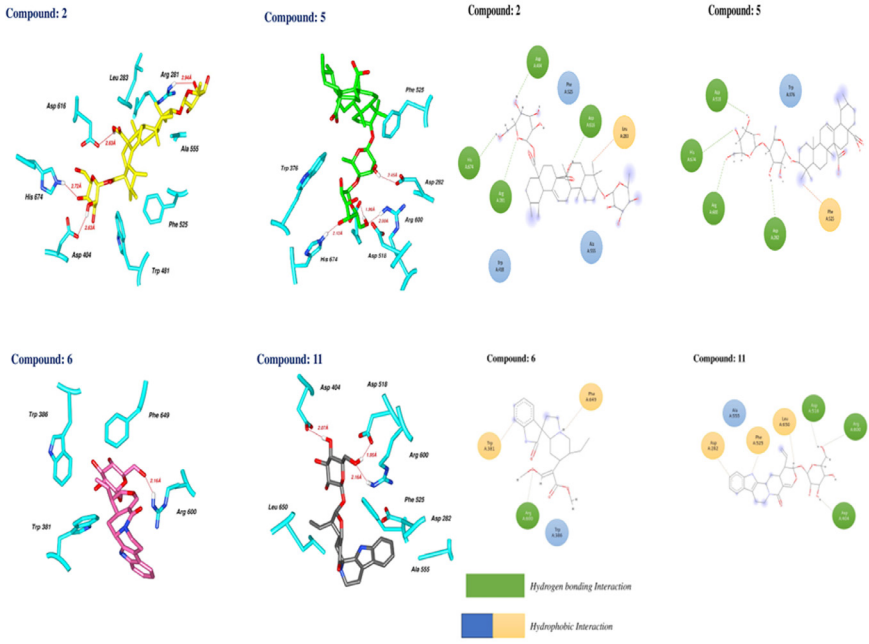

Figure 6. Molecular docking interactions between terpenoids 2 and 5 and alkaloids 6 and 11 with α-glucosidase (PDB: 5NN5). 3D interaction in the right and 2D interactions in the left.

The biochemical basis of most anti-diabetic drugs involves inhibiting the catalytic activities of carbohydrate metabolizing enzymes such as human pancreatic α-amylase and α-glucosidase, which reduces blood sugar levels by suppressing carbohydrate digestion and glucose uptake, making them the primary targets in controlling blood glucose in diabetes mellitus patients[71]. Thus, terpenoids 2, 5, 8, 9, 16, 17, and alkaloids 1, 6, 11, 13, 14, 16, 17, 19 might be potent antidiabetic drugs.

Docking analysis of Angiotensin Converting Enzyme (ACE)

Both alkaloids and terpenoids resided well in the binding site of ACE receptor, virtually show similar docking score as shown in Table 3. In general, terpenoids and alkaloids had higher docking scores when interacting with the ACE receptor than captopril, which is recognized inhibitor of this receptor.

Table 3. Docking score of the alkaloids and terpenoids compounds targeting ACE receptor

Terpenoids	Docking Score (kcal/mol)	Alkaloids	Docking Score (kcal/mol)
Compound: 1	-4.20691	Compound: 1	-6.52445
Compound: 2	-5.3765	Compound: 2	-5.38772
Compound: 3	-4.19894	Compound: 3	-5.98851
Compound: 4	-8.53989	Compound: 4	-6.90636
Compound: 5	-5.55693	Compound: 5	-7.18063
Compound: 6	-3.88615	Compound: 6	-6.27578
Compound: 7	-6.54263	Compound: 7	-7.35921
Compound: 8	-8.765	Compound: 8	-6.86186
Compound: 9	-5.55732	Compound: 9	-6.23907
Compound: 10	-4.87211	Compound: 10	-7.52613
Compound: 11	-4.60608	Compound: 11	-7.48866
Compound: 12	-4.72709	Compound: 12	-5.82266
Compound: 13	-4.32381	Compound: 13	-7.16123
Compound: 14	-5.36818	Compound: 14	-6.22365
Compound: 15	-4.45572	Compound: 15	-6.31605
Compound: 16	-4.71778	Compound: 16	-6.64717
Compound: 17	-6.45235	Compound: 17	-6.71206
Compound: 18	-3.15279	Compound: 18	-5.97653
		Compound: 19	-8.30466
		Compound: 20	-6.14573
		Compound: 21	-8.13562
		Compound: 22	-6.47229
Captopril	-5.31	Captopril	-5.31

The interaction pattern of terpenoids 4 and 7 and alkaloids 19 and 10 have been analyzed and presented in Figure 7. Compound 4 established three hydrogen bonds with the protein's Ala-354, Gln-369 and Asp-377 residues, with bond distances measuring 2.60, 3.08, 2.00 Å, respectively. On the other hand,

compound 7 exhibited only hydrophobic interaction with Pro-163, Ala-354, Glu-376, Val-380, Phe-457, and Tyr-523 amino acid receptor. Compound 19 and 10 demonstrated favorable interaction pattern with ACE receptor. Herein, Compound 19 exhibited hydrogen bonds with Trp-279, Gln-281 and Ala-354 amino acid of the protein with a bond distance of 2.65, 2.79, and 2.82 Å, respectively. Further, hydrophobic interaction also observed between receptor and compound 19. Also compound 10 manifested two hydrogen bonds with Ala-354 and His-513 with bond distance 2.11, and 3.00 Å, respectively. Additionally compound 10 also engaged in hydrophobic interactions with Glu-162, Trp-279, Gln-369, Val-380 and Phe-457 amino acids of the protein. 2D interaction shows that these compounds exhibited both hydrogen bonding and hydrophobic interaction with ACE receptor (Figure 7). These findings support the plausible inhibitory activity of the high scoring compounds.

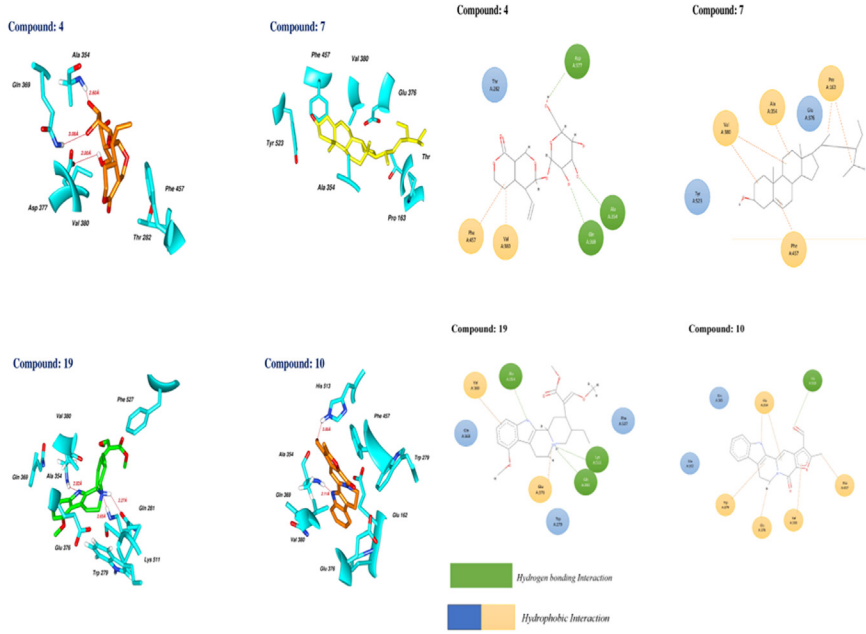

Figure 7. Molecular docking interactions between terpenoids 4 and 7 and alkaloids 19 and 10 with angiotensin converting enzyme (PDB: 108A). 3D interaction in the right and 2D interactions in the left.

ACE is essential for blood pressure regulation and electrolyte homeostasis through the renin–angiotensin–aldosterone system. So, ACE inhibitors are a first line of therapy for hypertension, heart failure, myocardial infarction and diabetic nephropathy[23]. However, terpenoids 4,5,7,8,17 and alkaloids 5,7,10,11, 19 might be potent antihypertensive drug candidates.

Docking analysis of Sodium Glucose co-transporter 2 (SGLT2)

The docking results of terpenoids and alkaloids with SGLT2 receptor shown a lower affinity than the other three suggested receptors namely α-glucosidase, α-amylase and ACE receptors. Table 4 presents docking result of terpenoids and alkaloids with SGLT2 receptor. Interestingly, the terpenoids exhibited better docking score compared to alkaloids when interacting with the receptor.

Table 4. Docking score of the alkaloids and terpenoids compounds targeting SGLT2

Terpenoids	Docking Score (kcal/mol)	Alkaloids	Docking Score (kcal/mol)
Compound: 1	-5.55716	Compound: 1	-4.95916
Compound: 2	-6.5534	Compound: 2	-4.73264
Compound: 3	-5.69784	Compound: 3	-4.91457
Compound: 4	-5.0918	Compound: 4	-4.84715
Compound: 5	-6.4528	Compound: 5	-4.65885
Compound: 6	-5.19954	Compound: 6	-4.84331
Compound: 7	-5.11214	Compound: 7	-4.90466
Compound: 8	-6.40594	Compound: 8	-4.58541
Compound: 9	-6.77291	Compound: 9	-4.49578
Compound: 10	-5.73278	Compound: 10	-4.64818
Compound: 11	-4.92561	Compound: 11	-5.76122
Compound: 12	-4.72267	Compound: 12	-4.81659
Compound: 13	-4.69988	Compound: 13	-5.17577
Compound: 14	-4.77389	Compound: 14	-4.90317
Compound: 15	-5.71305	Compound: 15	-4.91769
Compound: 16	-5.94821	Compound: 16	-4.92341
Compound: 17	-6.37138	Compound: 17	-5.18537
Compound: 18	-4.75509	Compound: 18	-4.75765
		Compound: 19	-4.94668
		Compound: 20	-4.84495
		Compound: 21	-5.48553
		Compound: 22	-4.75224
Empagliflozin	-4.87	Empagliflozin	-4.87

The interaction pattern of terpenoids 2 and 9 with SGLT2 receptor are shown in Figure 8. Compound 2 formed three hydrogen bonds with Tyr 570, Ile 572, and Lys 573 residues with bond distance of 2.45, 2.27, and 2.23 Å. Conversely, compound 9 only engaged in hydrophobic interaction with Tyr 570 and Ile 570 residues of the receptor. The Compound 11 demonstrated formation of one hydrogen bond with Lys 576 residue at a 2.64 Å. In contrast compound 21 form two hydrogen bonds with Ser 569 residue of the receptor, at 2.48 and 2.69 Å. It is noteworthy that both compounds also shown hydrophobic interaction with the SGLT2 receptor as presented in Figure 8. In general, terpenoids and alkaloids had higher docking scores when interacting with SGLT2 receptor than empagliflozin which is recognized inhibitor of this receptor. 2D interaction shows that these compounds exhibited both hydrogen bonding and hydrophobic interaction with SGLT2 receptor (Figure 8). These findings support the plausible inhibitory activity of the high scoring compounds.

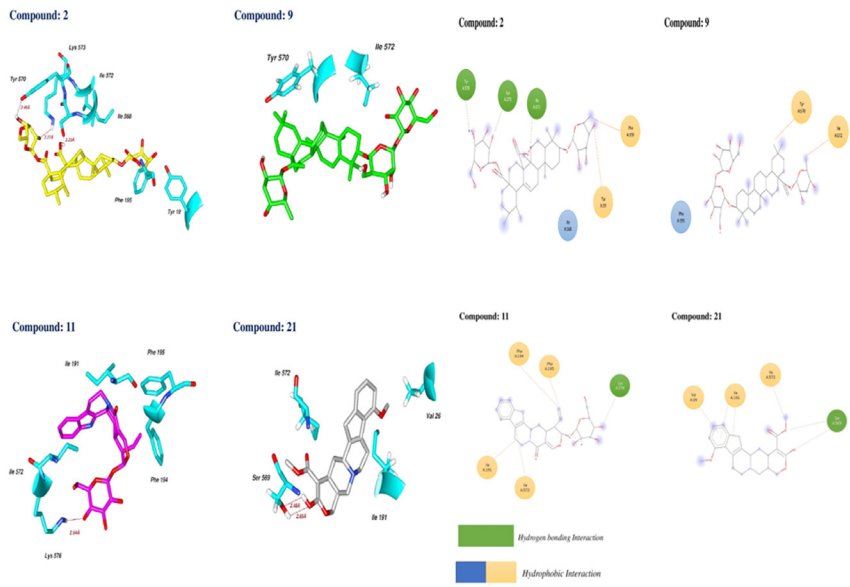

Figure 8. Molecular docking interactions between terpenoids 2 and 9, alkaloids 11 and 21 with sodium-glucose co-transporter 2 (PDB: 2XQ2). 3D interaction in the right and 2D interactions in the left.

However, sodium-glucose co-transporters are molecular targets for drugs to treat diabetes and obesity[22]. Thus, terpenoids 2,9 and alkaloids 11,21 might be potent antidiabetic drugs. However, all compounds appeared to be non-selective inhibitor of α-amylase, α-glucosidase, ACE, and SGLT2. It has been

reported that in most cases, diabetes is associated with high blood pressure[72]. Thus, these non-selective compounds might be suitable drug candidate for both diabetes and these complications management.

Pharmacokinetic of the most scoring compounds

Physicochemical data shown seven scoring compounds with highest probability of being absorbed by the gastrointestinal tract and to permeate to the brain, six scoring compounds with highest probability to permeate to the brain and seven scoring compounds non-permeant as shown BOILED-Egg prediction in Figure 9 and Table 5.

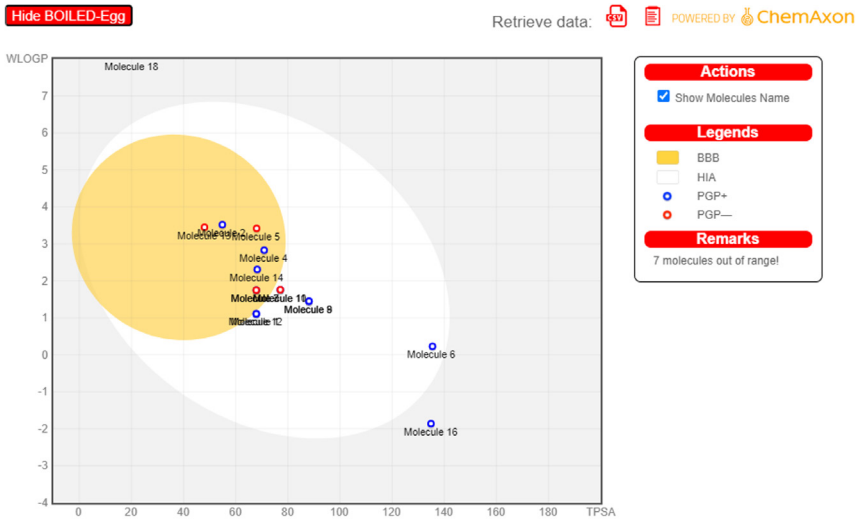

Figure 9. BOILED-Egg (Brain Or IntestinaL EstimateD permeation predictive model) prediction

Table 5. High scoring compounds ADME profiles

Compound	TPSA	Log P	Solubility	GI Absorption	BBB Permeability	CYP2D6 Inhibition
Alkaloid: 1	67.87	1.85	Soluble	High	No	Yes
Alkaloid: 5	54.86	3.09	Moderately	High	Yes	No
Alkaloid: 6	67.87	2.43	Soluble	High	Yes	Yes
Alkaloid: 7	70.91	2.52	Soluble	High	Yes	Yes
Alkaloid: 10	68.00	2.85	Soluble	High	Yes	No
Alkaloid: 11	135.48	0.90	Soluble	High	No	No
Alkaloid: 12	67.87	2.46	Soluble	High	Yes	Yes
Alkaloid: 13	88.10	2.12	Soluble	High	No	Yes
Alkaloid: 14	88.10	2.12	Soluble	High	No	Yes
Alkaloid: 16	77.10	2.41	Soluble	High	No	Yes
Alkaloid: 17	77.10	2.34	Soluble	High	No	Yes
Alkaloid: 18	67.87	1.83	Soluble	High	No	Yes
Alkaloid: 19	48.00	3.50	Moderately	High	Yes	Yes
Alkaloid: 21	68.23	2.47	Soluble	High	Yes	Yes
Terpenoid: 2	253.13	1.38	Moderately	Low	No	No
Terpenoid: 4	134.91	-0.78	Very	Low	No	No
Terpenoid: 5	232.90	2.15	Moderately	Low	No	No
Terpenoid: 7	20.23	7.24	Poorly	Low	No	No
Terpenoid: 8	312.05	0.69	Moderately	Low	No	No
Terpenoid: 9	257.68	1.74	Poorly	Low	No	No
Terpenoid: 16	236.06	2.38	Poorly	Low	No	No
Terpenoid: 17	212.67	3.11	Poorly	Low	No	No

TPSA: Total Polar Surface Area; Log P: Consensus Log P; GI: Gastrointestinal; BBB: Blood Brain Barrier; CYP2D6: Cytochrome P2D6.

Gastrointestinal absorption and brain access are two pharmacokinetic behaviors crucial to estimate at various stages of the drug discovery processes[26]. According to pharmacokinetic study, terpenoids are lowly absorbed by the gut. Then, they might be the good post-prandial drug for digestive enzymes inhibition as well as α-amylase and α-glucosidase. These compounds are probably metabolized and eliminated according to the failing of CYP2D6 inhibition. However, alkaloids are on the high gastrointestinal absorption, so must not be the suitable drug for gut and salivary enzyme inhibition. Alkaloids 5, 10, and

11 might be probably eliminated by cytochrome P450. Therefore, inhibition of cytochrome P450 is certainly one major cause of pharmacokinetics-related drug-drug interactions leading to toxic or other unwanted adverse effects due to the lower clearance and accumulation of the drug or its metabolites[27].

M. inermis ingredients have antihypertensive and hypoglycemic properties supported by its leading chemical composition. The virtual study reveals terpenoids and alkaloids isolated from *M. inermis* are potential various drugs. Our study provides an *in silico* interpretation of the antihypertensive and antidiabetic potential of *M. inermis* metabolites as well as providing sufficient evidence for future research with suitable targets on these agents and linking their pharmacological actions to the host. Thus, assuming that plant is a leading source of promising bioactive compounds. Herein, these various studies show the importance of the species in promoting traditional and complementary medicine. The species is relatively abundant in Burkina Faso and is growing rapidly. However, study reported the vulnerability of this species in its biotope like others due to overexploitation in traditional medicine. Thus, this species deserves to be safeguarded for future generations. Further study may allow identification or any pharmacophores adding for new class drugs with optimizing activities discovery.

STATEMENT OF ETHICS

Not applicable.

CONFLICT OF INTEREST STATEMENT

The authors declared no conflict of interest.

AUTHOR CONTRIBUTIONS

Concept – R.J.O, L.O.; Design – R.J.O., N.A.; Supervision – L.O., Z.U., G.A.O.; Data Collection and/or Processing – R.J.O., N.A., L.O.; Analysis and/or Interpretation – R.J.O., N.A.; Literature Search – R.J.O, L.O.; Writing – R.J.O., N.A.; Critical Reviews – L.O., Z.U., G.A.O.

FUNDING SOURCES

This research received no external funding.

ACKNOWLEDGMENTS

Not applicable.

REFERENCES

1. Olivier M, Zerbo P, Boussim JI, Guinko S. Les plantes des galeries forestières à usage traditionnel par les tradipraticiens de santé et les chasseurs Dozo Sénoufo du Burkina Faso. Int J Biol Chem Sci, 2013;6(5):2170-2191. Doi: 10.4314/ijbcs.v6i5.24

2. Stark TD, Mtui DJ, Balemba OB. Ethnopharmacological survey of plants used in the traditional treatment of gastrointestinal pain, inflammation and diarrhea in Africa: future perspectives for integration into modern medicine. Animals, 2013;3(1). Doi: 10.3390/ani3010158

3. Nergard CS, Ho TPT, Diallo D, Ballo N, Paulsen BS, Nordeng H. Attitudes and use of medicinal plants during pregnancy among women at health care centers in three regions of Mali, West-Africa. J Ethnobiol Ethnomed, 2015;11(1):1-11. Doi: 10.1186/s13002-015-0057-8

4. Ouedraogo Y, Guissou IP, Nacoulma OG. Biological and toxicological study of aqueous root extract from *Mitragyna inermis* (Willd oktze) Rubiaceae. Int J Pharmacol, 2007;3(1):80-85.

5. Asase GKA, Kokubun T, Grayer RJ, Kite G, Simmonds MSJ, Oteng-Yeboah AA, et al. Chemical constituents and antimicrobial activity of medicinal plants from Ghana: *Cassia sieberiana*, *Haematostaphis barteri*, *Mitragyna inermis* and *Pseudocedrela kotschyi*. Phyther Res, 2008;22(4):544-549. Doi: 10.1002/ptr

6. Umeh EU, Oluma HOA, Igoli JO. Antibacterial screening of four local plants using an indicator-based microdilution technique. Afr J Trad Comp Alt Med, 2005;2(3):238-243. Doi: 10.4314/ajtcam.v2i3.31121

7. Namadina MM, Kamal RM, Sunusi U, Abubakar DS, Sani H, Nuhu Y, et al. Pharmacognostic and antimicrobial study of *Mitragyna inermis* stem bark. Biol Environ Sci J Trop, 2019;16(1):104-115.

8. Zongo C, Akomo EFO, Savadogo A, Obame LC, Koudou J, Traore AS. *In vitro* antibacterial properties of total alkaloids extract from *Mitragyna inermis* (Willd.) O. Kuntze, a West African traditional medicinal plant. Asian J Plant Sci, 2009;8(2):172-177. Doi: 10.3923/ajps.2009.172.177

9. Abubakar IB, Kankara SS, Malami I, Danjuma JB, Muhammad YZ, Yahaya H, et al. Traditional medicinal plants used for treating emerging and re-emerging viral diseases in northern Nigeria. Eur J Integr Med, 2022;49(2022):1-28. Doi: 10.1016/j.eujim.2021.102094

10. Beuscher N, Bodinet C, Neumann-Haefelin D, Marston A, Hostettmann K. Antiviral activity of African medicinal plants. J Ethnopharmacol, 1994;42:101-109. Doi: 10.1016/0378-8741(94)90103-1

11. Garber A, Barnard L, Pickrell C. Review of whole plant extracts with activity against herpes simplex viruses *in vitro* and *in vivo*. J Evidence-Based Integr Med, 2021;26:1-57. Doi: 10.1177/2515690x20978394

12. Fiot J, Sanon S, Azas N, Mahioua V, Jansen O, Angenot L, et al. Phytochemical and pharmacological study of roots and leaves of *Guiera senegalensis* J.F. Gmel (Combretaceae). J Ethnopharmacol, 2006;106(2):173-178. Doi: 10.1016/j.jep.2005.12.030

13. Pierrot D, Sinou V, Sok-Siya Bun SS, Parzy D, Taudon N, Rodriguez J, et al. Design and synthesis of simplified speciophylline analogues and β-carbolines as active molecules against *Plasmodium falciparum*. Drug Dev Res, 2019;80(1):133-137. Doi: 10.1002/ddr.21494

14. Ouédraogo RJ, Muhammad J, Ouattara L, Muhammad NH, Khan F, Simjee SU, et al. Antiseizure activity of *Mitragyna inermis* in the Pentylenetetrazol (PTZ)-Induced Seizure Model in mice: involvement of flavonoids and alkaloids. Turkish J Pharm Sci, 2024;1(2):104-112. Doi: 10.4274/tjps.galenos.2023.14704

15. Wagner K, Brath H. A global view on the development of non communicable diseases. Prev Med, 2012;54:38-41. Doi: 10.1016/j.ypmed.2011.11.012

16. Boutayeb A. The double burden of communicable and non-communicable diseases in developing countries. Trans R Soc Trop Med Hyg, 2006;100:191-199. Doi: 10.1016/j.trstmh.2005.07.021

17. Konkon NG, Adjoungoua AL, Manda P, Simaga D, N'Guessan KE, Kone BD. Toxicological and phytochemical screening study of *Mitragyna inermis* (willd) O ktze (Rubiaceae), anti diabetic plant. J Med Plants Res, 2008;2(10):279-284.

18. Ouédraogo RJ, Aleem U, Ouattara L, Muhammad N, Ouédraogo GA, Jahan H, et al. Inhibition of advanced glycation end-products by *Tamarindus indica* and *Mitragyna inermis* extracts and effects on human hepatocyte and fibroblast viability. Molecules, 2023;28(393):1-14. Doi: 10.3390/molecules28010393

19. Traore F, Gasquet M, Laget M, Guiraud H, Di-Giorgio C, Azas N, et al. Toxicity and genotoxicity of antimalarial alkaloid rich extracts derived from *Mitragyna inermis* O. Kuntze and *Nauclea latifolia*. Phyther Res, 2000;14(8):608-611. Doi: 10.1002/1099-1573(200012)14:8<608::AID-PTR667>3.0.CO;2-D

20. Williams LK, Xiaohua Zhang X, Caner S, Tysoe C, Nguyen NT, Wicki J, et al. The amylase inhibitor montbretin A reveals a new glycosidase inhibition motif. Nat Chem Biol, 2015;11(9):691-696. Doi: 10.1038/nchembio.1865

21. Roig-Zamboni V, Cobucci-Ponzano B, Iacono R, Ferrara MC, Germany S, Bourne Y, et al. Structure of human lysosomal acid α-glucosidase–a guide for the treatment of Pompe disease. Nat Commun, 2017;8(1):1-10. Doi: 10.1038/s41467-017-01263-3

22. Watanabe A, Choe S, Chaptal V, Rosenberg JM, Wright EM, Grabe M, et al. The mechanism of sodium and substrate release from the binding pocket of vSGLT. Nature, 2010;468(7326):988-991. Doi: 10.1038/nature09580

23. Inducible K, Natesh R, Schwager SLU, Sturrock ED. Crystal structure of the human enzyme – lisinopril complex. Nature, 2003;1429(1995):1427-1429.

24. Islam F, Khan FA, Khan NM, Ahmad S, Alsaiari AA, Almehmadi M, et al. PEGylated graphene oxide as a nanodrug delivery vehicle for podophyllotoxin (GO / PEG / PTOX) and *in vitro* α-amylase/α-glucosidase inhibition activities. ACS Omega, 2023;8:20550-20560. Doi: 10.1021/acsomega.3c00888

25. Fang L, Geng M, Liu C, Wang J, Min W, Liu J. Structural and molecular basis of angiotensin-converting enzyme by computational modeling: insights into the mechanisms of different inhibitors. PLoS One, 2019;14(4):1–16. Doi: 10.1371/journal.pone.0215609

26. Daina A, Zoete V. A BOILED-Egg to predict gastrointestinal absorption and brain penetration of small molecules. Chem Med Chem, 2016;11:1117-1121. Doi: 10.1002/cmdc.201600182

27. Daina A, Michielin O, Zoete V. SwissADME: a free web tool to evaluate pharmacokinetics, drug-likeness and medicinal chemistry friendliness of small molecules. Sci Rep, 2016;7:1-13. Doi: 10.1038/srep42717

28. Pillay MS. Anatomy of the leaves and young stem of *Mitragyna inermis* (O. Kuntze). J Pharm Pharmacol, 1964;16(12):820-827. Doi: 10.1111/j.2042-7158.1964.tb07416.x

29. Shellard EJ, Wade A. The morphology and anatomy of the flowers of *Mitragyna inermis* (Willd.) O. Kuntze. J Pharm Pharmacol, 1969;21:102-112. Doi: 10.1111/j.2042-7158.1969.tb08358.x

30. Arbonnier M. Arbres, arbustes et lianes des zones sèches d'Afrique de l'Ouest. 3rd ed. Montpellier, France: Troisieme edition Cirad; 2002. p. 1-541.

31. Dénou A, Koudouvo K, Togola A, Haïdara M, Dembélé SM, Ballo FN, et al. Savoir traditionnel sur les plantes antipaludiques à propriétés analgésiques, utilisées dans le district de Bamako (Mali). J Appl Biosci, 2017;112(1):10985-10995. Doi: 10.4314/JAB.V112I1.3

32. MacLennan KJR, Kirkby WW. The eradication of *Glossina morsitans submorsitans* Newst. in part of a river flood plain in Northern Nigeria by chemical means. Bull Entomol Res, 1958;49(1):123-131. Doi: 10.1017/S0007485300053475

33. Seou E, Akame L, Boukpessi T. Diversité floristique et caractéristiques structurales des groupements végétaux du bassin de Zio (Sud-Togo). Physio-Géo, 2022;17(1):83-98. Doi: 10.4000/physio-geo.13984

34. Sambare O, Savadogo S, Ouédraogo I, Thiombiano A. Ecologie et diversité des forêts galeries et des savanes adjacentes du secteur sud-soudanien du Burkina Faso (Afrique de l'Ouest). J Anim Plant Sci, 2020;45(3):7992-8009. Doi: 10.35759/janmplsci.v45-3.4

35. Qasim M, Porembski S, Sattler D, Stein K, Thiombiano A, Lindner A. Vegetation structure and carbon stocks of two protected areas within the South-Sudanian Savannas of Burkina Faso. Environments, 2016;3(4):25. Doi: 10.3390/environments3040025

36. Chabi A, Lautenbach S, Orekan VOA, Kyei-Baffour N. Allometric models and aboveground biomass stocks of a West African Sudan Savannah watershed in Benin. Carbon Balance Manag, 2016;11(16):1-18. Doi: 10.1186/s13021-016-0058-5

37. Chabi A, Lautenbach S, Tondoh JE, Orekan VOA, Adu-Bredu S, Kyei-Baffour N, et al. The relevance of using in situ carbon and nitrogen data and satellite images to assess aboveground carbon and nitrogen stocks for supporting national REDD + programmes in Africa. Carbon Balance Manag, 2019;14(1):1-13. Doi: 10.1186/s13021-019-0127-7

38. Ganamé M, Bayen P, Ouédraogo I, Balima LH, Thiombiano A. Allometric models for improving aboveground biomass estimates in West African Savanna ecosystems. Trees For People, 2021;4:1-15. Doi: 10.1016/j.tfp.2021.100077

39. Zizka A, Thiombiano A, Dressler S, Nacoulma BMI, Ouédraogo A, Ouédraogo I, et al. Traditional plant use in Burkina Faso (West Africa): a national-scale analysis with focus on traditional medicine. J Ethnobiol Ethnomed, 2015;11(9):1-10. Doi: 10.1186/1746-4269-11-9

40. Hadonou-Yovo AG, Houessou LG, Lougbegnon TO, Adebi Y, Sinasson GKS, Semevo DF. Diversité et formes d'utilisation des espèces ligneuses de la Réserve de biosphère du Mono (Bénin). VertigO-la Rev électronique en Sci l'environnement, 2019;19(2):1-19. Doi: 10.4000/vertigo.26257

41. Agbani PO, Kafoutchoni KM, Salako KV, Kégbé AM, Karen H, Sinsin B. Traditional ecological knowledge-based assessment of threatened woody species and their potential substitutes in the Atakora mountain chain, a threatened hotspot of biodiversity in Northwestern Benin, West Africa. J Ethnobiol Ethnomed, 2018;14(21):1-19. Doi: 10.1186/s13002-018-0219-6

42. African plant database. Accessed May 20, 2023. Available from: https://africanplantdatabase.ch/en/nomen/89011

43. Konkon NG, Simaga D, Adjoungova AL, N'Guessan KE, Zırıhı GN, Kone BD. Etude Phytochimique De *Mitragyna inermis* (Willd) O. Ktze (Rubiaceae), Plante A Feuille Antidiabetique. Pharm Méd Trad Afr, 2006;14:73-80.

44. Pahaye DB, Bum EN, Taïwé GS, Ngoupaye GT, Sidiki N, Moto FCO, et al. Neuroprotective and antiamnesic effects of *Mitragyna inermis* Willd (Rubiaceae) on scopolamine-induced memory impairment in mice. Behav Neurol, 2017;1-11. Doi: 10.1155/2017/5952897

45. Wakirwa JH, Yawate UE, Zakama SG, Muazu J, Madu SJ. Phytochemical and antibacterial screening of the methanol leaf extract of *Mitragyna inermis* (Wild O. Ktze Rubiaceae). Int J Pharm Res Innov, 2013;6:1-6.

46. Alowanou GG, Azando EVB, Adenilé AD, Koudandé DO, Chrysostome CAM, Hounzangbé-Adoté SM. Evaluation of the *in vivo* anthelmintic properties of *Mitragyna inermis* (Willd.) as a livestock dewormer against parasitic hematophagous worm *Haemonchus contortus* infections in different breeds of lambs. Trop Anim Health Prod, 2019;52(1):309-319. Doi: 10.1007/s11250-019-02014-w

47. Onuh OA, Machunga-Mambula SS, Akin-Osanaiye BC. Phytochemical screening, chromatographic evaluation and antibacterial activity on stem bark extracts of *Mitragyna inermis*. Direct Res J Biol Biotechnol, 2019;5(2):17-23. Doi: 10.5281/zenodo.3246793

48. Ouedraogo Y, Nacoulma O, Guissou IP. Évaluation *in vivo* et *in vitro* de la toxicité des extraits aqueux d'écorces de tige et de racines de *Mitragyna inermis* (Willd). O. Ktz (Rubiaceae). Pharm Méd Trad Afr, 2001;1(10):13-29.

49. Ouedraogo Y. Activity study of aqueous extract of bark roots of *Mitragyna inermis* Willd Oktze-Rubiaceae on biological elements, support of immunity among the rabbit. [PhD Thesis]. Burkina Faso: University of Ouagadougou; 2003.

50. Timothy SY, Wazis CH, Helga BI, Maina A, Bomai HI. Anticonvulsant screening of the aqueous and ethanol extracts of *Mitragyna inermis* Bark. Int J Pharm Ther, 2015;5(5):358-363.

51. Sangare M, Ategbo JM, Attakpa ES, Klotoe JR, Guinnin FFG, Zibrila AI, et al. Phytochemical screening and toxicological study of the aqueous extract of stem bark of *Mitragyna inermis* (Wild) O. Kundze (Rubiaceae), a traditional medicine plant. Int J Adv Res, 2017;5(3):746-751. Doi: 10.21474/IJAR01/3567

52. Onuh OA, Odugbo M, Oladipo OO, Olobayotan IW. Phytochemical investigation of the crude and fractionated extracts of two Nigerian herbs, *Mitragyna inermis* (Wild) and *Lawsonia inermis* (Linn). 2021. Doi: 10.1101/2021.06.02.446752

53. Ouédraogo RJ, Somda MB, Ouattara L, Kagambega W, Ouoba P, Ouédraogo GA. Evaluation of the antioxidant and A-amylase inhibitory activities of *Mitragyna inermis* (Willd) O. Kuntze and *Tamarindus indica* Linn. J Exp Biol Agric Sci, 2020;8(5):676-682. Doi: 10.18006/2020.8(5).676.682

54. Ouédraogo RJ, Ouattara L, Kabre P, Sanou Y, Somda MB, Ouoba P, et al. Season and ecotype effects on soluble phenolic compounds content and antioxidant potential of *Tamarindus indica* and *Mitragyna inermis*. J Pharm Pharmacol, 2022;10(5):143-156. Doi: 10.17265/2328-2150/2022.05.001

55. Atta-ur-Rahman F. Studies in natural products chemistry. 25th ed. Karachi, Pakistan: Elsevier Book Aid International; 2015. p. 1-523.

56. Cheng ZH, Yu BY, Yang XW. 27-Nor-triterpenoid glycosides from *Mitragyna inermis*. Phytochemistry, 2002;61(4):379-382. Doi: 10.1016/s0031-9422(02)00244-3

57. Cheng ZH, Yu BY, Yang XW, Zhang J. Triterpenoid saponins from bark *Mitragyna inermis*. Zhongguo Zhongyao Zazhi, 2002;27(4):276-277.

58. Adoum OA, Nenge HP, Chedi B. The steroidal component and hypoglycaemic effect of stem bark extract of *Mitragyna inermis* (Wild) O. Kundze (Rubiaceae) in alloxan induced diabetic wistar rats. Int J Appl Biol Pharm Technol, 2012;3(2):169-174.

59. Donfack EV, Lenta BN, Kongue MDT, Fongang YF, Ngouela S, Tsamo E, et al. Naucleactonin D, an indole alkaloid and other chemical constituents from roots and fruits of *Mitragyna inermis*. Z Naturforsch, 2012;67(11):1159-1165.

60. Toure H, Balansard G, Pauli AM, Scotto AM. Pharmacological investigation of alkaloids from leaves of *Mitragyna inermis* (Rubiaceae). J Ethnopharmacol, 1996;54(1):59-62. Doi: 10.1016/0378-8741(96)01446-8

61. Martins D, Nunez CV. Secondary metabolites from Rubiaceae species. Molecules, 2015;20(7):13422-13495. Doi: 10.3390/molecules200713422

62. Tibiri A, Boria S, Traoré TK, Ouédraogo N, Nikièma A, Ganaba S, et al. Countrywide survey of plants used for liver disease management by traditional healers in Burkina Faso. Front Pharmacol, 2020;11(563751):1-14. Doi: 10.3389/fphar.2020.563751

63. Pare D, Hilou A, Ouedraogo N, Guenne S. Ethnobotanical study of medicinal plants used as anti-obesity remedies in the nomad and hunter communities of Burkina Faso. Medicines, 2016;3(9):1-24. Doi: 10.3390/medicines3020009

64. Holaly GE, Karou DS, Gnoula C, Agbodeka K, Anani K, Tchacondo T, et al. Étude ethnobotanique des plantes utilisées dans le traitement du diabète dans la médecine traditionnelle de la région Maritime du Togo. Pan Afr Med J, 2015;20. Doi: 10.11604/pamj.2015.20.437.5660

65. Sy GY, Sarr A, Dièye AM, Faye B. Myorelaxant and antispasmodic effects of the aqueous extract of *Mitragyna inermis* barks on Wistar rat ileum. Fitoterapia, 2004;75(5):447-450. Doi: 10.1016/j.fitote.2004.03.006

66. Asase A, Yohonu DT. Ethnobotanical study of herbal medicines for management of diabetes mellitus in Dangme West District of southern Ghana. J Herb Med, 2016;6(4):204-209. Doi: 10.1016/j.hermed.2016.07.002

67. Adinortey MB, Agbeko R, Boison D, Ekloh W, Kuatsienu LE, Biney EE, et al. Phytomedicines used for diabetes mellitus in Ghana: a systematic search and review of preclinical and clinical evidence. Evid Based Complement Altern Med, 2019;1-23. Doi: 10.1155/2019/6021209

68. Ouédraogo S, Ranaivo HR, Ndiaye M, Kaboré ZI, Guissou IP, Bucher B, et al. Cardiovascular properties of aqueous extract from *Mitragyna inermis* (wild). J Ethnopharmacol, 2004;93(2-3):345-350. Doi: 10.1016/j.jep.2004.04.002

69. Alamin MA, Yagi AI, Yagi SM. Evaluation of antidiabetic activity of plants used in Western Sudan. Asian Pac J Trop Biomed, 2015;5(5):395-402. Doi: 10.1016/S2221-1691(15)30375-0

70. Funke I, Melzig MF. Traditionally used plants in diabetes therapy-phytotherapeutics as inhibitors of α-amylase activity. Rev Bras Farmacogn, 2006;16(1):1-5. Doi: 10.1590/S0102-695X2006000100002

71. Chukwuma IF, Nworah FN, Apeh VO, Omeje KO, Nweze EJ, Asogwa CD, et al. Phytochemical characterization, functional nutrition, and anti-diabetic potentials of *Leptadenia hastata* (pers) Decne leaves: *in silico* and *in vitro* studies. Bioinform Biol Insights, 2022;16:1-17. Doi: 10.1177/11779322221115436

72. Tielmans A, Laloi-Michelin M, Coupaye M, Virally M, Meas T, Guillausseau PJ. Drug treatment of type 2 diabetes. Presse Medicale, 2007;36(2):269-278. Doi: 10.1016/j.lpm.2006.10.017

Acta Pharm. Sci. Vol 63:(1), 2025
Original article
DOI: 10.23893/1307-2080.APS6303

Formulation and characterization of lercanidipine HCl nanoparticles as fast-dissolving sublingual film

Zahraa A. ALSAFAR, Fatima J. JAWAD*

Baghdad University, College of Pharmacy, Department of Pharmaceutics, Baghdad, Iraq

ABSTRACT

Calcium channel blocker lercanidipine HCl treats hypertension and angina pectoris. It is a biopharmaceutical classification system (BCS) class II drug due to its poor water solubility. First-pass metabolism and low solubility reduce lercanidipine HCl oral bioavailability to 10%. This research aims to improve the dissolution rate of lercanidipine HCl by developing a nanosuspension and then transforming it into a sublingual fast-dissolving film with rapid disintegration, simple administration, and stability that will enhance patient adherence. The solvent-antisolvent precipitation technique produced lercanidipine HCl nanosuspension. Sublingual fast-dissolving films contain lercanidipine HCl nanoparticles produced by solvent casting. The dissolution rate increased significantly in nanosuspension. Film formulations using 50% polyvinyl alcohol and 30% glycerin produced excellent results. Formula F4 is optimal due to its 25-second disintegration and 99.8% in vitro drug release in 4 minutes. The study observed that lercanidipine HCl sublingual film offered an effective drug delivery system with improved disintegration and patient compliance.

Keywords: lercanidipine HCl, nanoparticles, PVA, solvent casting, sublingual film

*Corresponding author: Fatima J. JAWAD
E-mail: drfatimajalal@copharm.uobaghdad.edu.iq
ORCIDs:
Zahraa A. ALSAFAR: 0009-0004-7839-916X
Fatima J. JAWAD: 0000-0002-4906-6241
(Received 07 Mar 2024, Accepted 24 Apr 2024)

INTRODUCTION

Lercanidipine HCl (LER) is a dihydropyridine calcium channel blocker used to treat hypertension and alleviate angina pectoris. The antihypertensive effect of LER is due to its direct relaxation of vascular smooth muscle, leading to a decrease in total peripheral resistance and consequently lowering blood pressure[1]. Lercanidipine HCl is categorized as a biopharmaceutical classification system (BCS) class II drug because of its poor water solubility. The drug is very lipophilic with a Log P value of 6.4 at 20-25°C. The oral bioavailability of LER is about 10%, and its absorption from the gastrointestinal tract is erratic, mainly caused by extensive first-pass metabolism and poor solubility[2]. Nanotechnology currently provides many techniques for improving the dissolution of poorly water-soluble drugs. Nanoparticles are attracting significant interest from formulation researchers due to developments in formulation technology. Pharmaceutical nanoparticles are submicron-sized solid drug carriers that may or may not be biodegradable[3]. Nanoparticles are produced using a top-down technique without a need for a solvent. In contrast, the bottom-up technique requires an organic solvent mixed with immiscible water, causing the drug to precipitate because of its poor water solubility. The different types of nanoparticles comprise nanosuspensions, polymeric nanoparticles, lipid nanoparticles, and others[4]. Nanosuspensions are colloidal particle systems that are nanosized. Nanosuspensions enhance the solubility and dissolution of low-water-soluble drugs by their small particle sizes and large surface areas. Furthermore, they may modify the drug's pharmacokinetics to improve its effectiveness and safety. These advantages could increase the bioavailability of low-soluble drugs[5].

Ensuring solution stability via transformation to a solid state without aggregation is essential for successfully manufacturing and scaling up nanosuspensions. Formulating nanosuspensions into the polymer matrix of oral films stabilizes them by avoiding aggregation and allows for resuspension when dissolved[6]. Fast-dissolving films have been increasingly utilized in pharmaceutical manufacturing. Fast-dissolving dosage types have resolved difficulties with medication delivery to pediatric and older adults. This convenience offers marketing benefits and increases compliance among patients[7]. Films are usually made using either the solvent-casting technique or the hot melt extrusion technique. The solvent-casting process involves dissolving or dispersing the polymer and drug in an aqueous solvent and then casting a film by solvent evaporation. During extrusion, the drug and excipients are combined in a dry condition, heated, and then extruded in a molten state[8]. Sublingual films accel-

erate the onset of drug action by enhancing drug bioavailability through direct absorption into the circulatory system from the sublingual area, bypassing the gastrointestinal tract and hepatic first-pass metabolism. Sublingual films have advantages as they disintegrate fast when placed into contact with the tongue, without the need for liquid intake. They also provide correct dosing, painless administration, easy handling, and simple storage[9]. The project aims to develop lercanidipine HCl nanosuspension and convert it into sublingual film formulations to enhance stability and improve patient compliance.

METHODOLOGY

Materials

Lercanidipine HCl (LER) was obtained from Hyper Chem Company in China, Soluplus (SLU) was acquired from Kathy in China, methanol was purchased from Panreac Applichem in Spain, Polyvinyl alcohol cold (PVAc) from BASF in Germany, Hydroxypropyl methylcellulose E5 (HPMC E5) supplied by Baoji in china, Glycerin (GL) was obtained from BDH Chemical Ltd, Vanilla and Cross povidone from Chemical point in Germany, Mannitol supplied by Hopkin & Willims LTD in England and Sodium Lauryl Sulfate (SLS) was supplied by Alpha Chemika in India.

Methods

Preparation of lercanidipine HCl nanosuspension

Lercanidipine HCl nanosuspensions were produced using the solvent/anti-solvent precipitation process. 10 mg of LER powder was dissolved in 3 mL of methanol at room temperature and then added to 10 mL of deionized water containing soluplus as a stabilizer. The resultant solution was maintained at 37°C. A plastic syringe with a needle was put directly into an aqueous solution containing a stabilizer and drops of the drug's organic solution (organic phase) were at a 1 mL/min rate. The drug-to-stabilizer ratios used in generating the nanosuspension were 1:2. The mixture was agitated on a magnetic stirrer at 1500 rpm for 60 minutes to facilitate the evaporation of the volatile solvent[10,11].

Lercanidipine HCl nanosuspension fabrication as fast-dissolving sublingual films

Previously, lercanidipine HCl nanoparticles were synthesized via a solvent/anti-solvent method. Sublingual films of LER nanoparticles and pure LER were prepared via solvent-casting, as shown in Table 1. The hydrophilic film-forming polymer (PVAc, HPMC E5, or a combination of both) was dispersed in 10 mL of deionized water at 60°C using a magnetic stirrer for one hour estab-

lished at 1000 rpm until the polymer had completely dissolved. After cooling, a plasticizer (glycerin) was added to the mixture. Mannitol (a cooling and sweetening agent), vanilla (a flavoring agent), and cross povidone (an effective super disintegrant) were dissolved in 2 mL of deionized water. The solution obtained was then mixed with the polymeric solution while stirring continuously for 1 hour, creating a transparent solution. LER nanosuspension formulations were produced using a total volume of 10 mL. The formulations were added to the polymer solution and stirred for 2 hours to distribute the drug particles equally inside the polymer matrix, resulting in a more uniform and consistent formulation. The resulting dispersion was covered and left in a cool place for at least 24 hours in order to allow any air bubbles to escape. After being cast onto a Petri dish with a diameter of 6 cm, the final homogenous dispersion was dried for 24 hours at 40°C in an oven. Following drying, the films were divided into 2*3 cm^2 fragments, coated in aluminum foil, and kept in a cold place. A Petri dish with 28 cm^2 in surface area can accommodate four films. Each film has a surface area of 6 cm^2 and contains LER nanoparticles equal to 10 mg LER. Table 1 demonstrates how LER films F9 were created by adding LER to a polymer solution after it had already been dissolved in 3 mL of methanol[12].

Table 1. Sublingual film composition of lercanidipine HCl nanoparticles

Ingredient (mg)	F1	F2	F3	F4	F5	F6	F7	F8	F9
LER (mg)	10	10	10	10	10	10	10	10	10
Soluplus (mg)	20	20	20	20	20	20	20	20	_
PVAc (mg)	60 (50%)	–	30 (25%)	60 (50%)	54 (45%)	–	27 (22.5%)	54 (45%)	60 (50%)
HPMC E5 (mg)	–	60 (50%)	30 (25%)	–	–	54 (45%)	27 (22.5%)	–	–
Glycerin (mg)	15 (25%)	15 (25%)	15 (25%)	18 (30%)	13.5 (25%)	13.5 (25%)	13.5 (25%)	16.2 (30%)	18 (30%)
Mannitol (mg)	6	6	6	6	6	6	6	6	6
Cross povidone (mg)	6	6	6	6	6	6	6	6	6
Vanilla (mg)	2	2	2	2	2	2	2	2	2

Evaluation of lercanidipine HCl nanosuspension

Measurements of the particle size and polydispersity index

The Malvern Zetasizer Nano Laser, manufactured by Ultra Rate Company in the USA, was used to analyze the size and distribution of lercanidipine HCl nanosuspension by dynamic light scattering (DLS) at room temperature. Both the polydispersity index (PDI) and particle size (PS) are determined[13].

Assessment of drug content

Methanol and a specific quantity of nanosuspension (1 mL) were mixed in a 10 mL volumetric flask. The sample was sonicated for one hour and filtered using a 0.45 µm filter syringe. The samples were analyzed using a UV-visible spectrophotometer with a wavelength of 236 nm, where the drug in methanol showed its peak absorption[14]. The drug content was calculated using the following equation:

Drug content = (Practical conc./Theoretical conc.) x 100% (Equation 1)

Measurement of entrapment efficiency

A 4mL sample of lercanidipine HCl nanosuspension was placed in an Amicon ultra-4 centrifugal filter with a molecular weight cut-off of 10 KD. The sample was centrifuged for 30 minutes at 4000 rpm to evaluate the entrapment efficiency (%EE) and quantify the amount of drug contained in the nanoparticles. The amount of unbound LER was determined using UV spectrophotometry at the maximum absorption wavelength of 236 nm[15]. The entrapment efficiency was determined using the following equation:

%EE = Actual amount of drug - Amount of free drug / Actual amount of drug x 100% (Equation 2)

Determination of *in-vitro* dissolution profile

The dissolution test for lercanidipine HCl nanosuspension formulation was conducted using USP apparatus type II (paddle type). A dialysis membrane with a molecular weight cutoff of 8000–14000 was loaded with a nanosuspension volume containing 10 mg of LER. The dialysis membrane was attached to the paddle and immersed in a 200 mL solution of pH 6.8 phosphate buffer containing 1% SLS. The paddle rotated at 50 revolutions per minute while the temperature was kept constant at 37 ± 0.5°C. At specific time points (5, 10, 15, 20, 25, 30, and 45 minutes), a 5 mL sample was taken out and substituted with a new dissolution media to maintain the sink condition. The amount of LER was determined using spectrophotometry at the specified wavelength of 239 nm for this medium[16].

Evaluation of lercanidipine HCl fast dissolving sublingual film

Visual appearance

Evaluate the formulated films for their visual characteristics. Films should be visually inspected for their appearance[17].

Disintegration time of the film

10 mL of phosphate buffer with a pH of 6.8 was added to a Petri dish. A film was placed on the surface of the buffer, and the time it took for the film to break down completely was measured. Estimations were conducted for three films, and the range was calculated[18]. The disintegration time varies according to the formulation, but it usually takes five to thirty seconds[19].

Film thickness

An electronic Vernier caliper is utilized to measure each film's thickness at five locations, including the center and four corners. The average standard deviation of five replicate measurements determines the outcomes[20].

Variations in film weight

Weight variation is examined by using ten randomly chosen films separately on an electronic scale and measuring the average weights. The weight of the acceptable film should not deviate substantially from the weighted average[21].

Measurement of folding endurance

Folding endurance demonstrates the film's flexibility. The measurement was taken manually by pressing the two sides of the film between the thumb and index finger. The film was frequently folded in the center until it broke. The number of times the film was folded before breaking was recorded as the folding endurance. The average of the triplicate observations is provided[22].

Drug content

The films were dissolved in 100 mL of phosphate buffer solution with a pH of 6.8, and 1% SLS was added. The mixture was stirred for 30 minutes using a magnetic stirrer. Samples are taken from the solution and filtered using a syringe filter with a pore size of 0.45 μm. The samples were analyzed for absorbance at a wavelength of 239 nm using a UV spectrophotometer. The amount was calculated using an equation developed from the calibration curve of LER in a buffer solution with a pH of 6.8, containing 1% SLS[23].

Surface pH study

The pH of a film is measured by placing it in a petri dish, dissolving the film with 2mL of distilled water, and then determining the pH by contacting the film surface with a pH meter electrode. It is essential to determine surface pH because acidic or basic pH might lead to oral mucous irritation[24].

In vitro dissolution study of the films

The drug was released from the films using USP dissolution apparatus type II. The dissolution media comprised 200 mL of phosphate buffer pH 6.8 solution with 1% SLS, maintained at a set temperature of 37 ± 0.5°C and stirred at a rate of 50 rpm. 5 mL samples were taken at particular times (1, 2, 3, 4, 5, 6, 7, 8, 9, 10, and 15 minutes) and substituted with the same amount of new dissolution media. The obtained sample was filtered with a 0.45 µm syringe filter. The samples were analyzed using spectrophotometry at a wavelength of 239 nm[25].

Compatibility test by FTIR

Fourier Transform Infrared (FTIR) analysis was used to evaluate the compatibility between lercanidipine HCl nanoparticles and the excipients in the film formulation. A comparison examination was performed between the spectra of LER nanoparticles and the selected film formulation to confirm the absence of interactions and the existence of the drug's distinctive peaks. FTIR spectroscopy ranges from 4000 to 400 cm^{-1} [26].

Statistical analysis

Statistically significant findings were determined for probability values below 0.05, while statistically insignificant findings were classified for values equal to or over 0.05 all measurements and values repeated three times and reported the results as the mean ± standard deviation (SD)[27,28].

RESULTS and DISCUSSION

Evaluation of lercanidipine HCl nanosuspension

The Zeta Sizer was used to analyze a sample of lercanidipine HCl nanosuspension. The investigation obtained a particle size value of 92.94 nm and a polydispersity index (PDI) that was 0.2515. The drug content percentage of the LER nanosuspension formula was determined to be 99.2% ± 0.2516. The results met the criteria stated in the British Pharmacopoeia (BP) and were within the acceptable range of 95% to 110%[29]. The entrapment efficiency of LER was estimated to be 97.76% ± 1.0598. The drug's high encapsulation efficiency is due to its poor solubility in the exterior phase and high solubility in the organic

solvent. As a result, less drug gets transferred into the outer aqueous phase[30]. The lercanidipine HCl nanosuspension demonstrated 100% release after 20 minutes, but the pure lercanidipine HCl powder released just 33.6% after the same time interval, as seen in Figure 1. The similarity factor value estimated is 12.37, which is less than 50. The LER nanosuspension and the pure LER powder show significant variations in dissolution characteristics[31].

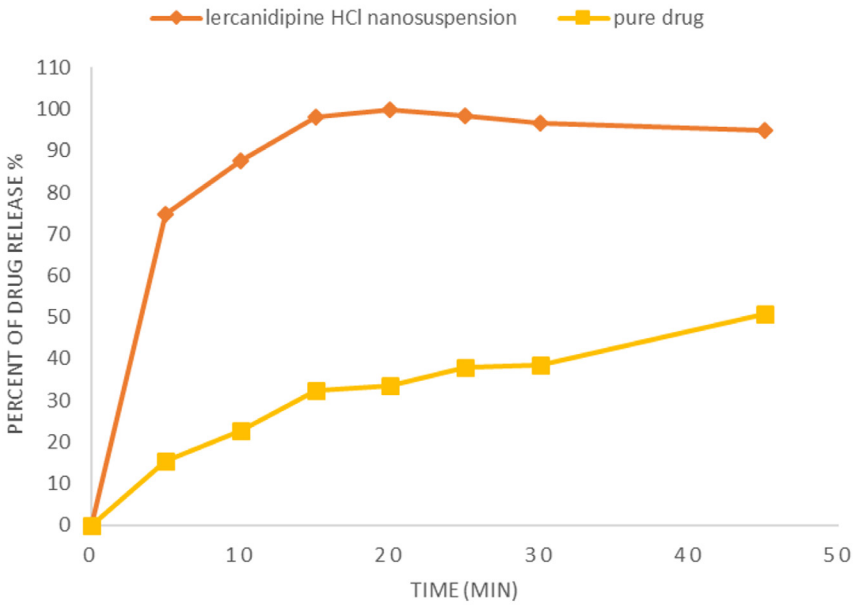

Figure 1. The dissolution patterns of the pure lercanidipine HCl and lercanidipine HCl nanosuspension in 6.8 buffer containing 1% SLS.

Evaluation of lercanidipine HCl fast dissolving sublingual film

Visual appearance

The polymer formulations, including HPMC E5 (F2, F6), exhibited high adhesion, making them difficult to remove from the Petri dish. Formulas F3 and F7, which included a combination of HPMC E5 and PVAc, displayed no transparency, brittleness, or stickiness in their appearance. The formulations containing PVAc (F1, F4, F5, F8, and F9) displayed a uniform, clear appearance with a smooth and homogeneous surface texture. That is seen in Figure 2. PVAc was selected as the best film-forming polymer because it produced a good film that could be separated from the Petri dish and the drug was distributed uniformly through the film. In contrast, HPMC is a film-forming polymer with good film-forming ability, but it did not generate satisfactory outcomes to give an excellent film because the drug is insoluble in water[32].

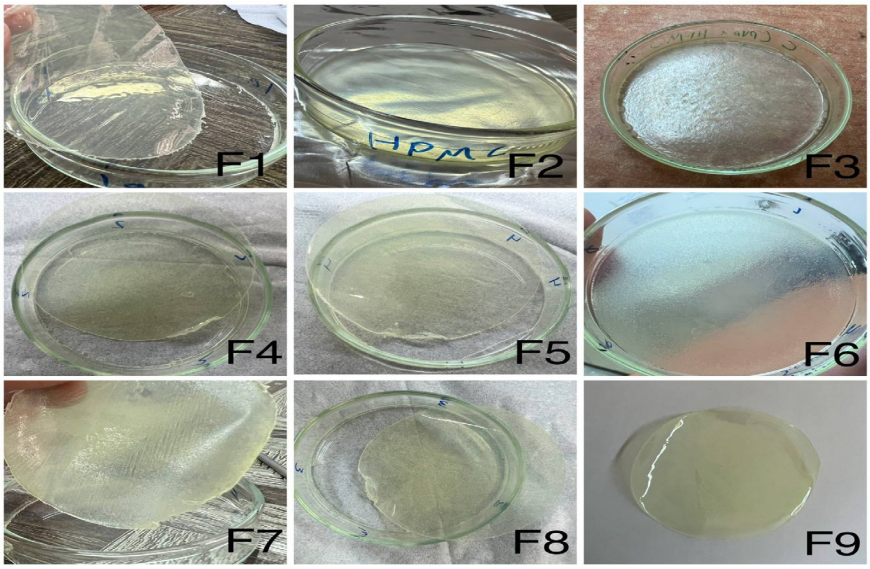

Figure 2. Displays the physical appearance of lercanidipine HCl films

Disintegration time of the film

The evaluation of *in vitro* disintegration demonstrated the following results for film disintegration times: 28 ± 1.0 seconds for F1, 25 ± 1.0 seconds for F4, 27 ± 1.5 seconds for F5, and 30 ± 1.0 seconds for F8. Cross-povidone causes film disintegration in a second for all films. Cross-povidone enhances disintegration by rapidly absorbing saliva into the film, resulting in volume expansion and hydrostatic pressures. This leads to rapid disintegration in the oral cavity, with wicking and swelling mechanisms as the main processes[33].

Film thickness

The average film thickness estimates for all formulations are displayed in Table 2. The thickness ranged from 0.108 ± 0.0083 to 0.124 ± 0.023 mm. A low standard deviation result suggests that the film formulation procedure is reproducible, producing films with uniform thickness and accurate dose in each film[34].

Variations in film weight

The measured weight of the films F1, F4, F5, and F8 were 117.8 ± 4.3, 121.6 ± 3.8, 110.8 ± 2.9, and 112.1 ± 6.4, respectively. The results demonstrate that the films average weight corresponds to the original formulations weight.

Measurement of folding endurance

All films in the study exhibited a folding endurance of more than 300, demonstrating the suitability and toughness of the polymers used, as shown in Table 2. Folding endurance of >300 reflects excellent flexibility[35]. The plasticizer enhanced the flexibility of the films, leading to an improvement in their folding endurance. After adding glycerin, the film became more flexible, and its folding endurance improved[36].

Drug content

The drug content in the film preparation was found to be 99% ± 0.3 for (F1), 100.7% ± 0.08 for (F4), 98.8% ± 0.19 for (F5), and 98.5% ± 0.05 for (F8). The outcomes illustrate that the drug nanoparticles are distributed equally within the film, confirming the effectiveness of the film manufacturing procedure as a uniform film and elevated drug content[37].

Surface pH study

The pH of the films ranged between 6.6 and 6.8. All these pH levels are compatible with the pH of the oral mucosa. The films are non-irritating to the oral cavity, making them acceptable for utilization[38].

Table 2. Displays the physicochemical properties of the prepared lercanidipine HCl sublingual films

F. Code	Drug content	Weight of film (mg)	Film thickness (mm)	Surface pH	Folding endurance	*In vitro* DT (sec)
F1	99% ± 0.3	117.8 ± 4.3	0.116 ± 0.011	6.6 ± 0.2	>300	28 ± 1.0
F4	100.7% ± 0.08	121.6 ± 3.8	0.108 ± 0.0083	6.7 ± 0.05	>300	25 ± 1.0
F5	98.8% ± 0.19	110.8 ± 2.9	0.124 ± 0.023	6.8 ± 0.11	>300	27 ± 1.5
F8	98.5% ± 0.05	112.1 ± 6.4	0.119 ± 0.011	6.6 ± 0.1	>300	30 ± 1.0

In vitro dissolution study of the films

The films that included PVAc polymer (F1, F4, F5, and F8) were found to release (78.6, 99.8, 77, and 92.5) %, respectively, after four minutes. Consequently, F4 demonstrated a greater release of its contents in an in vitro application. Figure 3 illustrates this result. Compared to this, the pure lercanidipine HCl film (F9) exhibited a release rate of just 41.8% for the same duration of time. The research project comprised a comparison of the release patterns of films that included F1, F4, F5, and F8, as well as a film that contained pure lercanidipine HCl (F9), which acted as a reference. The similarity factor f2 was used for comparison. Based on the information shown in Table 3, it was concluded that the value of the similarity factor obtained is less than 50. The LER nanoparticle films and the pure LER film show significant variations in dissolution characteristics.

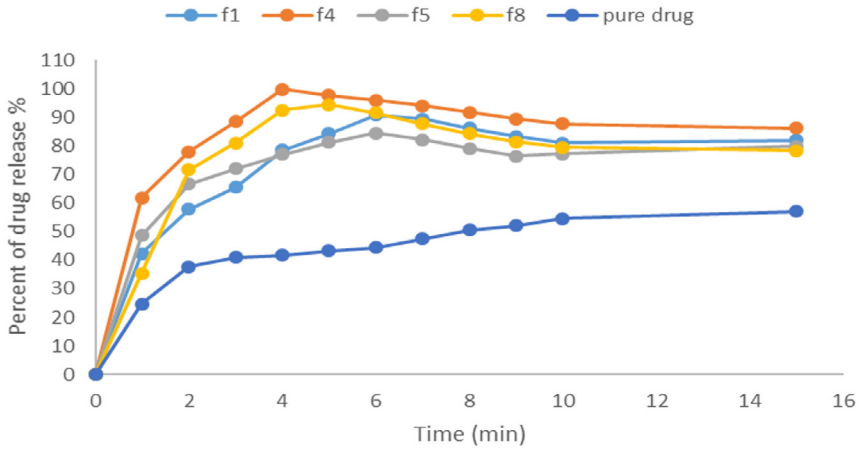

Figure 3. The *in vitro* dissolution of the pure lercanidipine HCl sublingual film and lercanidipine HCl nanoparticle films in phosphate buffer at a pH of 6.8 and 1% SLS.

Table 3. The similarity factor f2 results compare the release patterns of sublingual films containing lercanidipine HCl nanoparticles with those including pure lercanidipine HCl

F. Code	f2 factor
F1	25.13
F4	18.68
F5	26.61
F8	22.56

Characterization of the selected formula

The formulation identified as F4, including PVAc at 50% of the film weight and glycerin at 30% of the polymer weight, was selected as the preferred choice based on the disintegration time, weight uniformity, surface pH, drug content, Film thickness, and dissolution profile, as illustrated in Table 4.

Table 4. The features of the optimal lercanidipine HCl nanoparticle sublingual film

Parameter	F4
Drug content	100.7% ± 0.08
Disintegration time	25 ± 1.0
Weight	121.6 ± 3.8
Thickness	0.108 ± 0.0083
Surface pH	6.7 ± 0.05
Folding endurance	> 300
Drug release %	99.8 %

Compatibility test by FTIR

Figures 4 and 5 exhibit the Fourier Transform Infrared (FTIR) spectra of lercanidipine HCl nanoparticles and the best film preparation (F4), respectively. The optimized film formulation (F4) FTIR showed distinct peaks, which corresponded to those of the drug. This indicates no interaction between the drug and excipients in the film preparation[39].

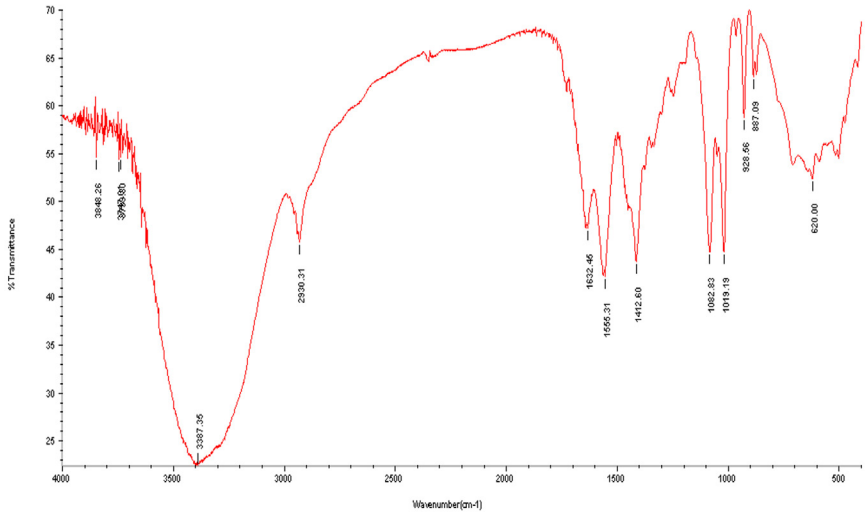

Figure 4. The FTIR spectra of lercanidipine HCl nanoparticles

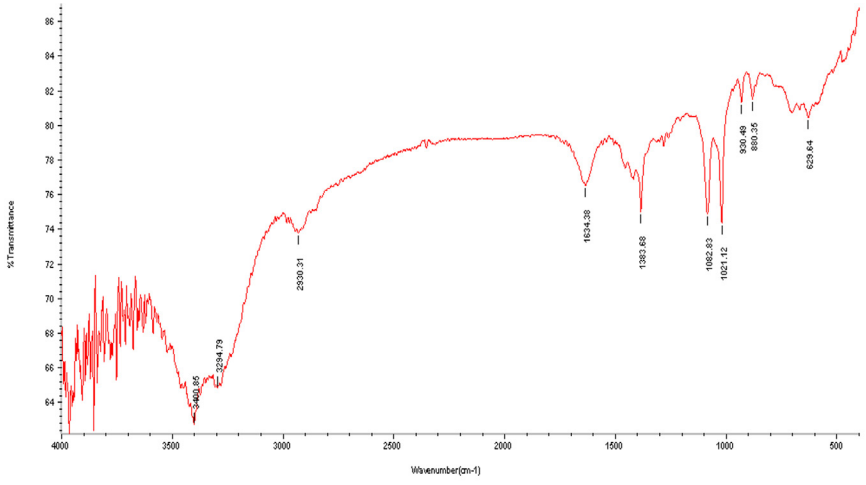

Figure 5. The FTIR spectra of the optimal film preparation (F4)

STATEMENT OF ETHICS

Ethics approval is not required in this study, as no human and experimental animal samples are not involved.

CONFLICT OF INTEREST STATEMENT

The authors declared no conflict of interest.

AUTHORS CONTRIBUTIONS

Zahraa A. Alsafar collected data, analyzed and interpreted results, and prepared the initial manuscript. Zahraa A. Alsafar and Fatima J. Jawad participated in the final version of the text. Fatima J. Jawad supervised the project.

FUNDING SOURCES

Authors have no conflict of interests, and the work was not supported or funded by any drug company.

ACKNOWLEDGMENTS

The authors thank the Department of Pharmaceutics at the College of Pharmacy, University of Baghdad, for providing assistance in conducting the study.

REFERENCES

1. Hajdys J, Fularski P, Leszto K, Majchrowicz G, Stabrawa M, Młynarska E, et al. New insights into the nephroprotective potential of lercanidipine. Int J Mol Sci, 2023;24(18):14048. Doi: 10.3390/ijms241814048

2. Suthar V, Butani S, Gohel M. Solid self-emulsified nanostructures of lercanidipine hydrochloride: a potential approach to improve the fraction of the dose absorbed. J Drug Deliv Sci Technol, 2016;31:11-21. Doi: 10.1016/j.jddst.2015.11.001

3. Al-lami MS, Oudah MH, Rahi FA. Preparation and characterization of domperidone nanoparticles for dissolution improvement. Iraqi J Pharm Sci, 2018;27(1):39-52. Doi: 10.31351/vol27iss1pp39-52

4. Muhesen RA, Rajab NA. Formulation and characterization of olmesartan medoxomil as a nanoparticle. Res J Pharm Technol, 2023;16(7):3314-3320. Doi: 10.52711/0974-360X.2023.00547

5. Pınar SG, Oktay AN, Karaküçük AE, Çelebi N. Formulation strategies of nanosuspensions for various administration routes. Pharmaceutics, 2023;15(5):1520. Doi: 10.3390/pharmaceutics15051520

6. Sinha S. Nanoparticles loaded in consumable polymeric oral films: a smart dosage form design for oral administration. GSC Biol Pharm Sci, 2020;12(1):7-14. Doi: 10.30574/gscbps.2020.12.1.0153

7. Al-Nemrawi NK, Dave RH. Formulation and characterization of acetaminophen nanoparticles in orally disintegrating films. Drug Deliv, 2016;23(2):540-549. Doi: 10.3109/10717544.2014.936987

8. Bharti K, Mittal P, Mishra B. Formulation and characterization of fast dissolving oral films containing buspirone hydrochloride nanoparticles using design of experiment. J Drug Deliv Sci Technol, 2019;49:420-432. Doi: 10.1016/j.jddst.2018.12.013

9. Habib BA, Abd El-Samiae AS, El-Houssieny BM, Tag R. Formulation, characterization, optimization, and in-vivo performance of febuxostat self-nano-emulsifying system loaded sublingual films. Drug Deliv, 2021;28(1):1321-1333. Doi: 10.1080/10717544.2021.1927247

10. Shariare MH, Sharmin S, Jahan I, Reza H, Mohsin K. The impact of process parameters on carrier free paracetamol nanosuspension prepared using different stabilizers by antisolvent precipitation method. J Drug Deliv Sci Technol, 2018;43:122-128. Doi: 10.1016/j.jddst.2017.10.001

11. Abbas HK, Wais FM, Abood AN. Preparation and evaluation of ketoprofen nanosuspension using solvent evaporation technique. Iraqi J Pharm Sci, 2017:41-55. Doi: 10.31351/vol26iss2pp41-55

12. Shen C, Shen B, Xu H, Bai J, Dai L, Lv Q, et al. Formulation and optimization of a novel oral fast dissolving film containing drug nanoparticles by Box–Behnken design–response surface methodology. Drug Dev Ind Pharm, 2014;40(5):649-656. Doi: 10.3109/03639045.2014.884116

13. Jassim ZE, Hussein AA. Formulation and evaluation of clopidogrel tablet incorporating drug nanoparticles. Int J Pharm Sci, 2014:838-851.

14. Qureshia MJ, Phina FF, Patrob S. Enhanced solubility and dissolution rate of clopidogrel by nanosuspension: formulation via high pressure homogenization technique and optimization using Box Behnken design response surface methodology. J Appl Pharm Sci, 2017;7(2):106-113. Doi: 10.7324/JAPS.2017.70213

15. Toma NM, Abdulrasool AA. Formulation and evaluation of montelukast sodium nanoparticles for transdermal delivery. Int J Drug Deliv Technol, 2021;11(2):530-538.

16. Alwan RM, Rajab NA. Nanosuspensions of Selexipag: formulation, characterization, and *in vitro* evaluation. Iraqi J Pharm Sci, 2021;30(1):144-153. Doi: 10.31351/vol30iss1pp144-153

17. Kshirsagar T, Jaiswal N, Chavan G, Zambre K, Ramkrushna S, Dinesh D. Formulation & evaluation of fast dissolving oral film. World J Pharm Res, 2021;10(9):503-561.

18. Bala R, Sharma S. Formulation optimization and evaluation of fast dissolving film of aprepitant by using design of experiment. Bull Fac Pharm Cairo Univ, 2018;56(2):159-168. Doi: 10.1016/j.bfopcu.2018.04.002

19. Sheoran R. Fast dissolving oral films: a review with future prospects. Int J Pharm Pharm Res, 2018;12(2):15-32.

20. Abbas IK, Rajab NA, Hussein AA. Formulation and *in-vitro* evaluation of darifenacin hydrobromide as buccal films. Iraqi J Pharm Sci, 2019;28(2):83-94. Doi: 10.31351/vol28iss2pp83-94

21. Sumi S, Alam MN, Chowdury MI, Mazumdar MM, Chowdhury S, Alam SA. Effective development and evaluation of oral thin film of etoricoxib. World J Pharm Res, 2015;4:257-272.

22. Rashid A, Khalid SH, Irfan M, Asghar S, Rizg WY, Sabei FY, et al. *In vitro* and *in vivo* evaluation of composite oral fast disintegrating film: an innovative strategy for the codelivery of ranitidine HCl and flurbiprofen. Pharmaceutics, 2023;15(7):1987. Doi: 10.3390/pharmaceutics15071987

23. Al-Kubati SS, Ahmed MA, Emad NA. Palatable levocetirizine dihydrochloride solid dispersed fast-dissolving films: formulation and *in vitro* and *in vivo* characterization. Sci World J, 2022;2022. Doi: 10.1155/2022/1552602

24. Irfan M, Rabel S, Bukhtar Q, Qadir MI, Jabeen F, Khan A. Orally disintegrating films: a modern expansion in drug delivery system. Saudi Pharm J, 2016;24(5):537-546. Doi: 10.1016/j.jsps.2015.02.024

25. Mady OY, Abulmeaty MMA, Donia AA, Al-Khureif AA, Al-Shoubki AA, Abudawood M, et al. Formulation and bioavailability of novel mucoadhesive buccal films for candesartan cilexetil in rats. Membranes, 2021;11(9):659. Doi: 10.3390/membranes11090659

26. Dharmasthala S, Shabaraya AR, Andrade GS, Shriram RG, Hebbar S, Dubey A. Fast dissolving oral film of piroxicam: solubility enhancement by forming an inclusion complex with β-cyclodextrin, formulation and evaluation. J Young Pharm, 2019;11(1):1-6. Doi: 10.5530/jyp.2019.11.1

27. Jabur MS, Manna MJ, Mohammed HR, Baqir LS, Abdulamir HA. Ocular hypotensive effect for the topical amlodipine 0.5% eye drop. Lat Am J Pharm, 2023;42:311-314.

28. Abdulhussein HA, Alwasiti EAR, Khiro NK, Nile AK. The potential impact of vascular endothelial growth factor rs699947 polymorphisms on breast tumors susceptibility in a sample of Iraqi females. Acta Pharm Sci, 2024;62:(2): 268-277. Doi: 10.23893/1307-2080.APS6217

29. Hussien RM, Ghareeb MM. Formulation and characterization of isradipine nanoparticle for dissolution enhancement. Iraqi J Pharm Sci, 2021;30(1):218-225. Doi: 10.31351/vol30iss1pp218-225

30. Asfour MH, Mohsen AM. Formulation and evaluation of pH-sensitive rutin nanospheres against colon carcinoma using HCT-116 cell line. J Adv Res, 2018;9:17-26. Doi: 10.1016/j.jare.2017.10.003

31. Santos Júnior AdF, Barbosa IS, Santos VL, Silva RL, Caetite Junior E. Test of dissolution and comparison of *in vitro* dissolution profiles of coated ranitidine tablets marketed in Bahia, Brazil. Braz J Pharm Sci, 2014;50:83-89. Doi: 10.1590/S1984-82502011000100008

32. Jassim ZE, Mohammed MF, Sadeq ZA. Formulation and evaluation of fast dissolving film of lornoxicam. Asian J Pharm Clin Res, 2018;11(9):217-223. Doi: 10.22159/ajpcr.2018.v11i9.27098

33. Sumaiyah S, Mentari J, Suryanto S. The effect of crospovidone on the dissolution profile of amlodipine besylate from fast orally dissolving film. Open Access Maced J Med Sci, 2019;7(22):3811. Doi: 10.3889/oamjms.2019.510

34. Kaewkroek K, Petchsomrit A, Septama AW, Wiwattanapatapee R. Development of starch/chitosan expandable films as a gastroretentive carrier for ginger extract-loaded solid dispersion. Saudi Pharm J, 2022;30(2):120-131. Doi: 10.1016/j.jsps.2021.12.017

35. Rani KC, Parfati N, Aryani NLD, Winantari AN, Fitriani EW, Pradana AT, et al. Development, evaluation, and molecular docking of oral dissolving film of atenolol. Pharmaceutics, 2021;13(10):1727. Doi: 10.3390/pharmaceutics13101727

36. Kittipongpatana OS, Trisopon K, Wattanaarsakit P, Kittipongpatana N. Fabrication and characterization of orodispersible composite film from hydroxypropylmethyl cellulose-crosslinked carboxymethyl rice starch. Membranes, 2022;12(6):594. Doi: 10.3390/membranes12060594

37. Krull SM. Formulation and dissolution of polymer strip films for the delivery of poorly water-soluble drug nanoparticles. [Doctoral thesis]. New Jersey: New Jersey Institute of Technology; 2017.

38. Gayathri D, Jayakumari LS. Evaluation of commercial arrowroot starch/CMC film for buccal drug delivery of glipizide. Polímeros, 2020;29:e2019047. Doi: 10.1590/0104-1428.06619

39. Shaikh F, Patel VB. Enhancement of dissolution of Lercanidipine hydrochloride using solid dispersion technique. Res J Recent Sci, 2015;2277:2502.

Acta Pharm. Sci. Vol 63:(1), 2025
Original article
DOI: 10.23893/1307-2080.APS6304

The role of hypoxia-inducible factor 1 alpha and peroxisome proliferator activated receptor gamma coactivator 1 alpha in the diagnosis of breast cancer

Doaa Y. R. ALGBURI[1*], Bashar Abass ABDULHASSAN[2], Omar F. ABDUL-RASHEED[1]
Ahmed Zuhair ALSAMMARRAIE[3]

1 Al-Nahrain University, College of Medicine, Department of Chemistry and Biochemistry, Baghdad, Iraq
2 Al-Nahrain University, College of Medicine, Department of Surgery, Baghdad, Iraq
3 Ministry of Health and Environment, Oncology Teaching Hospital, Baghdad, Iraq

ABSTRACT

This study aimed to assess the possible association between hypoxia-inducible factor 1 (HIF-α1) and proliferator activated receptor gamma coactivator 1 (PGC-α1) levels in early and advanced breast cancer patients and to study the correlation between these parameters in a case-control study conducted on 40 females with breast cancer categorized into early and advanced stages, with 20 patients in each group, collected from the Medical City and Oncology teaching hospital, Baghdad, Iraq, between June and October 2023. The levels of HIF-α1 and PGC-α1 were measured in the serum of breast cancer patients by ELISA technique and compared with 40 age- and gender- matched controls, which showed that the levels of HIF-1α and PGC-1α increased significantly in the early and advanced stages in comparison with controls, which indicates that the markers can be used as diagnostic markers for breast cancer in the early and advanced stages.

Keywords: HIF-1α, PGC-1α, breast cancer, diagnostic markers

*Corresponding author: Doaa Y. R. ALGBURI
E-mail: duaa.yrj@ibnsina.edu.iq
ORCIDs:
Doaa Y. R. ALGBURI: 0009-0002-5636-9547
Bashar Abass ABDULHASSAN: 0000-0002-0519-0021
Omar F. ABDUL-RASHEED: 0000-0003-3016-9176
Ahmed Zuhair ALSAMMARRAIE: 0000-0002-7419-961X
(Received 20 Jan 2024, Accepted 26 Feb 2024)

INTRODUCTION

Breast cancer is the most frequently diagnosed cancer and a major cause of death in women worldwide, diagnostic marker for breast cancer typically involves a combination of various tests and procedures[1]. However, there are several key markers and tests commonly used in the diagnostic process for breast cancer such as carcinoembryonic antigen (CEA), alpha fetoprotein (AFP), carbohydrate antigen 125 (CA125), carbohydrate antigen 199 (CA199) and carbohydrate antigen 153 (CA153)[2]. Mammography is a standard screening tool for detecting breast abnormalities and breast ultrasound is frequently employed alongside mammography to differentiate between solid masses and fluid-filled cysts which enhances the diagnostic capabilities. Breast Magnetic Resonance Imaging (MRI) can provide detailed images of the breast and is often used for further evaluation, especially in high-risk cases in addition to Biopsy which is considered as definitive diagnosis of breast cancer[3]. Both Fine Needle Aspiration Cytology (FNAC) and Tru-Cut biopsy demonstrate commendable diagnostic accuracy. However, Tru-Cut biopsy exhibits higher accuracy compared to FNAC for detecting this pathological condition[4].

Circulating Tumor Markers are generally not specific enough for a definitive diagnosis, for example CEA is not specific to breast cancer, and elevated levels can also be seen in other conditions, such as colorectal cancer. CEA is more commonly used in monitoring the progression of the disease and evaluating the response to treatment rather than for the initial diagnosis[5]. Another example is CA 15-3 which is a protein that may be elevated in the circulation of breast cancer patients, particularly those with advanced or metastatic disease. CA 15-3 also not specific to breast cancer and can be elevated in other conditions include endometriosis, pelvic inflammatory disease and liver disease. It can also be increased during pregnancy[6]. CA 15-3 is often used as a tumor marker for monitoring disease progression and treatment response rather than for diagnostic purposes[7].

When cells encounter low levels of oxygen (Hypoxia)[8], HIF plays a pivotal role in coordinating cellular reactions to hypoxia by controlling the expression of genes associated with oxygen homeostasis, angiogenesis, and glycolysis which is crucial for cells to cope with this challenges[1]. Even under normoxic (normal oxygen) conditions, the heightened expression of HIF-1α in breast tumors is evident, indicating that the irregularities in HIF-1α regulation within these tumors are not exclusively tied to low oxygen levels[9]. The peroxisome proliferator-activated receptor gamma coactivator 1-alph (PGC-1α) functions as a co-activator for steroid and receptor of nuclear, participating in adaptive ther-

mogenesis, fatty-acid oxidation, energy metabolism, thyroid hormone receptors, homeostasis of cellular cholesterol, and gluconeogenesis[10]. The processes underlying tumor invasion, proliferation, progression, and metastatic potential remain not clear, but recent findings suggest that in invasive tumors, tumor cells primarily rely on mitochondrial respiration. In this context, oxidative phosphorylation activated processes by PGC-1α appears to play a significant role[11]. The correlation between PGC-1α and HIF-1α has undergone thorough examination, revealing that in the context of angiogenesis, PGC-1α induces vascular endothelial growth factor (VEGF) expression without reliance on HIF-1α. Nevertheless, it can be postulated that PGC-1α-induced mitochondrial respiration may lead to reduced oxygen levels and an augmentation in the production of reactive oxygen species (ROS)[12].

This study aimed to assess the possible association between Hypoxia-Inducible Factor1 HIF-α1 and proliferator activated receptor gamma coactivator PGC-α1 level with early and advance breast cancer patients, and to study the correlation between these parameters.

METHODOLOGY

Study design

This study is case-control research conducted at Al-Nahrain University's College of Medicine, department of chemistry and biochemistry. The research proposal was authorized by the Al-Nahrain University College of Medicine's Ethical Committee. Forty female Iraqi patients with breast cancer were documented by histopathology and collected in from Al- Oncology teaching hospital Medical City, Baghdad, Iraq. Blood samples were obtained from all patients upon their consent, following hospitalization and before the initiation of any medication. The study was conducted between May 2022 and December 2022. All participants included in the study were aged between 18 and 60 years.

1. Control group: Includes 40 samples of apparently healthy-aged and sex-matched volunteers.

2. Case group: Includes 40 (18 early, 22 advance stage) samples with confirmed breast cancer, diagnosed by true cut histopathology.

Exclusion criteria

Female with tumor other than breast cancer, pregnant and lactating women, viral infected women, women who exposure to radiotherapy and chemotherapy taken.

Blood sample collection and storage

Approximately 5 ml of blood samples were collected from the participants. The blood was allowed to clot at room temperature for 15 minutes, and then the serum was separated by centrifugation at 3000 rpm for 10 minutes. The isolated serum was stored in a -4°C freezer until it was ready to be used in the study, Human HIF-1a and PCG-1a kit was measured using Elisa Human Reader, purchased from Cloud-Clone Corp Company, USA. Other tests include urea, creatinine, ALT, AST, ALP.

Statistical analysis

The study data were analyzed utilizing SPSS software version 20. Numeric variables were presented as mean, standard error (SE) and standard deviation (SD), and statistical comparisons were conducted through ANOVA, followed by the post-hoc Tukey test. A significance level of $p \leq 0.05$ was considered statistically significant. Categorical variables were expressed as numbers and analyzed using cross-tabulation to evaluate the frequency and percentage of each variable within the studied groups.

RESULTS and DISCUSSIONS

Age and body mass index (BMI) of the studied groups were summarized in Table 1 which showed non-significant differences in age and BMI among all studied groups.

Table 1. Age and BMI of the patients with early and advance stages in comparison with controls

		N	Mean	SD	SE	p^a	p^b	p^c	p^d	p^e
Age	Control	40	43.4	6.62	1.48	0.923	0.972	0.992	0.926	0.708
	Early Stage	22	42.62	5.25	1.46					
	Advance Stage	18	42.91	4.46	1.34					
	All Patients	40	42.75	4.8	0.98					
BMI	Control	40	26.88	1.24	0.28	0.397	0.137	0.75	0.131	0.058
	Early	22	27.63	2.06	0.57					
	Advance	18	28.13	1.49	0.49					
	All Patients	40	27.84	1.83	0.39					

P^a value between controls and early-stage patients; P^b value between controls and advance-stage patients; P^c value between early- and advance-stage patients; P^d value among controls, early- and advance-stage patients (ANOVA test); P^e value between controls and all patients; SD: Standard deviation; SE: Standard error.

Table 2 showed that the levels of HIF-1α and PGC-1α increased significantly ($p<0.001$) in the early and advanced stages in comparison with controls, and these two subgroups were non-significantly different from each other. On the other hand, CEA and CA 15-3 showed a different manner of increment in that the levels of these markers increase non-significantly in early stages in comparison with controls whereas advanced stages patients showed the significant increase in comparison with both controls and early stages patients with breast cancer.

Table 2. Levels of HIF-1α, PGC-1α, CEA and CA 15-3 in all studied groups

		N	Mean	SD	SE	Pa	Pb	Pc	Pd	Pe
HIF-1α	Control	40	1.58	0.31	0.07	<0.001	<0.001	0.821	<0.001	<0.001
	Early	22	3.91	1.59	0.44					
	Advance	18	4.22	1.87	0.56					
	All Patients	40	4.05	1.69	0.35					
PGC-1α	Control	40	1.07	0.1	0.02	<0.001	<0.001	0.944	<0.001	<0.001
	Early	22	2.62	1.01	0.28					
	Advance	18	2.72	0.97	0.29					
	All Patients	40	2.67	0.97	0.2					
CEA	Control	40	0.51	0.2	0.04	0.275	<0.001	0.004	<0.001	0.001
	Early	22	1.2	0.48	0.13					
	Advance	18	2.94	2.43	0.73					
	All Patients	40	1.99	1.86	0.38					
CA 15-3	Control	40	13.27	4.77	1.07	0.938	0.002	0.011	0.002	0.482
	Early	22	14.05	3.94	1.09					
	Advance	18	22.14	10.47	3.16					
	All Patients	40	17.76	8.53	1.74					

P^a value between controls and early-stage patients; P^b value between controls and advance-stage patients; P^c value between early- and advance-stage patients; P^d value among controls, early- and advance-stage patients (ANOVA test) P^e value between controls and all patients; SD: Standard deviation; SE: Standard error.

Results illustrated in Table 3 showed that PGC-1α levels were positively and significantly correlated with ALP (r=0.470, p=0.02) and with CEA (r=0.467, p=0.021). Additionally, CEA and CA15-3 were also correlated positively and significantly (p=0.624, p=0.001).

Table 3. Correlation among all studied groups in patients with breast cancer

		BMI	Urea	Cr	ALT	AST	ALP	HIF-1α	PGC-1α	CEA	CA 15-3
HIF-1α	r	-0.002	0.285	-0.011	-0.24	0.056	-0.051	-	-0.234	0.106	0.309
	p	0.994	0.177	0.96	0.258	0.795	0.811	-	0.27	0.621	0.142
PGC-1α	r	-0.054	0.346	0.08	0.311	0.198	0.470*	-0.234	-	0.467*	0.304
	p	0.813	0.098	0.709	0.139	0.354	0.02	0.27	-	0.021	0.148
CEA	r	0.112	0.367	0.144	0.02	0.361	0.084	0.106	0.467*	-	0.624**
	p	0.619	0.078	0.503	0.926	0.083	0.695	0.621	0.021	-	0.001
CA 15-3	r	0.308	0.192	0.012	0.17	0.134	0.049	0.309	0.304	0.624**	-
	p	0.164	0.368	0.955	0.427	0.532	0.819	0.142	0.148	0.001	-

r: Pearson correlation coefficient; p: Significance; Cr: Creatinine.

Table 4 and Figure 1 showed that PGC-1α showed the highest AUC of 1 with sensitivity and specificity of 100% in patients with breast cancer when compared with controls, followed by CEA that showed AUC, sensitivity, and specificity of 0.972, 91.7%, and 85%, respectively, and HIF-1α with 0.958, 91.7%, and 100%, respectively. The only marker that showed a low value was CA 15-3 with 0.704, 66.7%, and 70%, respectively. An interesting finding is that CEA when combined with CA 15-3 provides a higher AUC of 0.981 with perfect sensitivity (100 %) and excellent specificity (91.7).

Table 4. ROC curve results of HIF-1α, PGC-1α, CEA and CA 15-3 between breast cancer patients' group and controls

Parameters	AUC	Cut-Off value	Sensitivity (%)	Specificity (%)
HIF-1α	0.958	2.433	91.7	100
PGC-1α	1.000	1.24	100	100
CEA	0.972	0.745	91.7	85
CA 15-3	0.704	14.35	66.7	70
Combination of CEA and CA 15-3	0.981	-	100	91.7

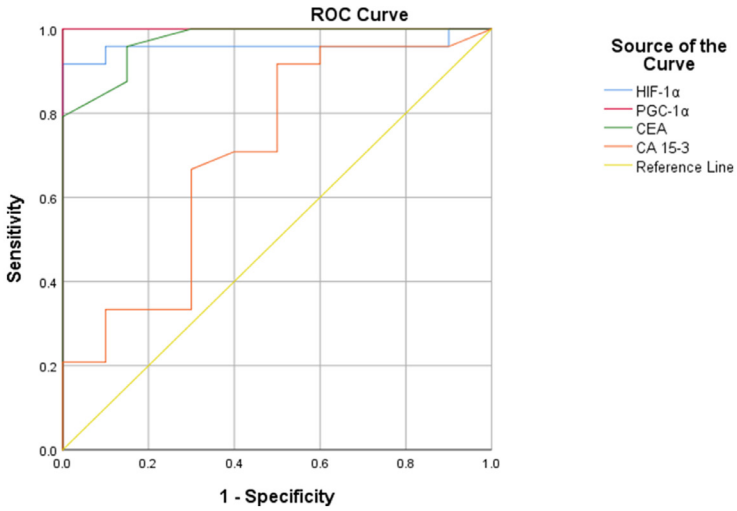

Figure 1. ROC curve results of HIF-1α, PGC-1α, CEA and CA 15-3 between breast cancer patients and controls

These markers are not definitive for breast cancer diagnosis, and decisions regarding treatment and monitoring should be made based on a comprehensive assessment by healthcare professionals so that not used as diagnostic markers. In Hypoxic Microenvironment Rapid tumor growth in the early stages can outpace the development of new blood vessels, leading to areas of inadequate oxygen supply or hypoxia[13]. HIF-1α is highly responsive to low oxygen levels, and its stabilization occurs in response to hypoxia. In early breast cancer, regions of hypoxia trigger the accumulation and activation of HIF-1α. The early tumor microenvironment relies on angiogenesis to provide the necessary blood supply for sustained growth HIF-1α triggers the production of pro-angiogenic molecules, including Vascular Endothelial Growth Factor (VEGF). Promoting the formation of new blood vessels to support the growing tumor[14].

In advanced breast cancer, the tumor outgrows its existing blood supply, resulting in persistent and widespread hypoxia. The chronic hypoxic conditions contribute to sustained activation and accumulation of HIF-1α in cancer cells. Metastatic Spread in advanced breast cancer is often characterized by increased metastatic potential. HIF-1α is involved in the induction of genes associated with invasion and metastasis, facilitating the spread of cancer cells to distant organs. The microenvironment of advanced tumors undergoes dynamic changes, including fluctuations in oxygen levels[15]. These changes can further activate HIF-1α as cancer cells adapt to the evolving conditions. Therapeutic Resistance to treatment modalities, such as chemotherapy and radiation, can

induce hypoxia in tumor regions. In response to these therapies, cancer cells may upregulate HIF-1α as a survival mechanism, contributing to resistance against treatment[16]. PGC-1α is known for its role in regulating cellular energy metabolism. In cancer cells, including breast cancer, there can be metabolic adaptations to support the increased energy demands of rapidly dividing cells. Elevated PGC-1α might contribute to these adaptations[17]. PGC-1α is a key regulator of mitochondrial biogenesis and function. Breast cancer cells often exhibit changes in rely on mitochondrial metabolism to fulfill their energy requirements. Increased PGC-1α expression may be a part of these adaptations[18].

PGC-1α is involved in the cellular response to oxidative stress. Breast cancer cells may experience higher levels of oxidative stress due to various factors, and an elevation in PGC-1α could be part of the cellular response to mitigate oxidative damage.PGC-1α expression can be influenced by hormonal signaling pathways. Breast cancer, especially hormone receptor-positive subtypes, is influenced by hormonal factors. Changes in hormonal signaling in breast cancer cells may contribute to alterations in PGC-1α expression[19]. Dysregulation of genes involved in the PGC-1α pathway through genetic mutations or epigenetic modifications might contribute to elevated PGC-1α expression in breast cancer[20]. In the early stages of breast cancer, alterations in cellular metabolism and mitochondrial function may be critical for tumor initiation and growth[21,22]. Elevated PGC-1α might support these early metabolic adaptations. In advanced stages, where tumors become more aggressive and may develop resistance to treatment, PGC-1α could contribute to sustaining the high energy demands of rapidly dividing cancer cells and promoting cell survival [23,24].

This study shows that the increasing in Hypoxia-Inducible Factor1 Alpha and Peroxisome Proliferator Activated Receptor Gamma Coactivator 1 Alpha (HIF-1α and PGC-1α) associated with breast cancer in early and advance stage, positive significant correlations were demonstrated between age and PGC-1α, HIF-1α and AST. That PGC-1α showed the highest AUC with sensitivity and specificity of 100% in patients with breast cancer when compared with controls, followed by HIF-1α.

STATEMENTS OF ETHICS

The study received approval from the "Institute Review Board (IRB) of Al-Nahrain University/College of Medicine" on April 30, 2023 (38/2023) with a number 20221276.

CONFLICT OF INTEREST STATEMENT

No conflict of interest was declared by the authors.

AUTHOR CONTRIBUTIONS

Design – Abdul-Rasheed OF, Alsammarraie AZ; Acquisition of Data – Algburi DYR, Abdulhassan BA, Alsammarraie AZ; Analysis of Data – Algburi DYR, Abdulhassan BA; Drafting of the Manuscript – Algburi DYR, Abdulhassan BA, Abdul-Rasheed OF; Critical Revision of the Manuscript – Abdulhassan BA, Abdul-Rasheed OF, Alsammarraie AZ; Statistical Analysis – Algburi DYR, Alsammarraie AZ; Technical or Financial Support – Algburi DYR, Abdulhassan BA, Abdul-Rasheed OF; Supervision – Abdulhassan BA, Abdul-Rasheed OF, Alsammarraie AZ.

FUNDING SOURCES

The work was not supported or funded by any organization, university or drug company.

ACKNOWLEDGMENTS

The author is grateful to staff of the Department of Chemistry and Biochemistry, Medical Research Unit / Division of Molecular Biology-College of Medicine Al-Nahrain University, Baghdad, Iraq for their facilities in performing this study and also to the head and staff members of Oncology Teaching Hospital, Medical City, Baghdad, Iraq.

REFERENCES

1. Alrubaye YSJ, Mohammed MB, Abdulamir HA. Exosome and breast cancer. Res J Pharm Tech, 2022;15(3):1393-1397. Doi: 10.52711 /0974-360X.2022.00232

2. Luo J, Xiao J, Yang Y, Chen G, Hu D, Zeng J. Strategies for five tumour markers in the screening and diagnosis of female breast cancer. Front Oncol, 2023;12:1055855. Doi: 10.3389/fonc.2022.1055855

3. Beňačka R, Szabóová D, Guľašová Z, Hertelyová Z, Radoňák J. Classic and new markers in diagnostics and classification of breast cancer. Cancers, 2022;14(21):5444. Doi: 10.3390/cancers14215444

4. Masood A, Muhammad TA, Rehana R, Muhammad BGH, Abdul R, Lailama SS. Comparative analysis of the diagnostic accuracy of fine-needle aspiration cytology (fnac) versus true-cut biopsy in the detection of malignancy within detectable breast masses. J Popul Ther Clin Pharmacol, 2023;30(17):1276-1281. Doi: 10.53555/jptcp.v30i17.2738

5. Filella X, Rodríguez-Garcia M, Fernández-Galán E. Clinical usefulness of circulating tumor markers. Clin Chem Lab Med, 2022;61(5):895-905. Doi: 10.1515/cclm-2022-1090

6. Canadian Cancer Society. Accessed February 19, 2024. Available from: https://cancer.ca/en/treatments/tests-and-procedures/cancer-antigen-15-3-ca-15-3

7. Fakhari A, Gharepapagh E, Dabiri S, Gilani N. Correlation of cancer antigen 15-3 (CA15-3) serum level and bony metastases in breast cancer patients. Med J Islam Repub Iran, 2019;33:142. Doi: 10.34171/mjiri.33.142

8. Rakoff-Nahoum S. Why cancer and inflammation? Yale J Biol Med, 2006;79(3-4):123-130.

9. Poorva G, Chantal V, Sanchareeka D, Li Z. Mitochondria targeting as an effective strategy for cancer therapy. Int J Mol Sci, 2020;21(9):3363. Doi: 10.3390/ijms21093363

10. Haijiang Wu, Xinna D, Yonghong Shi. PGC-1α, glucose metabolism and type 2 diabetes mellitus. J Endocrinol, 2016;229(3):R99–R115. Doi: 10.1530/JOE-16-0021

11. Brito LG, Schiavon VF, Andrade JM, Tiezzi DG, Peria FM, Marana HR. Expression of hypoxia-inducible factor 1-α and vascular endothelial growth factor-C in locally advanced breast cancer patients. Clinics (Sao Paulo), 2011;66(8):1313-1320. Doi: 10.1590/s1807-59322011000800002

12. Cai FF, Xu C, Pan X, Cai L, Lin XY, Chen S, et al. Prognostic value of plasma levels of HIF-1a and PGC-1a in breast cancer. Oncotarget, 2016;7(47):77793-77806. Doi: 10.18632/oncotarget.12796

13. He Z, Chen Z, Tan M, Elingarami S, Liu Y, Li T, et al. A review on methods for diagnosis of breast cancer cells and tissues. Cell Prolif, 2020;53(7):e12822. Doi: 10.1111/cpr.12822

14. Zimna A, Kurpisz M. Hypoxia-Inducible Factor-1 in Physiological and pathophysiological angiogenesis: applications and therapies. Biomed Res Int, 2015;2015(1):549412. Doi: 10.1155/2015/549412

15. Bader SB, Dewhirst MW, Hammond EM. Cyclic hypoxia: an update on its characteristics, methods to measure it and biological implications in cancer. Cancers, 2020;13(1):23. Doi: 10.3390/cancers13010023

16. Sebestyén A, Kopper L, Dankó T, Tímár J. Hypoxia signaling in cancer: from basics to clinical practice. Pathol Oncol Res, 2021;27:1609802. Doi: 10.3389/pore.2021.1609802

17. Bost F, Kaminski L. The metabolic modulator PGC-1α in cancer. Am J Cancer Res, 2019;9(2):198-211.

18. Abu Shelbayeh O, Arroum T, Morris S, Busch KB. PGC-1α is a master regulator of mitochondrial lifecycle and ros stress response. Antioxidants, 2023;12(5):1075. Doi: 10.3390/antiox12051075

19. Wang L, Zhang S, Wang X. The metabolic mechanisms of breast cancer metastasis. Front Oncol, 2021;10:602416. Doi: 10.3389/fonc.2020.602416

20. Oka SI, Sabry AD, Cawley KM, Warren JS. Multiple levels of PGC-1α dysregulation in heart failure. Front Cardiovasc Med, 2020;7:2. Doi: 10.3389/fcvm.2020.00002

21. Avagliano A, Ruocco MR, Aliotta F, Belviso I, Accurso A, Masone S, et al. Mitochondrial flexibility of breast cancers: a growth advantage and a therapeutic opportunity. Cells, 2019;8(5):401. Doi: 10.3390/cells8050401

22. Zakic T, Kalezic A, Drvendzija Z, Udicki M, Ivkovic Kapicl T, et al. Breast cancer: mitochondria-centered metabolic alterations in tumor and associated adipose tissue. Cells, 2024;13(2):155. Doi: 10.3390/cells13020155

23. Mastropasqua F, Girolimetti G, Shoshan M. PGC1α: friend or foe in cancer? Genes, 2018;9(1):48. Doi: 10.3390/genes9010048

24. Andrzejewski S, Klimcakova E, Johnson RM, Tabariès S, Annis MG, McGuirk S, et al. PGC-1α promotes breast cancer metastasis and confers bioenergetic flexibility against metabolic drugs. Cell Metab, 2017;26(5):778-787.e5. Doi: 10.1016/j.cmet.2017.09.006

Acta Pharm. Sci. Vol 63:(1), 2025
Original article
DOI: 10.23893/1307-2080.APS6305

What can Google Trends and Wikipedia-Pageview analysis tell us about sustainability and sustainable diets?

Hatice Merve BAYRAM, Arda OZTURKCAN*

Istanbul Gelisim University, Faculty of Health Sciences, Department of Nutrition and Dietetics, Istanbul, Türkiye

ABSTRACT

The study aimed to determine the public interest in sustainability and sustainability diet-related topics. Wikipedia Pageviews analysis and Google Trends data were used for the relative internet search popularity on "sustainability" and diet-related topics from 1 July 2015 to 1 May 2023. "Sustainability" was particularly popular in European countries. "Climatarian diet" was a new term, and only three countries were searched. Relative Search Volume increased most dynamically for the topics "Sustainability", "Sustainable diet", "Plant-based diet", "Mediterranean diet", and "Pescetarianism", while page views increased most dynamically for the topics "Plant-based diet", "Flexitarianism", and "Mediterranean diet". According to both Wikipedia and Google Trends, there was a positive correlation between "Sustainability" and "Healthy diet", "Plant-based diet", "Mediterranean diet", "Veganism", "Raw foodism", and "Pescetarianism". Understanding the public's interest in sustainability and sustainable diets is critical to developing and choosing strategies for transitioning to sustainable diets.

Keywords: sustainability, sustainable diets, Google Trends, Wikipedia, pageviews analysis

*Corresponding author: Arda OZTURKCAN
E-mail: turkcana@hotmail.com
ORCIDs:
Hatice Merve BAYRAM: 0000-0002-7073-2907
Arda OZTURKCAN: 0000-0001-7982-6988
(Received 25 Jan 2024, Accepted 29 Feb 2024)

INTRODUCTION

Sustainable food systems and diets are gaining popularity in a variety of scientific sectors. A sustainable food system ensures food security and nutrition for everyone without undermining the economic, social, and environmental underpinnings for future generations' food security and nutrition[1].

Sustainable diets are defined as "diets protective and respectful of biodiversity and ecosystems, culturally acceptable, accessible, economically fair and affordable; nutritionally adequate, safe and healthy; while optimizing natural and human resources" according to the Food and Agriculture Organization (FAO)[2]. Additionally, it is thought that food is the single most powerful lever for improving human health and environmental sustainability on the planet[3]. The World Health Organization (WHO) recommends that fruit, vegetables, legumes, nuts, and whole grains are important parts of a healthy diet, and free sugars, salt, and fat must be limited[4]. A study showed that the adoption of sustainable diets in middle- and high-income countries can positively affect both health and the environment, while the adoption of sustainable diets in low-income countries may result in more resource expenditure, which may limit sustainability[5]. Additionally, diets that positively affect health and environmentally sustainable diets do not cover each other. Since a nutritionally adequate diet may have a high environmental impact, a diet with low greenhouse gas emissions may be nutritionally inadequate[6]. Therefore, popular-based dietary modifications could benefit both health and the environment[7,8].

There is a greater interest in sustainable and related diets. Animal-based diets were associated with higher greenhouse gas emissions (GHGE), whereas higher consumption of plant-based diets was associated with lower GHGE[1,9]. Additionally, animal-based products include harmful nutrients such as sodium, saturated fat, and added sugars[10]. Therefore, reduced consumption of animal-based products may result in higher sustainability, health advantages, and a decline in disease risks[1]. The Climatarian diet is consistent with a range of environmentally motivated diets (including plant-based and flexitarian), that aims to reduce the carbon footprint from food consumption and mitigate climate change. The diet typically does not include rigid restrictions, but rather focuses on mindfulness about food-related emissions and may include a variety of behaviours to reduce one's carbon footprint from food intake (e.g., lowering meat consumption)[3,11]. However, a healthy diet and Mediterranean diet include a higher number of animal-based products (meat and dairy products) than a Climatarian diet[3,12].

Big Data is currently a hot topic in many industries and academia. "Big Data" are informational resources/assets with such a great volume, speed, and variety that they necessitate specialized technology and analytical methodologies to transform them into value[13]. In today's digital world, a variety of tools have emerged that make it easier to understand and predict social changes in "big data", which includes high amounts of data and resources[14,15]. Data collected during internet searches is one type of Big Data that can provide significant insights and information on population behaviour and interests. Google is the global search leader between 2015 and 2023 with an 84.69% usage rate, and one tool Google Trends a free and publicly accessible online portal from Google that allows people to interact with Internet search data[14,16].

However, two new characteristics have recently been assigned to Big Data: variability and veracity. The consistency of the data across time is represented by variability, whereas the accuracy, credibility, and truthfulness of the data are represented by veracity[14]. Wikipedia is a non-profit, free online encyclopedia that is created and maintained by volunteers from all over the world. It is trustworthy for users due to labelled articles based on their appearance[17]. Wikitrends has a similar function to Google Trends and is an attractive new analytics platform for Wikipedia that provides a variety of visualizations of Wikipedia pages[18]. These analytics tools have demonstrated promise for identifying the level of public awareness.

Food systems have a critical role in causing climate change, and food consumption is one of the most important climate change mitigation options in the food systems[1]. Therefore, it is important to evaluate the knowledge levels of consumers about sustainability and dietary patterns. The aim of this study was to determine the public interest in sustainability and sustainable diet-related topics such as sustainable diet, healthy diet, plant-based diet, Climatarian diet, flexitarianism, Japanese diet, Mediterranean diet, Nordic diet, vegetarianism, veganism, raw foodism, fruitarianism, pescetarianism.

METHODOLOGY

Wikipedia Pageviews statistics

Wikipedia, an important encyclopedia portal, is one of the top five most popular domains on the global internet[15]. Wikipedia Pageviews statistics (https://pageviews.wmcloud.org/) is a freely available tool for Wikipedia pages that shows how many people have visited an article in a given period since July 2015.

Google Trends tool

Google Trends (https://trends.google.com/trends/) is a freely available online tool that allows the analysis of a selected expression, in a chosen region and period since January 2004. Google Trends enabled the comparison of up to five terms at once.

The tool estimates the relative search volume (RSV) of queries made using the Google search engine. RSV is an index of search volume adjusted to the number of Google users in a given geographic area and time interval. RSV ranges from 0 to 100, with 100 indicating peak popularity (100% of popularity in a given time and location) and 0 indicating total disinterest (0% of popularity in a given period and location)[19,20].

Google Trends may qualify analyzed phrases as "search term" or "topic". Search terms are literal typed words, whereas Google Trends may suggest topics when it recognizes phrases linked to popular queries. Topics allow for easy comparison of the provided term across countries. For example, Google Trends will analyze the search term "diet" literally; thus, RSV will be highest in English-speaking countries, whereas the topic "diet" will include all queries linked with the query in all available languages[15,20].

Data collection

We used Google Trends and Wikipedia Pageviews statistics for collecting data from 1 July 2015 to 1 May 2023. We first used the Wikipedia tool Forge to access the pageview statistics of the countries related to the relevant terms (https://pageviews.wmcloud.org/langviews/). When the term "sustainability" was searched in tool forge, we found that a total of 60 languages were searched between 01.07.2015 and 01.05.2023. For Wikipedia pageviews statistics, we analyzed these 60 language-speaking countries. Although Wikipedia has a tool (Wikidata) that provides structured data on page views, we quickly perceived that many selected terms' pages were not registered in Wikipedia's category. Therefore, we manually verified if each selected term had a Wikipedia page. To do this, we used Google Search with the strings such as "site:en.wikipedia.org" (for the English version)", and the name of each selected term (e.g. sustainable diet site:en.wikipedia.org). Moreover, searches were conducted independently for each selected country using the filters "Country", "All Categories", and "Web Searches" for countries speaking these 60 languages for Google Trends.

The same search terms are used wherever possible between Google and Wikipedia searches. We determined the general topics as "sustainability" and diet-related terms such as "sustainable diet", "healthy diet", "plant-based diet",

"Climatarian diet", "flexitarianism", "Japanese diet", "Mediterranean diet", "Nordic diet", "vegetarianism", "veganism", "raw foodism", "fruitarianism", and "pescetarianism". We also searched "lacto-vegetarianism", "ovo-vegetarianism", and "lacto-ovo vegetarianism", however, the data were very limited. Therefore, we excluded these terms. We chose these diet-related terms according to the reports published reports by WHO and IPCC Reports[3,21]. Additionally, we have added the term Climatarian diet because it is an up-to-date term that covers the contents of sustainable diets[11].

Selected terms in all countries speaking these 60 languages were searched according to the official language of the countries. Then, countries without Google Trends RSVs were excluded. Hereby, Google Trends RSVs for Türkiye, Australia, Canada, the United Kingdom, Ireland, Germany, Spain, Mexico, Brazil, Netherlands, Belgium, Austria, Switzerland, France, The United States of America (USA), Greece, Russia, Poland, Czech Republic, Denmark, India, Norway, Croatia, Vietnam, Finland, and Sweden were included. No Wikipedia pageviews statistics and Google Trends RSVs could be retrieved for other countries (for sustainability).

Statistical analysis

Data were analyzed using SPSS version 24.0. Due to the structure of the data, non-parametric tests were used as a conservative approach. Jonckheere-Terpstra test was used to determine if there was a statistically significant trend of RSVs for sustainability, sustainable diet, healthy diet, plant-based diet, Climatarian diet, flexitarianism, Japanese diet, Mediterranean diet, Nordic diet, vegetarianism, veganism, raw foodism, fruitarianism, pescetarianism across time. The Kendall's Tau correlation coefficient was used to determine pairwise correlations between sustainability RSVs and RSVs of sustainable diet, healthy diet, plant-based diet, Climatarian diet, flexitarianism, Japanese diet, Mediterranean diet, Nordic diet, vegetarianism, veganism, raw foodism, fruitarianism, pescetarianism. We performed the seasonal Mann–Kendall test using XLSTAT Statistical Software for Excel to search for the presence of a significant secular trend of time series. For all statistical tests, a p-value of <0.05 was considered statistically significant.

RESULTS and DISCUSSION

According to Wikipedia pageviews results, healthy diet, plant-based diet, Climatarian diet, and Mediterranean diet showed positive trends (22.05%, 9109,52%, 420.53%, and 7,14%, respectively), however, sustainability, sustainable diet, flexitarianism, vegetarianism, veganism, raw-foodism, fruitari-

anism, and pescetarianism were decreased over time (%4.15, %31.89, %18.51, %44.96, %62.16, %66.49, %38.29, %22.97, respectively). Based on the Google Trends RSVs, sustainability, sustainable diet, plant-based diet, flexitarianism, Mediterranean diet, fruitarianism, and pescetarianism increased (226.91%, 224.74%, 92.91%, 779.07%, 361.83%, 65.55%, and 565.08%, respectively), whereas healthy diet, Climatarian diet, Japanese diet, Nordic diet, vegetarianism, and raw foodism decreased between 2015 to 2023 (29.63%, 50.77%, 33.08%, 70.07%, 45.04%, 41.03%). The term "veganism" was found no changes over time (Figure 1).

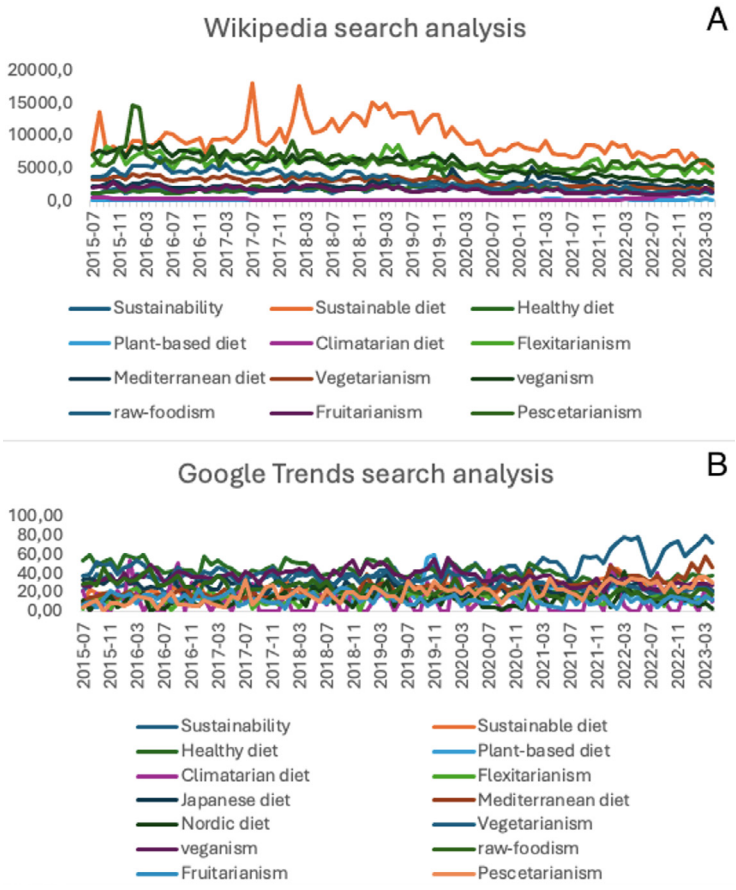

Figure 1. Search volume for the terms "sustainability, sustainable diet, healthy diet, plant-based diet, climatarian diet, flexitarianism, Japanese diet, Mediterranean diet, Nordic diet, vegetarianism, veganism, raw-foodism, fruitarianism, pescetarianism" across two online platforms (A: Wikipedia search analysis, B: Google Trends search analysis)

For all topics, Table 1 shows the top five countries with the highest worldwide RSV. Sustainability was particularly popular in European countries. Similarly, as many as three of the five top countries with the highest interest in the sustainable diet, healthy diet, plant-based diet, Mediterranean diet, raw foodism, and pescatarianism, included European countries. Climatarian diet was a new term, and only three countries were searched. Flexitarianism was popular mostly in Eastern European countries. The highest RSV for the Japanese diet, and Nordic diet were found in the USA and the United Kingdom. Vegetarianism and veganism were generally popular in United States countries. Fruitarianism was prevalent in the United States, European, and Asian countries.

Table 1. Top five countries with the highest page views and RSV by region of all related topics according to Google Trends data

Topic	Top 5 countries with the highest RSV
Sustainability	Australia (65.58), Netherlands (60.65), Switzerland (58.39), Canada (58.10), Russia (57.18)
Sustainable diet	France (40.43), Germany (40.28), USA (40.21), United Kingdom (34.94), India (20.46)
Healthy diet	Australia (73.64), USA (73.47), India (65.04), Canada (64.09), France (60.63)
Plant-based diet	USA (41.55), Germany (33.09), Türkiye (30.74), Poland (22.79), Canada (21.08)
Climatarian diet	United Kingdom (12.69), Australia (11.21), USA (10.91)
Flexitarianism	France (32.46), Russia (20.63), Australia (17.10), Brazil (16.02), Poland (15.01)
Japanese diet	USA (68.20), United Kingdom (53.97), Russia (46.54), Brazil (35.01), India (34.67)
Mediterranean diet	Australia (50.37), Canada (44.64), United Kingdom (44.20), France (39.93), Poland (36.36)
Nordic diet	United Kingdom (25.43), Canada (24.42), USA (16.61), Australia (15.48), France (13.46)
Vegetarianism	Poland (65.78), Brazil (56.42), United Kingdom (50.74), USA (48.98), Russia (48.54)
Veganism	USA (60.24), Germany (59.52), Spain (58.64), Mexico (57.92), Canada (57.65)
Raw-foodism	Germany (63.68), Austria (54.21), Switzerland (49.68), Russia (44.76), Türkiye (25.70)
Fruitarianism	Brazil (26.08), Vietnam (20.70), Poland (17.39), Russia (16.96), Spain (14.35)
Pescatarianism	Russia (36.35), United Kingdom (32.00), Canada (31.74), USA (31.37), Australia (22.88)

Table 2 shows the correlation between sustainability and diet-related topics. There was a positive correlation between sustainability and healthy diet, plant-based diet, Mediterranean diet, veganism, raw foodism, and pescetarianism according to both Wikipedia and Google Trends. Sustainability showed a positive correlation between sustainable diet in Google Trends (τ=0.201, p<0.001), whereas it showed a negative correlation in Wikipedia (τ=-0.563, p<0.001). Based on Wikipedia, sustainability presented a positive and moderate correlation with flexitarianism (τ=0.465, p<0.001), vegetarianism (τ=0.422, p<0.001), and a positive weak correlation with fruitarianism (τ=0.278, p<0.001). Japanese diet and the Nordic diet were weakly associated with sustainability according to Google Trends (τ=0.090, p<0.001, τ=0.111, p<0.001, respectively).

Table 2. Sustainability correlations with diet-related topics

	Wikipedia Pageviews Statistics	**Google Trends RSVs**
	τ; p	τ; p
Sustainability vs Sustainable diet	-0.563, <0.001**	0.210; <0.001**
Sustainability vs Healthy diet	0.383, <0.001**	0.133, <0.001**
Sustainability vs Plant-based diet	0.097, <0.001**	0.061, <0.001**
Sustainability vs Climatarian diet	-0.509, <0.001**	0.026, 0.574
Sustainability vs Flexitarianism	0.465, <0.001**	-0.023, 0.217
Sustainability vs Japanese diet	-	0.090, <0.001**
Sustainability vs Mediterranean diet	0.477, <0.001**	0.190, <0.001**
Sustainability vs Nordic diet	-	0.111, <0.001**
Sustainability vs Vegetarianism	0.422, <0.001**	0.011, 0.437
Sustainability vs Veganism	0.453, <0.001**	0.115, <0.001**
Sustainability vs Raw-foodism	0.204, <0.001**	0.087, <0.001**
Sustainability vs Fruitarianism	0.278, <0.001**	-0.018, 0.346
Sustainability vs Pescatarianism	0.366, <0.001**	0.156, <0.001**

Table 3 shows the time-series analysis of all related topics according to Google Trends. The RSV most dynamically increased over the observational period for topics sustainability (τ=0.778, p<0.001), sustainable diet (τ=0.378, p=0.002), plant-based diet (τ=0.484, p=0.006), the Mediterranean diet (τ=0.738, p<0.001), and pescetarianism (τ=0.494, p=0.004); whereas the RSV most rapidly decreased for Healthy diet (τ=-0.680, p<0.001), Japanese diet (τ:=-0.235, p: 0.027), vegetarianism (τ=-0.794, p<0.001), and raw-foodism (τ=-0.659, p<0.001).

Table 3. Time-series analysis of all related topics according to Google Trends

Topic	The month with the highest seasonal component (RSV)	The month with the lowest seasonal component (RSV)	Seasonal Mann–Kendall test (τ, p)	Mean ± SS
Sustainability	April (59.62)	July (36.50)	0.778, <0.001**	50.01 ± 16.01
Sustainable diet	May (50.42)	July (25.25)	0.378, 0.002*	37.57 ± 23.22
Healthy diet	January (83.6)	December (51.18)	-0.680, 0.001**	63.77 ± 15.35
Plant-based diet	February (31.8)	July (23.06)	0.484, 0.006**	26.90 ± 23.17
Climatarian diet	March (19.87)	May (2.57)	-0.133, 0.210	11.80 ± 24.63
Flexitarianism	May (21.57)	August (6.00)	0.127, 0.206	12.59 ± 22.81
Japanese diet	January (77.62)	October (49.00)	-0.235, 0.027*	61.09 ± 17.58
Mediterranean diet	January (64.68)	December (28.06)	0.738, < 0.001**	40.08 ± 18.10
Nordic diet	June (30.71)	December (11.31)	0.127, 0.314	21.02 ± 21.47
Vegetarianism	November (58.81)	July (36.12)	-0.794, < 0.001**	49.86 ± 18.58
Veganism	January (51.62)	August (35.31)	-0.227, 0.225	41.96 ± 23.30
Raw-foodism	February (13.37)	August (3.75)	-0.659, 0.001**	8.86 ± 19.03
Fruitarianism	May (16.92)	August (4.68)	-0.195, 0.066	9.48 ± 15.91
Pescatarianism	July (42.93)	May (20.64)	0.494, 0.004*	31.68 ± 22.99

Table 4 shows the time-series analysis of all related topics according to Wikipedia. The pageviews most dynamically increased over the observational period for topics plant-based diet (τ=0.921, p<0.001), flexitarianism (τ=0.595, p=0.004), the Mediterranean diet (τ=0.413, p: 0.022); whereas the pageviews most rapidly decreased for Climatarian diet (τ=-0.722, p<0.001), vegetarianism (τ=-0.690, p=0.001), veganism (τ=-0.818, p<0.001), raw-foodism (τ=-0.802, p<0.001), fruitarianism (τ=-0.683, p<0.001), and pescetarianism (τ=-0.579, p=0.004).

Table 4. Time-series analysis of all related topics according to Wikipedia Pageviews Statistics

Topic	Seasonal Mann–Kendall test (τ, p)	Mean ± SS	The month with the highest seasonal component	The month with the lowest seasonal component
Sustainability	-0.135, 0.462	822.67 ± 187.01	January (1008.75)	December (715.00)
Sustainable diet	-0.183, 0.349	28668.56 ± 7867.05	February (31056.37)	December (24644.50)
Healthy diet	0.222, 0.264	18517.71 ± 16632.84	November (25739.25)	June (14983.00)
Plant-based diet	0.921, <0.001**	122.50 ± 161.70	March (181.00)	July (81.125)
Climatarian diet	-0.722, <0.001**	606.96 ± 1168.21	March (1059.25)	July (285.00)
Flexitarianism	0.595, 0.004*	51133.27 ± 12375.34	May (57337.14)	July (41531.25)
Mediterranean diet	0.413, 0.022*	41533.93 ± 18921.92	January (61840.75)	December (31282.37)
Vegetarianism	-0.690, 0.001**	45060.93 ± 10064.61	January (48426.00)	June (42410.42)
Veganism	-0.817, <0.001**	77735.26 ± 20420.61	January (89374.37)	June (71864.14)
Raw-foodism	-0.802, < 0.001**	9355.10 ± 2832.08	March (11108.25)	December (8507.62)
Fruitarianism	-0.683, < 0.001**	14216.08 ± 4333.54	July (15984.62)	December (12233.62)
Pescetarianism	-0.579, 0.004*	99600.03 ± 33359.75	January (131628.25)	June (89847.71)

Over the past decade, public interest in sustainability has increased, with consumers increasingly seeking information on their food consumption decisions' environmental and human health effects[22]. In this study, we used Wikipedia pageviews statistics and Google Trends, to our knowledge this was explored for the first time, to determine the public interest in sustainability and dietary patterns related to sustainability. We found that the RSV most dynamically increased over the observational period for topics sustainability, sustainable diet, plant-based diet, Mediterranean diet, and pescetarianism, whereas the pageviews most dynamically increased over the observational period for topics plant-based diet, flexitarianism, and Mediterranean diet. There was a positive correlation between sustainability and healthy diet, plant-based diet, Mediterranean diet, veganism, raw foodism, and pescetarianism according to both Wikipedia Pageviews statistics and Google Trends.

Sustainability has been a global concern in the last 50 years, but it is now vital[23]. Global Sustainable Development Report seeks to strengthen the science-policy interface as an evidence-based instrument to support policymakers and other stakeholders in the implementation of the 2030 Agenda across the social, economic, and environmental dimensions of sustainable development[24]. Therefore, the knowledge of the public about sustainability and related terms may be important to be a guide. A study reported that public interest in environmental sustainability increased significantly between 2009 and 2019 according to Google Trends[22]. Similarly, it was observed that there was a positive trend in sustainability from 2010 to 2021 in European countries using Google Trends[15]. We found that the interest in sustainability increased according to Google Trends, whereas the interest in sustainability did not change according to Wikipedia page views over time. However, Wikipedia is an encyclopedia that provides more scientific data than Google Trends. Therefore, it is not possible for scientific interest in the issues to fully coincide with the interest of the public.

The FAO defines sustainable diets as "diets with low environmental impacts which contribute to food and nutrition security and healthy life for present and future generations. Sustainable diets are protective and respectful of biodiversity and ecosystems, culturally acceptable, accessible, economically fair and affordable; nutritionally adequate, safe and healthy; while optimizing natural and human resources"[2]. This definition is quite complex, encompassing environmental, social, and economic factors. However, consumers' food choices play a key role in the transition to more sustainable diets. Therefore, it is of great importance to understand how consumers interpret the concept of "sustainability" according to their eating habits. A study found that the mean European RSVs for food sustainability significantly increased from 2010 to 2021[15]. However, a recent systematic review determined that consumers struggle to define "sustainability", and to estimate the environmental impact of their food choices[25]. According to Google Trends, there was an increasing trend in sustainable diet over time in this study, not Wikipedia page views. It is possible that the results are contradictory because the changes in sustainable diet and food sustainability and public interest in these concepts occurred simultaneously but in some unrelated ways.

According to the WHO, a healthy diet is defined as the type of diet essential for health, well-being, optimal growth, and development. A healthy diet should also be more environmentally sustainable as it is associated with lower greenhouse gas emissions, less freshwater, and land mass use[4]. It was observed that the interest in healthy diet from 2010 to 2021 increased in the Northern

and Western European regions by using Google Trends[17]. Another study, using Google Trends, showed that the interest in healthy diet globally decreased from 1 January 2004 to 30 June 2020[26]. We found that interest in a healthy diet decreased according to Google Trends, whereas it increased according to Wikipedia Pageviews. Time-series analysis showed that interest in a healthy diet followed a negative trend according to Google Trends, while there was no statistically significant trend according to Wikipedia Pageviews over time. While our results were similar to the study evaluating the worldwide, the other study may have been different as it only included the European region.

The Mediterranean diet is thought the most beneficial type of diet, so we chose it[27]. A study showed that according to Google Trends, from 2004 to 2019, interest in the Mediterranean diet increased[20]. Another study showed that statistically significant seasonal differences were found for the Mediterranean (the mean pageviews were highest in spring) from 2015 to 2021 according to Wikipedia[14]. We found that global interest in the Mediterranean diet increased according to both Google Trends and Wikipedia from July 2015 to May 2023, and the mean Pageviews were highest at the beginning of the year. New Year's resolutions appear to be a fantastic opportunity to influence the establishment of new health goals.

The Climatarian diet is a new term that refers to a group of environmentally oriented diets (including plant-based and flexitarian diets)[3,11]. It was observed that the interest in plant-based diet increased from 2004 to 2019 according to Google Trends, and it was most popular in the USA[20]. According to the literature, only one study evaluated the interest in flexitarianism, and that found that the interest in flexitarianism from 2010 to 2021 increased in most European countries by using Google Trends[15]. The present study showed that the plant-based diet increased according to both Google Trends and Wikipedia, however, flexitarianism increased, and the Climatarian diet decreased according to only Wikipedia. Similarly, we found that the term plant-based diet is most popular in the USA. We did not find any statistically significant in the term flexitarianism and Climatarian diet according to Google Trends, and compared to Portugal-Numes et al., the mismatch in these findings may lie in the regional specificity[15]. Additionally, the Climatarian diet is a new term, and only three countries searched this term in our findings.

Vegetarian diets (including fruitarianism, pescetarianism, and raw foodism) reduce greenhouse emissions compared to omnivore diets[28]. Therefore, we searched these terms in addition to other vegetarian diets such as lacto-ovo, ovo, and lacto. However, the data about lacto-ovo, ovo, and lacto vegetarianism is not enough to analyze, thus they were excluded. It was observed that

global interest in raw foodism, pescetarianism, veganism, and vegetarianism increased according to Google Trends from 2004 to 2019[20]. A study showed that statistically significant seasonal differences were found for vegetarian (the mean pageviews highest in spring), and pescetarianism diets (the mean pageviews highest in winter) from 2015 to 2021 according to Wikipedia Pageviews[14]. We found that the trend in pescetarianism significantly increased, however vegetarianism and raw-foodism significantly decreased according to Google Trends; and vegetarianism, raw-foodism, veganism, pescetarianism, and fruitarianism significantly decreased according to Wikipedia. The reason for this difference may be due to the fact that we analyzed the years July 2015 to May 2023 in order to compare both Google Trends and Wikipedia data.

The study has some limitations. First, Wikipedia pageviews analysis does not contain precise location data, making it difficult to locate viewers due to its privacy policy. Summary data is available for each Wikipedia language providing the page view rate by country, and a page's language can be used as a rough proxy for its geography[29]. However, Wikipedia pageviews statistics have advantages over other metadata in measuring public interest. They reflect the search for information about a topic and involve the highest amount of user interaction[30]. Second, Google Trends contains precise location data, but it does not provide real-time usage data and more precise time intervals, which reduces predicting capability. Also, these results lack transparency, as there is no clear data on the methods used by Google to calculate RSVs[26]. Third, both Google Trends and Wikipedia Pageviews statistics do not provide user characteristics. Therefore, the results cannot be generalized to Internet users.

On the contrary, the study has some strengths. In the study, firstly, using Wikipedia pageviews statistics, a total of 60 languages containing the word "sustainability" were searched. In this context, sustainability and diet-related terms were all researched with Google Trends RSVs in all 60 languages-speaking countries. Therefore, the study provides a valuable resource for future studies.

In conclusion, here it was explored, for the first time, public interest in sustainability and sustainable diet-related topics. According to our results, there was a growing interest in sustainability, sustainable diet, plant-based diet, Mediterranean diet, and pescetarianism according to the RSVs, whereas the page views most dynamically increased over the observational period for topics plant-based diet, flexitarianism, and Mediterranean diet. We believe that more research is needed to reflect real life in this field, however, Google Trends and Wikipedia pageviews statistics have the potential to be useful tools. Understanding the public's interest in sustainability and sustainable diets is criti-

cal to developing and choosing strategies for transitioning to sustainable diets. Therefore, our findings could help scientists, practitioners, policymakers, as well as the public who are interested in diet-related topics. Moreover, artificial intelligence has begun to support search tools as of 2023. Currently, Microsoft Bing is using Chat GPT, etc., and Google has started its algorithm and Google Bard, whereas Wikipedia still uses its algorithm called page view statistics. In summary, Google searches and Wikipedia with their algorithm and give these results in Google trends and Wikipedia pageviews statistics, this study can be an important source for the question of how this will change with artificial intelligence in the future.

STATEMENT OF ETHICS

Not applicable.

CONFLICT OF INTEREST STATEMENT

No conflict of interest was declared by the authors.

AUTHOR CONTRIBUTIONS

Design: HMB, AÖ; Acquisition of Data: HMB; Analysis of Data: HMB; Statistical Analysis: HMB, Drafting of the Manuscript: HMB; Critical Revision of the Manuscript: AÖ; Statistical Analysis: HMB; Supervision: AÖ.

FUNDING SOURCES

The authors declared that this study received no financial support.

ACKNOWLEDGMENTS

This paper presents a research study that used Google Trends and Wikipedia-Page view analysis. All authors had access to the data and played an important role in writing the paper.

REFERENCES

1. Bayram HM, Ozturkcan SA. Greenhouse gas emissions in the food system: current and alternative dietary scenarios. Med J Nutrition Metab, 2022;15(4):463-477. Doi: 10.3233/MNM-220006

2. Food and Agriculture Organization. International Scientific Symposium: Biodiversity and Sustainable Diets United Against Hunger; 2010; Rome, Italy.

3. Willett W, Rockström J, Loken B, Springmann M, Lang T, Vermeulen S, et al. Food in the anthropocene: the EAT-*Lancet* commission on healthy diets from sustainable food systems. Lancet, 2019;393(10170):447-492. Doi: 10.1016/S0140-6736(18)31788-4

4. World Health Organization. Accessed July 10, 2023. Available from: https://www.who.int/newsroom/fact-sheets/detail/healthy-diet

5. Springmann M, Wiebe K, Mason-D'Croz D, Sulser TB, Rayner M, Scarborough P. Health and nutritional aspects of sustainable diet strategies and their association with environmental impacts: a global modelling analysis with country-level detail. Lancet Planet Health, 2018;2(10):e451-e461. Doi: 10.1016/S2542-5196(18)30206-7

6. Macdiarmid JI. Is a healthy diet an environmentally sustainable diet? Proc Nutr Soc, 2013;72(1):13-20. Doi: 10.1017/S0029665112002893

7. Nelson ME, Hamm MW, Hu FB, Abrams SA, Griffin TS. Alignment of healthy dietary patterns and environmental sustainability: a systematic review. Adv Nutr, 2016;7(6):1005-1025. Doi: 10.3945/an.116.012567

8. Perignon M, Vieux F, Soler LG, Masset G, Darmon N. Improving diet sustainability through evolution of food choices: review of epidemiological studies on the environmental impact of diets. Nutr Rev, 2017;75(1):2-17. Doi: 10.1093/nutrit/nuw043

9. Clune S, Crossin E, Verghese K. Systematic review of greenhouse gas emissions for different fresh food categories. J Clean Prod, 2017;140:766-783. Doi: 10.1016/j.jclepro.2016.04.082

10. Soedamah-Muthu SS, De Goede J. Dairy consumption and cardiometabolic diseases: systematic review and updated meta-analyses of prospective cohort studies. Curr Nutr Rep, 2018;7(4):171-182. Doi: 10.1007/s13668-018-0253-y

11. Lohmann PM, Gsottbauer E, Doherty A, Kontoleon A. Do carbon footprint labels promote climatarian diets? Evidence from a large-scale field experiment. J Environ Econ Manag, 2022;114:102693. Doi: 10.1016/j.jeem.2022.102693

12. World Health Organization. Accessed July 10, 2023. Available from: https://apps.who.int/iris/bitstream/handle/10665/329409/9789241516648-eng.pdf

13. De Mauro A, Greco M, Grimaldi M. What is big data? A consensual definition and a review of key research topics. AIP Conf Proc, 2015;1644:97-104. Doi: 10.1063/1.4907823

14. Nucci D, Santangelo OE, Nardi M, Provenzano S, Gianfredi V. Wikipedia, Google Trends and diet: assessment of temporal trends in the internet users' searches in Italy before and during COVID-19 pandemic. Nutrients, 2021;13(11):3683. Doi: 10.3390/nu13113683

15. Portugal-Nunes C, Nunes FM, Saraiva C, Gonçalves C. Public interest in food sustainability: an infodemiology study of Google Trends Data in Europe from 2010–2021. Int J Food Sci Nutr, 2023;74(1):95-106. Doi: 10.1080/09637486.2022.2151988

16. Bianchi T. Accessed July 10, 2023. Available from: https://www.statista.com/statistics/216573/worldwide-market-share-of-search-engines/

17. Al Qundus J, Paschke A, Kumar S, Gupta S. Calculating trust in domain analysis: theoretical trust model. Int J Inf Manag, 2019;48:1-11. Doi: 10.1016/j.ijinfomgt.2019.01.012

18. Gerguis MN, Salama C, El-Kharashi MW. Natural language processing and information systems. 22nd International Conference on Applications of Natural Language to Information Systems; 2017; Liège, Belgium. Liège (Belgium): Springer International Publishing; 2017.

19. Nuti SV, Wayda B, Ranasinghe I, Wang S, Dreyer RP, Chen SI, et al. The use of Google Trends in health care research: a systematic review. PLOS One, 2014;9(10):e109583. Doi: 10.1371/journal.pone.0109583

20. Kamiński M, Skonieczna-Żydecka K, Nowak JK, Stachowska E. Global and local diet popularity rankings, their secular trends, and seasonal variation in Google Trends data. Nutrition, 2020;79:110759. Doi: 10.1016/j.nut.2020.110759

21. Mbow C, Rosenzweig C, Barioni LG, Benton TG, Herrero M, Krishnapillai M, et al. Climate Change and Land: an IPCC special report on climate change, desertification, land degradation, sustainable land management, food security, and greenhouse gas fluxes in terrestrial ecosystems. Geneva: IPCC; 2019. p. 437-550.

22. Tulloch AI, Miller A, Dean AJ. Does scientific interest in the nature impacts of food align with consumer information-seeking behavior? Sustain Sci, 2021;16:1029-1043. Doi: 10.1007/s11625-021-00920-3

23. Independent Group of Scientists appointed by the Secretary-General. Global Sustainable Development Report 2019: The Future is Now – Science for Achieving Sustainable Development. New York: United Nations; 2019. p. 120-125.

24. Independent Group of Scientists appointed by the Secretary-General. Global Sustainable Development Report 2023: Times of crisis, times of change: Science for accelerating transformations to sustainable development. New York: United Nations; 2023. p. 1-21.

25. van Bussel LM, Kuijsten A, Mars M, van't Veer P. Consumers' perceptions on food-related sustainability: a systematic review. J Clean Prod, 2022;342:130904. Doi: 10.1016/j.jclepro.2022.130904

26. Palomo-Llinares R, Sánchez-Tormo J, Wanden-Berghe C, Sanz-Valero J. Trends and seasonality of information searches carried out through google on nutrition and healthy diet in relation to occupational health: infodemiological study. Nutrients, 2021;13(12):4300. Doi: 10.3390/nu13124300

27. Katz DL, Meller S. Can we say what diet is best for health? Annu Rev Public Health, 2014;35:83-103. Doi: 10.1146/annurev-publhealth-032013-182351

28. Kustar A, Patino-Echeverri D. A review of environmental life cycle assessments of diets: plant-based solutions are truly sustainable, even in the form of fast foods. Sustainability. 2021;13(17):9926. Doi: 10.3390/su13179926

29. Mittermeier JC, Roll U, Matthews TJ, Grenyer R. A season for all things: phenological imprints in Wikipedia usage and their relevance to conservation. PLoS Biology, 2019;17:e3000146. Doi: 10.1371/journal.pbio.3000146

30. Yu AZ, Ronen S, Hu KZ, Hidalgo CA. Pantheon 1.0, a manually verified dataset of globally famous biographies. Sci Data, 2016;3:150075. Doi: 10.1038/sdata.2015.75

Acta Pharm. Sci. Vol 63:(1), 2025
Original article
DOI: 10.23893/1307-2080.APS6306

Determination of some components in *Valencia albedo* and monitoring its bioeffects in experimental mice

May EBRAHEEM*, Dima AL DIAB

Tishreen University, Faculty of Pharmacy, Department of Analytical and Food Chemistry, Lattakia, Syrian Arab Republic

ABSTRACT

This study aims to identify the most important components in the albedo layer of Valencia (*Citrus sinensis*) fruit peel, and to evaluate the effect of albedo on weight and blood glucose levels in experimental rats. The percentage of moisture, ash, fat, protein, carbohydrate and dietary fibers in albedo were (61.94, 3.57, 1.51, 3.19, 78.2, 13.45), respectively, and the content of phenolic compounds in albedo was 19.9 g GAE/kg. The albedo powder in the mice diet led to a decrease in weight or to preventing its gain compared to the diet without albedo powder in a statistically significant way ($p<0.05$), the addition of albedo powder to the diet also led to a decrease in blood glucose levels in the mice of the second group compared to the first group, but with a statistically insignificant difference ($p>0.05$).

Keywords: Valencia fruit, albedo, weight, blood glucose, diet, experimental rats

INTRODUCTION

Citrus species are known as one of the most widely grown products in the world, as it is cultivated in more than 100 countries. The global production of citrus is estimated at about 88-115 million tons annually[1]. Brazil is considered the most productive country of citrus in the world[2], while Syria ranks third in the Arab world in citrus production and twentieth in the world as its production of about one million tons represents about 1% of global production[3].

*Corresponding author: May EBRAHEEM
E-mail: may.ebraheem@tishreen.edu.sy
ORCIDs:
May EBRAHEEM: 0009-0007-4592-285X
Dima AL DIAB: 0009-0007-8957-6717
(Received 2 Sep 2023, Accepted 4 Mar 2024)

Citrus is the largest genus in the Rutaceae family, which consists of 150 genera and about 1,600 species, but the exact number of species is still unclear[4]. Among the types of citrus fruits, orange production constitutes the largest portion of the total world production, followed by mandarins, then lemons, and finally grifons. The most common sweet orange is the 'Valencia' as it is among the most widely cultivated varieties worldwide, due largely to their high productivity[5,6].

The orange fruit consists of an outer layer (peel) and an inner substance (pulp). The outer shell is divided into two parts: an outer part is the colored part (epicarp or exocarp) and is called flavedo, and an inner part is the white part (mesocarp) and is called albedo. The inner substance (pulp) is called endocarp and contains vesicles with juice[7].

Citrus fruits are consumed fresh, or the different parts of the fruits are used in many fields (foods and pharmaceutical industries)[4]. Citrus fruits are also consumed after they have been processed and converted into many forms of products where the most common product of citrus fruits is fresh or concentrated juice. It is estimated that the industrial processing of citrus fruits uses 33% of citrus fruits to produce juice[8]. The process of converting citrus fruits to obtain juices generates a large amount of by-products (residues) that reach about 50-70% of the weight of the fruit, most of it are peels (60-65%)[9].

Citrus waste is often thrown into landfills or rivers, which causes environmental and water pollution[10]. As another option, citrus waste is also disposed of by burning[11].

Although citrus by-products are sometimes called citrus waste, they still contain large amounts of valuable compounds[12]. So, the concept of recycling and reuse is necessary in order to reduce the waste generated and the associated damages. In addition, this may reduce the excessive consumption of raw materials and increase economic profits and allow the use of the biological value of citrus waste[13], especially that citrus by-products are rich in contents of high health and economic value, such as proteins, fats, sugars, essential oils and vitamins, in addition to containing polyphenols and dietary fibers[8].

Phenolic compounds are plant secondary metabolites; have lots of beneficial effects on human health. There are currently about 8,000 polyphenols, generally classified into flavonoids and non-flavonoids (phenolic acids, coumarins, stilbenes and lignans)[14]. Flavonoids are classified into subclasses including flavones, flavanones, isoflavanones, flavonols, isoflavanoids, anthocyanidins, and catechins[15]. The flavanones are the most present in citrus fruits among the flavonoid groups, and the flavanones are more concentrated in the albedo and membranes than in juice bags[4]. The most important flavonoids found in

sweet oranges are hesperidin, hesperitin, diosmin, and diosmetin, in addition to narirutin[16]. Phenolic compounds structure is rich in hydroxyl groups which enable these compounds to be antioxidants and scavenge free radicals[17,18]. Antioxidants are important for health and disease prevention by reducing the damage caused by free radicals[18-20], like its anti-inflammatory[14,21], antibacterial and antifungal activity, beside its anti-hyperglycemic[22,23], and anticoagulant effects[24]. In addition, several in vitro studies have been conducted to evaluate the effects of citrus flavonoids on obesity. It has been found to have an effect on obesity by multiple mechanisms[25,26]. It was also found that effects on total body weight were more pronounced in studies using citrus peel extracts instead of standardized flavonoids, which indicates the possibility of synergy between the different phenols present in the peels[27].

Dietary fibers have been defined by The National Academy of Sciences as indigestible carbohydrates and lignin present in plants[28]. Dietary fibers are often classified based on their water solubility into water-soluble fibers (SDF) such as pectin and gum arabic, and insoluble fibers (IDF) such as cellulose, hemicellulose, and lignin. Citrus waste is a good source of dietary fiber where the main part of citrus waste in terms of dietary fiber content is albedo[16]. Albedo is a rich source of dietary fiber, especially pectin[9], as the proportion of pectin in orange albedo reaches 12-28%[29]. Studies indicate that increasing dietary fiber in the daily diet is very important for maintaining good health[16]. Frequent consumption of dietary fiber is associated with a lower risk of chronic diseases such as cardiovascular disease, diabetes, and obesity[30]. Considerable research has been conducted to evaluate the effect of dietary fiber on body weight, and it has shown an inverse relationship between fiber intake and body weight gain[31].

Albedo has better qualities than other sources of dietary fiber due to the presence of associated bioactive compounds such as flavonoids (mainly flavanones) and vitamins, which may lead to more health-promoting effects in addition to those found in dietary fiber[32].

Due to the spread of Obesity and Diabetes in addition to diseases and discarders related to them; and the possibility of reducing the risk of these diseases by regular and frequent consumption of vegetables and fruits (especially since there has been increased interest in using natural products instead of artificial ones in treating diseases). The importance of this research is the possibility of usage of the large amount of citrus waste and its ingredients in the treatment or prevention of diseases.

Therefore, the aim of this research is to study the biological effects of Valencia orange waste on body weight and blood glucose in experimental rats.

METHODOLOGY

Instruments

Analytical balance (RADWAG, AS 220/C/2), Air oven (Janat instruments), Electric grinder, Glucometer (O2 BG-202), Spectrophotometer (Jasco V-530 UV), Water bath Ultrasonic (K & H Industries).

Orange sample collection and preparation for the study

The fruits of Valencia (*Citrus sinensis*) were collected from the local market in Lattakia in the season of 2022, the fruits were washed and peeled manually, then the albedo was separated and cut into small pieces and dried in the air oven. Afterward, it was ground into a fine powder and kept in the refrigerator (-4°C) until use[33].

Chemical analysis

Moisture content, total ash, protein and fiber content were calculated by using AOAC Standard Method. Moisture content was determined by an oven method (drying until constant weight)[34]. Ash content was determined by using a muffle furnace maintained at 550°C for five hours[35]. Protein was determined by the Kjeldahl method, fiber was obtained by digesting sample with H_2SO_4 and NaOH followed by incinerating in muffle furnace at 550°C[34,36]. Fat was determined using hexane as a solvent, where about 0.5 g of the sample was weighed and soaked in 10 ml of hexane for a week (the tube was covered well), then hexane was taken with the fat substance in a clean and weighed plastic can, and left at room temperature until the hexane evaporated completely and the fat substance remained in the can (until weight stability), and the weight of the can with the oil substance was recorded. The percentage of fat in the sample was calculated according to the law:

Fat (%) = weight of the fat substance x 100 / weight of the sample

= (weight of the can with the fat substance - weight of the empty can) x 100 / weight of the sample

Carbohydrate content was calculated from the difference of 100 – [% moisture + % ash + % protein + % fibre + % fat][37].

Determination of pectin

The amount of pectin was determined in the dried, unground pieces of albedo using acid hydrolysis[38].

Extraction and determination of phenolic compounds

Phenolic compounds were extracted using the Ultrasound water bath[39]. About 5g of the sample was weighed and placed in a beaker with 50ml of ethanol 80%, then the beaker was placed in the water bath at a temperature of 35-40°C for half an hour, after that, the mixture was left to cool at room temperature, then filtered, and the extract was kept in the refrigerator until the levels of phenolic compounds were determined. For the determination of phenolic compounds levels, the Folin-Ciocalteu method was used[40].

Experimental animals

The study included normal adult female mice of the Balb-C species, ages (2-4) months and weighing (15-35) grams. They were placed in special cages that allow them to eat food and drink water easily, at room temperature (24 ± 2)°C in 12/12-hour light/dark cycles. The experiment was conducted in the laboratory of the experimental animal incubator at the Faculty of Pharmacy, Tishreen University, Syria. Ethical approval number: 524.

Experimental design

Eighteen mice were divided into two groups (n=9 in each group). The experiment lasted eight weeks. In the first week, mice were left to adapt to the laboratory conditions and were given normal food without additives. In the second week until the eighth week, each group was given its own food, as follows[41]:

1. First group (Normal Diet: ND): normal food without additives

2. Second group (Normal Diet with albedo: ND+A): normal food with albedo

Table 1 shows the food components of each group with their proportions:

Table 1. Food components of each group with their proportions

Component	First group	Second group
bread	80%	60%
corn	20%	20%
albedo	-	20%

The food was prepared by weighing the dry ingredients, then kneading it with water until it becomes a dough that can be formed, then the dough was formed in the form of small pieces and air-dried.

The weight of the mice was measured once a week, and the blood sugar was measured in the last week after fasting for 16 hours by taking a drop of blood from the caudal vein and using the O2 BG-202 strip glucometer. These measurements were taken for each mouse separately.

Statistical analysis

The statistical study was conducted using the SPSS version 26 program, the Independent Samples T Test was used. P values lower than 0.05 were defined as statistically significant and corresponded to a confidence level of (95%).

RESULTS and DISCUSSION

Chemical analysis

Table 2 shows the values of the components that were determined in the albedo (Mean ± SD):

Table 2. Values of the components in the albedo (Mean ± SD)

Component (%)	
Moisture	61.94 ± 1.003
Ash	3.57 ± 0.33
Fat	1.51 ± 0.34
Protein	3.19 ± 0.33
Carbohydrate	78.2
Fiber	13.45 ± 0.71
Pectin	7.03

The result of moisture in the albedo was close to moisture levels in other studies, where it was 62.67% and 65.46%[42,43]. In a study conducted in Tunisia; researchers showed that citrus peels contain a very high level of water, up to 75%, this provides a suitable environment for mold growth, so it must be used immediately or stored under appropriate conditions until it is used[39]. The value of ash in our study converged with the result of a study conducted in 2021, where the percentage of ash was 3.21%[42]. According to a Brazilian study, the value of ash in the current study is considered a high value. The high ash value indicates that orange albedo contains a high content of minerals such as calcium, potassium, sodium, iron, copper, copper and magnesium[2,44].

The results of fat and carbohydrate in this study (1.51% and 78.2%, respectively) was higher than the fat and carbohydrate values reported by some other studies (0.27% and 57.15%, respectively)[45,46], while the value of protein (3.19%) was lower than the value reported by F. Omajasola et al. which was 4.69%[46].

The percentage of fiber in the albedo was 13.45%, which is higher than the value found by Mohammad et al. in Egypt (9.92%)[47], but lower than the value found by another study, where it was 27.67%[46]. Orange peel has a high level of fiber, and its unique physical and chemical properties make it suitable for food applications[47].

The result of pectin in this study was 7.03%, which is consistent with the result of the study conducted by Al-haj in 2022, where it found that the percentage of pectin in albedo ranges between (5.34-13.57%), depending on the time of harvesting the fruit[38].

The level of phenolic compounds was found to be equal to (19.9 ± 0.132) g GAE/kg, which is close to the value measured in one study, which was 17.16 g/kg[48], and higher than the result in a study conducted in Greece by Athanasiadis et al. where it was 9.2 g/kg[49] The levels of phenolic compounds in Valencia peel indicate a good antioxidant activity, as the higher the total content of phenolic substances, the higher the antioxidant capacity[50]. In addition, it gives an indication of the presence of antimicrobial activity according to some researchers[51].

The difference in the values of phenolic compounds between this study and some other studies may be due to the different solutions used to extract the phenolic compounds, or to the difference in the temperature at which the peels were dried, as it was found to affect the extraction yield of the phenolic compounds (drying at 80°C allows obtaining higher content of phenolic compounds compared to drying at 60°C and at 40°C for a longer period of time)[37,52].

In general, the difference in the levels of nutrient compounds in citrus cultivars or within the same cultivar can be attributed to climatic factors (type of soil, exposure to sunlight, rainfall...), genetic factors (diversity), and agricultural factors (maturity stage, fertilization, and irrigation...) and the analytical methods used[37].

It can be concluded that orange albedo has important properties and can be a promising source of nutritional compounds which play an important role in evaluating food quality such as dietary fiber and phenolic compounds and can be used as natural sources of functional ingredients or food additives[53], in addition to their good content of proteins and carbohydrates.

Effect on weight

Obesity is a chronic disease associated with an increase in the mass of adipose tissue, abnormal fat distribution and weight gain equal to or greater than 20% of normal weight[54]. Basically, obesity is a typical consequence of an imbalance

between calories in and calories out where the calories ingested are greater[55]. Obesity is a modifiable risk factor for type 2 diabetes, coronary heart disease, and hypertension[56]. The mainstay in the non-pharmacological treatment of obesity is diet and exercise. However, prescribing anti-obesity drugs can be a catalyst for obese patients who fail to achieve weight loss through diet and exercise[54]. Because of the adverse effects of these drugs; There has been a renewed interest in medicinal plants[57]. In recent years, the study of using citrus fruits in obesity and associated metabolic disorders prevention and treatment has attracted increasing attention[41].

Table 3 shows the total weights of the mice in the first week (the acclimation week), the second week, and the last week:

Table 3. Weights of the mice

	First group ND	Second group ND+A
Weight in 1st week	259	206
Weight in 2nd week	258	209
Weight in last week	277	210

Weight comparison between the Normal Diet group (ND) and the Normal Diet with Albedo group (ND+A)

For the effect of albedo on the weight of the mice; it was observed that the weight of the mice of the second group (ND+A) - where albedo was added to the diet - was significantly lower compared to the first group (ND) ($p<0.05$). That is, albedo prevented weight gain when added to the diet.

As mentioned earlier; albedo contains an important amount of fiber, especially pectin, and it also contains flavonoids. The effect of albedo on weight may be due to these two components.

These results agreed with the results of a study conducted by Osfor et al., which showed a decrease in body weight in rats fed a diet containing 20% *Citrus aurantium* albedo, which was attributed to a decrease in food consumption. This may be due to the high fiber content in albedo (about 10% relative to dry weight), specifically pectin, as the pectin present in orange peel can help reduce appetite [58].

These findings were supported by a study that investigated the effect of pectin on weight, which concluded that a high-fat diet with pectin led to weight loss

and reduced weight gain compared to a high-fat diet. This suggests that soluble fiber in diets may reduce weight gain caused by high nutrition. In general, dietary fiber may contribute to weight loss through several mechanisms including delaying gastric emptying (which give a feeling of fullness) and preventing fat absorption[59]. Thus, increasing the amounts of soluble dietary fiber in diet may be helpful method for weight reduction[60].

Studies that dealt with the effect of adding orange albedo on weight loss indicate the role of phenolic compounds as a study in Brazil determined content of phenolic compounds in albedo and the antioxidant activity of these compounds and indicated that the antioxidant activity of albedo and its beneficial metabolic effects may be linked to reducing oxidative stress associated with obesity. Therefore, this opens prospects for the development of food products based on the use of albedo for the prevention and treatment of obesity[61].

Citrus flavonoids have also effect on caloric intake[62], and inhibition of amylase function[63]. For example, some citrus flavonoids can suppress appetite by influencing hormones that control appetite (such as hesperidin and naringenin) or activating receptors that also suppress appetite (such as naringenin and naringenin), while both the flavonoids naringenin and nobiletin have been shown to increase energy expenditure in heat-producing brown adipose tissue[64].

Another anti-obesity strategy is to enhance lipolysis and reduce lipogenesis to reduce fat deposits by affecting enzymes. Some flavonoids, including naringenin, luteolin and hesperidin, have the ability to target enzymes such as fatty acid synthetase (FAS) and lipase Hormone-sensitive (HSL), which is involved in the mechanisms responsible for both the dissociation of existing fat cells or the generation of additional fat cells[62]. Additionally, hesperidin, neohesperidin, and luteolin have an inhibitory effect on the enzyme pancreatic lipase (PL) which is involved in the digestion of triglycerides leading to a strong effectiveness in the treatment of obesity as well[65]. In addition, naringenin, hesperidin, and quercetin were found to support the targeting of adipocytes (fat cells) through the process of apoptosis and thus reduce adipocyte numbers[66].

Effect on blood glucose levels

Diabetes mellitus is a chronic metabolic disorder characterized by higher blood sugar levels than normal values, it is caused by the inability of the pancreas to produce sufficient insulin, or it results from the ineffective use of the insulin that is produced[67].

There is a condition called “prediabetes” which is a chronic metabolic condition in which blood glucose values are higher than the upper limit that is con-

sidered normal, but less than the lower limit for diagnosing diabetes[68]. Prediabetes progresses to diabetes in up to 70% of individuals during their lifetime[69]. This condition may be reversible through lifestyle modification, by adopting a healthier diet and increasing levels of physical activity[68].

In our study the blood glucose values of the mice were measured in the last week of the experiment, after a 16-hour fasting, where a drop of blood was taken from the caudal vein, Table 4 shows the blood sugar values of the mice in each group:

Table 4. Blood sugar values of the mice

	ND	ND+A
1	**134***	61
2	**88**	74
3	**66**	61
4	**64**	78
5	**62**	58
6	**62**	**L
7	**85**	58
8	**85**	72
9	**62**	57
Mean ± SD	**71.75 ± 11.91**	64.87 ± 7.98

*Outlier excluded
**Low value not measured by instrument (L<30mg/dl)

Comparison of blood glucose levels between the Normal Diet group (ND) and the Normal Diet with Albedo group (ND+A)

Our results showed that ND+A mice had lower blood sugar values than the first group that ate a normal diet without albedo, but in no significant difference ($p>0.05$).

These results do not agree with the results of a study showed that the rats' intake of albedo in the proportions of 10% and 20% as a source of fiber in food significantly reduced blood glucose levels. This may be due to the presence of dietary fiber and polyphenols[58].

A lot of studies have examined the relationship between dietary fiber and diabetes. large number of reports indicate that soluble fiber (which includes pectin) can significantly improve glycemic control[70]. In general, dietary fiber can reduce blood glucose by increasing satiety by different mechanisms: increasing chewing, forming a gel in the stomach that delays gastric emptying, and reducing the interaction between lumenal contents and digestive enzymes, and thus reduces glucose absorption[71].

A study carried out in China on pectin extracted from orange peels has confirmed that experimental rats which consumed pectin had significant increase in hepatic glycogen content, and thus can reduce blood glucose, meaning that citrus pectin can enhances insulin sensitivity by stimulating hepatic glycogen synthesis. Pectin improved glucose tolerance, as was shown by Fasting Blood Glucose (FBG) and the Oral Glucose Tolerance Tests (OGTT), meaning that pectin reduced insulin resistance, which led to improvements in glucose metabolism[72].

In addition to pectin, phenolic compounds in albedo have beneficial effects on pancreatic cells by neutralizing oxidative stress due to their antioxidant activity, since previous studies have shown that high blood sugar leads to deterioration of pancreatic cells due to oxidative stress[73]. Some studies investigated the effect of the flavonoid's hesperidin and naringenin on blood sugar in experimental rats, where a significantly lower blood glucose was observed compared to the control group. Another study has found hypoglycemic effect of both hesperidin and naringenin, this effect was mediated by changes in hepatic glucose-regulating enzyme activities in mice, as these compounds increased hepatic glucokinase (an enzyme involved in the conversion of glucose into glycogen) and glycogen, and decreased levels of the enzyme glucose-6-phosphatase (involved in the breakdown of hepatic glycogen into glucose units), in addition to an increase in plasma insulin levels at the end of the study[73]. Other studies provide evidence that naringenin can inhibit intestinal glucose uptake as well as renal glucose reabsorption[74] in addition to significantly increasing glucose uptake into muscle and liver cells, which contributes to reduce blood glucose[58].

Obesity and diabetes are among the widespread diseases in the world, and the medications used to treat it have many side effects. Our study suggests that adding the *Valencia albedo* to the diet may help prevent or slow the development of these diseases due to beneficial health effects of active ingredients, like dietary fibers and polyphenol, which have shown weight and blood sugar lowering effects by several mechanisms.

STATEMENTS OF ETHICS

The protocols used in this study were following the guide for the care and use of experimental animals. The experiment was conducted in the laboratory of the experimental animal incubator at the Faculty of Pharmacy, Tishreen University, Syria. Ethical approval number: 524.

CONFLICT OF INTEREST STATEMENT

All authors declare that there is no conflict of interest.

AUTHOR CONTRIBUTIONS

All authors contributed to data collection and analysis, methodology, review, editing, and study design. All authors contributed to revision and approval of the final manuscript.

FUNDING SOURCES

This study was funded by Tishreen University.

ACKNOWLEDGMENTS

All authors thank Tishreen University for supporting this study.

REFERENCES

1. Lagha-Benamrouche S, Madani K. Phenolic contents and antioxidant activity of orange varieties (*Citrus sinensis* L. and *Citrus aurantium* L.) cultivated in Algeria: peels and leaves. Ind Crop and Prod, 2013;50:723-730. Doi: 10.1016/j.indcrop.2013.07.048

2. Castro LAD, Lizi JM, Chagas EGLD, Carvalho RAD, Vanin FM. From orange juice by-product in the food industry to a functional ingredient: application in the circular economy. Foods, 2020;9(5):593. Doi: 10.3390/foods9050593

3. Food and Agriculture Organization (FAO). Citrus Fruit Statistical Compendium 2020. Rome: FAO; 2021.

4. Matheyambath AC, Padmanabhan P, Paliyath G. Citrus fruits. In: Encyclopedia of Food and Health. 2016. p. 136-140.

5. Seminara S, Bennici S, Di Guardo M, Caruso M, Gentile A, La Malfa S. et al. Sweet orange: evolution, characterization, varieties, and breeding perspectives. Agriculture, 2023;13(2):264. Doi: 10.3390/agriculture13020264

6. Singh J, Sharma V, Pandey K, Ahmed S, Kaur M, Sidhu GS. Horticultural classification of citrus cultivars. Citrus - Research, Dev and Biotech, 2021;1-24. Doi: 10.5772/intechopen.96243

7. Zahra N, Alim-un Nisa KI, Saeed MK, Ahmad I, Hina S. Nutritional evaluation and antioxidant activity of zest obtained from orange (*Citrus sinensis*) peels. Int J Appl Sci, 2017;9(1):7-10.

8. Khan UM, Sameen A, Aadil RM, Shahid M, Sezen S, Zarrabi A, et al. Citrus genus and its waste utilization: a review on health-promoting activities and industrial application. Evid Based Comp Altern Med, 2021;1-17. Doi: 10.1155/2021/2488804

9. Nieto G, Fernández-López J, Pérez-Álvarez JA, Peñalver R, Ros G. Viuda-Martos M,. Valorization of Citrus co-products: recovery of bioactive compounds and application in meat and meat products. Plants, 2021;10(6):1069. Doi: 10.3390/plants10061069

10. Ruiz B, Flotats X. Citrus essential oils and their influence on the anaerobic digestion process: an overview. Waste Manag, 2014;34(11):2063-2079. Doi: 10.1016/j.wasman.2014.06.026

11. Siles JA, Vargas F, Gutiérrez MC, Chica AF. Martín MA. Integral valorisation of waste orange peel using combustion, biomethanisation and co-composting technologies. Bioresour Techno, 2016;211:173-182. Doi: 10.1016/j.biortech.2016.03.056

12. Chen Y, Tyler JB, Ruihong Z, Zhongli. Citrus. In: Integrated Processing Technologies for Food and Agricultural By-Products. Academic Press; 2019. p. 217-242. Doi: 10.1016/B978-0-12-814138-0.00009-5

13. Russo C, Maugeri A, Lombardo GE, Musumeci L, Barreca D, Rapisarda,A, et al.. The second life of *Citrus* fruit waste: a valuable source of bioactive compounds. Molecules, 2021;26(19):5991. Doi: 10.3390/molecules26195991

14. Al Diab D, Hasan N, Nezam A. Use of albumin denaturation inhibition method to determine the anti-inflammatory activity of phenolic compounds in some locally available fruit juices. Tishreen University Journal-Medical Sciences Series, 2021;43(1).

15. Puri M, Verma ML, Mahale K. Processing of citrus peel for the extraction of flavonoids for biotechnological applications. In: Yamane K, Kato Y, editors. Handbook on flavonoids: dietary sources, properties and health benefits. Hauppauge, New York: Nova Science Publishers; 2012. p. 443-459.

16. Mahato N, Sharma K, Sinha M. Cho MH.Citrus waste derived nutra-/pharmaceuticals for health benefits: current trends and future perspectives. JFF, 2018;40:307-316. Doi: 10.1016/j.jff.2017.11.015

17. Al Asaad N, Al Diab D. Determination of total antioxidant activity of fruit juices widely consumed in Syria. Res J of Phar and Tech, 2017;10(4):957-962. Doi: 10.5958/0974-360X.2017.00174.3

18. Aldiab D. Usage of phenolic extract of grape waste as natural antioxidant for milk proteins. JCHPS, 2018;11:196-200.

19. Al Asaad N, Al Diab D. Antioxidant activity and phenolic content of eight mediterranean fruit juices. Int J of Pharm Sci and Nanotech, 2016;9(3):3299-3304.

20. Sahunie A, Al-Diab D. Effect of rosemary and marjoram extracts on oxidative stability during heat treatment of sunflower oil. TUJ-MSS, 2023;45(1):293-305.

21. Nezam A, Al Diab D, Hasan N. In-vitro anti-inflammatory activity of total phenolic content of some fruit juices in Syria. Res J of Phar and Tech, 2021;14(7):3685-3688. Doi: 10.52711/0974-360X.2021.00637

22. Al-Diab D, Nasser S. Study of some factors affecting the levels of phenolic compounds and their antioxidant activity in some functional juices. TUJ-MSS, 2018;40(5).

23. Alsalti AA, Hasan N, Aldiab D. *In-vitro* and *in-vivo* hypoglycemic efficacy of *Rosa damascena* petals extracts. Bull Pharm Sci Assiut Uni, 2022; 45(2):593-604. Doi: 10.21608/bfsa.2022.271532

24. Ahmad A, Hasan N, Aldiab D. Study of the anticoagulant efficacy of Damask rose extract *in vitro*. TUJ-MSS, 2023;45(3):319-335.

25. Sergeev IN, Li S, Ho CT, Rawson NE, Dushenkov S. Polymethoxyflavones activate Ca2+-dependent apoptotic targets in adipocytes. J Agri Food Chem, 2009;57(13):5771-5776. Doi: 10.1021/jf901071k

26. Kanda K, Nishi K, Kadota A, Nishimoto S, Liu MC, Sugahara T. Nobiletin suppresses adipocyte differentiation of 3T3-L1 cells by an insulin and IBMX mixture induction. Biochim Biophys Acta, 2012;1820(4):461-468. Doi: 10.1016/j.bbagen.2011.11.015

27. Nakajima VM, Macedo GA, Macedo JA. Citrus bioactive phenolics: role in the obesity treatment. Food Sci and Technol, 2014;59(2):1205-1212. Doi: 10.1016/j.lwt.2014.02.060

28. Ryan-Harshman M, & Aldoori W. New dietary reference intakes for macronutrients and fibre. Can Fam physician, 2006;52(2):177.

29. Alhaj R, Al-Diab D. Pectin from some citrus species (Valencia-Griffon) and determination of some extraction properties. TUJ-MSS, 2022;44(2):253-275.

30. Figuerola F, Hurtado ML, Estévez AM, Chiffelle I, Asenjo F. Fibre concentrates from apple pomace and citrus peel as potential fibre sources for food enrichment. Food Chem, 2005;91(3):395-401. Doi: 10.1016/j.foodchem.2004.04.036

31. Ötles S, & Ozgoz S. Health effects of dietary fiber. Acta Sci Pol Technol Aliment, 2014;13(2):191-202. Doi: 10.17306/J.AFS.2014.2.8

32. Bianchi F, Larsen N, de Mello Tieghi T, Adorno MAT, Kot W, Saad SMI, et al. Modulation of gut microbiota from obese individuals by *in vitro* fermentation of citrus pectin in combination with *Bifidobacterium longum* BB-46. Appl Microbiol Biotechnol, 2018;102(20):8827-8840. Doi: 10.1007/s00253-018-9234-8

33. Oberoi HS, Vadlani PV, Nanjundaswamy A, Bansal S, Singh S, Kaur S, et al. Enhanced ethanol production from Kinnow mandarin (*Citrus reticulata*) waste via a statistically optimized simultaneous saccharification and fermentation process. Bioresource Technology, 2011;102(2):1593-1601. Doi: 10.1016/j.biortech.2010.08.111

34. Ibrahim Y, Samra S, Aldiab D. Microbiological control of some powdered milk preparations available in local market. TUJ-MSS, 2023;45(1):357-371.

35. Park YW. Determination of Moisture and Ash contents of Foods. Handbook of Food Analysis. 1st ed. New York: Marcel Dekker Inc.; 1996. p. 9-92.

36. Manuha M. Determination of nutrients value in five generally consuming Sri-Lankan rice varieties with concern on weight reduction. Int Multidiscip Res J, 2018;7(8):183.

37. Abdelazem RE, Hefnawy H, El-Shorbagy GA. Chemical composition and phytochemical screening of *Citrus sinensis* (orange) peels. ZJAR, 2021;48(3):793-804. Doi: 10.21608/zjar.2021.191315

38. Al-Diab D, Al-haj R. Extraction and characterization of pectin from grapefruit (*Citrus paradisi*) and valencia (*Citrus sinensis*). TUJ-MSS, 2022;44(2):253-275.

39. M'hiri N. Proximate chemical composition of orange peel and variation of phenols and antioxidant activity during convective air drying. J New Sci, 2015;30(4):881-890.

40. Al Diab D, Hasan N, Nezam A. Using albumin denaturation inhibition method to determine the anti-inflammatory activity of phenolic compounds in some locally available fruit juices. TUJ-HSS, 2021;43(1).

41. El-Shazly AH, Ahmed NS, Mohamed AY, Elhossary GG, Elsebaee FM. The potential prophylactic effect of orange peel administration on fatty liver and hyperlipidemia in an animal model of diet induced obesity. Egypt J Food Sci, 2017;45(1):57-66.

42. Baioumy AA, Abedelmaksoud TG. Quality properties and storage stability of beef burger as influenced by addition of orange peels (albedo). Theory Pract Meat Process, 2021;6(1):33-38.

43. Ammar M. Producing of high fiber chicken meat nuggets by using different fiber sources. Middle East J Agric Res, 2017;6(2):415-423.

44. Silva JGS, Rebellato AP, Greiner R, Pallone JAL. Bioaccessibility of calcium, iron and magnesium in residues of citrus and characterization of macronutrients. Food Res Int, 2017;97:162-169. Doi: 10.1016/j.foodres.2017.04.005

45. Levent N. Utilization of Citrus Albedo in Tarhana Production. J Food Nutr Res, 2014;53(2):162-170.

46. Omojasola PF, Adejoro DO. Submerged fermentation of orange albedo to produce gibberellic acid using *Fusarium moniliforme* and *Aspergillus niger*. Jordan J Biol Sci, 2018;11(2):187-194.

47. Osfor MMH, Hegazy A, Abd El-Moaty M, Elmadbouly MA, Afify AMR, Elbahnasawy ASM. Hypo-cholesterolemic and hypoglycemic effects of orange albedo powder (*Citrus Aurantium* L.) on male albino rats. Int J Nutr Food Sci, 2013;2(2):70. Doi: 10.11648/j.ijnfs.20130202.17

48. Kadhom IM, Ibrahim NS, Al-zubaidy NA. Estimation of phenolic compounds and evaluation of their antioxidant activity of some parts of the orange plant (*Citrus sinensis* L.). Eur J Mol Clin Med, 2020;7(3):4811-4822.

49. Athanasiadis V, Chatzimitakos T, Kotsou K, Palaiogiannis D, Bozinou E, Lalas SI. Optimization of the extraction parameters for the isolation of bioactive compounds from Ooange peel waste. Sustainability, 2022;14(21):13926. Doi: 10.3390/su142113926

50. Gorinstein S, Martín-Belloso O, Park YS, Haruenkit R, Lojek A, Ĉı´ž M. Comparison of some biochemical characteristics of different citrus fruits. Food Chem, 2001;74(3):309-315. Doi: 10.1016/S0308-8146(01)00157-1

51. Arora M, Kaur P. Antimicrobial & antioxidant activity of orange pulp and peel. Int J Sci Res, 2013;2:412-415.

52. Aldiab D. Effect of preparation conditions on phenolic content and antioxidant activity of various teas and herbal teas. J of Chem and Pharm Sci, 2018;11(3):222-226.

53. Ibrahim HM, Hamed AA. Some physicochemical and functional properties of lemon and orange peels. Int J Curr Microbiol Appl Sci, 2018;7:4871-4885.

54. Wedamulla NE, Fan M, Choi YJ, Kim EK. Citrus peel as a renewable bioresource: transforming waste to food additives. J Func Foods, 2022;95:105163. Doi: 10.1016/j.jff.2022.105163

55. Vaidya V. Psychosocial aspects of obesity. Health and Treatment Strategies in Obesity, 2006;27:73-85.

56. Arika WM, Kibiti CM, Njagi JM, Ngugi MP. Anti-obesity effects of dichloromethane leaf extract of *Gnidia glauca* in high fat diet-induced obese rats. Heliyon, 2019;5(11). Doi: 10.1016/j.heliyon.2019.e02800

57. World Health Organization. Obesity and overweight fact sheet. Geneva: World Health Organization; 2018.

58. Osfor MMH, Hegazy A, Abd El-moaty M, Elmadbouly MA, Afify AMR, Elbahnasawy AS. Hypo-cholesterolemic and hypoglycemic effects of orange albedo powder (*Citrus aurantium* L.) on male albino rats. Int J Nutr Food Sci, 2013;2(2):70-76. Doi: https://doi.org/10.11648/j.ijnfs.20130202.17

59. de Vries J, Miller PE, Verbeke K. Effects of cereal fiber on bowel function: a systematic review of intervention trials. WJG, 2015;21(29):8952. Doi: 10.3748/wjg.v21.i29.8952

60. Lattimer JM, Haub MD. Effects of dietary fiber and its components on metabolic health. Nutrients, 2010;2(12):1266-1289.

61. da Rocha PDS. Antioxidant and anti-obesity effects of albedo Flour *Citrus sinensis*. Free Radic Biol Med, 2016;100:171. Doi: 10.1016/j.freeradbiomed.2016.10.450

62. Westerterp KR. Diet induced thermogenesis. Nutr & Metab, 2004;1(1):1-5. Doi: 10.1186/1743-7075-1-5

63. Nater UM, Rohleder N. Salivary alpha-amylase as a non-invasive biomarker for the sympathetic nervous system: current state of research. Psychoneuroendocrinology, 2009;34(4):486-496. Doi: 10.1016/j.psyneuen.2009.01.014

64. Wang Y, & Reuss LE. Citrus Flavonoid Effects on Obesity: Uni Florida IFAS Extension, 2017;(2):1-3.

65. Yun JW. Possible anti-obesity therapeutics from nature – a review. Phytochem, 2010;71(14-15):1625-1641. Doi: 10.1016/j.phytochem.2010.07.011

66. Herold C, Rennekampff HO, Engeli S. Apoptotic pathways in adipose tissue. Apoptosis, 2013;18:911-916. Doi: 10.1007/s10495-013-0848-0

67. Saeedi P, Petersohn I, Salpea P, Malanda B, Karuranga S, Unwin N, et al. Global and regional diabetes prevalence estimates for 2019 and projections for 2030 and 2045: results from the International Diabetes Federation Diabetes Atlas. Diabetes Res Clin Pract, 2019;157:107843. Doi: 10.1016/j.diabres.2019.107843

68. American Diabetes Association. Microvascular complications and foot care: standards of medical care in diabetes–2020. Diabetes Care, 2020;43:14-31. Doi: 10.2337/dc20-s011

69. Hostalek U. Global epidemiology of prediabetes-present and future perspectives. Clin Diabetes Endocrinol, 2019;5(1):5. Doi: 10.1186/s40842-019-0080-0

70. Bray JK, Chiu GS, McNeil LK, Moon ML, Wall R, Towers AE, et al. Switching from a high-fat cellulose diet to a high-fat pectin diet reverses certain obesity-related morbidities. Nutr & Metab, 2018;15:1-10. Doi: https://doi.org/10.1186/s12986-018-0294-7

71. Kaczmarczyk MM, Miller MJ, Freund GG. The health benefits of dietary fiber: beyond the usual suspects of type 2 diabetes mellitus, cardiovascular disease and colon cancer. Metab, 2012;61(8):1058-1066. Doi: 10.1016/j.metabol.2012.01.017

72. Liu Y, Dong M, Yang Z, Pan S. Anti-diabetic effect of citrus pectin in diabetic rats and potential mechanism via PI3K/Akt signaling pathway. Int J Biol Macromol, 2016;89:484-488. Doi: 10.1016/j.ijbiomac.2016.05.015

73. Jung UJ, Choi MS, Lee MK, Jeong KS. The hypoglycemic effects of hesperidin and naringin are partly mediated by hepatic glucose-regulating enzymes in C57BL/KsJ-db/db mice. The Journal of nutrition, 2004;134(10):2499-2503. Doi: 10.1093/jn/134.10.2499

74. Den Hartogh DJ& Tsiani E. Antidiabetic properties of naringenin: a citrus fruit polyphenol. Biomolecules, 2019;9(3):99. Doi: 10.3390/biom9030099

Acta Pharm. Sci. Vol 63:(1), 2025
Original article
DOI: 10.23893/1307-2080.APS6307

Effect of *Ocimum gratissimum* L. leaf extract on muscular atrophy in diabetic male wistar rats

Shehu-Tijani SHITTU[1*], Ibrahim BELLO[1], Seyyid Alli-Sisse SHITTU[1]
Maryam AKOR-DEWU[2], Taye LASISI[1]

1 University of Ibadan, Department of Physiology, Ibadan, Nigeria
2 Ahmadu Bello University, Department of Human Physiology, Zaria, Nigeria

ABSTRACT

Oxidative stress and inflammation precipitate muscular atrophy in diabetes mellitus. The antioxidant and anti-inflammatory activities of *Ocimum gratissimum L.* (OG) is well documented. Thus, the effect of OG on muscular atrophy in diabetic rats was investigated. Twenty rats grouped as Control, OG, Diab and Diab+OG were administered distilled water or OG for 28 days. Glycogen content was determined in gastrocnemius muscle, oxidative stress biomarkers were assessed in right rectus femoris and extensor digitorum longus muscles while histomorphometry analysis was done in the contralateral muscles. Elevated blood glucose and depleted glycogen content were observed in the Diab (204.75 ± 9.95mg/dl and 0.09 ± 0.03mg/ml) and reversed in Diab+OG (90.01 ± 26.50mg/dl and 0.36 ± 0.05mg/ml). The lengths of the rectus femoris and extensor digitorum longus muscles were reduced while malonaldehyde increased in Diab (0.420 ± 0.031µmol/l) compared with Diab+OG (0.370 ± 0.01µmol/l). In conclusion, OG prevented atrophy and promoted glycogenesis by decreasing lipid peroxidation in the skeletal muscles of diabetic rats.

Keywords: muscular atrophy, diabetes mellitus, oxidative stress, *Ocimum gratissimum* L.

*Corresponding author: Shehu-Tijani SHITTU
Email: st.shittu@ui.edu.ng
ORCID:
Shehu-Tijani SHITTU: 0000-0002-7115-1960
Ibrahim BELLO: 0009-0004-3228-3233
Seyyid Alli-Sisse SHITTU: 0000-0002-6220-9948
Maryam AKOR-DEWU: 0000-0002-6122-4492
Taye LASISI: 0000-0002-3056-7548
(Received 1 Nov 2023, Accepted 4 Mar 2024)

INTRODUCTION

Onset, progression and complications of diabetes mellitus are closely associated with oxidative stress resulting from prolonged hyperglycemia[1]. The characteristic uncontrolled hyperglycemia can directly increase free radical production through autoxidation of glucose[2], nonenzymatic reaction of glucose with protein leading to formation of Advanced Glycation End products[3], enhanced glucose channeling to the sorbitol pathway[4] and enzymatic induction of Nitric Oxide Synthase[5] among other pathways generating free radicals at different levels[6]. The increased expression of inducible nitric oxide synthase (iNOS) secondary to hyperglycemia is activated by inflammation-sensitive Nuclear Factor κappa B (NF-κB)[7] which contributes to muscle atrophy in diabetes mellitus[8].

Muscle atrophy results from imbalanced protein synthesis and degradation which is a stray in maintaining muscle homeostasis crucial for preserving the body's integrity and function[9,10]. Diabetic muscular atrophy (DMA) is a complication of diabetes mellitus characterized by proximal lower extremity muscle weakness, atrophy, pain, sensory disturbances, and even quadriplegia in severe cases[11]. Denervation associated with peripheral neuropathy in diabetes plays a significant role in the development of muscular atrophy[12]. The prevalence of diabetic neuropathy in Africa is 46% among diabetic patients[13] thus, the prevalence of diabetic muscle atrophy may equally be high given that Andreassen et al.[14] had demonstrated that the severity of neuropathy correlated directly with muscle atrophy in diabetic patients. Animal model of diabetes mellitus induced by streptozotocin were also shown to manifest DMA[15,16].

Muscle atrophy is closely related to two major protein degradation pathways, the ubiquitin-proteasome system (UPS) and the autophagy-lysosome pathway (ALP). It is also related to the protein synthesis pathways, such as the insulin-like growth factor 1– phosphoinositide-3-kinase–Akt/protein kinase B–mammalian target of rapamycin (IGF1–PI3K–Akt/PKB–mTOR) pathway and IGF-1-AKT- Forkhead box O (FoxO) pathways[17,18]. Insulin resistance in type 2 diabetes mellitus inhibits protein synthesis by inhibiting the IGF-1-PI3K-AKT/PKB-mTOR pathway and activates the UPS and ALP through the IGF-1-AKT-FoxO signaling pathway thereby promoting muscle atrophy while muscle atrophy in type 1 diabetes mellitus is mediated by the FoxO-driven protein degradation pathway[10]. The links between all these pathways are inflammation and oxidative stress hence, therapeutic agents targeting any of these links in addition to glycemic control have been found beneficial in ameliorating diabetic muscular atrophy. For instance, Punkt et al.[15], Brocca et al.[19], and Ono et al.[20] explored the antioxidants target while

Bako et al.[21] and Cea et al.[22] documented the role of inflammation. Exploration of agents with antioxidants and anti-inflammatory properties would therefore be a desirable progress in ameliorating DMA. A good candidate with such property is *Ocimum gratissimum* (OG), Africa basil/sweet basil, a plant belonging to *Lamiaceae* family native to Africa, Asia and South America. In Nigeria, it is known as *efinrin*, *Nehonwu*, and *ai daya ta guda* by the Yoruba, Igbo and Hausa, respectively[23]. Its bioactive compounds include phytochemicals (oleanolic acid, caffeic acid, ellagic acid, epicatechin, sinapic acid, rosmarinic acid, chlorogenic acid, luteolin, apigenin, nepetoidin, xanthomicrol, nevadensin, salvigenin, gallic acid, catechin, quercetin, rutin, and kaempferol) and essential oils (camphene, β-caryophyllene, α- and β-pinene, α-humulene, sabinene, β-myrcene, limonene, 1,8-cineole, trans-β-ocimene, linalool, α- and δ-terpineol, eugenol, α-copaene, β-elemene, p-cymene, thymol, and carvacrol)[24]. Several studies have documented its hypoglycaemic[25,26], antioxidant[27] and anti-inflammatory[28,29] activities. This study therefore investigated the effect of aqueous leaf extract of OG on skeletal muscle atrophy in streptozotocin-induced diabetic male Wistar rats.

METHODOLOGY

Animal

Twenty male Wistar rats weighing between 180 and 230 g were used for this study. They were housed in the Department of Physiology Postgraduate Animal House, College of Medicine, University of Ibadan, Ibadan, Nigeria. The rats were housed in plastic cages with perforated lids and allowed to acclimatize for two weeks at a standard room temperature, humidity, and a natural photoperiod of 12 hours of light/dark cycle. They were allowed free access to standard rat chow (Ladokun Feeds®) and tap water. All experimental protocols were conducted in strict adherence to institutional guideline on the use of laboratory animals for experiments based on the NIH publication No. 85-23 guidelines.

Preparation of aqueous leaf extract *of Ocimum gratissimum L.*

The fresh leaves of *Ocimum gratissimum L.* were collected from Ibadan metropolis and identified and authenticated at the Forest Research Institute of Nigeria (FHI.110026). The leaves were separated from their stalk, rinsed with water to remove dirt, and air-dried for three (3) weeks at room temperature. They were pulverized to fine powder, 1 kg of the pulverized leaves was macerated for 24 hours in distilled water, filtered and the filtrate was collected in a round bottom flask for concentration in a rotary evaporator set at a temperature of 40°C to yield 13.26 % aqueous extract.

Induction of diabetes mellitus

Diabetes mellitus was induced by a single intraperitoneal dose of 65 mg/kg of freshly prepared Streptozotocin, STZ (Sigma®, St Loius, USA) in cold 50 mM sodium citrate buffer, pH 4.5. Fasting Blood Glucose was assessed after 72 hours of induction and animals with Fasting Blood Glucose level ≥ 200 mg/dL were confirmed as diabetic.

Experimental design

The animals were randomly divided into 4 groups (n=5) as follows:

I - Control, Normal rats administered distilled water

II - OG, Normal rats administered *Ocimum gratissimum* (400 mg/kg bwt)

III - Diab, Diabetic rats administered distilled water

IV - Diab+OG, Diabetic rats administered *Ocimum gratissimum* (400 mg/kg bwt)

The administered 400 mg/kg bwt of OG was established in earlier studies as being the effective therapeutic dose[27]. All administrations were done by oral gavage for 28 consecutive days. The weight and fasting blood glucose of all the rats were taken before and after the experiment. Blood was obtained by once-off tail prick and glucose levels determined using Accu-Chek® Glucometer (Roche, Germany).

Sample collection

Following an overnight fast, the animals were anaesthetized by 100 mg/kg Ketamine, *i.p.* (Ketanir®, Aculife Healthcare Pvt Ltd, India) and muscle samples were obtained. The gastrocnemius muscle was obtained for the determination of glycogen content, the right rectus femoris and extensor digitorum longus muscles were obtained separately for homogenization in phosphate buffer saline, PBS (pH 7.4) for markers of oxidative stress while their left counterparts were fixed separately in 10% formalin for histology and histomorphometry analysis.

Determination of muscle glycogen content

The glycogen content of the gastrocnemius muscle was determined by the Anthrone method as previously reported[30]. Briefly, gastrocnemius muscle was digested in 30% KOH overheat, washed twice by 95% ethanol and centrifuged to obtain glycogen precipitate. The precipitate was reconstituted with distilled water followed by stepwise addition of concentrated HCl, 88% formic acid and anthrone reagent then mixed thoroughly. It was incubated at 100°C for 10 min-

utes to obtain a blue colored solution. Absorbance of the solution was recorded at 630 nm against a reagent blank. Several dilutions of 0.2 mg/mL of glycogen standard were similarly treated to obtain a standard curve from which the glycogen concentrations of the samples were determined.

Determination of oxidative stress biomarkers

Oxidative stress biomarkers, Malondialdehyde, Superoxide Dismutase (SOD) and Catalase activity were determined in the supernatant of the homogenized right rectus femoris and extensor digitorum longus muscles.

Malondialdehyde (MDA) was determined according to the method described by Hagege et al.[31]. Briefly, 0.5ml of supernatant was aliquoted into 1ml of TCA-TBA-HCL solution (15 g of trichloroacetic acid and 0.375 g of thiobarbituric acid dissolved in 100 ml of 0.25 N hydrochloric acid) and incubated for 15 minutes in boiling water (100°C). After cooling, the mixture was centrifuged at 1000 g for 10 minutes and supernatant was read at 535 nm against the blank. The malondialdehyde concentration of the sample can be calculated using extinction coefficient of $1.56\times.10^{5}m^{-1}cm^{-1.}$

$$\text{MDA concentration} = \frac{O.D\ x\ V\ x\ 1000}{a\ x\ v\ x\ I\ x\ Y}$$

Where O.D=absorbance of sample test at 535 nm; V = total volume of the reaction = 1.5 ml; a = molar estimation coefficient of product=1.56×; I=light path = 1 cm; v=volume of sample used=0.5 ml.

Superoxide Dismutase (SOD) activity was determined according to the method of Misra and Fridovich[32]. Briefly, 0.2 ml of supernatant (test) or distilled water (reference) was added to 2.5 ml of 0.05 M Carbonate buffer (pH 10.2) was then added and incubated at room temperature. 0.3 ml of 0.3 mM adrenaline solution was added to the test and each of the reference solutions and were mixed by inversion and read using the spectrophotometer at 420 nm within 3 minutes.

$$\text{Inhibition} = \frac{O.D_{Ref} - O.D_{Test}}{O.D_{Ref}} \times 100$$

1 unit of SOD activity was taken as the amount of SOD required to cause 50 % inhibition of the auto-oxidation of adrenaline to adrenochrome.

Catalase activity was determined using a method based on the reaction of undecomposed hydrogen peroxide with ammonium molybdate to produce a yellowish color[33]. Briefly, 0.2 ml of supernatant was incubated with 1 ml of substrate solution (65 mmol/ml hydrogen peroxide in 60 mMol/l sodium–potassium phosphate buffer, pH 7.4) at 37°C for three minutes. The reaction was

stopped with 1 ml of 4 % ammonium molybdate in 12.5 mM H_2SO_4 and read at 305 nm wavelength.

Histomorphometry analysis

The fixed left rectus femoris and extensor digitorum longus muscles were taken for heamatoxylin and Eosin histological preparation using standard methods. Diameters of longitudinal and cross sections of the muscles were measured in microns using the measurements plug-in on AmScope 3.7, a computer enabled digital camera and software.

Statistical analysis

The data from each group was expressed as mean ± standard error of the mean (mean ± SEM) and analyzed using ANOVA and Tukey's post hoc test. $P<0.05$ was considered significant. All analyses were performed using GraphPad prism®, version 7.

RESULTS and DISCUSSION

Effects of *Ocimum gratissimum* L. leaf extract on body weight in normal and diabetic rats

As shown in Figure 1, Diabetes caused significant weight loss in Diab group when their initial weight (200.5 ± 2.52 g) was compared with their final weight (174.5 ± 9.18 g). The weight loss effect of diabetes was however abolished by OG treatment in Diab+OG group (Initial= 202.25 ± 4.33 g, Final = 195.5 ± 9.05 g).

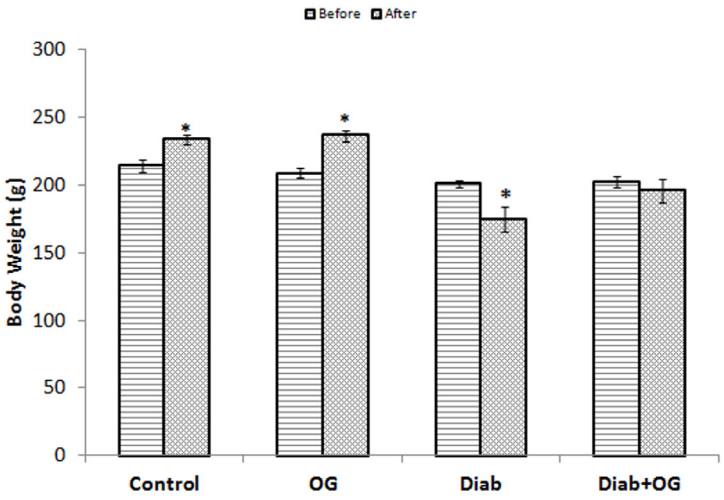

Figure 1. Effect of *Ocimum gratissimum* leaf extract on body weight in streptozotocin-induced diabetic male Wistar rats. *p<0.05 Before vs After

Effects of *Ocimum gratissimum* L. leaf extract on fasting blood glucose in normal and diabetic rats

Ocimum gratissimum leaf extract caused significant reduction in the fasting blood glucose level of animals in the Diab+OG (90.01 ± 26.50 mg/dl) when compared with the Diab (204.75 ± 9.95 mg/dl), Figure 2.

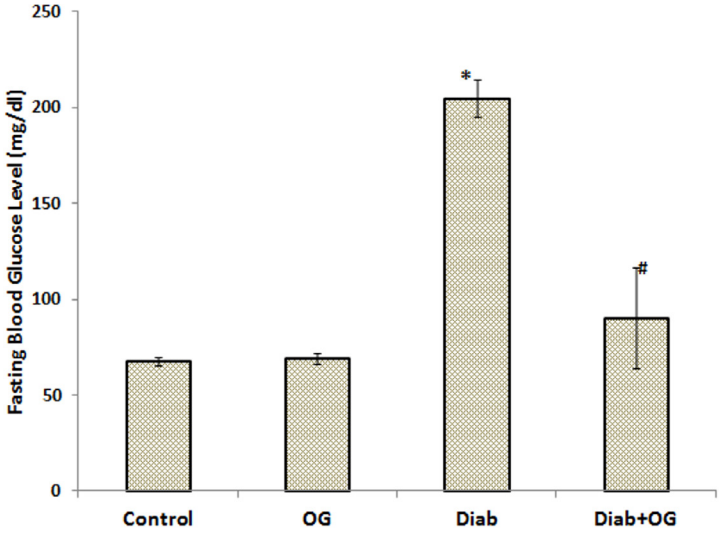

Figure 2. Effect of *Ocimum gratissimum* leaf extract on fasting blood glucose in normal and streptozotocin-induced diabetic male Wistar rats. *p<0.05 vs Control, #p<0.05 vs Diab

Effects of *Occimum gratissimum* L. leaf extract on glycogen content of the gastrocnemius muscles of normal and diabetic rats

Glycogen content was significantly depleted in the gastrocnemius muscle of the Diab group (0.09 ± 0.03 mg/ml) compared with the control (0.37 ± 0.07 mg/ml). The glycogen depletion was however reversed in the Diab+OG group (0.36 ± 0.05 mg/ml) compared with the Diab group (0.09 ± 0.03 mg/ml), as shown in Figure 3.

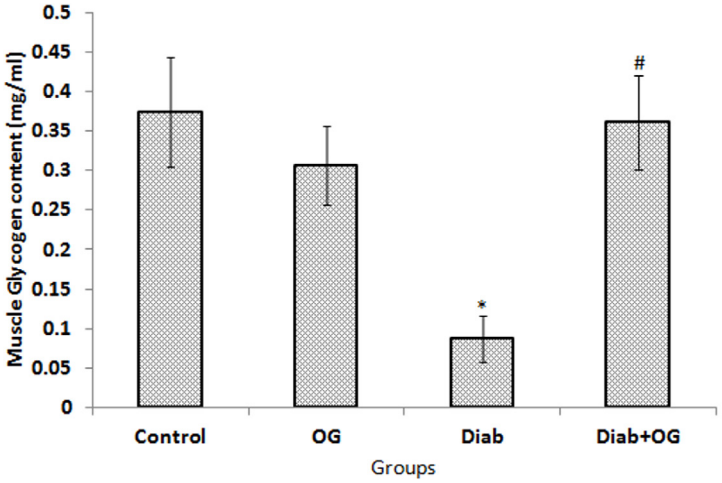

Figure 3. Effect of *Ocimum gratissimum* leaf extract on muscle glycogen content in normal and streptozotocin-induced diabetic male Wistar rats. *p<0.05 vs Control, #p<0.05 vs Diab

Effects of *Occimum gratissimum* L. leaf extract on transverse and longitudinal dimensions of rectus femoris and extensor digitorum longus muscles in normal and diabetic rats

As shown in Table 1, the size of the rectus femoris muscle was significantly decreased in the Diab group (Transverse dimension=248.97 ± 7.36 μm; Longitudinal dimension=250.93 ± 7.82 μm) when compared with the control (Transverse dimension=372.03 ± 18.23 μm; Longitudinal dimension=327.97 ± 14.22 μm). The reduction in size was however reversed by treatment with OG in the Diab+OG group when compared with the Diab group (Transverse dimension=297.18 ± 12.36 μm vs 248.97 ± 7.36 μm; Longitudinal dimension=317.37 ± 10.12 μm vs 250.93 ± 7.82 μm).

Table 1. Effects of *Ocimum gratissimum* L. leaf extract on transverse and longitudinal dimensions of rectus femoris and extensor digitorum longus muscles in normal and streptozotocin-induced diabetic rats

	RECTUS FEMORIS length (µm)		EXTENSOR DIGITORIS length (µm)	
	Transverse	Longitudinal	Transverse	Longitudinal
Control	372.03 ± 18.23	327.97 ± 14.22	283.44 ± 13.72	289.72 ± 9.74
OG	372.56 ± 32.49	333.19 ± 11.29	273.66 ± 13.44	273.63 ± 9.47
Diab	248.97 ± 7.36*	250.93 ± 7.82*	227.59 ± 10.85*	261.58 ± 9.83*
Diab+OG	297.18 ± 12.36*#	317.37 ± 10.12#	238.88 ± 5.83*	262.04 ± 10.09*

*p<0.05 vs Control; #p<0.05 vs Diab

In the extensor digitorum longus muscle, both the transverse (227.59 ± 10.85 µm) and longitudinal (261.58 ± 9.83 µm) dimensions were significantly reduced in the Diab group compared with the control (283.44 ± 13.72 µm; 289.72 ± 9.74 µm). Treatment with OG in the Diab+OG had no effect on the diabetes-induced size reduction of the extensor digitorum muscle, Table 1.

Effect of *Ocimum gratissimum* L. leaf extract on oxidative stress biomarkers in the rectus femoris muscle of normal and diabetic rats

As shown in Table 2, MDA level in the Rectus Femoris muscle was significantly reduced in the Diab+OG group compared with the Diab group. While SOD activity was not different across all the groups, catalase activity was significantly decreased in the Diab group (0.008 ± 0.0004 Activity/mg protein) compared with control (0.010 ± 0.0002 Activity/mg protein) and the Diab+OG group (0.009 ± 0.0005 Activity/mg protein).

Table 2. Effect of *Ocimum gratissimum* L. leaf extract on Oxidative stress biomarkers in rectus femoris in normal and streptozotocin-induced diabetic male Wistar rats

	Control	OG	Diab	Diab+OG
MDA (µmol/l)	0.402 ± 0.019	0.414 ± 0.019	0.420 ± 0.031	0.370 ± 0.01#
SOD (Activity/mg protein)	2.03 ± 0.03	1.98 ± 0.04	2 ± 0.06	2 ± 0.04
Catalase (Activity/mg protein)	0.01 ± 0.0002	0.011 ± 0.0006	0.008 ± 0.0004*	0.009 ± 0.0005#

*p<0.05 vs Control; #p<0.05 vs Diab

Effect of *Ocimum gratissimum* L. leaf extract on oxidative stress biomarkers in the extensor digitorum longus muscle of normal and diabetic rats

The MDA level of the Extensor Digitorum Longus Muscle of the Diab group (0.485 ± 0.025 μmol/l) was significantly elevated when compared with the control (0.388 ± 0.004 μmol/l). The elevated MDA was significantly reduced in the Diab+OG group (0.403 ± 0.03 μmol/l) when compared with the Diab group (0.485 ± 0.025 μmol/l). Extensor Digitorum Longus Muscle SOD and catalase activities were however not different across all the groups, Table 3.

Table 3. Effect of *Ocimum gratissimum* L. on Oxidative Stress Biomarkers in Extensor Digitorum Longus Muscle in normal and streptozotocin-induced diabetic male Wistar rats

	Control	OG	Diab	Diab+OG
MDA (μmol/l)	0.388 ± 0.004	0.394 ± 0.018	0.485 ± 0.025*	0.403 ± 0.03#
SOD (Activity/mg protein)	2.124 ± 0.04	2.131 ± 0.02	2.117 ± 0.03	2.287 ± 0.12
Catalase (Activity/mg protein)	0.01 ± 0.0006	0.00859 ± 0.0004	0.0089 ± 0.0005	0.00944 ± 0.0002

*$p<0.05$ vs Control; #$p<0.05$ vs Diab

This study was designed to examine the effect of *Ocimum gratissimum* leaf extract on diabetes-induced muscular atrophy in male Wistar rats. The abolishment of weight loss and reduction in fasting blood glucose level observed in the OG treated diabetic animals in this study are in agreement with the well documented effects of OG[25,26].

Skeletal muscle is the largest reservoir of glycogen, containing about fourfold of what is contained in the liver postprandially and is depleted by 65% in type 1 or 25% in type 2 diabetes mellitus patients[34,35]. The observed significant depletion in the glycogen content of the gastrocnemius muscle in the present study agrees with these earlier reports. Inhibition of glycogen synthase[36] and stimulation of glycogen phosphorylase[37] activities are contributing factors in the diabetes-induced glycogen depletion and are major therapeutic targets. Earlier on, Shittu et al.[30] reported that OG inhibited glycogen phosphorylase activity in liver of streptozotocin-induced diabetic rats and the restoration of glycogen

content in the gastrocnemius muscle of OG-treated diabetic rats in the current study is in conformity with this earlier finding. Other studies also showed that stimulating glycogen synthase activity by inhibiting its phosphorylating enzyme, glycogen synthase kinase 3β (GSK-3β) promotes muscle glycogen and insulin sensitivity[38,39]. The restoration of muscle glycogen in the OG treated rats in this study may be linked with the absence of diabetes-induced weight loss given that a recent study in human documented that lowered muscle glycogen is associated with reduction in body mass[40].

The reduction in glycogen synthesis by GSK-3β activity occurs through the PI3K/Akt signaling pathway[41] which is also implicated in free radical production/oxidative stress induction[42] therefore, the increased MDA level in Extensor Digitorum Longus Muscle matching glycogen depletion in the gastrocnemius muscle observed in the diabetic animals of the present study may not be surprising. Elevated skeletal muscle oxidative stress is a well-documented phenomenon in diabetes mellitus[16,43-45] and treatment with antioxidants were found to be ameliorative[15,46]. The decreased MDA level and increased Catalase activity observed in the OG treated diabetic animals of this study are consistent with documented antioxidant property of OG[27]. The high phenol content of OG can be adduced to its antioxidant effect[24] and studies using phenol-rich fraction of OG reported superior antioxidants potentials compared to other fractions[47,48].

Histomorphometry analysis in this study showed significant muscular atrophy in both the rectus femoris and extensor digitorum longus muscles of the diabetic rats. Treatment with OG reverses the observed diabetes-induced muscular dystrophy. Such reversal by antioxidant treatments had been documented to increase skeletal muscle weights, strengths and fiber size in type1 diabetic rats[49] which corroborated with the effect of *OG* in the transverse and longitudinal dimensions of the rectus femoris and extensor digitorum longus muscles of diabetic rats. The anti-inflammatory property of OG[28,29] may also be involved in the prevention of muscular atrophy given that plants with anti-inflammatory properties reverse diabetes-induced muscle atrophy via the MPK/SIRT1 pathway[50].

O*cimum gratissimum* leaf extract prevented atrophy and promoted glycogenesis by decreasing lipid peroxidation in the skeletal muscles of STZ-induced diabetic male Wistar rats. The interaction between OG and glycogen synthase activity requires further elucidation.

STATEMENT OF ETHICS

All experimental protocols were conducted in strict adherence to institutional guideline on the use of laboratory animals for experiments based on the NIH publication No. 85-23 guidelines. The ethical approval number is UI-ACUREC/100-1023/13.

CONFLICT OF INTEREST STATEMENT

No conflict of interest was declared by the authors.

AUTHOR CONTRIBUTIONS

Design – Shittu ST, Lasisi T; Acquisition of data – Shittu ST, Bello I; Analysis of data – Shittu ST, Shittu SA, Bello I; Drafting of the manuscript – Shittu ST, Bello I; Critical revision of the manuscript – Akor-Dewu M, Lasisi T; Statistical analysis – Shittu ST, Bello I, Shittu SA; Technical or financial support – Shittu ST, Bello I, Shittu SA, Akor-Dewu I, Lasisi T; Supervision – Akor-Dewu I, Lasisi T.

FUNDING STATEMENT

The study did not receive any external funding.

ACKNOWLEDGMENTS

We appreciate Dr T.A. Jarikre of the Department of Veterinary Pathology, University of Ibadan, Ibadan, Nigeria for his assistance with the histomorphometry.

REFERENCES

1. Rösen P, Nawroth PP, King G, Möller W, Tritschler HJ, Packer L. The role of oxidative stress in the onset and progression of diabetes and its complications: a summary of a congress series sponsored by UNESCO-MCBN, the American Diabetes Association and the German Diabetes Society. Diabetes Metab Res Rev, 2001;17(3):189-212. Doi:10.1002/dmrr.196

2. Turko IV, Marcondes S, Murad F. Diabetes-associated nitration of tyrosine and inactivation of succinyl-CoA:3-oxoacid CoA-transferase. Am J Physiol Heart Circ Physiol, 2001;281(6):H2289-2294. Doi: 10.1152/ajpheart.2001.281.6.H2289

3. Gillery P. Produits avancés de glycation (AGE), radicaux libres et diabète [Advanced glycation end products (AGEs), free radicals and diabetes]. J Soc Biol, 2001;195(4):387-390.

4. Lorenzi M. The polyol pathway as a mechanism for diabetic retinopathy: attractive, elusive, and resilient. J Diabetes Res, 2007;10. Doi:10.1155/2007/61038

5. Johansen JS, Harris AK, Rychly DJ, Ergul A. Oxidative stress and the use of antioxidants in diabetes: linking basic science to clinical practice. Cardiovasc Diabetol, 2005;4:5. Doi: 10.1186/1475-2840-4-5

6. Robertson RP. Chronic oxidative stress as a central mechanism for glucose toxicity in pancreatic islet beta cells in diabetes. J Biol Chem, 2004;279(41):42351-42354. Doi: 10.1074/jbc.R400019200

7. Jia J, Liu Y, Zhang X, Liu X, Qi J. Regulation of iNOS expression by NF-κB in human lens epithelial cells treated with high levels of glucose. Invest Ophthalmol Vis Sci, 2013; 54(7):5070-5077. Doi: 10.1167/iovs.13-11796

8. Perry BD, Caldow MK, Brennan-Speranza TC, Sbaraglia M, Jerums G, Garnham A, et al. Muscle atrophy in patients with type 2 diabetes mellitus: roles of inflammatory pathways, physical activity and exercise. Exerc Immunol Rev, 2016;22:94-109.

9. Yin L, Li N, Jia W, Wang N, Liang M, Yang X, et al. Skeletal muscle atrophy: from mechanisms to treatments. Pharmacol Res, 2021;172:105807. Doi: 10.1016/j.phrs.2021.105807

10. Shen Y, Li M, Wang K, Qi G, Liu H, Wang W, et al. Diabetic muscular atrophy: molecular mechanisms and promising therapies. Front Endocrinol, 2022;13:917113. Doi: 10.3389/fendo.2022.917113

11. Mahashabde M, Chaudhary G, Kanchi G, Rohatgi S, Rao P, Patil R, et al. An unusual case of critical illness polyneuromyopathy. Indian J Crit Care Med, 2020;24:133-135. Doi: 10.5005/jp-journals-10071-23346

12. Parasoglou P, Rao S, Slade JM. Declining skeletal muscle function in diabetic peripheral neuropathy. Clin Ther, 2017;39(6):1085-1103. Doi: 10.1016/j.clinthera.2017.05.001

13. Shiferaw WS, Akalu TY, Work Y, Aynalem YA. Prevalence of diabetic peripheral neuropathy in Africa: a systematic review and meta-analysis. BMC Endocr Disord, 2020;20(1):49. Doi: 10.1186/s12902-020-0534-5

14. Andreassen CS, Jakobsen J, Ringgaard S, Ejskjaer N, Andersen H. Accelerated atrophy of lower leg and foot muscles—a follow-up study of long-term diabetic polyneuropathy using magnetic resonance imaging (MRI). Diabetologia, 2009;52(6):1182-1191. Doi: 10.1007/s00125-009-1320-0

15. Punkt K, Psinia L, Welt K, Barth W, Asmussen G. Effects on skeletal muscle fibres of diabetes and *Ginkgo biloba* extract treatment. Acta Histochem, 1999;101:53-69. Doi: 10.1016/S0065-1281(99)80008-7

16. Aughsteen AA, Khair AB, Suleiman AA. Quantitative morphometric study of the skeletal muscles of normal and streptozotocin-diabetic rats. J Pancreas, 2006;7(4):382-389.

17. Pohl C, Dikic I. Cellular quality control by the ubiquitin-proteasome system and autophagy. Science, 2019;366(6467):818-822. Doi: 10.1126/science.aax3769

18. Milan G, Romanello V, Pescatore F, Armani A, Paik JH, Frasson L, et al. Regulation of autophagy and the ubiquitin-proteasome system by the FoxO transcriptional network during muscle atrophy. Nat Commun, 2015;6:6670. Doi: 10.1038/ncomms7670

19. Brocca L, D'Antona G, Bachi A, Pellegrino MA. Amino acid supplements improve native antioxidant enzyme expression in the skeletal muscle of diabetic mice. Am J Cardiol, 2008;101(11A):57E-62E. Doi: 10.1016/j.amjcard.2008.03.002

20. Ono T, Takada S, Kinugawa S, Tsutsui H. Curcumin ameliorates skeletal muscle atrophy in type 1 diabetic mice by inhibiting protein ubiquitination. Exp Physiol, 2015;100:1052-1063. Doi: 10.1113/EP085049

21. Bako HY, Ibrahim MA, Isah MS, Ibrahim S. Inhibition of jak-stat and NF-κB signalling systems could be a novel therapeutic target against insulin resistance and type 2 diabetes. Life Sci, 2019;239:117045. Doi: 10.1016/j.lfs.2019.117045

22. Cea LA, Vásquez W, Hernández-Salinas R, Vielma AZ, Castillo-Ruiz M, Velarde V. Skeletal muscle atrophy induced by diabetes is mediated by non-selective channels and prevented by boldine. Biomolecules, 2023;13:708. Doi: 10.3390/biom13040708

23. Ayinla MT, Dada SO, Shittu ST, Olayaki LA, Akiode AO, Ojulari SL. Anti-hyperlipidemic effect of aqueous leaf extract of *Ocimum gratissimum* in alloxan induced diabetic rats. J. Med. Med. Sci, 2011;3(12):360-363. Doi: 10.5897/IJMMS.9000022

24. Ugbogu OC, Emmanuel O, Agi GO, Ibe C, Ekweogu CN, Ude VC, et al. A review on the traditional uses, phytochemistry, and pharmacological activities of clove basil (*Ocimum gratissimum* L.). Heliyon, 2021;7(11):e08404. Doi: 10.1016/j.heliyon.2021.e08404

25. Aguiyi JC, Obi CI, Gang SS, Igweh AC. Hypoglycaemic activity of *Ocimum gratissimum* in rats. Fitoterapia, 2000;71:444446. Doi: 10.1016/s0367-326x(00)00143-x

26. Okoduwa SIR, Umar IA, James DB, Inuwa HM. Anti-diabetic potential of *Ocimum gratissimum* leaf fraction in fortified diet fed streptozotocin-treated diabetic rats. Medicines, 2017;4:E73. Doi: 10.3390/medicines4040073

27. Shittu ST, Oyeyemi WA, Lasisi TJ, Shittu SA, Lawal TT, Olujobi ST. Aqueous leaf extract of *Ocimum gratissimum* improves hematological parameters in alloxan-induced diabetic rats via its antioxidant properties. Int J App Basic Med Res, 2016;6:96-100. Doi: 10.4103/2229-516X.179016

28. Ajayi AM, Ologe MO, Ben-Azu B, Okhale SE, Adzu B, Ademowo OG. *Ocimum gratissimum* Linn. leaf extract inhibits free radical generation and suppressed inflammation in carrageenan-induced inflammation models in rats. J Basic Clin Physiol Pharmacol, 2017;28(6):531-541. Doi: 10.1515/jbcpp-2016-0096

29. Anusmitha KM, Aruna M, Job JT, Narayanankutty A, Benil PB, Rajagopal R, Alfarhan A, et al. Phytochemical analysis, antioxidant, anti-inflammatory, anti-genotoxic, and anticancer activities of different Ocimum plant extracts prepared by ultrasound-assisted method. Physiol Mol Plant Pathol, 2022;117:101746. Doi: 10.1016/j.pmpp.2021.101746

30. Shittu ST, Oyeyemi WA, Shittu SA, Lasisi TJ. *Ocimum gratissimum* inhibits glycogen phosphorylase activity without changes in hepatic nuclear factor kappa B (NF-κB) and inducible nitric oxide synthase (iNOS) in streptozotocin-induced diabetic rats. Nig Med Pract, 2018;73(1-2):10-17

31. Feutrys HD, Krsnik-Rasol M, Poder D, Menez JF. Estimation of free and bound MDA in plant extracts. Comparison between spectrophotometric and HPLC methods. In: Chen T, Zhang B, editors. Plant lipid metabolism [Internet]. Dordrecht: Springer; 1995 [cited 2023 Nov 01]. p. 259-261.

32. Misra HP. Fridovich I. The role of superoxide anion in the autoxidation of epinephrine and a simple assay for superoxide dismutase. J Bio Chem, 1972;247(10):3170-3175. Doi: 10.1016/s0021-9258(19)45228-9

33. Góth L. A simple method for determination of serum catalase activity and revision of reference range. Clin Chim Acta, 1991;196(2-3):143-151. Doi: 10.1016/0009-8981(91)90067-m

34. Roch-Norlund AE, Bergstrom J, Castenfors H, and Hultman E. Muscle glycogen in patients with diabetes mellitus. Acta Med Scand, 1970;187:445-453. Doi: 10.1111/j.0954-6820.1970.tb02969.x

35. He J, Kelley DE. Muscle glycogen content in type 2 diabetes mellitus. Am J Physiol – Endocrinol, 2004;287(5): E1002-E1007. Doi: 10.1152/ajpendo.00015.2004

36. Svetlana EN, Theodore PC, Leslie C, Sunder M, Kyong SP, Robert RH. Impaired muscle glycogen synthase in type 2 diabetes is associated with diminished phosphatidylinositol 3-kinase activation. J Clin Endocrinol Metab, 2001;86(9):4307-4314. Doi: 10.1210/jcem.86.9.7872

37. Kantsadi AL, Parmenopoulou V, Bakalov DN, Snelgrove L, Stravodimos GA, Chatzileontiadou DS et al. Glycogen phosphorylase as a target for type 2 diabetes: synthetic, biochemical, structural and computational evaluation of novel N-acyl-N´-(β-D-glucopyranosyl) urea inhibitors. Curr Top Med Chem, 2015;15(23):2373-2389. Doi: 10.2174/1568026615666150619142253

38. Kaidanovich-Beilin O, Eldar-Finkelman H. Long-term treatment with novel glycogen synthase kinase-3 inhibitor improves glucose homeostasis in ob/ob mice: molecular characterization in liver and muscle. J Pharmacol Exp Ther, 2006;316(1):17-24. Doi: 10.1124/jpet.105.090266

39. Ponnusamy R, Giriraj K, Magesh Selvakumar AM, Thangaraj P, Sathyanarayanan S, Antunes de Souza Araújo A, et al. Glycogen synthase kinase 3β inhibition and insulin-receptor binding enhancement of compounds isolated from wild leafy vegetable Acalypha alnifolia, Phytomed Plus, 2022;2(1):100216. Doi: 10.1016/j.phyplu.2022.100216

40. Schytz CT, Ørtenblad N, Birkholm TA, Plomgaard P, Nybo L, Kolnes KJ, et al. Lowered muscle glycogen reduces body mass with no effect on short-term exercise performance in men. Scand J Med Sci Sports, 2023;33:1054-1071. Doi: 10.1111/sms.14354

41. Dokken BB, Sloniger JA, Henriksen EJ. Acute selective glycogen synthase kinase-3 inhibition enhances insulin signaling in prediabetic insulin-resistant rat skeletal muscle. Am J Physiol Endocrinol Metab, 2005;288:E1188-E1194. Doi: 10.1152/ajpendo.00547.2004

42. Le Belle JE, Orozco NM, Paucar AA, et al. Proliferative neural stem cells have high endogenous ROS levels that regulate self-renewal and neurogenesis in a PI3K/Akt-dependant manner. Cell Stem Cell, 2011;8(1):59-71. Doi: 10.1016/j.stem.2010.11.028

43. Klueber KM, Feczko JD, Schmidt G, Watkins JB. Skeletal muscle in the diabetic mouse: histochemical and morphometric analysis. Anat Rec, 1989;225:41-45. Doi: 10.1002/ar.1092250107

44. Medina-Sanchez M, Rodriguez-Sanchez C, Vega-Alvarez JA, Menedez-Pelaez A, Perez-Casas A. Proximal skeletal muscle alterations in streptozotocin-diabetic rats: a histochemical and morphometric analysis. Am J Anat, 1991;191:48-56. Doi: 10.1002/aja.1001910105

45. Ozaki K, Matsuura T, Narama I. Histochemical and morphometrical analysis of skeletal muscle in spontaneous diabetic WBN/Kob rat. Acta Neuropathol, 2001;102:264-270. Doi: 10.1007/s004010100363

46. Call JA, Chain KH, Martin KS, Lira VA, Okutsu M, Zhang M, et al. Enhanced skeletal muscle expression of extracellular superoxide dismutase mitigates streptozotocin-induced diabetic cardiomyopathy by reducing oxidative stress and aberrant cell signaling. Circ Heart Fail, 2015; 8(1):188-197. Doi: 10.1161/CIRCHEARTFAILURE.114.001540

47. Ajayi AM, Umukoro S, Ben-Azu B, Bulus A, Ademowo OG. Toxicity and protective effect of phenolic-enriched ethylacetate fraction of *Ocimum gratissimum* (Linn.) leaf against acute inflammation and oxidative stress in rats. Drug Dev Res, 2017;78:135-145. Doi: 10.1002/ddr.21384

48. Alabi QK, Akomolafe RO, Omole JG, Aturamu A, Ige MS, Kayode OO, et al. Polyphenol-rich extract of *Ocimum gratissimum* leaves prevented toxic effects of cyclophosphamide on the kidney function of Wistar rats. BMC Complement Med Ther, 2021;21:274. Doi: 10.1186/s12906-021-03447-3

49. Oyenihi AB, Langa SOP, Mukaratirwa S, Masola B. Effects of *Centella asiatica* on skeletal muscle structure and key enzymes of glucose and glycogen metabolism in type 2 diabetic rats. Biomed Pharmacother, 2019;112:108715. Doi: 10.1016/j.biopha.2019.108715

50. Li J, Zhang Y, Yu F, Pan Y, Zhang Z, He Y, et al. Proteoglycan extracted from *Ganoderma lucidum* ameliorated diabetes-induced muscle atrophy via the AMPK/SIRT1 pathway in vivo and in vitro. ACS Omega, 2023;8(33):30359-30373. Doi: 10.1021/acsomega.3c03513

Acta Pharm. Sci. Vol 63:(1), 2025
Original article
DOI: 10.23893/1307-2080.APS6308

Trends of antibiotic consumption in pediatric inpatients, a retrospective study in Lviv, Ukraine

Oksana HORODNYCHA, Andriy ZIMENKOVSKY, Tetiana RYVAK*

Danylo Halytsky Lviv National Medical University, Faculty of Pharmacy, Department of HealthCare Management, Pharmacotherapy and Clinical Pharmacy, Lviv, Ukraine

ABSTRACT

The objective of this study was to assess the consumption of antibiotics in children using the «AWaRe» classification of antibiotics (WHO, 2017) and metrics such as days of therapy (DoT) and length of therapy (LoT) per 1000 patient-days (PD). Antibiotics were administrated to 91.1% of inpatients in 2019 and 68.2% in 2021 ($p<0.05$). The main reason for antibiotic prescription was acute bronchitis in both study periods. Total DoT/1000 PD increased from 717.0 in 2019 to 760.0 in 2021 ($p<0.05$), and total LoT/1000 PD from 679.0 to 717.4 ($p<0.05$). Administration of antibiotics from the Access group decreased from 2.1% in 2019 to 1.8% in 2021 ($p>0.05$), antibiotics from the Watch group increased from 90.7% to 97.3% ($p>0.05$). Although a statistically significant reduction in the antimicrobial prescription rate, we found a considerable increase in (1) prescription antibiotics with a high risk of antimicrobial resistance, and (2) the main units of antimicrobial consumption.

Keywords: antibiotics, antimicrobial consumption, hospitals, children, inpatients

*Corresponding author: Tetiana RYVAK
E-mail: tanusha1905@gmail.com
ORCIDs:
Oksana HORODNYCHA: 0000-0002-6373-1447
Andriy ZIMENKOVSKY: 0000-0002-9649-293X
Tetiana RYVAK: 0000-0002-9491-1109
(Received 22 Dec 2023, Accepted 12 Mar 2024)

INTRODUCTION

Nowadays, antibiotics are one of the most prescribed medicines in the pediatric population, especially in hospital wards[1,2,3]. The prevalence of antibiotic prescription in hospitalized children varies significantly in different countries, with the worldwide average at 37%[4]. Simultaneously, a high rate of antimicrobial administrations is unnecessary or incorrect, accounting for up to 50% of total antibiotic prescriptions[5].

This group of medicines is responsible for numerous adverse reactions, notably gastrointestinal and hematological disorders[6]. Furthermore, inappropriate use and overconsumption of antibiotics significantly increase the risk of drug-resistant pathogen occurrence and spreading[7]. According to the World Health Organization (WHO) reports, antimicrobial resistance is one of ten global public health threats associated with a high rate of morbidity and mortality[8]. About 1.3 million deaths per year worldwide are directly related to drug-resistant bacteria defining antimicrobial resistance as a frequent cause of fatalities[9].

Davey P. et al. found that reducing antibiotic use in hospitals decreases the risk of antimicrobial resistance[7]. Different metrics evaluate the antimicrobial prescribing trends in hospitals[10]. For instance, the defined daily dose (DDD) is a technical unit of antimicrobial consumption in hospitalized adults. Although this is the most commonly used unit, it has some limitations for pediatrics[11]. Thus, alternative metrics, such as (1) days of therapy (DoT) and (2) the length of therapy (LoT), describe the quantification of antimicrobial utilization in children[4,11]. Also, the AWaRe classification lets practitioners reduce the use of antibiotics with a high potential for antimicrobial resistance[12]. Overall, the analysis of antibiotic consumption in inpatient children is essential. Not only does it optimize antibiotic treatment, but also it helps to implement different interventions of antimicrobial policy[7,11]. Numerous studies in Canada[13], Spain[14], and Germany[15-17] report that the calculation of the abovementioned metrics evaluates the effectiveness of antibiotic stewardship programs.

Though overconsumption and inappropriate use of antibiotics in pediatrics are not new issues, there is little available information about this problem in Ukraine. With this background, we aimed to (1) define the trends of antimicrobial consumption in hospitalized children, (2) identify the problem areas of antibiotic prescription and (3) highlight the necessity of antimicrobial stewardship programs development and implementation in Ukraine.

METHODOLOGY

Definitions

AWaRe classification – a grading of antibiotics into three groups (Access, Watch, and Reserve), developed by WHO to support antibiotic stewardship efforts. The background of this classification is the impact of different antibiotics and antibiotic classes on antimicrobial resistance[12].

Days of therapy (DoT) – the number of days a patient receives an antimicrobial agent irrespective of single and daily doses. All doses of one antibiotic received throughout a day are 1 DoT. If patients received more than one antibiotic, we calculated DoT for each antimicrobial agent[17,18].

Length of therapy (LoT) – the number of days a patient receives antimicrobials (one or more)[17,18].

Data collection and analysis

This retrospective study was conducted in the Pediatric Unit in one of Lviv city hospitals. This Unit admits children aged 1 to 18 years due to different somatic diseases (with respiratory system disorders prevalence). We acquired copies of medical records (123 in March 2019 and 129 in March 2021) with an agreement with the hospital administration. The reason for choosing March was that it is a time of the year with a steady medium number of inpatients in this Unit. Information regarding demographic (age, gender) and clinical (diagnosis, comorbidity, allergy, administration of antibiotics) characteristics we extracted from the medical records. Antibiotic consumption was assessed using the AwaRe classification12 and units such as DoT and LoT[4,11,15,17]. These units were standardized per 1000 patient days (PD) (taking into account the length of stay of each patient) and compared in 2 study periods (2019 and 2021).

Limitations

Necessary information we obtained retrospectively from paper medical records. The analysis of this type of documentation requires a lot of time and human resources. Thus, medical records of patients admitted to the hospital in 1 month (from 1 to 31 March 2019 and 2021) were enrolled. Consequently, we did not calculate the annual total antibiotics consumption but managed to evaluate its tendency. The quantification of antimicrobial utilization measured as DoT and LoT per 1000 PD did not include doses and frequency regimen of antibiotic treatment, which is another disadvantage of this study. Carrying out the research only in Pediatric Unit and only in one hospital restricts the generalizability of our findings. Further studies are needed to evaluate antimicrobial consumption in other wards and hospitals.

Statistical analysis

The statistical analysis was performed with SPSS Trial. Qualitative variables were summarized as frequency (n) and percentage (%), while quantitative variables were described as mean with standard deviations (SD). To test the difference between the two study periods (2019 and 2021), the Mann–Whitney U test was used for quantitative variables and Chi-square or Fisher's tests for qualitative variables14. The value of $p<0.05$ was statistically significant. This research received ethical approval from the Human Research Ethics Committee of Danylo Halytsky Lviv National Medical University in December 2019 (Protocol No. 10).

RESULTS and DISCUSSION

Overall, 252 pediatric inpatients were included in the study sample (123 in 2019 and 129 in 2021). Among them, 91.1% in 2019 and 68.2% in 2021 received at least one antibiotic ($p<0.05$). The main characteristics of hospitalized children distributed by study periods are presented in Table 1.

Table 1. Main characteristics of inpatient children who received antibiotics

Characteristics	2019		2021		p
	n	%	n	%	
Number of patients	112		88		
Gender					
male	53	47.3	39	44.3	0.672
female	59	52.7	49	55.7	
Age (min-max)	1-16		1-17		
from 1 to 5 years	64	57.1	56	63.6	
from 5 to 12 years	40	35.7	27	30.7	
from 12 to 18 years	8	7.2	5	5.7	
Mean age ± SD, years	5.5 ± 3.7		5.1 ± 3.8		0.348
Allergy					
yes	4	3.6	3	3.4	0.951
no	108	96.4	85	96.6	
Co-morbidity					
yes	15	13.4	18	20.5	0.182
no	97	86.6	70	79.5	
Diagnosis					
acute bronchitis	72	64.3	62	70.5	0.357
community-acquired pneumonia	39	34.8	14	15.9	0.003
others*	1	0.9	12	13.6	

*Others in 2019: acute pyelonephritis (n=1); others in 2021: acute laryngotracheitis (n=4), acute obstructive laryngitis (n=2), acute nasopharyngitis (n=1), chronic sinusitis (n=1), acute pansinusitis (n=1), asthma (n=1), systemic inflammatory response syndrome of infectious origin (after COVID-19) without organ failure (n=1), functional disorder of stomach (n=1)

There were no statistically significant differences ($p>0.05$) in gender, age, allergy, and co-morbidity in 2019 and 2021. The main reason for antibiotic administration in both study periods was acute bronchitis (64.3% vs 70.5% in 2019 and 2021, respectively, $p>0.05$), followed by community-acquired pneumonia, the rate of which decreased significantly from 34.8% in 2019 to 15.9% in 2021 ($p<0.05$).

The total number of prescribed antibiotics was 139 in 2019 and 107 in 2021 (mean 1.2 ± 0.5 vs 1.2 ± 0.4, respectively, $p=0.826$; minimum one antibiotic, maximum three antibiotics in both periods).

According to the «AWaRe» classification, 90.7% of antimicrobials in the first period of study and 97.3% in the second period of study were from the Watch group ($p>0.05$). Ceftriaxone (43.2% and 29.0% in 2019 and 2021, respectively, $p<0.05$), azithromycin (18.0% and 18.7%, $p>0.05$), cefotaxime (9.4% and 40.2%, $p<0.05$) and cefoperazone (9.4% and 3.8%, $p>0.05$) presented the most common antibiotics from Watch group. The rate of antimicrobials from the Access group was 2.1% and 1.8% in the first and second periods of the study, respectively ($p>0.05$). This group involved amikacin (1.4% and 0.9% in 2019 and 2021), furazidin (0.7% in 2019) and sulfamethoxazole + trimethoprim (0.9% in 2021). The Reserve group (imipenem + cilastatin) was administrated only in 2019. The prevalence of this group accounted for 0.7% of the total antibiotics prescribed. Moreover, 6.5% of antimicrobials in 2019, and 0.9% in 2021 ($p<0.05$) were classified by AWaRe classification as not recommended. In 2019, this category included cefoperazone + sulbactam (5.8%) and ceftriaxone + sulbactam (0.7%), in 2021 – cefoperazone + sulbactam (0.9%).

The total number of PD in the first period was 1000, and in the second period – 700 (Table 2). Total DoT decreased from 717 to 532 days and total LoT from 679 to 503 days. However, standardized DoT per 1000 PD increased from 717.0 to 760.0 (+6%) with an average 5.2 ± 1.6 and 7.1 ± 2.3 in 2019 and 2021, respectively ($p<0.05$). Simultaneously, standardized LoT per 1000 PD rose from 679.0 to 717.4 with an average from 6.1 ± 1.9 to 8.2 ± 2.7 in 2019 and 2021, respectively ($p<0.05$).

Table 2. Summary of the antibiotic consumption data in 2019 and 2021

Antibiotic consumption data	2019	2021	p
Patient days (PD)	1000	700	
Days of therapy (DoT) Total DoT Total DoT/1000 PD Mean DoT/1000 PD ± SD	 717 717.0 5.2 ± 1.6	 532 760.0 7.1 ± 2.3	 <0.05
Length of therapy (LoT) Total LoT Total LoT/1000 PD Mean LoT/1000 PD ± SD	 679 679.0 6.1 ± 1.9	 503 717.4 8.2 ± 2.7	 <0.05

SD – standard deviation

There was a predominance of third-generation cephalosporins consumption (measured as DOT) in both study periods. These antibiotics accounted for 70.7% and 76.3% of total DoT in 2019 and 2021, respectively (Table 3). The highest rate of DoT in 2019 accounted for ceftriaxone (42.0%), and in 2021 - for cefotaxime (35.9%). Also, the consumption of macrolides was relatively high (17.7% of total DOT in 2019 and 18.4% in 2021).

Table 3. Comparison of detailed antibiotic consumption in 2019 and 2021

Antibiotics	2019			2021			Difference	
	Total DoT	DoT / 1000 PD	%	Total DoT	DoT / 1000 PD	%	DoT / 1000 PD	%
Third-generation cephalosporins	**507**	**507.0**	**70.7**	**406**	**580.0**	**76.3**	**73**	**14.4**
Ceftriaxone	301	301.0	42.0	182	260.0	34.2	-41	-13.6
Ceftriaxone, combinations	5	5.0	0.7	0	0	0	-5	-100.0
Cefoperazone	66	66.0	9.2	20	28.6	3.8	-37.4	-56.7
Cefoperazone + sulbactam	45	45.0	6.3	7	10.0	1.3	-35	-77.8
Cefotaxime	71	71.0	9.9	191	272.9	35.9	201.9	284.4
Cefpodoxime	19	19.0	2.6	4	5.7	0.8	-13.3	-70.0
Cefixime	0	0	0	2	2.9	0.4	2.9	-
Macrolides	**127**	**127.0**	**17.7**	**98**	**140.0**	**18.4**	**13.0**	**10.5**
Azithromycin	127	127.0	17.7	91	130.0	17.1	3.0	2.4
Clarithromycin	0	0	0	7	10.0	1.3	10.0	-
Fluoroquinolones	**38**	**38.0**	**5.3**	**0**	**0**	**0**	**-38.0**	**-100.0**
Ciprofloxacin	24	24.0	3.3	0	0	0	-24.0	-100.0
Levofloxacin	14	14.0	2.0	0	0	0	-14.0	-100.0
Fourth-generation cephalosporins	**17**	**17.0**	**2.4**	**13**	**18.6**	**2.4**	**1.6**	**9.4**
Cefepime	17	17.0	2.4	13	18.6	2.4	1.6	9.4
Carbapenems	**11**	**11.0**	**1.5**	**5**	**7.1**	**0.9**	**-3.9**	**-35.5**
Meropenem	0	0	0	5	7.1	0.9	7.1	-
Imipenem/ cilastatin	11	11.0	1.5	0	0	0	-11	-100.0
Aminoglycosides	**9**	**9.0**	**1.3**	**3**	**4.3**	**0.6**	**-4.7**	**-52.2**
Amikacin	9	9.0	1.3	3	4.3	0.6	-4.7	-52.2
Second-generation cephalosporins	**5**	**5.0**	**0.7**	**0**	**0**	**0**	**-5.0**	**-100.0**
Cefuroxime	5	5.0	0.7	0	0	0	-5.0	-100.0
Nitrofurans	**3**	**3.0**	**0.4**	**0**	**0**	**0**	**-3.0**	**-100.0**
Furazidin	3	3.0	0.4	0	0	0	-3.0	-100.0
Sulfonamides	**0**	**0**	**0**	**7**	**10.0**	**1.3**	**10.0**	**-**
Sulfamethoxazole + trimethoprim	0	0	0	7	10.0	1.3	10.0	-
Total	**717**	**717.0**	**100.0**	**532**	**760.0**	**100.0**	**43.0**	**6.0**

As far as we know, this was the first study in Ukraine that described and evaluated the trends of antimicrobial consumption in hospitalized children. Overall, the frequency of antimicrobial treatment of hospitalized patients under 18 years differs worldwide, with the prevalence from 25% to 94% of inpatients in some European[19] and African[1] countries, respectively. This variety could be related to different factors, for instance, (1) the occurrence of infectious diseases[20], (2) the level of income in the county, and, consequently, the ability to perform the precise laboratory testing of the infection's origin, (3) medical staff experience and their attitude towards the antimicrobial resistance[19], (4) insufficient state regulation of antibiotic administration[20, 21], etc. Also, the rate of antimicrobial prescription depends on the type of hospital setting[22]. The pediatric intensive care units, neonatal units[22], and pediatric medical wards[22,23] are the settings with the highest level of antibiotic consumption. According to our results, the rate of antibiotic administration for inpatient children was high in both study periods and surpassed the pooled worldwide prevalence (37%)[4]. At the same time, the percentage of inpatients who received antibiotics decreased significantly from 91.1% in 2019 to 68.2% in 2021 ($p<0.05$), which could be related to different efforts directed to reduce antimicrobial utilization in Ukraine[24].

Children aged 1 to 5 years were most vulnerable to antibiotic prescriptions, similar to other studies[22,23,25]. In our case, females received antibiotics more often, which is content with results from Lithuania[22] and differs from findings in the United States[25], Latvia[22], and some other countries[20,23] with male predominance.

Scientific literature reports that respiratory tract infections are one of the main reasons for antibiotics prescription[19,22,23,26,27]. Our findings match this information because acute bronchitis was the most common diagnosis in both study periods. At the same time, it is known that upper respiratory tract infections are usually viral (for instance, up to 95% of acute bronchitis cases), with limited evidence-based data about the beneficial effects of antibiotics[28]. However, we cannot affirm the excessive use of antibiotics in this study due to its retrospective design.

We found third-generation cephalosporins (mainly ceftriaxone in 2019 and cefotaxime in 2021) the most common antibiotics. Also, the rate of macrolides (mainly azithromycin) was high. This result is similar to findings in numerous recent studies[22,23,29]. These cephalosporins and macrolides present the Watch group of antibiotics, the total rate of which increased from 90.7% to 97.3% ($p>0.05$). This tendency reflects the permanent problem of overusing broad-spectrum antibiotics with a high risk of resistance. According to the WHO rec-

ommendations[12], antibiotics from the Watch group should not exceed 40% of total antimicrobial consumption. Not only in Ukraine but also in other countries, such as Canada[30], China[26], Pakistan[27], and others[20,31], antibiotics with a high risk of resistance prevail. At the same time, the Access group presented about 2% of the total number of antibiotics in both study periods instead of recommended at least 60%[12]. This distribution indicates the inappropriateness of antibiotic use and the needfulness of antibiotic stewardship programs for inpatient children.

The global overuse of antibiotics, especially in hospitalized adults and children, defined the necessity of different metrics for evaluating antibiotic consumption[16,17]. Numerous units, such as (1) DDD, (2) DoT, (3) LoT per 1000 PD, and some others, describe antibiotic utilization in patients[10,20]. However, DoT and LoT are more applicable for pediatrics[16,17]. According to recent studies, in general pediatric wards, total antibiotic consumption varies from 392[16] to 483 DoT per 1000 PD[17]. In this study, the overall antibiotic utilization was much higher in both study periods (717.0 versus 760.0 DoT per 1000 PD, mean 5.2 ± 1.6 versus 7.1 ± 2.3 DoT per 1000 PD in 2019 and 2021, respectively, $p<0.05$). Moreover, our results demonstrate the same changes in LOT per 1000 PD (679.0 versus 717.4 LoT per 1000 PD, mean 6.1 ± 1.9 versus 8.2 ± 2.7 LoT per 1000 PD days in 2019 and 2021, respectively, $p<0.05$). Compared with other studies, the overall antibiotic LoT per 1000 PD was considerably higher than published data in general pediatric wards (no more than 377 LoT per 1000 PD)[17] and similar to pediatric intensive care units with 667 to 750 LoT per 1000 PD[15]. Thus, we found the deterioration of metrics that describe antibiotic consumption in hospitalized children. Many published reports show the efficacy of antibiotic stewardship programs in providing optimization of antimicrobial utilization[1,13,15-17]. These findings define further steps in this area in Ukraine.

Detailed analysis of antibiotic utilization revealed that third-generation cephalosporins accounted for 70.7% in 2019 and 76.3% in 2021 of total DoT per 1000 PD. The consumption of ceftriaxone, the most commonly used antibiotic in 2019, reduced by 41 DoT/1000 PD (-13.6%) in 2021. At the same time, the consumption of cefotaxime increased by 201.9 DoT/1000 PD (+284.4%), which was the most used antibiotic in 2021. These results differ from other studies, where penicillins and second-generation cephalosporins prevailed[16,17]. Moreover, scientific literature indicates a decrease in cephalosporins administration and an increase in penicillin consumption[16,17]. Notably, the reduction of third-generation cephalosporins (most common in intensive care units[15,16]) prescription ensures decreasing the risk of antimicrobial resistance and numerous other conditions, such as *Clostridium difficile* infections[32], immune hemolytic anemia[33], etc.

The consumption of macrolides was relatively high (17.7% and 18.4% of total DoT per 1000 PD in 2019 and 2021, respectively), with an increase of 13 DOT/1000 PD (+10.5%) in 2021. This result is much higher than in other studies (1.8-6.9%)[16]. In 2019 macrolides were followed by fluoroquinolones, usually associated with multiple adverse drug reactions in children[34]. However, in 2021 we found no one case of fluoroquinolones administration (-100.0%), which is a positive change in pediatrics[32].

Antibiotics are common medicines in pediatric inpatients. The rate of antibiotic prescriptions is high. However, a statistically significant reduction in patient rates received antimicrobials was found. Although this positive change, we established a statistically significant increase in main metrics of antimicrobial consumption such as (1) days of therapy and (2) length of therapy per 1000 patient days. Also, we found the deterioration of a permanent problem associated with the prescription of antibiotics with a high risk of resistance. Thus, there is a necessity for effective interventions to improve antibiotic therapy in hospitalized children in Ukraine.

STATEMENT OF ETHICS

The study received ethical approval from the Human Research Ethics Committee of Danylo Halytsky Lviv National Medical University (Protocol No.10 of 16.12.2019).

CONFLICT OF INTEREST STATEMENT

The authors report no conflict of interest**.**

AUTHOR CONTRIBUTIONS

Concept – Horodnycha O, Zimenkovsky A, Ryvak T (authors contributed equally); Design – Horodnycha O, Zimenkovsky A, Ryvak T (authors contributed equally); Data Collection and Processing – Horodnycha O; Statistical Analysis and Interpretation – Horodnycha O; Literature Search – Horodnycha O, Ryvak T; Drafting of the Manuscript – Horodnycha O, Ryvak T; Critical Revision of the Manuscript – Zimenkovsky A.

FUNDING SOURCES

This work was not supported or funded by any company or organization.

ACKNOWLEDGMENTS

None.

REFERENCES

1. Korang SK, Safi S, Nava C, Greisen G, Gupta M, Lausten-Thomsen U, et al. Antibiotic regimens for late-onset neonatal sepsis. Cochrane Database Syst Rev, 2021;5(5):CD013836. Doi: 10.1002/14651858.CD013836.pub2

2. Rudnick W, Conly J, Thirion DJG, Choi K, Pelude L, Cayen J, et al. Antimicrobial use among paediatric inpatients at hospital sites within the Canadian Nosocomial Infection Surveillance Program, 2017/2018. Antimicrob Resist Infect Control, 2023;12(1):35. Doi: 10.1186/s13756-023-01219-x

3. Oğuz E, Bebitoğlu BT, Nuhoğlu Ç, Çağ Y, Hodzic A, Temel F, et al. Evaluation of antibiotic use among hospitalised patients in a paediatric department of a training hospital in Turkey. Int J Clin Pract, 2021;75(3):e13782. Doi: 10.1111/ijcp.13782

4. Araujo da Silva AR, Albernaz de Almeida Dias DC, Marques AF, Biscaia di Biase C, Murni IK, Dramowski A, et al. Role of antimicrobial stewardship programmes in children: a systematic review. J Hosp Infect, 2018;99(2):117-123. Doi: 10.1016/j.jhin.2017.08.003

5. Nasso C, Scarfone A, Pirrotta I, Rottura M, Giorgi DA, Pallio G, et al. Appropriateness of antibiotic prescribing in hospitalized children: a focus on the real-world scenario of the different paediatric subspecialties. Front Pharmacol, 2022;13:890398. Doi: 10.3389/fphar.2022.890398

6. Bulik NB, Farcaş A, Bucşa C, Iaru I, Oniga O. Safety of antibiotics in hospitalized children in Romania: a prospective observational study. Pharmaceuticals, 2022;15(6):713. Doi: 10.3390/ph15060713

7. Davey P, Marwick CA, Scott CL, Charani E, McNeil K, Brown E, et al. Interventions to improve antibiotic prescribing practices for hospital inpatients. Cochrane Database Syst Rev, 2017;2(2):CD003543. Doi: 10.1002/14651858.CD003543.pub4

8. World Health Organization. Accessed November 6, 2024. Available from: https://www.who.int/news-room/fact-sheets/detail/antimicrobial-resistance

9. Antimicrobial Resistance Collaborators. Global burden of bacterial antimicrobial resistance in 2019: a systematic analysis. Lancet, 2022;399(10325):629-655. Doi: 10.1016/S0140-6736(21)02724-0

10. D'Amore C, Ciofi Degli Atti ML, Zotti C, Prato R, Guareschi G, Spiazzi R, et al. Use of multiple metrics to assess antibiotic use in Italian children's hospitals. Sci Rep, 2021;11(1):3543. Doi: 10.1038/s41598-021-83026-1

11. Quaak CH, Cové E, Driessen GJ, Tramper-Stranders GA. Trends in paediatric inpatient antibiotic therapy in a secondary care setting. Eur J Pediatr, 2018;177(8):1271-1278. Doi: 10.1007/s00431-018-3185-z

12. World Health Organization. Accessed November 6, 2024. Available from: https://www.who.int/publications/i/item/2021-aware-classification

13. Thampi N, Shah PS, Nelson S, Agarwal A, Steinberg M, Diambomba Y, et al. Prospective audit and feedback on antibiotic use in neonatal intensive care: a retrospective cohort study. BMC Pediatr, 2019;19(1):105. Doi: 10.1186/s12887-019-1481-z

14. Fresán-Ruiz E, Izurieta-Pacheco AC, Girona-Alarcón M, de Carlos-Vicente JC, Bustinza-Arriortua A, Slocker-Barrio M. On behalf of the Pediatric-Envin-Helics study group. Antimicrobial stewardship improvement in pediatric intensive care units in Spain-what have we learned? Children, 2022;9(6):902. Doi: 10.3390/children9060902

15. Renk H, Sarmisak E, Spott C, Kumpf M, Hofbeck M, Hölzl F. Antibiotic stewardship in the PICU: impact of ward rounds led by paediatric infectious diseases specialists on antibiotic consumption. Sci Rep, 2020;10(1):8826. Doi: 10.1038/s41598-020-65671-0

16. Grewer-Katona G, Hüebner J, Pecar A, Wolf GK. Opportunities for antibiotic stewardship interventions in a pediatric hospital. J Pediatr Infect Dis, 2022;17(2):83-89. Doi: 10.1055/s-0042-1744559

17. Kreitmeyr K, von Both U, Pecar A, Borde JP, Mikolajczyk R, Huebner J. Pediatric antibiotic stewardship: successful interventions to reduce broad-spectrum antibiotic use on general pediatric wards. Infection, 2017;45(4):493-504. Doi: 10.1007/s15010-017-1009-0

18. Grau S, Bou G, Fondevilla E, Nicolás J, Rodríguez-Maresca M, Martínez-Martínez L. How to measure and monitor antimicrobial consumption and resistance. Enferm Infec Microbiol Clin, 2013;31(4):16-24. Doi: 10.1016/S0213-005X(13)70128-9

19. Covino M, Buonsenso D, Gatto A, Morello R, Curatole A, Simeoni B, et al. Determinants of antibiotic prescriptions in a large cohort of children discharged from a pediatric emergency department. Eur J Pediatr, 2022;181(5):2017-2030. Doi: 10.1007/s00431-022-04386-y

20. Kitt E, Hayes M, Ballester L, Sewawa K, Mulale U, Mazhani L, et al. Assessing antibiotic utilization among pediatric patients in Gaborone, Botswana. SAGE Open Medicine, 2022;10:20503121221104437. Doi: 10.1177/20503121221104437

21. Worldwide Antimicrobial Resistance National/International Network Group (WARNING) Collaborators. Ten golden rules for optimal antibiotic use in hospital settings: the WARNING call to action. World J Emerg Surg, 2023;18(1):50. Doi: 10.1186/s13017-023-00518-3

22. Sviestina I, Usonis V, Gurksniene V, Burokiene S, Ivaskeviciene I, Mozgis D. Prescription of antibiotics in Riga and Vilnius tertiary children's hospitals. Eur J Hosp Pharm, 2018;25(4):189-194. Doi: 10.1136/ejhpharm-2016-001124

23. Baidya S, Hazra A, Datta S, Das AK. A study of antimicrobial use in children admitted to pediatric medicine ward of a tertiary care hospital. Indian J Pharmacol, 2017;49(1):10-15. Doi: 10.4103/0253-7613.201034

24. The Order of Cabinet of Ministers of Ukraine. Accessed November 6, 2024. Available from: https://zakon.rada.gov.ua/laws/show/116-2019-%D1%80#Text

25. Wattles BA, Smith MJ, Feygin Y, Jawad KS, Bhadury S, Sun J, et al. Recurrent antibiotic use in Kentucky children with 6 years of continuous Medicaid enrollment. J Pediatric Infect Dis Soc, 2022;11(11):492-497. Doi: 10.1093/jpids/piac079

26. Wang CN, Tong J, Yi B, Huttner BD, Cheng Y, Li S, et al. Antibiotic use among hospitalized children and neonates in China: results from quarterly point prevalence surveys in 2019. Front Pharmacol, 2021;12:601561. Doi: 10.3389/fphar.2021.601561

27. Mustafa ZU, Salman M, Yasir M, Godman B, Majeed HA, Kanwal M, et al. Antibiotic consumption among hospitalized neonates and children in Punjab province, Pakistan. Expert Rev Anti Infect Ther, 2022;20(6):931-939. Doi: 10.1080/14787210.2021.1986388

28. National Institue for Health and Care Excellence. Accessed November 6, 2024. Available from: https:www.nice.org.uk/guidance/ng120

29. Simsek B, Senbayrak S, Balik R, Nuhoglu C. Trends of inpatient antibiotic consumption in a children's clinic. Mediterr J Infect Microb Antimicrob, 2021;10:35. Doi: 10.4274/mjima.galenos.2021.2021.35

30. Blackburn J, Barrowman N, Bowes J, Tsampalieros A, Le Saux N. Canadian Pediatric Antimicrobial Stewardship Group. Establishing benchmarks for antimicrobial use in Canadian Children's Hospitals: results from 2 national point prevalence surveys. Pediatr Infect Dis J, 2021;40(10):899-905. Doi: 10.1097/INF.0000000000003170

31. Hsia Y, Lee BR, Versporten A, Yang Y, Bielicki J, Jackson C, et al. Use of the WHO Access, Watch, and Reserve classification to define patterns of hospital antibiotic use (AWaRe): an analysis of paediatric survey data from 56 countries. Lancet Glob Health, 2019;7(7):e861-e871. Doi: 10.1016/S2214-109X(19)30071-3

32. Savage TJ, Sandora TJ. *Clostridioides difficile* infection in children: the role of infection prevention and antimicrobial stewardship. J Pediatric Infect Dis Soc, 2021;10:64-68. Doi: 0.1093/jpids/piab052

33. Zeng L, Wang C, Jiang M, Chen K, Zhong H, Chen Z, et al. Safety of ceftriaxone in pediatrics: a systematic review. Arch Dis Child, 2020;105(10):981-985. Doi: 10.1136/archdischild-2019-317950

34. Kong W, Mao W, Zhang L, Wu Y. Disproportionality analysis of quinolone safety in children using data from the FDA adverse event reporting system (FAERS). Front Pediatr, 2023;10:1069504. Doi: 10.3389/fped.2022.1069504

Acta Pharm. Sci. Vol 63:(1), 2025
Original article
DOI: 10.23893/1307-2080.APS6309

Stability indicating RP-HPLC method development for ondansetron hydrochloride estimation in bulk

Prathamesh SHIROLE[1], Dhanashree P. SANAP[2*], Kisan JADHAV[2]

1 University of Mumbai, School of Pharmacy, Department of Quality Assurance, Navi Mumbai, India
2 University of Mumbai, School of Pharmacy, Department of Pharmaceutics, Navi Mumbai, India

ABSTRACT

To determine ondansetron hydrochloride in bulk drug, an easy, fast, sensitive, and discerning stability-indicating (RP-HPLC) approach is proposed. Ondansetron hydrochloride was eluted from C18 column (4.6 × 250 mm, 5 µm) and mobile phase containing methanol, acetonitrile and water (50: 30: 20 v/v/v). According to ICH Q2 (R1) guidelines, the entire analytical technique validation was completed. The results of the retrieval study, which was conducted at working concentration levels between 80 to 120%, ranged from 99% to 101%. With a linear regression curve (R^2=0.9941), the linearity was assessed in the working concentration range of 5-35 µg mL^{-1}, with a limit of quantitation (LOQ) and detection (LOD) of 0.2559 µg mL^{-1} and 0.7755 µg mL^{-1}, respectively. Ondansetron hydrochloride showed a retention time of 4.997 min. The approach exhibited good recovery with relative standard deviations under 2% for intra and inter-day precision.

Keywords: ondansetron hydrochloride, RP-HPLC, ICH guidelines, validation, stability studies

*Corresponding author: Dhanashree P. SANAP
E-mail: dhanashree.sanap@bvcop.in
ORCIDs:
Prathamesh SHIROLE: 0009-0007-1474-1175
Dhanashree P. SANAP: 0000-0002-4794-7598
Kisan JADHAV: 0000-0001-7563-3935
(Received 26 Jul 2023, Accepted 22 Mar 2024)

INTRODUCTION

1,2,3,9-tetrahydro-9-methyl-3-[(2-methyl-1H-imidazol-1-yl)methyl]-4H-carbazol-4one(ondansetron), the antiemetic drug is a selective inhibitor of type 3 serotonin (5-HT) receptors[1,2]. It has the chemical formula $C_{18}H_{19}N_3O$ (Figure 1) and a molecular weight of 293.4 g mol^{-1}, respectively[3,4]. From the literature survey, various methods UV[1,5], HPLC[6,7], HPTLC[8], LC-ESI-MS/MS[9], Spectrofluorimetry[10], were reported for the analysis of ondansetron hydrochloride.

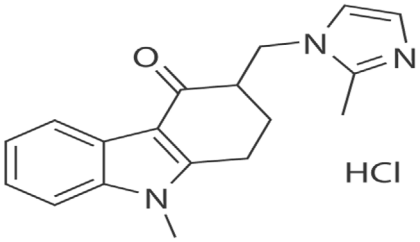

Figure 1. Structure of ondansetron hydrochloride

Pharmaceutical parameter analysis is an essential step in the entire process of developing drugs. Therefore, easy and fast methods are required for checking the quality of commercial formulations. To improve knowledge of the stability of the active pharmaceutical ingredient (API) and drug product stability, and to assist the development of analytical methodology and to achieve details on the degradation products, forced degradation studies are utilised. The purpose of this work was to create a stability-indicating reversed-phase high-performance liquid chromatography (RP-HPLC) method for analysing ondansetron (OND) in pharmaceutical formulations.

METHODOLOGY

Instruments

UV experimentation was performed using a Shimadzu UV- 1800 double beam UV/vis spectrophotometer with a 1 nm spectral bandwidth and a thickness of 1 cm quartz cells, and the calibrated analytical balance (Mettler Toledo) was used.

Shimadzu UFLC (LC 2030) system was used to carry out the chromatographic analysis, AutoSampler, SPD-20 prominence UV/VIS detector. Lab Solutions software was used to check and process the output signals. The analytical column was Hemochrom Intsil C18 – 5U (4.6 mm × 250 mm).

Materials

M/s ZIM Laboratories, B-21/22, MIDC Area, Kalmeshwar, Nagpur, Maharashtra, provided the bulk drug Ondansetron hydrochloride as a gift sample. HPLC-grade chemicals were used (Finar Ltd., Ahmedabad, Avantor Performance Materials India Private Ltd., Thane) and distilled water was used for mobile phase preparation. Before use, solutions and solvents were filtered via a membrane filter (0.45 μm pore size) and then degassed by sonication.

Analytical method development

Wavelength detection

Accurately weighed 10 mg of ondansetron, was transferred to a 100 mL volumetric flask, and distilled water was used to make up the final concentration. About 20 μg mL^{-1} standard solution of OND was prepared using distilled water and scanned in a range of 200-400 nm to determine the maximum wavelength (Figure 2).

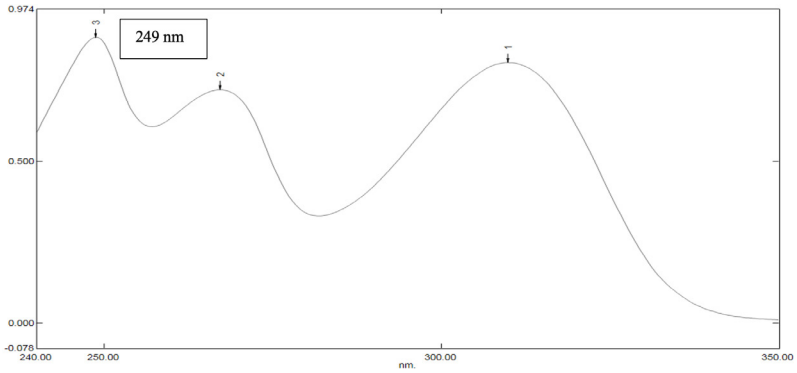

Figure 2. UV Spectrum of pure ondansetron

Chromatographic parameters

To achieve a sharp peak and adequate resolution of OND, various ratios of mobile phase consisting of water and methanol, acetonitrile and water were tried. When methanol: distilled water (80:20 % v/v) was tried, R_t was obtained at 7.296 min with tailing. Further changes were done by taking methanol: acetonitrile: distilled water (60: 20: 20 v/v/v) which showed R_t at 5.21 min along with peak tailing. By adjusting the mobile phase composition, column packing, flow rate, temperature, and detection wavelength, the method was improved, and the impact on retention time and peak form was observed (Figure 3).

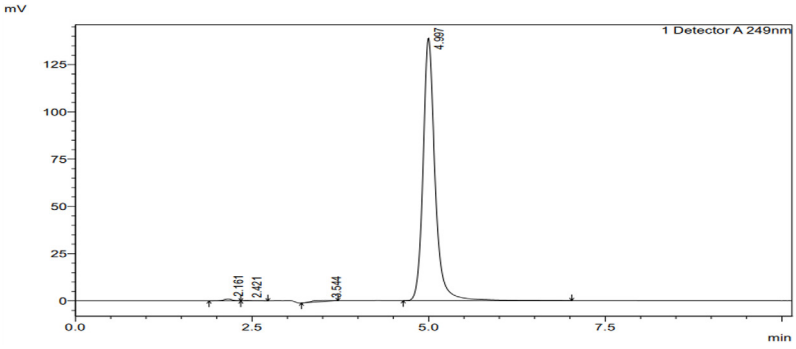

Figure 3. HPLC chromatogram of ondansetron hydrochloride

Sample and standard stock solution preparation

100 mg of OND were dissolved in 100 mL of distilled water (1000 μg mL^{-1}) to create a standard stock solution. 1.0 mL was pipetted out from the above solution and diluted with distilled water in a 10 mL volumetric flask to get a solution of 100 μg mL^{-1}.

Validation of an analytical method

Linearity determination

Aliquots of 0.5, 1.0, 1.5, 2.0, 2.5, 3.0, and 3.5 mL from the aforementioned stock solution were taken in volumetric flasks of 10 mL and diluted with distilled water to get a final concentration in the range of 5-35 μg mL^{-1} [11]. To produce the calibration curve, a graph of the peak area vs drug concentration was created (Figure 4).

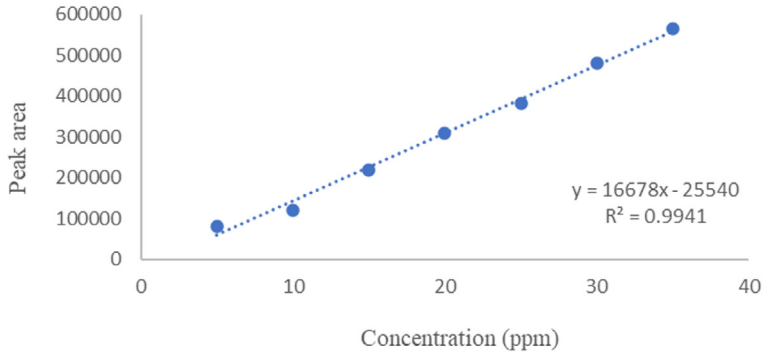

Figure 4. Standard plot of ondansetron hydrochloride

Precision

Repeatability and intermediate precision are two alternative levels of accuracy that can be used. Repeatability is the term used to describe the application of the analytical technique within the laboratory across a shorter period that was assessed by analysing the samples on the same day. Six replicates of the sample injection were used to test repeatability. The three distinct OND concentrations, 5, 20, and 35 μg mL^{-1} were examined three times on the same day to evaluate the intra-day precision. The three concentrations described above were examined for inter-day precision over three consecutive days to determine day-to-day variability[12,13].

Accuracy

Recovery studies were used to determine accuracy at levels of 80 %, 100 % and 120 % using the standard addition method, the sample was then supplemented with a known concentration of OND and it was then exposed to the suggested HPLC procedure[12,14]. Three accuracy studies were carried out, with the results of each research being used to calculate the % recovery and RSD %.

Robustness

By making minor, deliberate changes to a few parameters, the robustness of the technique was investigated. The rate of flow, detection wavelength and mobile phase composition were changed by ± 0.2 mL/min, ± 2nm and ± 10 mL, respectively. At a concentration of 20 μg mL^{-1}, robustness tests were conducted[15,16].

Limit of Detection (LOD) and Quantitation (LOQ)

According to the ICH, a process limit of quantitation is the smallest amount of analyte that can be quantitatively recognised in a sample, whereas a process limit of detection is the lowest concentration of analyte that can occasionally be detected but not exactly defined as a value[17,18,19]. LOD and LOQ were determined using the formula below:

$$LOD = 3.3 \times \sigma / S \text{ and } LOQ = 10 \times \sigma / S$$

σ=regression line's y-intercept standard deviation

S=calibration curve's slope

Marketed formulation analysis

The marketed tablet dosage formulation of OND (Vomikind MD 4, Mankind Pharma Limited) was used for the determination of tablet drug content by the proposed method. A precise 10 mg dose of ondansetron hydrochloride from

the formulation was taken in a 100 mL volumetric flask and then distilled water was added up to 50 mL and sonicated for 10 min, final volume was made up to 100 mL with the distilled water. For analysis, the resultant solution was further diluted to a concentration of 25 µg mL^{-1} and filtered using a 0.45 µm filter (Figure 5).

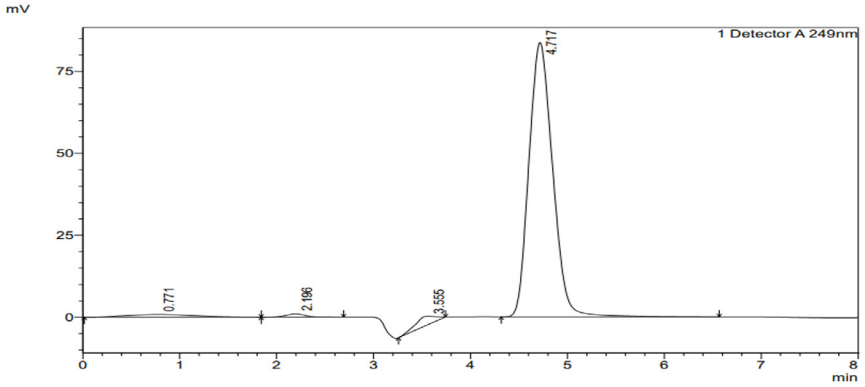

Figure 5. HPLC chromatogram of ondansetron hydrochloride marketed tablet

Forced degradation studies

According to ICH stability criteria, various stress factors, including acidic, alkaline, thermal, peroxide, and photolytic conditions, were used[11,15,20-27] and their blank chromatograph was taken as exhibited in Figure 6 ([a] to [e]).

(a)

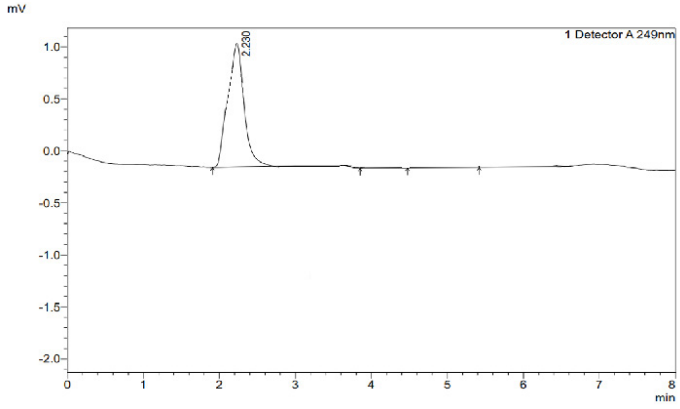

(b)

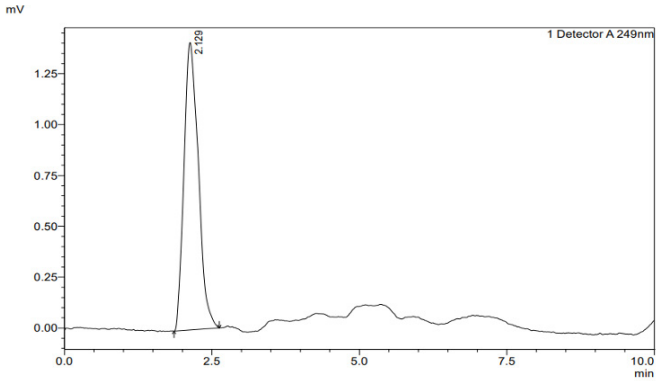
mV
1 Detector A 249nm
2.129
1.25
1.00
0.75
0.50
0.25
0.00
0.0
2.5
5.0
7.5
10.0
min

(c)

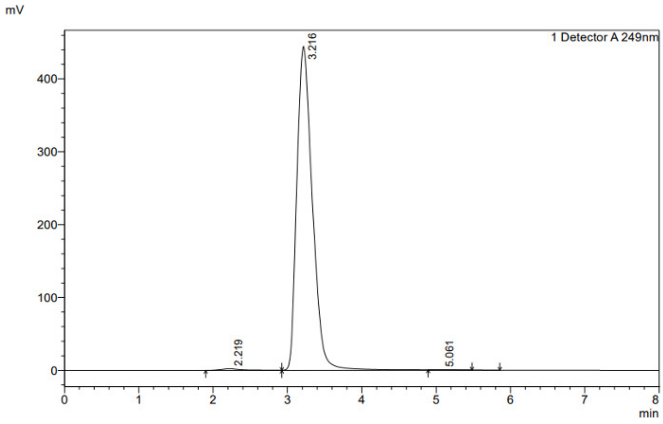
mV
1 Detector A 249nm
3.216
400
300
200
100
0
2.219
5.061
0
1
2
3
4
5
6
7
8
min

(d)

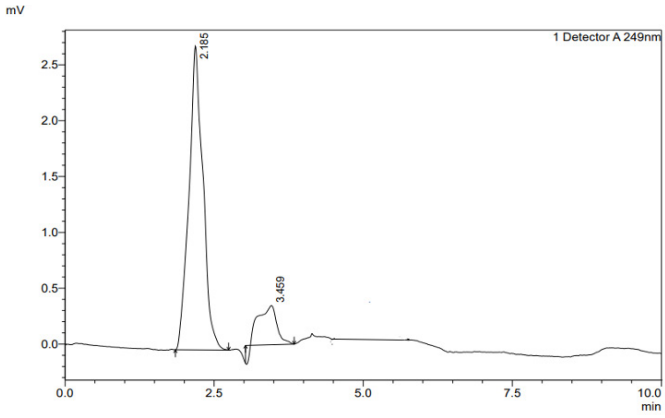
mV
1 Detector A 249nm
2.185
2.5
2.0
1.5
1.0
0.5
0.0
3.459
0.0
2.5
5.0
7.5
10.0
min

(e)

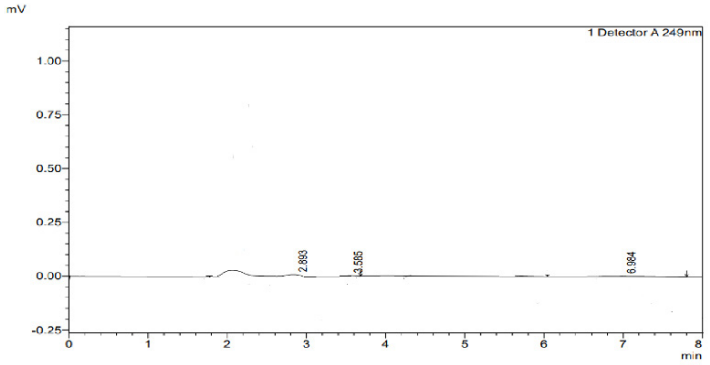

Figure 6. Blank degradation chromatogram of ondansetron (a) acidic degradation; (b) alkaline degradation; (c) peroxide degradation; (d) photolytic degradation; (e) thermal degradation

Thermal degradation

A 25 mL volumetric flask was filled with 5 mL of the standard stock solution, diluent was added, and the combination was heated at 105°C for 6 h. The solution was filtered using a 0.45 µm nylon syringe filter, with some of the filtrate being discarded. Without using the sample, prepare the thermal degradation blank in the same way.

Peroxide degradation

5 mL of the standard stock solution was transferred to a 25 mL volumetric flask, to which 2 mL of 30% H_2O_2 were added. A small amount of diluent was also added, and the mixture was heated at 60°C for 30 min. After cooling, diluent was added to increase volume. A small portion of the solution was discarded after the solution was filtered using a 0.45 µm nylon syringe filter. In the same way, prepare the peroxide degradation blank without utilising the sample.

Acid degradation

A small amount of diluent was added, 5 mL of the standard stock solution and 2 mL of 0.05M HCl were added to a 25 mL volumetric flask, and the mixture was heated at 60°C for 30 min. By adding 2 mL of 0.05M NaOH, the capacity was filled with diluent to neutralise the solution once it has cooled. A small portion of the fluid was eliminated after filtering it with a 0.45 µm nylon syringe filter. Without utilising the sample, prepare the acid degradation blank according to the same procedure[28].

Alkaline degradation

5 mL of the standard stock solution and 2 mL of 0.05M NaOH were added to a 25 mL volumetric flask, some diluent, and heated for 30 min at 60°C. By adding 2 mL of 0.05M HCl and cooling the solution, the solution is neutralised. The volume is then made up with diluent. With a 0.45 µm nylon syringe filter, the solution was filtered, with a small quantity of solution being discarded. Without using the sample, prepare the alkaline degradation blank in the same way.

Photolytic degradation

5 mL of the sample was obtained and placed in a 25 ml volumetric flask using the standard solutions. Diluent was then added to produce the volume, and the sample was then exposed to sunlight for 12 h. The solution was filtered using a 0.45 µm nylon syringe filter, with some of the filtrate being discarded. Without utilising the sample, prepare the photolytic degradation blank in the same way[29].

RESULTS and DISCUSSION

Analytical method development

The choice of an appropriate mobile phase is a crucial step in the development of the HPLC method. The existing literature on OND was used to guide the trial-and-error process of choosing and optimising the mobile phase. Various combinations of mobile phases were tried based on the polarity and solubility of ondansetron after a thorough literature survey. At first methanol: distilled water was used in the ratio of 70:30 and 80:20 %v/v, but no proper peak was observed. Then, acetonitrile: distilled water in a ratio of 80:20 and 70:30 %v/v was tried, and peak tailing of ondansetron was observed. After that, acetonitrile: distilled water (85:15 %v/v) showed a good peak, but the results were not reproducible. A further modification was done, and the mobile phase was changed methanol: acetonitrile: distilled water in the ratio 40:40:20 %v/v/v was optimized in that a broad peak was obtained. Furtherly, methanol: acetonitrile: distilled water in a ratio of 50:30:20 %v/v/v was used which gave well resolved peak without tailing.

After the selection of the appropriate mobile phase, further optimization was carried out to set chromatographic parameters like flow rate, column temperature and injection volume to get a well-resolved peak. Different flow rates range from 0.5-1.5 mL/min, column temperature in the range of 25°C-40°C and injection volume in the range of 5-20 µL. The column temperature was maintained at 30°C for better results. To minimize the carryover of a drug, the

injection volume was set at 5 µL, which shows good sensitivity and to decrease the backpressure of the column, the flow rate was kept at 1.0 mL/min.

About 20 µg mL^{-1} standard solution of OND was prepared using distilled water and scanned in a range of 200 - 400 nm. The maximum absorbance was found at 249 nm (Figure 2).

The final mobile phase included methanol, acetonitrile, and distilled water in the ratio 50: 30: 20 v/v/v to get a resolved sharp peak. The injection volume was 5 µL with a flow rate of 1.0 mL min^{-1} and the eluent was obtained at 249 nm and a 30°C column temperature. According to these specifications, the retention time of the OND peak was 4.997 min (Figure 3).

Using distilled water, acetonitrile, and methanol as the mobile phase, with a flow rate of 1 mL/min, a good peak symmetry and a decent resolution for ondansetron hydrochloride were obtained.

Analytical method validation

With a linear correlation coefficient of 0.9941, it was discovered that the linearity of OND was in the range of 5-35 µg mL^{-1} (Figure 5) and all the quantitative parameters were estimated as listed in Table 1.

For intraday and interday precision, the RSD % was discovered to be in the range of 0.65% - 1.84% and 0.27% - 2.24%, respectively. (Table 2[a] and 2[b]). The % recovery for Ondansetron was found in the range of 98.61% - 102.50% which shows there is no interference from the excipient. Table 3 shows the results of the accuracy studies. Robustness revealed that no changes were observed in the chromatogram of OND, hence, we may claim that the suggested method is reliable (Table 4).

Table 1. Quantitative and validation parameters

Parameter	Ondansetron hydrochloride
λ_{max} (nm)	249
Beer' law limits (µg mL^{-1})	5 - 35
Regression equation	16678x - 25540
Correlation coefficient (R^2)	0.9941
Accuracy	98.61% - 102.50%
Precision (intraday)	0.65 - 1.84 RSD %
Precision (interday)	0.27 - 2.24 RSD %
Robustness	0.06 - 2.00 RSD %
LOD and LOQ	0.2559 µg mL^{-1} and 0.7755 µg mL^{-1}

Table 2. Result of intra-day and inter-day precision

	Concentration (µg mL^{-1})	Peak Area			RSD %		
		Morning*	Afternoon*	Evening*	Morning	Afternoon	Evening
Intra-day precision	2	0.0883	0.0893	0.0916	0.65%	1.70%	1.66%
	12	0.5043	0.5026	0.5067	1.09%	1.84%	1.34%
	22	0.9400	0.9380	0.9416	1.33%	1.46%	1.44%
	Concentration (µg mL^{-1})	Peak Area			RSD %		
		Day I*	Day II*	Day III*	Day I	Day II	Day III
Inter-day precision	2	78844.7	88469	88042.7	1.64%	0.53%	0.27%
	12	312396	317032	326994	2.02%	1.90%	0.80%
	22	576312	525265	669645	2.24%	1.42%	1.81%

* Mean of three replicates n=3

Table 3. Result of accuracy studies

Concentration of the sample (µg ml^{-1})	Concentration of drug added (µg ml^{-1})	Percent of spiked	Recovered amount* (µg ml^{-1})	Percent recovery
10	8	80%	17.75	98.61%
10	10	100%	20.41	102.05%
10	12	120%	22.55	102.50%

* Mean of three replicates n=3

Table 4. Result of robustness

Parameters	Variation	R_t	Peak Area	Mean	RSD %
Flow rate	0.8ml/min	5.971	272335	273890	2.00
		5.902	269348		
		5.953	279987		
	1.2ml/min	5.971	175493	178334.3	1.39
		5.902	179423		
		5.953	180087		
Wavelength	247 nm	4.757	207645	207773.3	0.06
		4.765	207772		
		4.773	207903		
	251 nm	4.765	195290	196412.3	0.54
		4.773	196539		
		4.781	197408		
Mobile phase ratio	Methanol: ACN: Water (40: 40: 20)	4.781	198412	199872	0.67
		4.492	200152		
		4.608	201052		
	Methanol: ACN: Water (60: 30: 10)	3.999	235275	233223	1.22
		4.052	234436		
		4.115	229958		

The sensitivity of the technique was assessed by calculating the LOD and LOQ, which were found to be 0.2559 μg mL^{-1} and 0.7755 μg mL^{-1}, respectively.

Studies on the stability of Ondansetron under various stresses revealed the following degradation behaviour.

The percent degradation of ondansetron is calculated by using the following formula:

Percentage Degradation (%) = Peak area of degraded compound/Peak area of pure compound x 100

Acidic degradation occurred at retention times of 4.2 and 5.8 min (Figure 7[a], and the % degradation is 18.01%. The degradation product in alkali degradation was observed at retention times of 4.1 and 5.7 min (Figure 7[b]) and the % degradation is 19.16%. In peroxide, photolytic and thermal degradation, the % degradation was found to be 34.49%, 3.98%, and 12.55%, respectively (Table 5) (Figure 7[c], [d], and [e]).

(a)

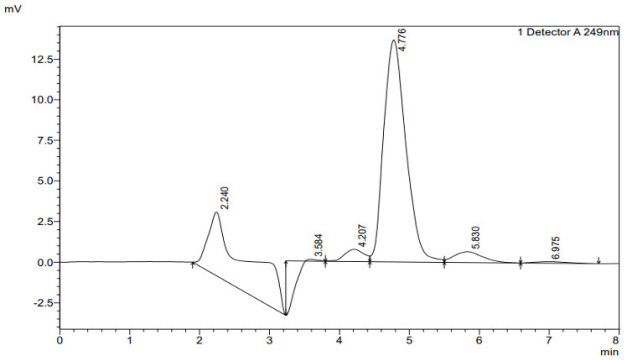

(b)

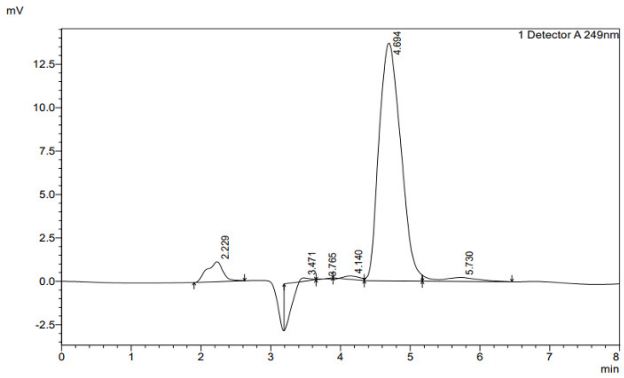

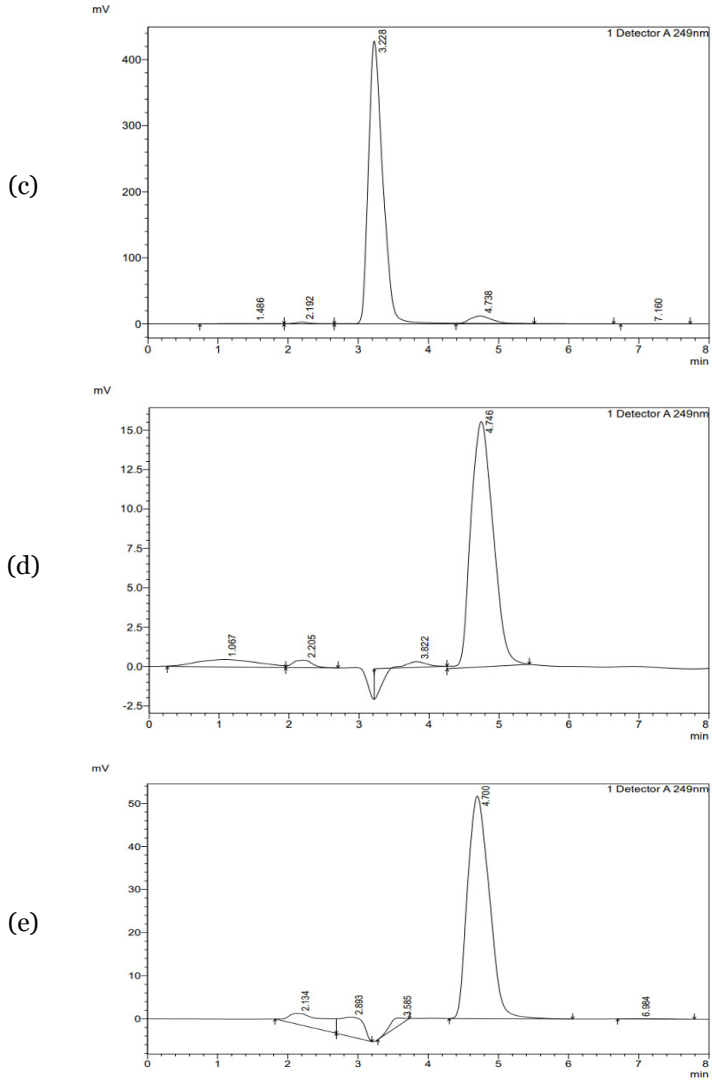

Figure 7. Degradation chromatogram of ondansetron (a) Acidic degradation; (b) Alkaline degradation; (c) Peroxide degradation; (d) Photolytic degradation; (e) Thermal degradation

Table 5. Result of forced-degradation studies

Condition of Stress	Exposure Period	Temperature (ºC)	New Degradation peaks			Degradation Rate (%)
			No of degradation peak observed	R_t (min)	RRT	
Acidic	30 min	60ºC	2	Peak 1: 4.207	Peak 1: 0.881	18.01
				Peak 2: 5.830	Peak 2: 1.220	
Alkaline	30 min	60ºC	2	Peak 1: 4.140	Peak 1: 0.882	19.16
				Peak 2: 5.730	Peak 2: 1.221	
Peroxide	30 min	60ºC	0	-	-	34.49
Photolytic	12 h	Sunlight	1	Peak 1: 3.822	Peak 1: 0.805	3.98
Thermal	6 h	105ºC	0	-	-	12.55

The method that was devised is simple, quick, linear, accurate, exact, and specific. The method's reliability and accuracy are demonstrated by the results of the validation studies. The investigation findings demonstrated that the method is appropriate for identifying ondansetron in bulk and tablet dosage forms without interference from degradation products, and it is advised for regular quality control analysis of the drug ondansetron in pharmaceutical formulation.

STATEMENT OF ETHICS

This study does not require ethical permission to be carried out.

CONFLICT OF INTEREST STATEMENT

No conflicts of interest exist, according to the authors, with the publishing of this paper.

AUTHOR CONTRIBUTIONS

Concept – K.J., P.S., D.S.; Design – K.J., D.S., P.S.; Supervision – D.S.; Resources – D.S., P.S.; Materials – K.J.; Data Collection and/or Processing – D.S., P.S.; Analysis – K.J., D.Ş., P.S.; Literature Search – P.S, D.Ş.; Writing – D.S.; Critical Reviews – D.S., K.J.

FUNDING SOURCES

This research received no specific grant from any funding agency in the public, commercial, or not-for-profit sectors.

ACKNOWLEDGMENT

The instruments and facilities were provided by Bharati Vidyapeeth's College of Pharmacy in CBD Belapur, Navi Mumbai, which the authors gratefully acknowledge. The authors are appreciative of Zim Laboratories, Kalmeshwar, Dist. Nagpur (M.S.), India for providing a gift sample of ondansetron hydrochloride.

REFERENCES

1. Akhtar J, Chaturvedi R, Shrivastava B, Dubey S. Spectrophotometric methods for simultaneous estimation of rabeprazole sodium and ondansetron hydrochloride in combined dosage form. Res J PharmTechnol, 2011;4(6):925-927. Doi: 10.5958/0974-360X

2. Polawar P, Shivhare U, Bhusari K, Mathur V. Development and validation of spectrophotometric method of analysis for fexofenadine HCl. Res J PharmTechnol, 2008;1(4):539-540.

3. The United States Pharmacopoeia. USP 35-NF 33, Revis. Bull, Official 2015. p. 4066.

4. Jhansi K, Chiranjeevi P, Rao KP, Rao YS, Deepthi R. A validated UV spectrophotometric method for the estimation of esomeprazole magnesium trihydrate in bulk and commercial dosage form. J Global Trends Pharm Sci, 2020;11(4):8754-8760.

5. Kolte R, Tambe V, Vichare V, Patil M. Simultaneous spectrophotometric estimation of omeprazole and ondansetron hydrochloride by first order derivative spectroscopy method in combined dosage form. Asian J Res Chem, 2012;5(6):787-790.

6. Liu J, Stewart JT. High-performance liquid chromatographic analysis of ondansetron enantiomers in human serum using a reversed-phase cellulose-based chiral stationary phase and solid-phase extraction. J Chromatogr B, 1997;694:179-184. Doi: 10.1016/S0378-4347(97)00112-6

7. Rajan N, Basha KA. HPLC method development for determination of glyoxal content in ondansetron HCl drug substances by derivatization with 2,4 DNPH. J Liq Chromatogr Relat Technol, 2014; 37(19):2800-2808. Doi: 10.1080/10826076.2013.873871

8. Mujtaba A, Kohli K, Ali J, Baboota S. Development of HPTLC method for the estimation of ondansetron hydrochloride in bulk drug and sublingual tablets. Drug Test Anal, 2013;5(2):122-125. Doi: 10.1002/dta.311

9. Moreira RF, Salvadori MC, Azevedo CP, Silva DO, Borges DC, Moreno RA. Development and validation of a rapid and sensitive LC-ESI-MS/MS method for ondansetron quantification in human plasma and its application in comparative bioavailability study. Biomed Chromatogr, 2010;24(11): 1220-1227. Doi: 10.1002/bmc.1431

10. Sambhani NG, Biju VMN, Starvin AM. Determination of ondansetron by spectrofluorimetry: application to forced degradation study, pharmaceuticals and human plasma. J Fluoresc, 2019;29(1): 203-209. Doi: 10.1007/s10895-018-2329-x

11. Kalal DJ, Redasani VK. Stability-indicating RP-HPLC method development and validation for estimation of mupirocin calcium in bulk and in pharmaceutical formulation. Future J Pharm Sci, 2022; 8(21):305-315. Doi: 10.1186/s43094-022-00412-w

12. Basha MD, Praveena B, Srinidhi M, Rahaman SK. Method development and validation of ondansetron in bulk and pharmaceutical dosage form by stability-indicating RP-HPLC method. Int J PharmTech Resh, 2013;5(1):86-98.

13. Haque A, Shahriar M, Parvin N, Ashraful Islam SM. Validated RP-HPLC method for estimation of ranitidine hydrochloride, domperidone and naproxen in solid dosage form. Asian J Pharm Anal, 2011; 1(3):59-63.

14. Annapurna MM, Venkatesh B, Kumar JSP. Chaitanya SM. Stability indicating RP-HPLC method for determination of ondansetron. J Chem Pharm Sci, 2017;10(2):764-767.

15. Singh PK, Subas CD. Development and validation of a stability indicating RP-HPLC method for determination of ondansetron in orally disintegrating films. Int J Resh in Pharm and Sci, 2013;3(1):57-66.

16. Rakam GK, Mallik A, Sucharitha CH. Method development and validation of reverse phase high performance liquid chromatography method for estimation of ondansetron and pantoprazole in their tablet dosage form. Indian J Pharm Sci, 2022;84(2):483-492. Doi: 10.36468/pharmaceutical-sciences.942

17. Sheshala R, Darwis Y, Khan N. Development and validation of an RP–LC–UV method for the determination of ondansetron: application to pharmaceutical dosage forms. Chromatographia, 2009;70(1):75-81. Doi: 10.1365/s10337-009-1117-9

18. Siddiqui K, Dubey B. Analytical method development and validation of ondansetron and telmisartan in tablet dosage form by RP-UPLC method. J Drug Deliv Ther, 2022;12(4):112-127. Doi: 10.22270/jddt.v12i4-S.5548

19. Rao GK, Vadrevu S, Haripriya M. Method development and validation for simultaneous estimation of omeprazole and domperidone by RP-HPLC. Asian J Pharm Anal, 2015;5(4):195-205. Doi: 10.5958/2231-5675.2015.00031.9

20. Ragab MAA, El Yazbi FA, Hassan EM, Khamis EF, Hamdy MAA. Green HPTLC and stability-indicating RP-HPLC for the assay of dextromethorphan hydrobromide and menthol in their lozenges. Ann Pharma Fr, 2020;78(5):368-378. Doi: 10.1016/j.pharma.2020.04.006

21. Sonawane S, Jadhav S, Rahade P, Chhajed S, Kshirsagar S. Development and validation of stability indicating method for estimation of chlorthalidone in bulk and tablets with the use of experimental design in forced degradation experiments. Scientifica, 2016:1-9. Doi: 10.1155/2016/4286482

22. Charde MS, Welankiwar AS, Chakole RD. Development of force degradation profile of atenolol and chlorthalidone in combine tablet dosage form by RP-HPLC. Int J Pharm Chem, 2014;4(3):92-98.

23. Shah BP, Jain S, Prajapati KK, Mansuri NY. Stability indicating HPLC method development: a review. Int J Pharm Sci and Resh, 2012;3(9):2978-2988. Doi: 10.13040/IJPSR.0975-8232.3(9).2978-88

24. Kongkiatpaiboon S, Duangdee N, Chewchinda S, Poachanukoon O, Amnuaypattanapon K. Development and validation of stability indicating HPLC method for determination of adrenaline tartrate. J King Saud Univ Sci, 2019;31(1):48-51. Doi: 10.1016/j.jksus.2017.05.016

25. Alani H, Alashkar I, Karabet F. Development and validation of stability-indicating RP-HPLC method for the determination of levocabastine hcl in bulk drug and in ophthalmic suspensions. Arab J Chem, 2017;10(2):3097-3107. Doi: 10.1016/j.arabjc.2013.11.051

26. Babu GR, Rao JS, Kumar SK, Reddy JP. Stability indicating liquid chromatographic method for aripiprazole. Asian J Pharma Anal, 2011;1(1):3-7.

27. Bhavya B, Nagaraju P, Mounika V, Priyadarshini G. Stability indicating RP-HPLC method development and validation for simultaneous estimation of albendazole and ivermectin in pharmaceutical dosage form. Asian J Pharm Anal, 2017;7(1):6-14. Doi: 10.5958/2231-5675.2017.00002.3

28. Pinaz AK, Muralikrishna KS. Method development and acid degradation study of rivaroxaban by RP-HPLC in bulk. Asian J Pharm Anal, 2013;3(2):62-65.

29. Gupta A, Rawat S, Pandey A. Method development and photolytic degradation study of doxofylline by RP-HPLC and LC-MS/MS. Asian J Pharm Anal, 2011;1(2):29-33.

Acta Pharm. Sci. Vol 63:(1), 2025
Original article
DOI: 10.23893/1307-2080.APS6310

Phyto-metabolomic investigation and anti-migratory potential of *Moringa oleifera* Lam. and *Moringa peregrina* (Forssk.) Fiori against hepatic carcinoma cell line

Ezzat E. A. OSMAN[1*], El-Sayed S. ABDEL-HAMEED[1], Mohamed A. SHEMIS[2]
Samah MAMDOUH[2]

1 Theodor Bilharz Research Institute, Department of Medicinal Chemistry, 12411, Giza, Egypt
2 Theodor Bilharz Research Institute, Department of Biochemistry and Molecular Biology, 12411, Giza, Egypt

ABSTRACT

The present study aims to characterize the active ingredients of *Moringa oleifera* (MO) and *Moringa peregrina* (MP) leaf extracts and evaluate their cytotoxic and anti-migration efficacies against liver cancer cells (HepG2). The chemical profiling of the aqueous and methanolic extracts of both *Moringa* species was carried out using LC-ESI-MS led to identifying of 37 compounds classified as flavonoids, phenolic acids, glucosinolate, and phenyl ethanoid. The MTT assay was used to assess the cytotoxic effect, which revealed to, the increasing of the MO and MP extracts' concentration adversely decreased the treated cells' viability. Treating of HepG2 cells by MO and MP for different time intervals effectively inhibited wound closure, while the cells migratory ability in the treated cells was decreased. This study reports that MO and MP extracts exhibited promising cytotoxic effects and inhibited migration of highly metastatic HepG2 cell lines, which may be due to the presence of polyphenolic compounds.

Keywords: *Moringa*, anti-migration, HepG2, LC-ESI-MS, phenolic compounds

*Corresponding author: Ezzat E. A. OSMAN
E-mail: ezzat_ea@yahoo.com; e.abdellateef@tbri.gov.eg
ORCIDs:
Ezzat E. A. OSMAN: 0000-0001-8893-3662
El-Sayed S. ABDEL-HAMEED: 0000-0002-0482-2170
Mohamed A. SHEMIS: 0000-0003-2493-7466
Samah MAMDOUH: 0000-0001-5979-3189
(Received 14 Mar 2023, Accepted 28 Sep 2023)

INTRODUCTION

Cancer is one of the leading causes of death globally, and the incidence of this group of diseases will continue to grow because of the increasing ageing of the population[1]. Hepatocellular carcinoma (HCC) is a frequent primary liver malignancy that primarily affects individuals, and it is the third leading cause of death worldwide[2]. The incidence of HCC has increased globally over the past 20 years, and in some countries, including the USA, it is anticipated to continue to rise through the year 2030[1]. The standard treatment for HCC mainly involves liver transplantation, surgical resection and chemotherapy[3]. Unfortunately, surgical resections are not suitable for HCC patients with advanced stages, especially those with liver cancer metastasis[4]. In addition, the currently available chemotherapeutic drugs are not effective to treat advanced HCC because of acquired resistance to the treatment[5]. In this regard, it is necessary to find more effective compounds, which may provide a novel therapy for HCC treatment, especially in the advanced stage.

Although there have been significant advancements in cancer therapy, metastasis still accounts for more than 90% of cancer-related deaths[6]. However, to treat cancer more effectively, we should further focus on preventing the formation and growth of metastatic carcinoma cells. We should consider that inhibition of migration, associated with the process of metastasis, might be as important as inhibition of cell proliferation.

At present, there is no effective therapy that can be used for patients diagnosed with HCC. There is a need for chemopreventive products targeting middle-aged patients. This is because treatment results are not sustainable for the health system, which does not cover the population[7]. Developing such a product from traditional medicinal plants would facilitate better compliance among a lot of patients, as the use of traditional plants and herbs is culturally embedded into the local lifestyle[8].

In recent years, the use of plants in primary health care and phytotherapeutic research has increased owing to the identification of bioactive molecules in medicinal plants and growing interest in alternative medicines. The World Health Organization (WHO) estimates that 80% of people receive their main medical care from plant-based traditional medicine. Also, in the clinical studies, more than 50% of the anticancer medications used came from naturally occurring plant sources[9].

The *Moringa* genus (Moringaceae family) contains 13 species found in Asia and Africa. *Moringa* species possess many biological properties, including an-

ti-inflammatory, antioxidant, anticancer, and antihyperglycemic due to their high alkaloids, flavonoids, glucosides, terpenes, and glucosinolate contents[10]. *Moringa oleifer*a Lam. (MO) is the most widely known and utilized due to its broad spectrum of health benefits[11]. While *Moringa peregrina* (Forssk.) Fiori (MP) is a potential crop candidate and is renowned for its ability to withstand drought and for its rich nutritional and therapeutic benefits[12].

The present study aims to identify the active constituents of MO and MP extracts using LC-ESI-MS as well as evaluate their *in vitro* cytotoxic and anti-migratory effects on liver cancer cells.

METHODOLOGY

Collection of plant material

The leaves of MO were obtained from the Egyptian Scientific Association of *Moringa*, National Research Center. While MP leaves were obtained from the Orman Garden, Giza, Egypt. The samples of the two plants were kindly identified by Mrs. Therese Labib, a consultant in plant taxonomy at the Orman Garden. Voucher specimen numbers 27318 (MO) and 27319 (MP) were kept at the Department of Medicinal Chemistry, Theodor Bilharz Research Institute, Giza, Egypt. The leaves of both *Moringa* species were dried in the shade at room temperature, then crushed to a fine powder by the electric mill and kept for the extraction process.

Preparation of the extracts

One hundred grams of both *Moringa* species' dried leaf powder were extracted with 500 mL of pure methanol (MeOH). The filtrate was evaporated using a rotary evaporator (Buchi, Switzerland) under vacuum till dryness, this step was repeated three times to obtain semi solid crude MeOH ext. (17 g). Furthermore, 10 g of the dried MeOH ext. were fractionated by *n*-butanol (*n*-BuOH). The soluble constituents in *n*-BuOH were filtered and concentrated using a rotatory evaporator to obtain 5.24 g of a dry *n*-BuOH fraction (fr.). On the other hand, another amount of leaf powder (100 g) of each *Moringa* species was extracted using boiling H_2O (500 mL) for 6 hours (h) with stirring until all the soluble constituents dissolved in the solvent, followed by filtration. The aqueous filtrate was concentrated using a rotary evaporator and this step was repeated three times to obtain H_2O ext. (8.50 g). All extracts were stored in brown glass vials until further use.

LC-ESI-MS phytochemical analysis of MO and MP extracts

The aqueous (H_2O) and MeOH extracts of both MO and MP species were chemically investigated via liquid chromatography coupled with electrospray ionization mass spectrometry (LC-ESI-MS). The experiments were carried out according to El-Wakil et al.[13] with little modification using the LC system (Waters Alliance 2695, Waters, USA) and reversed-phase analytical column C18, 250 mm, and 5 μm particle size (Phenomenex, USA). The mobile phase consists of two eluents; A (H_2O + 0.1% formic acid) and B (CH_3CN: MeOH [1:1] +0.1% formic acid). The injection volume was 20 μL of 5 mg/mL of each extract, and the elution flow was 400 μL/min. The LC time program was as follows: 0.0–2.0 min (5% B), 2.0–10 min (5.0%–10% B), 10–70 min (10%–50% B), 70–80 min (50%–70% B), 80–95 min (70%–5% B) and 95–100 min (5% B). The ESI-MS spectra were calculated by scanning in the 50–1000 m/z range with the following parameters: the source temperature was set at 150 °C, the capillary voltage was at 3 kV, the cone voltage was at 70 eV, the desolvation gas flow was at 600 L/h, the desolvation temperature was at 350°C, and the cone gas flow was at 50 L/h. The compounds were assigned by retention time, and mass spectroscopic results were compared to literature data.

Cell culture maintenance

The HepG2 cells were acquired from Nawah Scientific Inc., (Mokattam, Cairo, Egypt). The cells were seeded in Dulbecco's Modified Eagle Medium (DMEM) additionally with 10% heat-inactivated fetal bovine serum (FBS) and 1% penicillin/streptomycin. Then, incubated in a humidified 5% CO_2 atmosphere at 37°C. Cell passage was between 12 and 15, at 75-85% confluence used for seeding and treatment throughout the experiment.

3-(4, 5-dimethylthiazol-2-yl)-2, 5-diphenyl-2H-tetrazolium bromide (MTT) assay

This assay is a sensitive, quantitative, and reliable colorimetric method that measures the viability of cells. The assay is based on the ability of mitochondrial lactate dehydrogenase enzymes (LDH) in viable cells to convert the water-soluble substrate of MTT into dark blue formazan crystals, which are water insoluble.

HepG2 cells were cultured in a 24-well plate to get a cell count of 500,000/well and grown for 24 h at 37°C to reach 85% confluency. Once the cells had adhered, they were treated with serial dilutions of MO and MP extracts (MeOH ext., H_2O ext. and *n*-BuOH fr.) with concentrations of 3.25, 6.25, 12.5, 25, 50, and 100 μg/mL. Untreated cells were used as the control and the plate was

incubated for 24 h at 37°C, then 10 µL of 5 mg/ml MTT reagent were added to each well and incubated again for 4 h in the dark. The supernatant was removed and 200 µL of dimethyl sulfoxide (DMSO) was added to each well, including the control. Followed by shaking and then the plate was kept in a dark place for about 10 min at room temperature. The absorbance of each well was recorded at 570 nm using a microplate reader (Molecular Devices Co., CA, USA). The viability percentage was calculated as follows:

$$\text{The cell viability \%} = (\text{OD of treated cells}/\text{OD of untreated cells}) \times 100$$

The drug concentrations needed to inhibit 50% of cell growth relative to untreated control cells were calculated as the half maximal inhibitory concentration (IC_{50}) values.

In-vitro wound healing migration assay

The migration of HepG2 was examined using the scratch assay method. Cells were plated at a density of $3x10^5$/well onto a coated 24-well plate for scratch wound assay and cultured overnight in 5% FBS-DMEM at 37°C and 5% CO_2. The cells were allowed to adhere. On the next day, a sterilized micro-pipette tip was used to scratch across the cell layer and horizontal scratches were introduced into the confluent monolayer. After removing the supernatant, the cells were treated with different extracts of both MO and MP at a concentration of 10 µg/mL. Images were taken using an inverted microscope at 0, 24, 48, 72, and 96 h. The plate was incubated in 5% CO_2 at 37°C in-between time points. To determine the migration rate, images were analyzed by MII Image View software version 3.7.

Statistical analysis

The data were calculated using the statistical package for social science, IBM SPSS Statistics for Windows, version 26 (IBM Corp., Armonk, N.Y., USA) and Microsoft Excel 2016. Continuous normally distributed variables were represented as Mean ± SD with a 95% confidence interval and using the frequencies and percentage for categorical variables; a p value<0.05 was considered statistically significant. The student's t-test was used to evaluate the means of normally distributed variables between groups. The Pearson correlation coefficient (r) was used to show the correlation between different parameters in this study. The migration rate was calculated by dividing the time spent in migration according to the formula: Rm = Wi–Wf / t; where Rm is the rate of cell migration, Wi is the average initial wound width, Wf is the average final wound width, and t is the duration of migration (in hours).

RESULTS and DISCUSSION

LC-ESI-MS phytochemical characterization of MO and MP extracts

The use of plant extracts, containing hundreds of chemicals as pharmaceutical agents, is no longer a black box or the primary obstacle to understanding their mechanisms of action and the contained active compounds[14]. Over the past three decades, there has been a significant rise in the use of herbal medicines and supplements, with at least 80% of people using them for some aspect of primary healthcare[15]. Multiple molecules of medicinal plant origin are currently used as drugs to combat cancer[16]. *Moringa* species contain numerous phytoconstituents, including alkaloids, flavonoids, phenolic acids, tannins, steroids, glucosinolates, saponins, and terpenes. Its diverse pharmacological benefits are a result of the variety of these phytochemicals in this genus[10].

In the present study, the phytochemical analysis of 70% MeOH and aqueous extracts of both *Moringa* leaf extracts was carried out by LC-ESI-MS. The identification of compounds was confirmed by mass fragmentation analysis, as shown in Figure 1. Figure 2 shows the total ion chromatograms of these extracts. A total of 37 polyphenolic compounds, including 20 flavonoids, 11 phenolic acids, 5 glucosinolates, and 1 phenyl ethanoid were identified, as shown in Table 1. These compounds were detailed tentatively identified and classified as follows:

Table 1. Tentative assignment of the chemical composition of MO and MP extracts

Comp. No.	t_R (Min)	MW	[$[M-H]^-$ m/z	MS fragments	Tentative assignment	MO		MP	
						MeOH ext.	H_2O ext.	MeOH ext.	H_2O ext.
1	2.92	342	341	179, 135	Caffeoyl-glucoside	-	-	+	+
2	3.00	192	191	173, 93, 85	Quinic acid	+	-	-	-
3	4.09	196	195	97, 80	Hydroxytyrosol acetate	+	+	+	+
4	7.26	361	360	259, 97	Glucosinolate derivatives	+	-	-	-
5	12.27	571	570	328, 275, 97	Glucomoringin	+	+	+	-
6	13.94	516	515	353, 341, 179 (100%), 135	3-Caffeoylquinic glycoside	-	-	-	+
7	17.03	330	329	191, 167 (100%), 135	Vanillic acid-4-*O*-β-D-glucopyranoside	-	+	-	-
8	17.53	354	353	191 (100%), 179, 150, 135	3-Caffeoylquinic acid	+	+	+	+
9	21.63	613	612	259, 97	4-(2′-*O*-Acetyl-α-L-rhamnopyranosyloxy) benzyl glucosinolate	-	-	+	-
10	22.21	338	337	191, 163 (100%), 119	3-Coumaroylquinic acid	+	+	+	+
11	23.63	338	337	191, 163, 119	3-Coumaroylquinic acid isomer	+	+	-	+
12	24.63	613	612	259, 97	4-(3′-*O*-Acetyl-α-L-rhamnopyranosyloxy) benzyl glucosinolate	-	-	+	-
13	25.97	354	353	191, 179 (100%), 173, 135	3-Caffeoylquinic acid isomer	+	+	+	+
14	27.47	626	625	463, 301	Quercetin-di-*O*-glycoside	-	-	+	+
15	31.15	338	337	191, 173 (100%), 163, 119	4-Coumaroylquinic acid	-	+	-	+
16	32.06	594	593	503, 473, 383, 353	Apigenin-6,8-di-C-glycopyranoside (Vicenin-2)	+	-	+	+
17	32.48	338	337	191, 173 (100%), 163, 119	4-Coumaroylquinic acid isomer	-	+	-	-
18	32.73	613	612	259, 97	4-(4′-*O*-Acetyl-α-L-rhamnopyranosyloxy) benzyl glucosinolate	-	-	+	-
19	33.07	594	593	503, 473, 383, 353	Apigenin-6,8-di-C-glycopyranoside (Vicenin-2) isomer	-	+	-	-
20	33.23	368	367	193, 173 (100%), 135	4-Feruloylquinic acid	-	+	-	+

21	36.32	626	625	609, 463, 301	Quercetin-di-*O*-glycoside isomer	-	-	+	+
22	39.99	432	431	341, 311 (100%), 283	Vitexin or isovitexin	-	-	+	-
23	41.50	432	431	341, 311 (100%), 283	Vitexin or isovitexin	-	-	+	-
24	42.50	610	609	463, 301, 179	Quercetin-3-*O*-rutinoside	+	+	+	+
25	43.42	464	463	301 (100%), 271, 179	Quercetin-3-*O*-glycoside	+	+	+	+
26	46.51	608	607	505, 463, 301 (100%), 179	Quercetin-hydroxymethylglutaroyl glycoside	-	-	+	-
27	47.01	506	505	463, 301 (100%), 271, 179	Quercetin-3-*O*-acetyl-glycoside	-	-	+	+
28	48.18	448	447	285 (100%), 255	Kaempferol-3-*O*-glycoside	-	-	+	+
29	48.51	506	505	301 (100%), 271, 179	Quercetin-3-*O*-acetyl-glycoside isomer	-	-	+	+
30	48.68	594	593	447, 285, 151	Kaempferol-3-*O*-rutinoside	+	+	-	-
31	49.43	624	623	447, 285, 151	Kaempferol-3-*O*-glycoside-glucoronoid	+	+	-	-
32	50.18	478	477	315, 151	Isorhamnetin 3-*O*-glycoside	+	+	-	-
33	50.35	302	301	271 (100%), 165	Quercetin	-	-	+	-
34	52.60	286	285	255, 179	Kaempferol	-	-	+	+
35	54.61	490	489	285 (100%), 255	Kaempferol-*O*-acetyl-glycoside	-	-	+	-
36	55.44	520	519	421, 315 (100%), 285	Isorhamnetin-*O*-acyl-glycoside	-	-	+	-
37	72.14	574	573	463, 301 (100%), 179	Quercetin derivative	-	-	+	-

Flavonoids

Flavonoids are the most abundant group of polyphenolic compounds detected in MO and MP extracts in which quercetin, kaempferol, apigenin and isorhamnetin derivatives are the major flavonoids. Compounds 14 and 21 (t_R=27.47 and 36.32 min, respectively) had $[M-H]^-$ at *m/z* 625 which afforded main fragments at *m/z* 463 $[M-H-162]^-$ and 301 $[M-H-(162\times2)]^-$ which means the presence of quercetin aglycon attached with two glycoside moieties. Thus, these compounds were assigned as quercetin-di-*O*-glycoside[17]. Compound

24 (t_R=42.50 min) represented a precursor ion at *m/z* 609 along with other fragment peaks at *m/z* 463, 301 and 179 which characteristics for quercetin-3-*O*-rutinoside. Compound 25 (t_R=43.42 min) exhibited an *m/z* 463 $[M-H]^-$ which was assigned as quercetin-3-*O*-glycoside. Compound 26 (t_R=46.51 min) showed a deprotonated molecule at *m/z* 607 was assigned as quercetin-hydroxymethylglutaroyl glycoside based on hydroxymethylglutaroyl moiety produced the ion *m*/z 463 $[M-H-144]^-$ and ion at *m/z* 301 $[M-H-144-162]^-$ of quercetin aglycone. Compounds 27 and 29 (t_R=47.01 and 48.51 min) afforded a $[M-H]^-$ at *m/z* 505 and product ions at 463 and 301 (quercetin) which reflect the elimination of acetyl and glycoside moieties, respectively. Thus, they were identified as quercetin-3-*O*-acetyl-glycoside. Compound 33 (t_R=50.35 min) was characterized as quercetin with m/z 301 along with product ions at *m/z* 271, 165. In addition, compound 37 (t_R=72.14 min) was annotated as a quercetin derivative with *m/z* 573 $[M-H]^-$ and product ions at m/z 463, 301, and 179.

Compound 34 (t_R=52.60 min) was characterized as kaempferol with *m/z* 285 $[M-H]^-$ and product ions at *m/z* 255 and 179. Compound 28 (t_R=48.18 min) was assigned as kaempferol-3-*O*-glycoside due to the existence of $[M-H]^-$ at *m/z* 447 and 285 $[M-H-162]^-$ due to the loss of the glycoside moiety. Compound 30 (t_R=48.68 min) was assigned as kaempferol-3-O-rutinoside with $[M-H]^-$ at *m/z* 593 and product ions at m/z 447 [M-H-146]- and 285 [M-H-146-162]- due the elimination of the rutinoside moiety. Compound 31 (t_R=49.43 min) was characterized as kaempferol-3-*O*-glycoside-glucuronide which had *m/z* 623 $[M-H]^-$ and product ions at *m/z* 447 $[M-H-176]^-$ and 285 $[M-H-176-162]^-$ due to the loss of the glucuronide and glycoside units, respectively. Moreover, Compound 35 (t_R=54.61 min) was identified as kaempferol-*O*-acetyl-glycoside due to the appearance of *m/z* 489 $[M-H]^-$ and main signal at *m/z* 285 $[M-H-204]^-$ corresponding to the elimination of the acetyl-glycoside unit. Compounds 32 and 36 (t_R=50.18 and 55.44 min) were assigned as isorhamnetin 3-*O*-glycoside and isorhamnetin-*O*-acyl-glycoside which had precursor ion peaks at *m/z* 477 and 519, respectively. Most of these compounds were identified before in MO leaf extracts. Most of these compounds were detected and identified in *M. oleifera* leaves which growing in different localities in the world as reported by Amaglo et al., Oldoni et al., Ralepelea et al.,and Abdel Shakour et al.[17-20].

Compounds 16 and 19 (t_R=32.06 and 33.07 min) exhibited a pseudomolecular ion peak at *m/z* 593 which fragments into 503, 473, 473, 383, and ions. These peaks represented characteristic fragment ions of an apigenin-6,8-di-C-glycopyranoside (vicenin-2). Meanwhile, compounds 22 and 23 (t_R=39.99 and 41.50 min, respectively) showed *m/z* 431 is consistent with the presence of the

apigenin 8-C-glucoside (vitexin) or and the apigenin-6-C glucoside (isovitexin) with a typical fragmentation pattern (*m/z* 341, 311 (100%) and 283), this compound was reported in *M. oleifera* leaf extract[17].

Phenolic acids

The identified phenolic acids in both *Moringa* species were 10 hydroxycinnamic acids and 1 benzoic acid derivative. hydroxycinnamic acids such as compound 1 (t_R=2.92 min) showed the $[M-H]^-$ ion at *m/z* value 341 corresponding to caffeoyl-*O*-glucoside[17]. Compound 6 (t_R=13.94 min) had a deprotonated molecular ion peak at *m/z* 515 with a typical fragmentation pattern of 3-caffeoylquinic glycoside[21]. Compound 7 (t_R=17.03 min) was characterized as vanillic acid-4-*O*-β-D-glucopyranoside with characteristic *m/z* ion at 329[22]. Compounds 8 and 13 (t_R=17.53 and 25.97 min, respectively) were afforded ion peaks at *m/z* 353 corresponding to 3-caffeoylquinic acid and its isomer. Compounds 10 and 11 (t_R=22.21 and 23.63 min, respectively) showed molecular ion peaks with *m/z* values of 337 along with characteristic fragments at *m/z* 191, 163 (100%) and 119 of 3-coumaroylquinic acid and its isomer. Compounds 15 and 17 (t_R=31.15 and 32.48 min, respectively) showed the same molecular ion peaks with *m/z* 337 with fragment ions at *m/z* 191, 173 (100%) and 119 characteristics for 4-coumaroylquinic acid and its isomer. Moreover, compound 20 (t_R=33.23 min) was identified as feruloylquinic acid, which had a characteristic *m/z* value of 367. While only one benzoic acid derivative was detected, such as compound 2 (t_R=3.00 min) which was assigned as quinic acid with an *m/z* value of 191[23]. Most of these phenolic acids were detected in *M. oleifera* and *M. ovalifolia* leaf extracts[17,21-23].

Glucosinolates

Glucosinolates are a class of alkaloids whose structures are characterized by a β-D-glucoside unit and an *O*-sulfated anomeric (Z)-thiohydroximate function linked to a variable side chain based on the plant species' metabolism of amino acids. Previous studies reported that, *M. oleifera* had several uncommon glucosinolates compounds with a second saccharide residue in the aglycon side chain, which possess a promising antioxidant and anticancer activities[24].

Compound 5 (t_R=12.27 min) exhibited a deprotonated molecule at *m/z* 570 which displayed fragment ions at *m/z* 424, 328, 275 and 97 corresponding to the deprotonated ion of glucomoringin. Compounds 9, 12, and 18 (t_R=21.63, 24.63 and 32.73 min, respectively) afforded a precursor ion peak at *m/z* 612 with the same fragmentation pattern (*m/z* 259, 97) of three glucosinolates isomers and their structures similar to glucomoringin, except for the presence of an acetyl group at C-2′, C-3′, and C-4′ on the α-L-rhamnopyranosyl

unit. They identified as 4-(-2′-*O*-acetyl-α-L-rhamnopyranosyloxy) benzyl glucosinolate, 4-(-3′-*O*-acetyl-α-L-rhamnopyranosyloxy) benzyl glucosinolate, 4-(-4′-*O*-acetyl-α-L-rhamnopyranosyloxy) benzyl glucosinolate. In addition, compound 4 (t_R=7.26 min) was assigned as a glucosinolate derivatives. These compounds possess promising antioxidant and anticancer activities as well as were reported in *M. oleifera* leaves but not reported in *M. peregrina*[20,24].

Phenylethanoids

Just one compound (compound **3**) was detected in both MO and MP extracts, with a precursor ion peak at *m/z* 195 and fragment ions at *m/z* 97 and 80. This compound was annotated as hydroxytyrosol acetate[25].

In present results (Table 1 and Figure 1), it appears that the H_2O ext. of both *Moringa* species (MO and MP) are rich in phenolic acids and the MP extracts are famous for quercetin and apigenin derivatives. In addition, the peak intensity of quercetin-3-*O*-rutinoside is much higher in MO extracts than in MP extracts while the intensity of quercetin-3-*O*-glycoside peak is much higher in MP extracts than in MO extracts. Moreover, MP MeOH ext. is rich in glucosinolate. Therefore, the presence of these phytochemicals in both species may be responsible for the plant bioactivities.

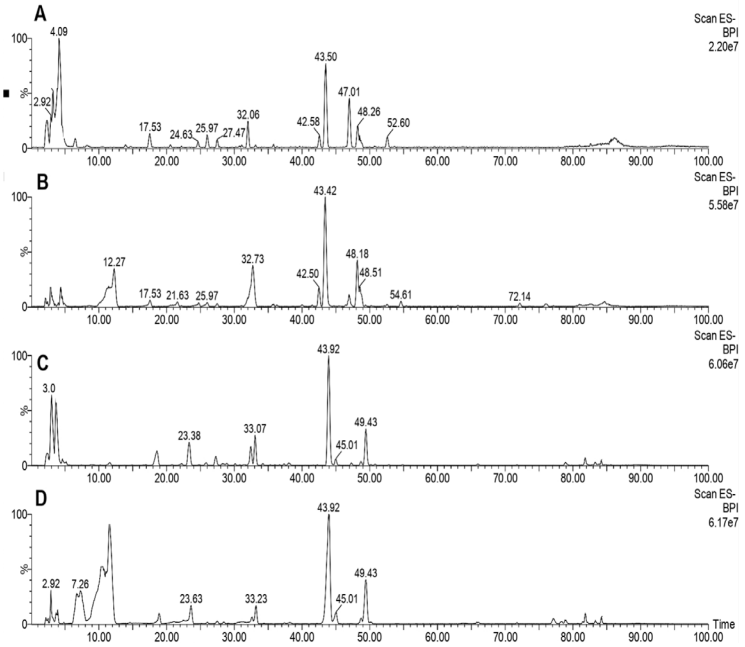

Figure 1. Total ion chromatograms (TIC) of (A) MP-H_2O, (B) MP-MeOH, (C) MO-H_2O and (D) MO-MeOH extracts

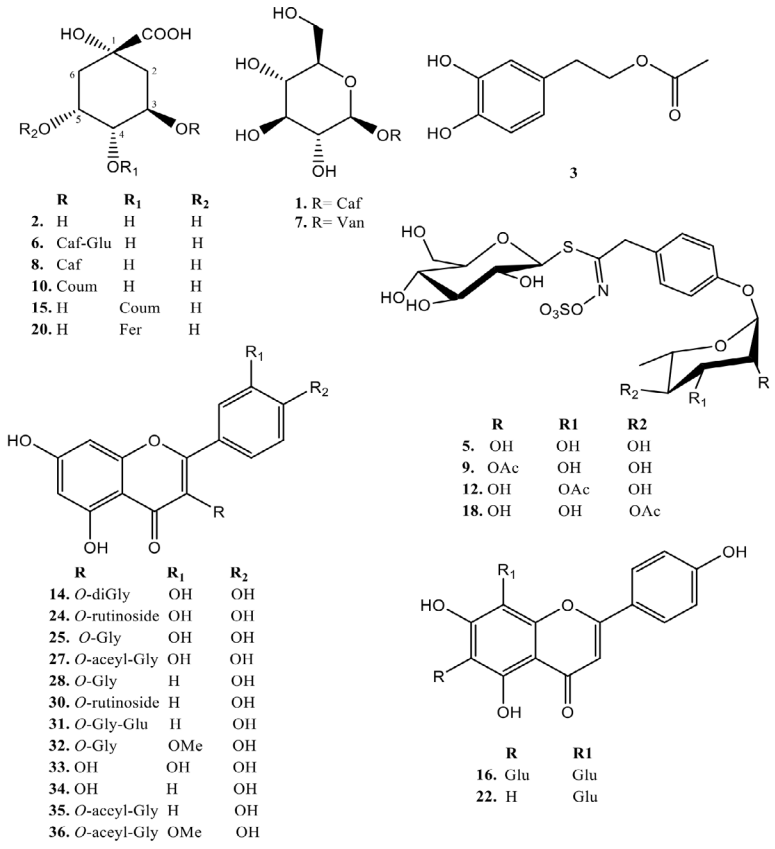

Figure 2. Structures of some identified compounds in H_2O and MeOH extracts of both *Moringa* species (MO and MP)

Effect of MO and MP extracts on cell viability

The development of new drugs from herbal plant ingredients has been the basic agenda in the R&D of the drug industry for many decades. Despite recent therapeutic advances in cancer treatment, metastasis remains the principal cause of cancer death. Recent work has uncovered the unique biology of metastasis-initiating cells that results in tumor growth in distant organs[6].

The cell culture wound closure assay is a useful method to examine cell migration, in which a scratch is generated on a confluent cell monolayer. The speed of wound closure and cell migration can be quantified by taking snapshot pictures with a regular inverted microscope at several time intervals[26].

Herein, the cytotoxic effect of MO and MP extracts on HCC, HepG2 cell lines was studied using various gradient concentrations of the two species of *Moringa* extracts using the MTT assay. The different fractions have been treated with increasing concentrations (1.563 -100 µg/mL) for 24 h. The obtained results showed clearly that increasing the concentration of the MO and MP extracts adversely decreased the viability of the treated HepG2 cells. Moreover, the highest concentration applied (100 µg/mL) showed the highest decrease in cell viability in all fractions. The data were analyzed by the Pearson correlation coefficient (r), which is a measure of linear correlation between two sets of data.

For MO, the mean of the viability of H_2O ext., MeOH ext. and *n*-BuOH fr. was 52.1 ± 15.7, 62.5 ± 7.7 and 52.0 ± 11.1, respectively, with correlation coefficient (r) -0.771, -0.976, and -0.66 with a significant effect of p value=0.042 and 0.107 for H_2O ext. and *n*-BuOH fr., respectively. A highly significant effect was observed for MeOH fr. with p<0.001 (Table 2). In addition, the lowest viability percentage of cells was observed for the H_2O ext. at concentrations of 100 and 50 µg/mL (Figure 3).

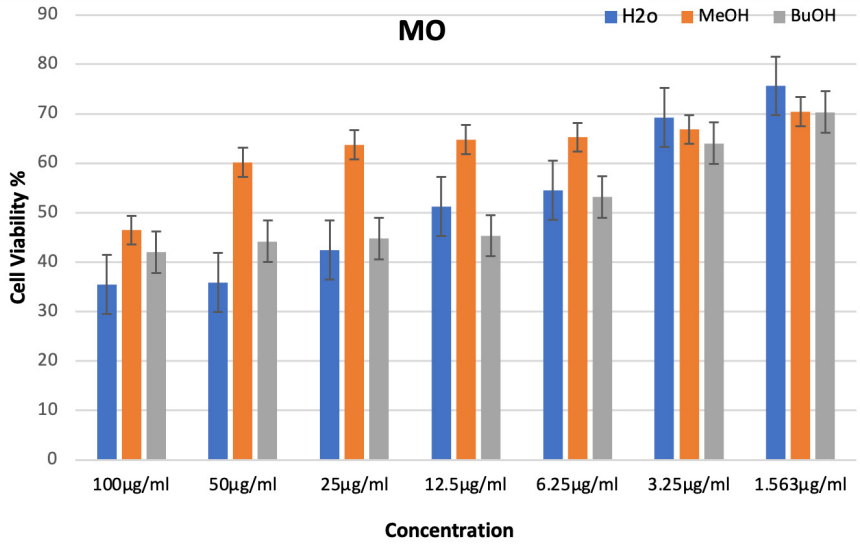

Figure 3. Effect of MO extracts on viability of HepG2 cells

While for MP, the mean of viability for H_2O ext., MeOH ext., and *n*-BuOH fr. was 51.6 ± 9.6, 44.8 ± 8.5 and 56.1 ± 5.0, respectively, with a correlation coefficient (r) -0.959, -0.792, and -0.997, respectively. The H_2O ext. and *n*-BuOH fr. showed a highly significant effect with p values=0.002 and <0.001, respectively. The non-significant effect was observed with MeOH ext. (p=0.06) as shown

in Table 2. Hence, the results exhibited that the lowest viability percentage of cells was observed for H_2O and MeOH extracts at a concentration of 100 µg/mL (Figure 4). These results showed that treatment with MO and MP extracts decreased the viability of HepG2 cells in a dose-dependent manner.

Table 2. The viability % of MP and MO extracts

Conc. (µg/mL)	Viability %					
	MP extracts			MP extracts		
	H_2O ext.	MeOH ext.	n-BuOH fr.	H_2O ext.	MeOH ext.	n-BuOH fr.
100	35.18	35.73	46.69	35.51	46.43	41.98
50	48.69	38.65	54.28	35.84	60.17	44.18
25	49.68	39.19	57.29	42.46	63.74	44.77
12.5	55.88	47.26	59.09	51.27	64.8	45.34
6.25	57	49.67	59.23	54.53	65.22	53.15
3.25	63.22	58.21	59.86	69.27	66.79	64
1.563	70.23	63.65	65.21	75.61	70.45	70.33
Mean of Viability	51.6 ± 9.6	44.8 ± 8.5	56.1 ± 5.0	52.1 ± 15.7	62.5 ± 7.7	52.0 ± 11.1
The correlation between the concentration and viability %	r=-0.959**, p=0.002	r=-0.792, p=0.06	r=-0.997**, p=<0.001	r=-0.771*, p=0.042	r=-0.976**, p= <0.001	r=-0.66*, p= 0.107
IC_{50} (µg/ml)	35.56	67.91	77.75	34.47	88.75	37.98

Viability is represented as Mean ± SD, while the correlation coefficient (r); the data were analyzed by Person correlation p=p. value.
*p. value<0.05 is significant, **p. value<0.01 is highly significant.

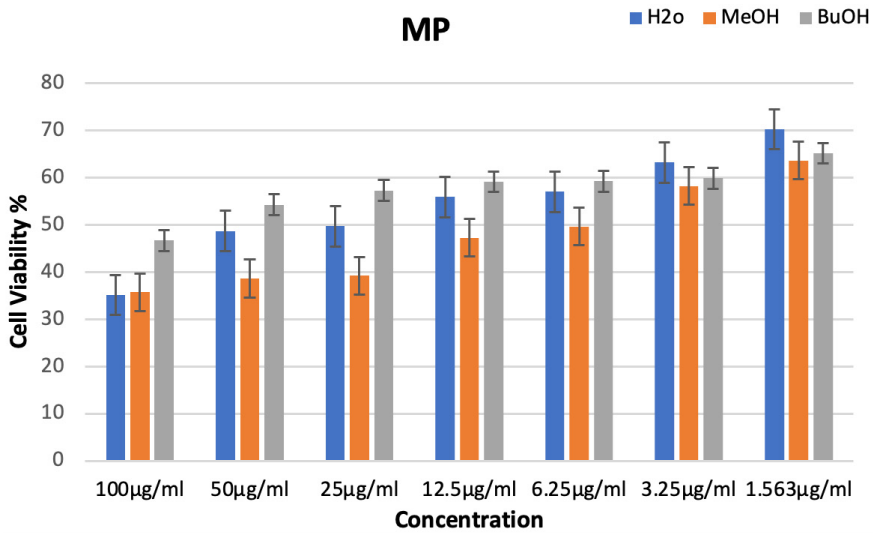

Figure 4. Effect of MP extracts on viability of HepG2 cells

The concentration of H_2O ext., MeOH ext., and an *n*-BuOH fr. of both MO and MP required to inhibit 50% of the cells (IC_{50}) was calculated. The results showed that the IC_{50} values of MO extracts on HepG2 cells were 34.473, 88.75, and 37.98 µg/mL for H_2O ext., MeOH ext. and *n*-BuOH fr., respectively. While the values recorded for MP extracts were 35.56, 67.91, and 77.75 µg/mL for H_2O ext., MeOH ext. and *n*-BuOH fr., respectively.

However, our results revealed that all the extracts have significant cytotoxic effects, and increasing the concentration of MO and MP extracts adversely decreased the viability of the treated HepG2 cells.

The IC_{50} curves determine the drug concentration that can inhibit the growth of tumor cells by half when compared to the cells grown with no exposure to the drug, low IC_{50} value means that the drug is effective at low concentrations, and thus will show lower systemic toxicity when administered to the patient. Interestingly, the three extracts mentioned above showed similar IC_{50} values close to this concentration and exhibited cytotoxic activity against HepG2 cells.

Our results are in agreement with those of Jung et al.[27] who reported that water extracts of *M. oleifera* leaves have been shown to inhibit the growth of liver cancer and also consistent with Mansour et al.[28] who mentioned that *M. peregrina* and *M. oleifera* leaves ethyl acetate extracts exhibited the highest inhibition activity against HCC HepG2 cell line (78% and 80.7% inhibition, respectively). Furthermore, the results of the present study are close to Emami et al.[29]. results who proved that HepG2 viability methanolic ext. was decreased

with increasing of extract concentration. Also, he mentioned that the IC_{50} for the MeOH ext. of a leaf of MO was 12.89 μg/mL which differs from our result as it indicated that the IC_{50} of MO-methanolic ext. was 88.75 μg/ml and this difference in the IC_{50} values may be attributed to the type of solvents and methods of extraction used. A different fraction that was not included in our study is isothiocyanate from MO (MIC-1) was evaluated for anticancer activity against 30 cancer cell lines including HepG2, which were treated with MIC-1 (0 or 10 μM) for 48 h. The research, conducted by Xie et al.[30] demonstrated that MIC-1 considerably reduced the HepG2 cell line's ability to proliferate and produced strong growth inhibitory effects on the cells with a high growth inhibitory rate.

It is clear from the current research why MO and MP extracts have potent anticancer properties against HepG2 cells. This may be because the plant's leaves contain promising polyphenolic compounds. As a result, it is evident that the polar solvents employed in the extraction procedure are capable of dissolving the active components from the source to the MP extracts, which demonstrated their anti-cancer effects in comparison to other extracts.

The anti-migration capacity of MO and MP extracts against HepG2 cells

Migration is a primary step in cancer metastasis. We studied the anti-migration potential of MO and MP extracts against the HepG2 cell line, wound healing assay was performed in the presence of various types of extracts. The 85% confluent HepG2 cell was wounded using a micro-pipette tip. After 24, 48, 72, and 96 h of incubation, the wound width was observed and imaged under an inverted microscope. The wound width was calculated as the average distance between the edges of the scratches.

Paired t-test was used to analyze the data, This test showed that the treatment with H_2O extract of MO for 72 h demonstrated a significant dependent migration inhibition of HepG2 cells with p=0.049, while for H_2O ext. of MP, the migration of HepG2 cells was inhibited and cells migrated slower following a 96 h incubation period with a significant p=0.016 and a decrease in wound width was observed as cell migration was induced, as shown in Table 3 and Figure 5. On the contrary, MeOH ext. of MO showed no inhibition for HepG2 cell migration as the cells had migrated into the scratched area and the untreated cells showed a less extensive wound with a significant p=0.047 after 72 h incubation whereas the treated cells migrated significantly more, while no significant anti-migration effect was observed for MeOH ext. of MP at all-time intervals (Table 4). A significant anti-migration effect of *n*-BuOH fr. of MO was observed with p=0.019, while *n*-BuOH fr. of MP showed no significant migration inhibition for HepG2 cells (Table 5).

Table 3. Comparison between H_2O extracts of MO and MP species on HepG2 regarding the anti-migration effect

Time (h)	MO (H_2O ext.)			MP (H_2O ext.)		
	Control	Drug	p. value	Control	Drug	p. value
0	3.1 9 ± 0.06	3.56 ± 0.40	0.158	3.74 ± 0.11	3.77 ± 0.40	0.216
24	2.23 ± 0.19	2.87 ± 0.77	0.218	2.63 ± 0.22	2.90 ± 0.80	0.15
48	1.39 ± 0.51	1.91 ± 0.78	0.335	1.81 ± 0.21	2.17 ± 0.59	0.256
72	0.19 ± 0.18	0.87 ± 0.62	0.049*	0.70 ± 0.23	0.85 ± 0.56	0.16
96	0.00 ± 0.00	0.00 ± 0.00	-	0.00 ± 0.00	0.05 ± 0.09	0.016*

The wound widths are represented as Mean ± SD; the data were analyzed by paired t test. *p. value<0.05 is significant, **p. value<0.01 is highly significant.

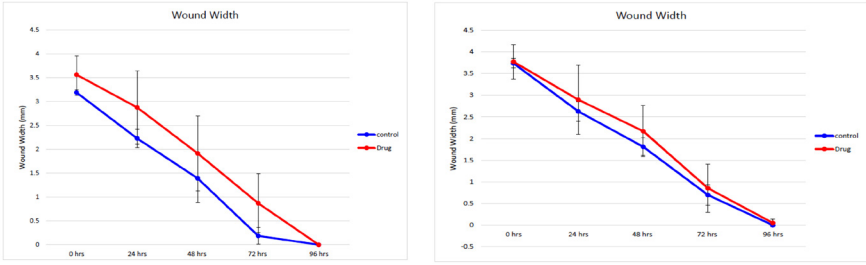

A) MO B) MP

Figure 5. Effect of H_2O extracts of MO and MP on HepG2 migration

Table 4. Comparison between MeOH extracts of MO and MP on HepG2 regarding anti-migration effect

Time (h)	MO (MeOH ext.)			MP (MeOH ext.)		
	Control	Drug	p. value	Control	Drug	p. value
0	4.02 ± 0.12	3.95 ± 0.13	0.97	3.90 ± 0.28	4.04 ± 0.73	0.128
24	3.28 ± 0.53	3.09 ± 0.11	0.115	2.13 ± 0.51	2.18 ± 0.99	0.216
48	2.30 ± 0.11	2.06 ± 0.13	0.795	0.44 ± 0.36	0.52 ± 0.89	0.092
72	1.05 ± 0.24	0.94 ± 0.05	0.047*	0.00 ± 0.00	0.00 ± 0.00	-
96	0.00 ± 0.00	0.00 ± 0.00	-	0.00 ± 0.00	0.00 ± 0.00	-

The wound widths are represented as Mean ± SD; the data were analyzed by paired t test. *p. value<0.05 is significant, **p. value<0.01 is highly significant.

Table 5. Comparison between *n*-BuOH fractions of MO and MP on HepG2 regarding the anti-migration effect

Time (h)	MO (*n*-BuOH fr.)			MP (*n*-BuOH fr.)		
	Control	Drug	p. value	Control	Drug	p. value
0	3.47 ± 0.02	3.57 ± 0.35	0.019*	4.76 ± 0.16	4.86 ± 0.20	0.393
24	2.32 ± 0.10	2.68 ± 0.27	0.09	2.76 ± 0.63	2.89 ± 0.21	0.099
48	1.76 ± 0.27	1.88 ± 0.10	0.112	1.16 ± 0.55	1.17 ± 0.16	0.147
72	0.47 ± 0.19	0.72 ± 0.31	0.337	0.00 ± 0.00	0.00 ± 0.00	-
96	0.00 ± 0.00	0.00 ± 0.00	-	0.00 ± 0.00	0.00 ± 0.00	-

The wound widths are represented as Mean ± SD; the data were analyzed by paired t test. *p. value<0.05 is significant, **p. value<0.01 is highly significant.

Comparison between MO and MP fractions regarding their anti-migration effect

Student t-test was used to analyze data, it was observed that MP-H_2O ext. gives a better anti-migration effect of HepG2 cells than MO-H_2O ext. following a 96 h incubation period with significant p=0.016 (Table 6, Figures 6 and 7). Also, a better effect was observed for MP-MeOH than MO at 0 hour with significant p=0.05, while at 24, 48, and 72 h, MO-MeOH showed a significantly better anti-migration effect for HepG2 cells than MP-MeOH with p=0.041, 0.028, and 0.041, respectively (Table 7). It was found that the MO-*n*-BuOH fr. Showed a better significant anti-migration effect than MP after 72 h incubation with p=0.033 (Table 8).

Table 6. Comparison between MO-H2O and MP-H_2O extracts regarding their anti-migration effect

Time (h)	MO-H_2O ext.	MP-H_2O ext.	p. value
0	3.56 ± 0.40	3.77 ± 0.40	0.991
24	2.87 ± 0.77	2.90 ± 0.80	0.882
48	1.91 ± 0.78	2.17 ± 0.59	0.461
72	0.87 ± 0.62	0.85 ± 0.56	0.797
96	0.00 ± 0.00	0.05 ± 0.09	0.016*

The wound widths are represented as Mean ± SD; the data were analyzed by student t test. *p. value<0.05 is significant, **p. value<0.01 is highly significant.

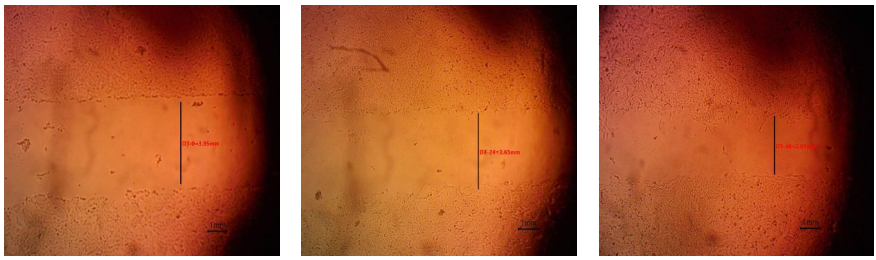

0 h 24 h 48 h

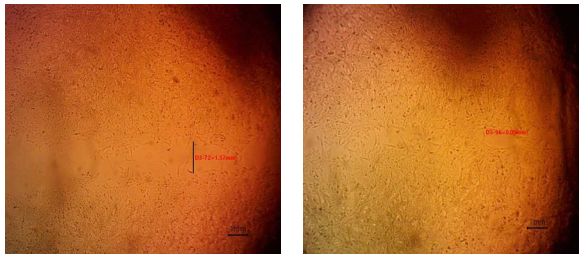

72 h 96 h

Figure 6. Effect of MO-H_2O ext. on cellular migration in HepG2 cells determined by wound healing assay (Images were taken at time zero, 24, 48, 72, and 96 h)

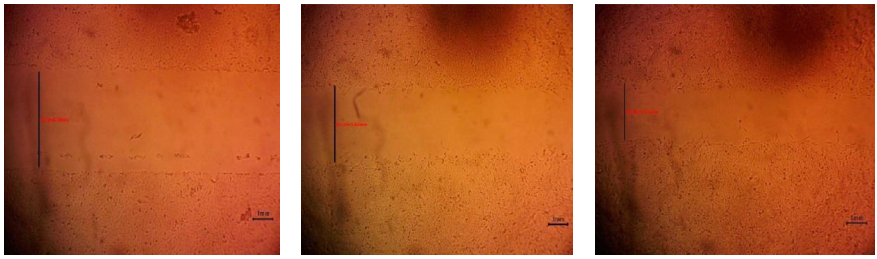

0 h 24 h 48 h

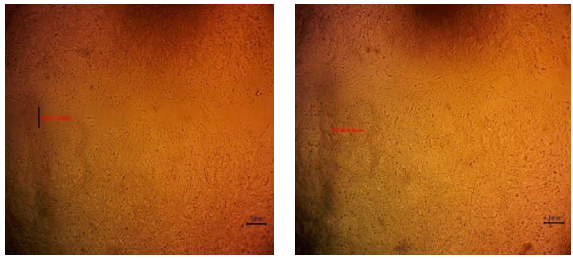

72 h 96 h

Figure 7. Effect of MP-H_2O ext. on cellular migration in HepG2 cells determined by wound healing assay. Images were taken at time zero, 24, 48, 72 and 96 hr.

Table 7. Comparison between MO-MeOH and MP-MeOH extracts regarding their anti-migration effect

Time (h)	MO- MeOH ext.	MP- MeOH ext.	p. value
0	3.95 ± 0.13	4.04 ± 0.73	0.05*
24	3.09 ± 0.11	2.18 ± 0.99	0.041*
48	2.06 ± 0.13	0.52 ± 0.89	0.028*
72	0.94 ± 0.05	0.00 ± 0.00	0.041*
96	0.00 ± 0.00	0.00 ± 0.00	-

The wound widths are represented as Mean ± SD; the data were analyzed by student t test. *p. value<0.05 is significant, **p. value<0.01 is highly significant.

Table 8. Comparison between MO-*n*-BuOH and MP-*n*-BuOH fractions regarding their anti-migration effect

Time (h)	MO- *n*-BuOH fr.	MP- *n*-BuOH fr.	p. value
0	3.57 ± 0.35	4.86 ± 0.20	0.231
24	2.68 ± 0.27	2.89 ± 0.21	0.522
48	1.88 ± 0.10	1.17 ± 0.16	0.221
72	0.72 ± 0.31	0.00 ± 0.00	0.033*
96	0.00 ± 0.00	0.00 ± 0.00	-

The wound widths are represented as Mean ± SD; the data were analyzed by student t test. *p. value<0.05 is significant, **p. value<0.01 is highly significant.

In the present study, we demonstrated for the first time that the aqueous extracts of MO and MP significantly inhibit HepG2 migration, as MO-H_2O ext. significantly inhibits the cell migration following 72 h incubation, whilst the significant anti-migration effect of MP-H_2O was observed after 96 h incubation, these results showed that MO and MP treatment inhibits the migration of HepG2 cells in a time-dependent manner.

Student t test proved a significant anti-migration effect of the MeOH ext. at all-time intervals and a non-significant suppression of cell migration for the *n*-BuOH fr. except after 72 h incubation; this means that the migration capacity of HepG2 cells decreased at specific time intervals which confirm the time-dependent manner of anti-migration.

Cell migration plays an important role in many physiological and pathological processes, such as tissue repair and tumor cell metastasis. Our study used a wound healing assay to determine the migration velocity of the HepG2 cell line. Statistical analysis showed that the migration rates of HepG2 cells treated with MO-MeOH and the MP-H_2O extracts were slower and significantly suppressed.

Migration rate

The wound healing assay is used to investigate cell migration. Cell migration is the movement of individual cells, cell sheets, and clusters from one location to another. Migration is considered the rate-limiting process during healing, and therefore migration process is a key part of investigating wound healing.

In the present comparative study between MO and MP, the Student t-test was used to calculate the migration rates of HepG2 cells for all extracts, it was found that the MeOH ext. of MO has a slower significant migration rate with p=0.01 but for the other extracts, they showed faster significant migration rate than the untreated cells with p=0.01. While for MP, the HepG2 cells treated with water ext. showed a slower significant migration rate with p=0.01 but for the cells treated with methanol and butanol extracts of MP, the migration rate of HepG2 cells was significantly faster than the untreated control with p=0.01 (Table 9 and Figure 8).

Table 9. The migration rate of both *Moringa* species extracts

Extract	MO			MP		
	Control	Drug	p. value	Control	Drug	p. value
H_2O ext.	3.18	3.55	0.01*	3.73	2.90	0.01*
MeOH ext.	4.00	3.93	0.01*	3.89	4.03	0.01*
n-BuOH fr.	3.46	3.56	0.01*	4.74	4.84	0.01*

Migration rate was calculated by dividing the time spent in migration according to the formula: Rm = Wi–Wf / t; where Rm is the rate of cell migration, Wi is the average initial wound width, Wf is the average final wound width, and t is duration of migration (in hours). The data were analyzed by student t test.
*p. value<0.05 is significant, **p. value<0.01 is highly significant.

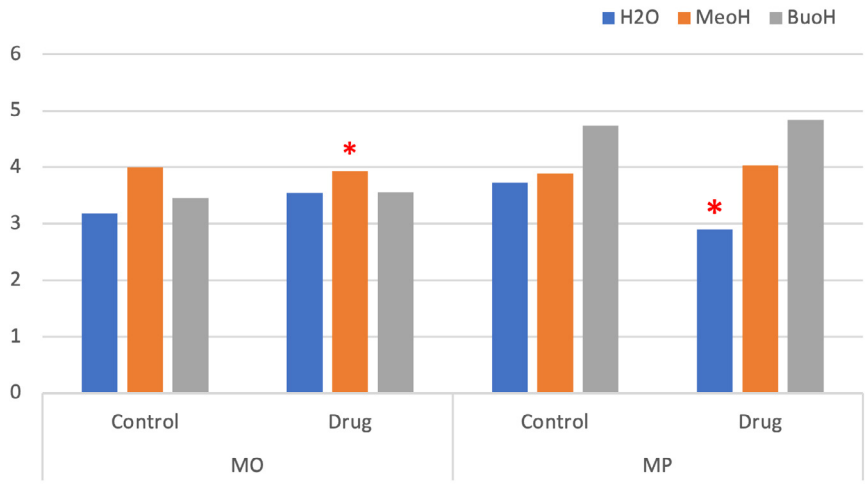

Figure 8. Migration rate within control comparison of MO and MP

The anti-migration effects of MO and MP have not been demonstrated before on liver cancer cell lines and accordingly, there is no available published research concerning this subject, so we discussed the migration effect of this medicinal plant on other cell lines. The study of Xie et al.[31] who examined the migratory inhibition of PC3 human prostate cancer cells by *M. oleifera* alkaloids (MOA) *in vitro*, they reported that MOA significantly suppress PC3 cell migration in a wound healing assay by inhibiting the expression of cyclooxygenase 2 (COX-2), and inhibiting the production of prostaglandin E2 (PGE2), these results agreed with Xie et al.[30] who assessed the effects of Isothiocyanate from *Moringa oleifera* (MIC-1) on the migration of renal cell carcinoma cell line (786-O and 769-P), the results showed that the exposure to MIC-1 (0, 1, and 2 μM) substantially reduced the migration ability of 786-O and 769-P cells and they mentioned that the cell migration rate of 786-O and 769-P cells decreased in the wound healing assay. The above results support our findings regarding the anti-migration effect of different fractions of *Moringa*. Additionally, to the best of our knowledge, this research is the first to demonstrate a substantial inhibition of HepG2 migration by the aqueous extracts of MO and MP, a treatment that may prevent the metastasis of HCC.

It can be concluded that the LC-ESI-MS analysis of H_2O and MeOH extracts of MO and MP leaves in negative ion mode led to characterize of major chemical constituents as flavonoid (*O*-and C-glycosides), phenolic acids, glucosinolates and phenyl ethanoid. The flavonoids consist mainly of the quercetin and kaempferol, isorhamnetin and apigenin derivatives including glycosides

and acetyl glycosides. The cytotoxic activity of MO and MP extracts on HepG2 cell lines showed IC_{50} values ranging from 34.473 to 88.75 μg/mL, in which the H_2O extracts of both *Moringa* species had the highest activities as well as exhibited significant antimigratory potential.

Hence, the promising cytotoxic and anti-migratory effects of MO and MP extracts could contribute to the development of a new anticancer drug for HCC from natural sources.

STATEMENT OF ETHICS

This study does not involve experiments on animals or human subjects.

CONFLICT OF INTEREST STATEMENT

All authors declare that there are no conflicts of interests.

AUTHOR CONTRIBUTIONS

Ezzat E.A. Osman: Study Design, Performing the Experiments, Data analysis, Writing, Preparing, and Editing the manuscript. Sayed S. Abdel-Hameed: Study Design, Data Interpretation, Writing, and Reviewing the manuscript. Mohamed A. Shemis: Study Design, Reviewing, and Editing the Manuscript. Samah Mamdouh: Performing the Experiments, Data Analysis, Writing and Preparing the Manuscript.

FUNDING SOURCES

The current research was not funded by any public, commercial or not-for-profit funding agency.

ACKNOWLEDGEMENTS

The authors thank Mrs. Therese Labib, a plant taxonomy consultant at the Orman Botanical Garden, Giza, Egypt, for authenticating the plants under investigation.

REFERENCES

1. World Health Organization. Accessed August 23, 2021. Available from: https://www.who.int/health-topics/cancer

2. Sia D, Villanueva A, Friedman SL, Llovet JM. Liver cancer cell of origin, molecular class, and effects on patient prognosis. Gastroenterol, 2017;152(4):745-761. Doi: 10.1053/j.gastro.2016.11.048

3. Llovet JM, Kelley RK, Villanueva A, Singal AG, Pikarsky E, Roayaie S, et al. Hepatocellular carcinoma. Nat Rev Dis Primers, 2021;7. Doi: 10.1038/s41572-020-00240-3

4. Benson AB, D`Angelica MI, Abbott DE, Anaya DA, Anders R, Are C, et al. Hepatobiliary cancers, version 2.2021, NCCN clinical practice guidelines in oncology. J Natl Compr Canc Netw, 2021;19 (5):541-565. Doi: 10.6004/jnccn.2021.0022

5. Yang J, Wu Y, Du D. Polydatin inhibits cell proliferation, invasion and migration, and induces cell apoptosis in hepatocellular carcinoma, Braz J Med Biol Res, 2018;51(4):1-9. Doi: 10.1590/1414-431X20176867

6. Ganesh K, Massagué J. Targeting metastatic cancer. Nat Med, 2021;27:34-44. Doi: 10.1038/s41591-020-01195-4

7. Rashed WM, Kandeil MAM, Mahmoud MO, Ezzat S. Hepatocellular Carcinoma (HCC) in Egypt: a comprehensive overview. J Egypt Nat Canc Inst, 2020;32(5):1-11. Doi: 10.1186/s43046-020-0016-x

8. Ssenku JE, Okurut SA, Namuli A, Kudamba A, Tugume P, Matovu P, et al. Medicinal plant use, conservation, and the associated traditional knowledge in rural communities in Eastern Uganda. Trop Med Health, 2022;50(39):1-10. Doi: 10.1186/s41182-022-00428-1

9. Al-Zharani M, Nasr FA, Abutaha N, Alqahtani AS, Noman OM, Mubarak M, et al. Apoptotic induction and anti-migratory effects of *Rhazya stricta* fruit extracts on a human breast cancer cell line. Molecules, 2019;24(21):3968. Doi: 10.3390/molecules24213968

10. Abd Rani N, Husain K, Kumolosas E. *Moringa* genus: a review of phytochemistry and pharmacology. Front Pharmacol, 2018;9(108):1-26. Doi: 10.3389/fphar.2018.00108

11. Mumtaz MZ, Kausar F, Hassan M, Javaid S, Malik A. Anticancer activities of phenolic compounds from *Moringa oleifera* leaves: *in vitro* and in silico mechanistic study. Beni-Suef Univ J Basic Appl Sci, 2021;10(12):1-11. Doi: 10.1186/s43088-021-00101-2

12. Soliman SA, Ismael AI, Abbas MS, Abd El- Lateaf HA, Mohamed ME. Comparative characteristics study of *Moringa* (*Moringa peregrina*), Terminalia (*Terminalia Billerica*) and Tiger nut (*Cyperus esculentus*) oils. Egypt J Chem, 2021;64(9):5241-5248. Doi: 10.21608/EJCHEM.2021.70105.3585

13. El-Wakil ES, Shaker S, Aboushousha T, Abdel-Hameed ES, Osman EEA. In vitro and in vivo anthelmintic and chemical studies of *Cyperus rotundus* L. extracts, BMC Complement Med Ther, 2023;23(15):1-17. Doi: 10.1186/s12906-023-03839-7

14. Pirintsos S, Panagiotopoulos A, Bariotakis M, Daskalakis V, Lionis C, Sourvinos G, et al. From traditional ethnopharmacology to modern natural drug discovery: a methodology discussion and specific examples. Molecules, 2022;27(13):4060. Doi: 10.3390/molecules27134060

15. Ekor M. The growing use of herbal medicines: issues relating to adverse reactions and challenges in monitoring safety. Front Pharmacol, 2014;4(177):1-10. Doi: 10.3389/fphar.2013.00177

16. Kuruppu AI, Paranagama P, Goonasekara CL. Medicinal plants commonly used against cancer in traditional medicine formulae in Sri Lanka. Saudi Pharm J, 2019;27(4):565-573. Doi: 10.1016/j.jsps.2019.02.004

17. Ralepelea FM, Chimukab L, Nuapiaa Y, Risenga I. UPLC-DAD-QTOF-MS/MS analysis of targeted poly-phenolic compounds from *Moringa oleifera* leaves as function of seasonal responses. S Afr J Bot, 2021;143(12):107-115. Doi: 10.1016/j.sajb.2021.07.032

18. Amaglo NK, Bennett RN, Lo Curto RB, Rosa EAS, Turco VL, Giuffrida A, et al. Profiling selected phytochemicals and nutrients in different tissues of the multipurpose tree *Moringa oleifera* L., grown in Ghana. Food Chem, 2010;122(4):1047-1054. Doi: 10.1016/j.foodchem.2010.03.073

19. Oldoni TLC, Merlin N, Karling M, Carpes ST, de Alencar SM, Morales RGF, et al. Bioguided extraction of phenolic compounds and UHPLC-ESI-Q-TOF-MS/MS characterization of extracts of *Moringa oleifera* leaves collected in Brazil. Food Res Int, 2019;125:108647. Doi: 10.1016/j.foodres.2019.108647

20. Abdel Shakour ZT, El-Akad RH, Elshamy AI, El Gend AG, Wessjohann LA, Farag MA. Dissection of *Moringa oleifera* leaf metabolome in context of its different extracts, origin and in relationship to its biological effects as analysed using molecular networking and chemometrics. Food Chem, 2023;399:133948. Doi: 10.1016/j.foodchem.2022.133948

21. Makita C, Chimuka L, Cukrowska E, Steenkamp PA, Kandawa-Schutz M, Ndhlala AR, et al. UPLC-qTOF-MS profiling of pharmacologically important chlorogenic acids and associated glycosides in *Moringa ovalifolia* leaf extracts. S Afr J Bot, 2017;108(23):193-199. Doi: 10.1016/j.sajb.2016.10.016

22. Gu X, Yang Y, Wang Z. Nutritional, phytochemical, antioxidant, α-glucosidase and α-amylase inhibitory properties of *Moringa oleifera* seeds. S Afr J Bot, 2020;133:151-160. Doi: 10.1016/j.sajb.2020.07.021

23. Braham F, Carvalho DO, Almeida CMR, Zaidi F, Magalhães JMCS, Guido LF, et al. Online HPLC-DPPH screening method for evaluation of radical scavenging phenols extracted from *Moringa oleifera* leaves. S Afr J Bot, 2020;129:146-154. Doi: 10.1016/j.sajb.2019.04.001

24. Maldini M, Maksoud SA, Natell F, Montoro P, Petretto GL, Foddai M, et al. *Moringa oleifera*: study of phenolics and glucosinolates by mass spectrometry. J Mass Spectrom, 2014;49(9):900-910. Doi: 10.1002/jms.3437

25. Oliveira-Alves SC, Vendramini-Costa DB, Cazarin CBB, Júnior MRM, Ferreira JPB, Silva AB, et al. Characterization of phenolic compounds in chia (*Salvia hispanica* L.) seeds, fiber flour and oil. Food Chem, 2017;232:295-305. Doi: 10.1016/j.foodchem.2017.04.002

26. Justus CR, Leffler N, Ruiz-Echevarria M, Yang LV. *In vitro* cell migration and invasion assays. J Vis Exp, 2014;1(88):51046. Doi: 10.3791/51046

27. Jung IL, Lee JH, Kang SC. A potential oral anticancer drug candidate, Moringa oleifera leaf extract, induces the apoptosis of human hepatocellular carcinoma cells. Oncol Lett, 2015;10(3):1597-1604. Doi: 10.3892/ol. 2015.3482

28. Mansour M, Mohamed MF, Elhalwagi A, El-Itriby HA, Shawki HH, Abdelhamid IA. *Moringa peregrina* leaves extracts induce apoptosis and cell cycle arrest of hepatocellular carcinoma. Biomed Res Int, 2019;2019(1):2698570. Doi: 10.1155/2019/2698570

29. Emami NA, Fazilati M, Daneshmand F, Habibollahi S. Cytotoxic Effects of *Moringa oleifera* leaf extract on human hepatoma cell line HepG-2. Jentashapir J Cell Mol Biol, 2020;11(2):e108527. Doi: 10.5812/jjcmb.108527

30. Xie J, Qian YY, Yang Y, Peng LJ, Mao JY, Yang MR, et al. Isothiocyanate from *Moringa oleifera* seeds inhibits the growth and migration of renal cancer cells by regulating the PTP1B-dependent Src/Ras/Raf/ERK signaling pathway. Front Cell Dev Biol, 2022;9:790618. Doi: 10.3389/fcell.2021.790618

31. Xie J, Luo FX, Shi CY, Jiang WW, Qian YY, Yang MR, et al. *Moringa oleifera* alkaloids inhibited PC3 cells growth and migration through the COX-2 mediated Wnt/β-catenin signaling pathway. Front Pharmacol, 2020;11:523962. Doi: 10.3389/fphar.2020.523962

Acta Pharm. Sci. Vol 63:(1), 2025
Original article
DOI: 10.23893/1307-2080.APS6311

In silico evaluation of some α7nAChR agonists in apical periodontitis: The role of the cholinergic anti-inflammatory pathway

Emine ERDAG[1*], Dilan KIRMIZI[2], Umut AKSOY[2], Ahmet Ozer SEHIRLI[3]

1 Near East University, Department of Pharmaceutical Chemistry, Faculty of Pharmacy, North Cyprus via Mersin 10, Türkiye
2 Near East University, Department of Endodontics, Faculty of Dentistry, North Cyprus via Mersin 10, Türkiye
3 Near East University, Department of Pharmacology, Faculty of Dentistry, North Cyprus via Mersin 10, Türkiye

ABSTRACT

Activation of the α7 nicotinic acetylcholine receptor, an important part of the cholinergic anti-inflammatory pathway, is considered a target macromolecule in the treatment of many inflammatory disorders. However, there are no molecular studies on the use of α7 nicotinic receptor agonists in apical periodontitis. In this study, we identified some α7 nicotinic acetylcholine receptor agonists that have been previously investigated for use mainly in diseases affecting the central nervous system. The selected ligands were examined in terms of binding affinity and receptor-ligand interactions on α7 nicotinic acetylcholine receptor using the molecular docking method. AutoDock Vina and GROMACS program packages were used in the molecular docking and simulation process. The results showed that B-973B, ABT-107, and GAT107 were the three most effective ligands in receptor binding affinity, respectively. This study explored the potential efficacy of α7 nicotinic acetylcholine receptor agonists in addressing apical periodontitis.

Keywords: α7nAChR, apical periodontitis, cholinergic pathway, inflammation, molecular docking

*Corresponding author: Emine ERDAG
E-mail: emine.erdag@neu.edu.tr
ORCIDs:
Emine ERDAG: 0000-0002-1431-935X
Dilan KIRMIZI: 0000-0003-0483-1736
Umut AKSOY: 0000-0001-7281-508X
Ahmet Ozer SEHIRLI: 0000-0002-5175-9290
(Received 24 Nov 2023, Accepted 2 Apr 2024)

INTRODUCTION

Inflammation resulting from pathological changes in the periapical tissue may result from the immunoinflammatory response of etiological factors such as microorganisms, toxins, harmful metabolic residues, or pulp tissue remaining in the root canal system associated with host infection[1]. Several inflammatory mediators such as cytokines, and growth factors begin to be altered by fibroblasts, endothelial cells, and immune cells with the spread of inflammation in periapical tissue[2]. Destruction of surrounding tissue occurs as part of the defense process, resulting in periapical bone resorption[3]. Host defense triggers an important complex process including diverse components such as cytokines and matrix metalloproteinases (MMPs)[4]. Various cytokines such as interleukins (IL) and TNF-α, affect osteoclast differentiation and activation to initiate bone destruction[2]. In addition, many inflammatory mediators play a role in the bone remodeling process. A hyperinflammatory environment can cause loss of alveolar bone by disrupting the balance between bone formation and destruction. In this context, the effect of host response modulation in the treatment process is considered[5].

Acetylcholine (ACh) is a neurotransmitter that has a significant impact on inflammation by binding to specific receptors on immune and tissue cells. Cells with both vagus nerve and neuronal networks are counted as ACh sources. Non-neuronal-derived ACh is also thought to be involved in the regulation of localized immune responses[6]. It has also been reported by Fujii et al. that oral epithelial cells represent functioning parts of the cholinergic system[7]. It is believed that ACh produced by epithelial cells can regulate periodontal tissue function both locally and within the same cell[6]. ACh is one of the important components of the cholinergic system that binds to nicotinic and muscarinic receptors. These receptors are found in the vast majority of non-neuronal human cells[8].

Nicotinic acetylcholine receptors (nAChRs) are ligand-gated ion channel proteins, and they mediate the influx of Na^+, Ca^{2+}, and K^+ ions. The increase of Ca^{2+} ions in the cell depends on the activation of nAChR. It also affects the activation of protein kinases A and C (PKA and PKC, respectively), Ca^{2+} calmodulin-dependent protein kinase (CaMK), phosphatidylinositol 3-kinase (PI3K), and adenylyl cyclase (AC), which are calcium-sensitive signal transduction protein kinase models. The nAChR structure consists of seven α subtypes; α2, α3, α4, α5, α6, α7, respectively[9].

The periodontal ligament fibroblasts express α7nACh receptors[10]. The anti-inflammatory pathway is regulated by the cholinergic system, primarily the alpha7 nicotinic acetylcholine receptor (α7nAChR). This pathway begins with

the distinctive features of inflammation that activate the afferent vagus nerve and the transmission of an informational stimulus to the brain about the inflammation that has occurred. ACh release is increased in inflamed peripheral tissues proximal to the nerve in association with efferent vagal nerve activity. Free AChs bind to α7nAChRs on immune-competent cells and thus play an active role in localized inflammatory processes. Essentially, the leading branch of the vagal nerve reflex is important in ensuring the activation of the immune system[6]. Whether the regulation of the vagal nerve on the periodontal immune response is not known yet. Thus, the anti-inflammatory effect of neuronal ACh, which is vagally released, on immune cells is controversial. There is evidence to suggest that ACh produced outside of neurons plays a role in regulating inflammation in specific areas[11].

Macrophages, monocytes, and B and T immune cells play an important role in the pathogenesis of periodontal disease. The α7nAChR found in immune cells in the periodontium is expressed during periodontal disease. A study observed high amounts of ACh in T cells and monocytes[12]. In another study on α7nAChR deficient (α7nAChR−/−) animals, susceptibility to bacterial lipopolysaccharide (LPS) was noted[13]. In the same study, the production of proinflammatory cytokines (TNF-α, IL-1β, and IL-6) was also observed. This observation proves that the α7nAChR is involved in the regulation of the anti-inflammatory pathway initiated by the cholinergic system and in the control of inflammation in response to pathogens[13]. Several research studies have noted that nicotine possesses the capacity to directly impact periodontal cells through nAChRs, resulting in pathophysiological consequences and the progression of tobacco-related ailments within these cellular structures[14]. In the literature, there is a study reported that inhibited bone destruction and decreased TNF-α expression were observed in animals administered nicotine and that it remarkably decreases synovial inflammation levels[15]. The α7nAChR agonist PHA 543613 was also shown to suppress IL-8 expression that was produced by *Porphyromonas gingivalis*. Although more investigation is required, it is hypothesized that ACh may be involved in the regulation of neutrophil chemotaxis in the periodontium[6].

In light of this information, it has been hypothesized that nicotine suppresses immune response via a cholinergic anti-inflammatory pathway, causing periodontal disease. There are no studies in the literature investigating the effect of nAChR agonists on the pathology of apical periodontitis. The selected ligands have shown efficacy as α7 nAChR agonists in previous clinical trials and many have been used as antidyskinetic agents in the treatment of Parkinson's disease and the treatment of schizophrenia, mainly to improve cognitive

functions[16]. According to the information we obtained from the literature, the selected ligands have generally been tested in disorders affecting the central nervous system. In addition, molecular docking studies of the ligands have not been performed before. Thus, it was aimed to demonstrate their usability as anti-inflammatory agents through the cholinergic anti-inflammatory pathway in the treatment of apical periodontitis and similar endodontic diseases. The cholinergic anti-inflammatory signaling cascade and the activity of α7 nAChR agonists in apical periodontitis were summarized in Figure 1.

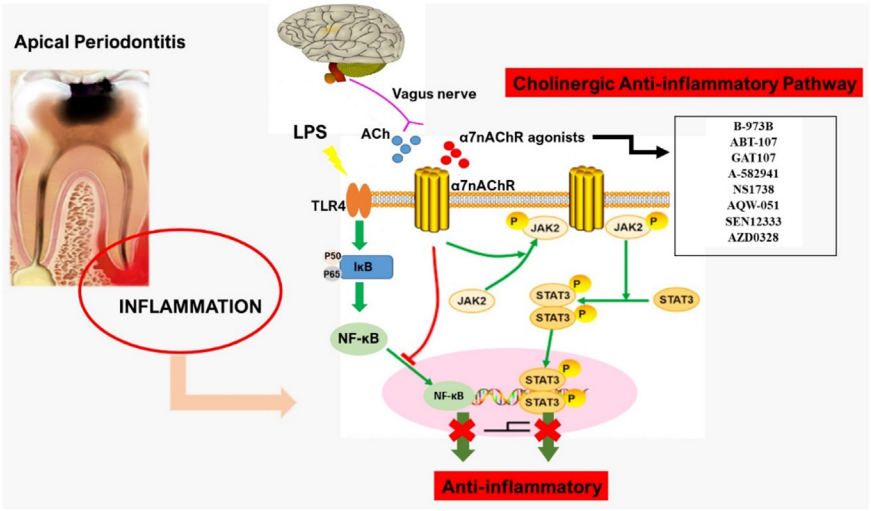

Figure 1. The cholinergic anti-inflammatory pathway and the role of α7 nAChR agonists in apical periodontitis

METHODOLOGY

Selection and preparation of data set

A molecular docking study was performed utilizing the crystallographic structures derived from the ligand binding domain of the α7 nAChR, an acetylcholine binding protein (AChBP) structure derived from *Lymnaea stagnalis* (PDB entry: 5J5I), and some selected α7 nicotinic acetylcholine receptor agonists were performed. The crystal structure of α7 nAChR, obtained from the Protein Data Bank (PDB) was illustrated in Figure 2. Before the docking procedure, we selected some specific α7 nAChR agonists as ligands; ABT-107 (PubChem CID 11151363), AZD0328 (PubChem CID 9794392), AQW-051 (PubChem CID 50914822), A-582941 (PubChem CID 11173546), B-973B (PubChem CID 137319851), NS1738 (PubChem CID 310378), GAT107 (PubChem CID 6554040), and SEN12333 (PubChem CID 45484303) were selected.

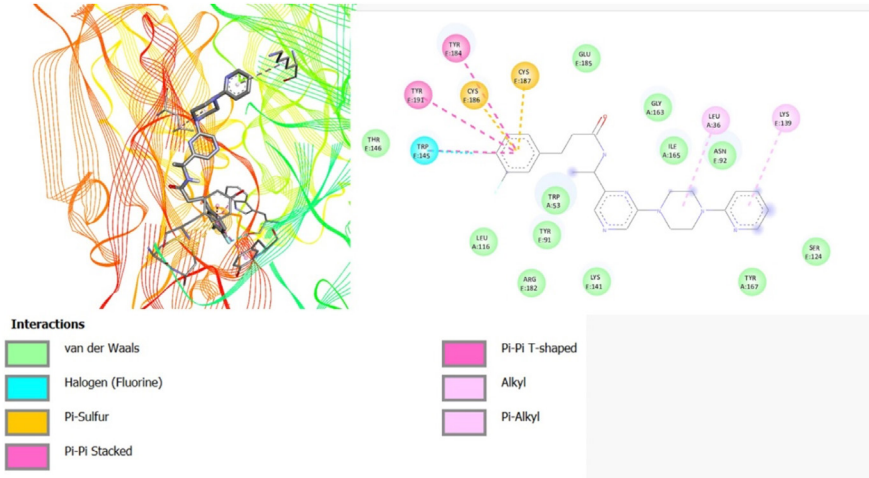

Figure 2. The 2D (on the right) and 3D (on the left) binding interactions of α7 nAChR and B-973B ligand. Green dotted lines; hydrogen bonds, pink lines; hydrophobic interactions, blue lines; halogen bonding, orange lines; electrostatic bonding.

The 2D representations of the selected ligands were obtained from the PubChem database. The ligands were subsequently extracted and converted into mol2 files using OpenBabel software, a preparatory step for molecular docking. Before initiating the molecular docking process, meticulous refinement was conducted on both the three-dimensional (3D) molecular structures of the ligands and the target protein, α7 nAChR. In this refinement procedure, all water molecules and heteroatoms were eliminated from the α7 nAChR structure. Subsequently, polar hydrogens were added, and Gasteiger charges were computed to enhance accuracy.

Following this structural refinement, the 3D conformation of α7 nAChR was saved as a PDBQT file. For the subsequent molecular docking analysis, AutoDock Vina and Discovery Studio Visualizer programs were employed to facilitate the extraction of diverse docking poses, as well as the calculation of binding affinities (ΔG) and the generation of ligand-receptor interaction profiles for the selected ligands. To comprehensively evaluate the performance of the chosen agonists on α7 nAChR, the docking study was carried out separately. Consistency was maintained throughout all docking procedures by employing a grid box with dimensions of 30 × 30 × 30 × 30 Å.

Molecular dynamics simulations

Utilizing the GROMACS molecular dynamics tool[17], we conducted molecular dynamics simulations. To simulate the protein-ligand complexes, GROMOS96 force field parameters were employed. To maintain charge neutrality within the protein-ligand complex, sodium ions (Na^+) and chloride ions (Cl) were added. Additionally, a simple point-charged water model was utilized to replicate water molecules.

The simulations were executed at a temperature of 310 K and a pressure of 1 bar, spanning a duration of 100 nanoseconds. This simulation protocol was consistent with a previously published methodology[18]. Throughout the simulations, we monitored protein-ligand interactions and assessed root-mean-square deviation (RMSD) characteristics to pinpoint the optimal conformations.

RESULTS and DISCUSSION

While the selected α7nAChR agonists have been extensively studied in diseases affecting the central nervous system, their application and potential efficacy in modulating inflammatory responses in apical periodontitis represent an unexplored and novel area of research. Our study is the first to investigate these ligands in this context, highlighting a new potential therapeutic pathway for a condition with a distinct inflammatory profile.

Table 1. Critical amino acid residues of α7 nAChR active site interacting with selected agonists, and their binding affinities

Name of Agonist	Binding Affinity, ΔG (kcal/mol)	Critical Amino Acid Residues
B-973B	-9.8	LEU36, TRP53, TYR91, LEU116, LYS139, LYS141, TRP145, THR146, GLY163, TYR167, ARG182, TYR184, GLU185, CYS186, CYS187, TYR191
ABT-107	-9.1	TRP53, LEU116, LYS139, LYS141, THR146, TYR167, ARG182, TYR184
GAT107	-8.9	TRP53, TYR91, LYS141, TRP145, ARG182, TYR184, CYS186, CYS187, TYR191
A-582941	-8.7	LEU116, TRP145, GLY163, TYR167, TYR184, CYS186, CYS187, TYR191
NS1738	-8.5	TYR91, CYS125, LYS139, ILE165, TYR167
AQW-051	-8.4	LEU36, TRP53, LEU106, TRP145, TYR184, GLU185, CYS186, CYS187, TYR191
SEN12333	-8.2	LEU36, TRP53, TYR184, CYS186, CYS187, TYR191
AZD0328	-7.4	ASP17, PRO79, SER81, TRP84, VAL85, LEU104

All ligands exhibited favorable binding affinities within the range of -9.8 to -7.4 kcal/mol. Table 1 provides a comprehensive summary of specific information concerning the interacting amino acid residues, types of interactions, and the binding affinities of the agonists. The binding affinity results derived from the ligands are presented in Table 1. The docking outcomes revealed that both ligands bound to their respective target receptors primarily through interactions involving hydrogen bonding and electrostatic bonds (Figure 3, Figure 4, and Figure 5). In this study, 3D and 2D receptor-ligand binding interactions obtained from molecular docking showed that all ligands interacted with amino acid residues which play critical roles in the sub- and complementary loops in receptor recognition and signal transduction. The findings indicated that B-973B exhibited the highest binding affinity (-9.8 kcal/mol) among the ligands. In addition, B-973B manifested bonding interactions with the receptor among all ligands tested.

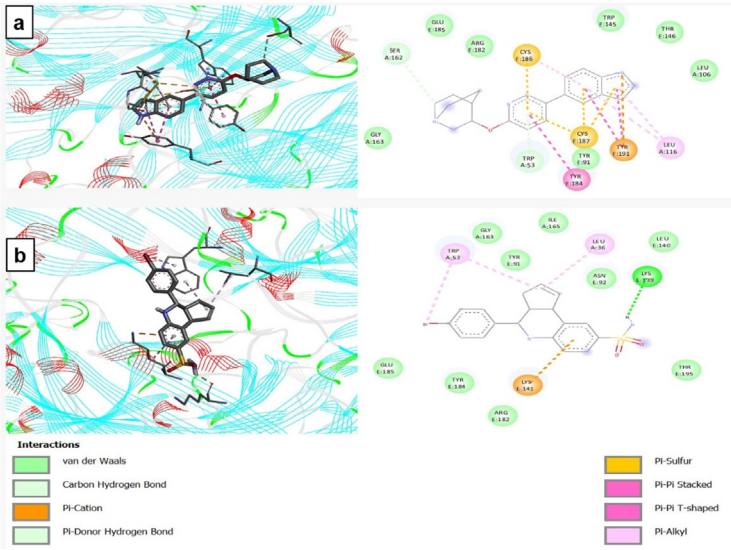

Figure 3. The 2D and 3D binding interactions of α7 nAChR with the ligands ABT-107 (a) and GAT107 (b). Green dotted lines; hydrogen bonds, pink lines; hydrophobic interactions, orange lines; electrostatic bonding.

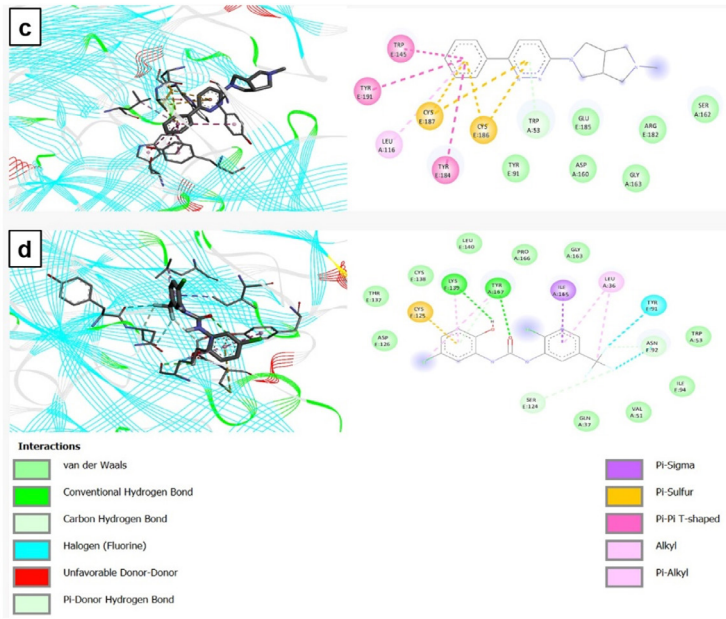

Figure 4. The 2D and 3D binding interactions of α7 nAChR and the ligands A-582941 (c) and NS1738 (d). Green dotted lines; hydrogen bonds, pink/purple lines; hydrophobic interactions, blue lines; halogen bonding, orange lines; electrostatic bonding.

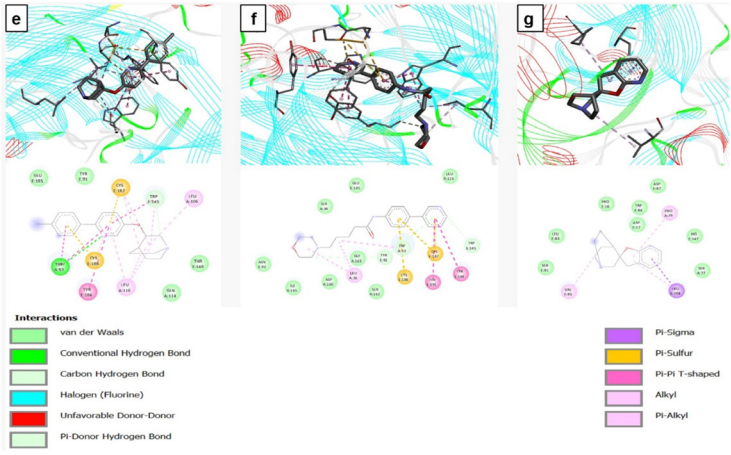

Figure 5. The 2D and 3D binding interactions of α7 nAChR and the ligands AQW-051 (e), SEN12333 (f), and AZD0328 (g). Green dotted lines; hydrogen bonds, pink/purple lines; hydrophobic interactions, blue lines; halogen bonding, orange lines; electrostatic bonding.

The conformational deviations in the receptor and the stability of the ligand in the receptor binding pocket were evaluated. A molecular dynamics (MD) simulation investigation was conducted to explore the interaction between the α7nAChR receptor and the most potent compound, B-973B ligand, which exhibited promising outcomes in the prior molecular docking analysis. The findings from this simulation reveal that the fluctuations observed throughout the 100 ns simulation period remain within the acceptable range of 1 to 3 Å.

Macrophages play an important role in the periodontal immune system by strengthening the defense against pathogens. Through the secretion of ACh, α7nAChR regulates the transmission of activation states and immunological responses of macrophages[6]. In the literature, several investigations have documented the utilization of macrophages for the identification of α7nAChR[19]. These studies have additionally revealed that the activation of macrophages plays a crucial role in modulating signaling pathways, resulting in the inhibition of NF-κB nuclear translocation and the subsequent reduction in the transcription of proinflammatory cytokines[19]. Additionally, it was discovered in research that modest dosages of nicotine had an inhibitory effect on the production of TNF-α and macrophage inflammatory protein 1 alpha (MIP-lα) in LPS-activated human peripheral monocytes[20]. All these states are moderated by 7nAChR, which in turn inhibits the NF-κB transcription factor by stopping the phosphorylation of IκBa (inhibitor of nuclear factor of kappa light polypeptide gene enhancer in B-cells, alpha)[20]. In addition, in some in vitro and in vivo studies in the literature, it has been observed that the JAK-2/STAT-3 pathway is also stimulated in α7nAChR activation. The release of STAT-3 proinflammatory cytokines is inhibited by the binding of nicotine to α7nAChR and activation of α7nAChR[21]. Activation of STAT-3 by the IL-10 receptor mediates the anti-inflammatory effect of IL-10. Studies have reported that only the specific down-regulation of proinflammatory cytokines can be induced by the activation of α7nAChR since it does not inhibit the production of IL-10[22].

Evidence on IgG-secreting B cells that have a role in the periodontal disease progression despite the effect of immune response on disease[23]. Under inflammatory conditions, T cells promote the differentiation of Th2 cells[24]. Th2 cells have anti-inflammatory responses and immune suppressive associated with periodontal disease[24]. While IL-17 production in CD4+ T cells in the blood is inhibited by Nicotine (nAChR agonist) through α7nAChR, α-bungarotoxin (α −BTX) provides the balance by showing an antagonistic effect[25]. The α7nAChR can differentiate into Treg cells, affect their immunosuppressive functions and nicotine increases the evidence of cytotoxic T-lymphocyte-associated antigen 4 (CTLA-4) and forkhead box 3 protein (FoxP3) and increases improvement of Treg cells into the central nervous system (CNS)[26].

Side effects occur in people who are addicted to cigarettes due to their continuous and high-dose exposure to nicotine throughout their lives. As a consequence of the location of nicotine in the central nervous system, it targets nicotinic acetylcholine receptors. In addition, there are non-neuronal nicotine binding sites in peripheral blood cells. Detailed examination of these regions has been proposed as an approach to understanding the pharmacological mechanisms in the tobacco addiction state[27]. The effects of tobacco on periodontal tissues and the causality of smoking with periodontitis have been reported by many researchers[27-29]. As a result of the inhibition of β-defensin by nicotine-induced *Porphyromonas gingivalis* LPS, it causes the progression of periodontal disease[29]. The increased IL-8 releases induced by *P. gingivalis* LPS or TNF-a decreases with nicotine activation[29]. This information implies that nicotine has a direct proinflammatory impact when present in the context of periodontal disease[6]. In previous studies, it has been observed that nicotine up-regulates IL-1β expression in periodontal cells[6, 29].

The ligand-binding core and regions of the α7 nAChR structure that play an important role in the analysis of signal transduction are covered with α7 residues[30]. Therefore, it is also critical for the recognition of ligand binding to the receptor. Recognition of ligand binding to the receptor is mediated by residues in loops A-C, the main subunit of the receptor, and loops D-E of the subunits, respectively[16,30]. Some critical amino acids in loops A and B of the main subunits are responsible for ligand binding and recognition. These amino acids are TYR91 in loop A and TRP145 in loop B. In loop C, the amino acids TYR184 and TYR191 play an important role in the transition to complementary subunits[16]. TRP53 in loop D, GLN114 in loop E, and LEU116 in loop E of the subunits enable ligand recognition mode and intra-unit communication inside the binding pocket. The ligand binding region of the receptor is surrounded by residues that are unique to the α7 subunit located throughout the C loop[16]. When the agonist binds to the receptor, these residues adopt a different conformation[30]. Conformational changes in the A, B, and C loops of the receptor during ligand binding led to the rearrangement of residues in the ligand binding site. The most important of these changes are the shifts of TYR91, TRP145, and TYR184. Also, TYR191 and TRP53 are the primary stabilizing residues[16].

The results obtained in our study showed that the selected ligands interact with these critical amino acid residues through different bonds. In particular, ligand B-973B, which was found to have the most effective binding affinity, interacted strongly with TYR184 and TYR191 via π- π stacked and π- π T-shaped interactions. Furthermore, TRP145 amino acid residue was observed to bind

with fluorine atoms in the ligand structure via halogen bonding. In addition, it is believed that the different interactions of the tested compounds with TRP53 and LEU116 amino acids, which are important in ligand recognition and signal transduction, as well as different types of bonding with ARG182 and GLU185 amino acids in the loop C region of the receptor, may affect the affinity of the α7-selectively bound agonist.

In general, as seen from the two-dimensional interactions, stabilizing interactions between the receptor and ligands were generally thought to consist of a π-cation bonding between the ligands and TRP145 amino acid residue due to the presence of an indole ring in its structure. The presence of the carbonyl functional group in the main chain of the amino acid TRP145 and the -OH group carried by TYR91 leads to the formation of hydrogen bonds between the ligands and the amino acid residues, which may constitute a component of stabilizing interactions. It is also concluded that extensive van der Waals contacts between the aliphatic part of the azabicyclo moiety and TYR184, CYS186, CYS187, and TRP145 in ligands such as ABT-107, AZD0328, or NS6784 may enhance the interactions.

The limitation in *silico* studies is to make calculations about the effects of chemical substances using computer simulations and present scientific data with estimated values. However, from a future perspective, preliminary data obtained from the *in silico* study can be evaluated and supported for use in *in vitro* and *in vivo* studies. Therefore, this molecular docking study may shed light on future *in vitro* and *in vivo* studies for apical periodontitis.

In summary, the binding affinity values obtained from the agonists selected as a result of the molecular docking study were compared. B-973B ligand, which was found to have the most effective binding affinity among them and showed a stable receptor-ligand relationship as a result of MD simulation, may be effective in reducing inflammation in the treatment of apical periodontitis and similar endodontic diseases. The results obtained may shed light on the use of the α7nAChR-mediated cholinergic anti-inflammatory pathway in apical periodontitis with effective α7nAChR agonists, mainly B-973B. In addition, this study may contribute to the design and synthesis of new α7nAChR agonists with halogen-substituted pyrazine propanamide derivatives similar to the molecular structure of B-973B, especially for use in LPS-induced apical periodontitis.

STATEMENT OF ETHICS

Not applicable.

CONFLICT OF INTEREST STATEMENT

The authors have no relevant financial or non-financial interests to disclose.

AUTHOR CONTRIBUTIONS

Emine Erdag: Design, Acquisition of Data, Analysis of Data, Drafting of the Manuscript. Dilan Kirmizi: Design, Acquisition of Data, Drafting of the Manuscript. Umut Aksoy: Supervision. Ahmet Ozer Sehirli: Supervision. All authors read and approved the final manuscript.

FUNDING SOURCES

Not applicable.

ACKNOWLEDGMENTS

Not applicable.

REFERENCES

1. Bronzato JD, Davidian MES, de Castro M, de-Jesus-Soares A, Ferraz CCR, Almeida JFA et al. Bacteria and virulence factors in periapical lesions associated with teeth following primary and secondary root canal treatment. Int Endod J, 2021;54(5):660-671. Doi: 10.1111/iej.13457

2. Galler KM, Weber M, Korkmaz Y, Widbiller M, Feuerer M. Inflammatory response mechanisms of the dentine-pulp complex and the periapical tissues. Int J Mol Sci, 2021;22:1480. Doi: 10.3390/ijms22031480

3. Aksoy U, Savtekin G, Şehirli AÖ, Kermeoğlu F, Kalender A, Özkayalar H, et al. Effects of alpha-lipoic acid therapy on experimentally induced apical periodontitis: a biochemical, histopathological and micro-CT analysis. Int Endod J, 2019;52(9):1317-1326. Doi: 10.1111/iej.13121

4. Zero DT, Zandona AF, Vail MM, Spolnik KJ. Dental caries and pulpal disease. Dent Clin North Am, 2011;55:29-46. Doi: 10.1016/j.cden.2010.08.010

5. Silva N, Abusleme L, Bravo D, Dutzan N, Garcia-Sesnich J, Vernal R et al. Host response mechanisms in periodontal diseases. J Appl Oral Sci, 2015;23:329-355. Doi: 10.1590/1678-775720140259

6. Zoheir N, Lappin DF, Nile CJ. Acetylcholine and the alpha 7 nicotinic receptor: a potential therapeutic target for the treatment of periodontal disease? Inflamm Res, 2012;61:915-926. Doi: 10.1007/s00011-012-0513-z

7. Fujii T, Mashimo M, Moriwaki Y, Misawa H, Ono S, Horiguchi K, et al. Expression and function of the cholinergic system in immune cells. Front Immunol, 2017;8:1085. Doi: 10.3389/fimmu.2017.01085

8. Prathumsap N, Ongnok B, Khuanjing T, Arinno A, Maneechote C, Apaijai N, et al. Acetylcholine receptor agonists provide cardioprotection in doxorubicin-induced cardiotoxicity via modulating muscarinic M2 and α7 nicotinic receptor expression. Transl Res, 2022;243:33-51. Doi: 10.1016/j.trsl.2021.12.005

9. Wills L, Ables JL, Braunscheidel KM, Caligiuri SPB, Elayouby KS, Fillinger C, et al. Neurobiological mechanisms of nicotine reward and aversion. Pharmacol Rev, 2022;74:271-310. Doi: 10.1124/pharmrev.121.000299

10. Wang XJ, Liu YF, Wang QY, Tsuruoka M, Ohta K, Wu SX, et al. Functional expression of α7 nicotinic acetylcholine receptors in human periodontal ligament fibroblasts and rat periodontal tissues. Cell Tissue Res, 2010;340:347-355. Doi: 10.1007/s00441-010-0949-9

11. Pereira MR, Leite PE. The involvement of parasympathetic and sympathetic nerve in the inflammatory reflex. J Cell Physiol, 2016;231:1862-1869. Doi: 10.1002/jcp.25307

12. Fujii T, Mashimo M, Moriwaki Y, Misawa H, Ono S, Horiguchi K, et al. Physiological functions of the cholinergic system in immune cells. J Pharmacol Sci, 2017;134:1-21. Doi: 10.1016/j.jphs.2017.05.002

13. Wang H, Yu M, Ochani M, Amella CA, Tanovic M, Susarla S, et al. The nicotinic acetylcholine receptor α7 subunit is an essential regulator of inflammation. Nature, 2023;421:384-388. Doi: 10.1038/nature01339

14. Faruk ER, Deveci E, Kalkanli S, Deveci B. The effects of nicotine on the incisive teeth and expression of vimentin in rats. Int. J. Morphol, 2013;31:516-519. Doi: 10.4067/S0717-95022013000200026.

15. Du H, Zhang X, Zeng Y, Huang X, Chen H, Wang S, et al. A novel phytochemical, DIM, inhibits proliferation, migration, invasion and TNF-α induced inflammatory cytokine produc-

tion of synovial fibroblasts from rheumatoid arthritis patients by targeting MAPK and AKT/mTOR signal pathway. Front Immunol, 2019;10:1620. Doi: 10.3389/fimmu.2019.01620

16. Papke RL, Horenstein NA. Therapeutic targeting of α7 nicotinic acetylcholine receptors. Pharmacol Rev, 2021;73:1118-1149. Doi: 10.1124/pharmrev.120.000097

17. Kutzner C, Kniep C, Cherian A, Nordstrom L, Grubmüller H, de Groot BL, et al. GROMACS in the cloud: a global supercomputer to speed up alchemical drug design. J Chem Inf Model, 2022;62:1691-1711. Doi: 10.1021/acs.jcim.2c00044

18. Branka AC, Wojciechowski KW. Generalization of nosé and nosé-hoover isothermal dynamics. Phys Rev E Stat Phys Plasmas Fluids Relat Interdiscip Topics, 2000;62:3281-3292. Doi: 10.1103/physreve.62.3281

19. Qi Y, Si D, Zhu L, Qi Y, Wu Z, Chen D, et al. High-fat diet-induced obesity affects alpha 7 nicotine acetylcholine receptor expressions in mouse lung myeloid cells. Sci Rep, 2020;10:18368. Doi: 10.1038/s41598-020-75414-w

20. Lin X, Tago K, Okazaki N, So T, Takahashi K, Mashino T, et al. The indole-hydantoin derivative exhibits anti-inflammatory activity by preventing the transactivation of NF-κB through the inhibition of NF-κB p65 phosphorylation at Ser276. Int Immunopharmacol, 2021;100:108092. Doi: 10.1016/j.intimp.2021.108092

21. Xie J, Li X, Zhang L, Liu C, Leung JW, Liu P, et al. Genistein-3'-sodium sulfonate ameliorates cerebral ischemia injuries by blocking neuroinflammation through the α7nAChR-JAK2/STAT3 signaling pathway in rats. Phytomedicine, 2021;93:153745. Doi: 10.1016/j.phymed.2021.153745

22. Soubh AA, El-Gazar AA, Mohamed EA, Awad AS, El-Abhar HS. Further insights for the role of Morin in mRTBI: Implication of non-canonical Wnt/PKC-α and JAK-2/STAT-3 signaling pathways. Int Immunopharmacol, 2021;100:108123. Doi: 10.1016/j.intimp.2021.108123

23. Volkov M, van Schie KA, van der Woude D. Autoantibodies and b cells: The abc of rheumatoid arthritis pathophysiology. Immunol Rev, 2020;294:148-163. Doi: 10.1111/imr.12829

24. Zheng Y, Chai L, Fan Y, Song YQ, Zee KY, Tu WW, et al. Th2 cell regulatory and effector molecules single nucleotide polymorphisms and periodontitis. J Leukoc Biol, 2020;108:1641-1654. Doi: 10.1002/JLB.4MA0720-698RR

25. Liu Z, Han B, Li P, Wang Z, Fan Q. Activation of α7nAChR by nicotine reduced the Th17 response in CD4(+)T lymphocytes. Immunol Invest, 2014;43:667-674. Doi: 10.3109/08820139.2014.914532

26. Lu J, Wu W. Cholinergic modulation of the immune system – a novel therapeutic target for myocardial inflammation. Int Immunopharmacol, 2021;93:107391. Doi: 10.1016/j.intimp.2021.107391

27. Apatzidou DA. The role of cigarette smoking in periodontal disease and treatment outcomes of dental implant therapy. Periodontol 2000, 2022;90:45-61. Doi: 10.1111/prd.12449

28. Nascimento GG, Leite FR, Scheutz F, Lopez R. Periodontitis: from infection to inflammation. Curr Oral Health Rep, 2017;4:301-308. Doi: 10.1007/s40496-017-0158-7

29. An N, Holl J, Wang X, Rausch MA, Andrukhov O, Rausch-Fan X. Potential suppressive effect of nicotine on the inflammatory response in oral epithelial cells: an *in vitro* study. Int J Environ Res Public Health, 2021;18:483. Doi: 10.3390/ijerph18020483

30. Weis WI, Kobilka BK. The molecular basis of g protein-coupled receptor activation. Annu Rev Biochem, 2018;87:897-919. Doi: 10.1146/annurev-biochem-060614-033910

Acta Pharm. Sci. Vol 63:(1), 2025
Original article
DOI: 10.23893/1307-2080.APS6312

Bioactivity of hexokinase II inhibitor ikarugamycin and relation with tissue factor in breast cancer cell lines

Vildan AKGUL OBEIDIN*, Feyza BAYRAMOGLU, Sevgi DISLI, Neslin EMEKLI

Istanbul Medipol University, Faculty of Medicine, Department of Biochemistry, Istanbul, Türkiye

ABSTRACT

Despite the understanding gained from scientific studies regarding Hexokinase II (HK2)'s involvement in cancer cell metabolism, there are no reports of directly inhibiting HK-2 enzyme to affect tissue factor (TF) activity in cancer cells. This study primarily investigates the complex mechanisms triggering neoplastic cell formation by examining the in vitro bioactivation of the Ikarugamycin (IKA) molecule, commonly used as an antibiotic. The IC50 values for MDA-MB-231 (TNBC) and MCF-7 (TPBC) cell lines are 24.1 μM and 19.25 μM, respectively. Furthermore, TF activation in breast cancer cell lines was demonstrated through Prothrombin Time (PT) analysis, showing that IKA effectively prolongs TF activation compared to Sodium Oxamate and Paclitaxel (Ptx), commonly used as a chemotherapeutic agent. Additionally, it was observed to be more effective in hormone-dependent MCF-7 breast cancer cell lines. Future studies should focus on investigating the changes in protein, enzyme, and gene levels of TF following treatment with IKA.

Keywords: hexokinase-2, tissue factor, breast cancer, glycolysis, anticancer-antibiotics

*Corresponding author: Vildan AKGUL OBEIDIN
E-mail: svakgul@gmail.com
ORCIDs:
Vildan AKGUL OBEIDIN: 0000-0003-0138-2445
Feyza BAYRAMOGLU: 0000-0002-0757-9743
Sevgi DISLI: 0009-0003-7801-4613
Neslin EMEKLI: 0000-0002-0109-5086
(Received 5 Feb 2024, Accepted 16 Apr 2024)

INTRODUCTION

Breast cancer is a prevalent malignancy typified by unregulated cellular proliferation within the breast tissue. According to the latest data, it is the most diagnosed cancer in women[1-2]. Various therapeutic modalities, including surgical interventions, radiotherapy, chemotherapy, and hormone therapy, may induce significant adverse effects that detrimentally impact the overall quality of life[3]. In this sense, it is important to search for new treatments that provide better results than current breast cancer treatment methods and at the same time reduce side effects.

Hexokinases (HKs) represent evolutionarily conserved enzymes pivotal in phosphorylating hexoses, six-carbon sugars. Their significance lies in mediating essential processes within cellular metabolism and play crucial roles in Adenosine Triphosphate (ATP) synthesis, glucose storage, NADH pool enrichment, and protein glycosylation. Among mammals, the well-characterized HK isozymes include HK1 through HK4[4-6]. Recent investigations have brought to light a fifth isozyme known as HKDC1 (HexoKinase Domain Containing protein 1)[7]. Noteworthy is the cytosolic localization of all HKs, except HK-1 and HK-2, which possess a distinctive N-terminal motif facilitating binding to mitochondria—an attribute absent in other isoforms.

The binding of HK-1 and HK-2 to mitochondria manifests cytoprotective effects in both healthy and neoplastic cells, enhancing their proficiency in glucose utilization. This unique feature underscores the intricate regulatory mechanisms through which hexokinases contribute to cellular homeostasis and function. These insights contribute to a comprehensive understanding of the diverse roles played by hexokinases in cellular processes critical for metabolic regulation and overall cellular health[5,8-10].

A key feature of many cancers, especially the most aggressive, is the ability to metabolize glucose at a high rate, a phenotype that is clinically detected using positron emission tomography (PET). This phenotype gives cancer cells, including those involved in metastasis, a competitive advantage over normal cells[8].

Especially, after the rapid entry of glucose into cancer cells through molecular glucose transporters, the overexpression of hexokinases, primarily HK-2, leads to high glycolytic activity through the interaction of numerous complex mechanisms[5]. This situation contributes to the continued proliferation of cancer cells (Figure 1). Numerous complex mechanisms facilitate the activation of tissue factor (TF). The initiation of TF activation is instigated by adenosine triphos-

phate (ATP), prompting the translocation of acid sphingomyelinase (A-SMase) to the plasma membrane. ATP stimulation augments the hydrolysis of sphingomyelin (SM) within the outer leaflet. Impeding the expression or activity of A-SMase not only diminishes ATP-induced sphingomyelin hydrolysis but also impedes the ATP-triggered decryption of the transcription factor[11-12]. Additionally, integrin mechanisms that trigger TF activation, particularly in breast cancers, are present. In breast cancer cells, TF plays a significant role in regulating the TF-VIIa-Protease-Activated Receptor 2 (PAR2) signaling pathway. TF is continually associated with β1 integrins on this pathway and participates in regulating the TF-VIIa-PAR2 signal. This signaling process is responsible for regulating the tumor microenvironment in breast cancer, supporting tumor cell migration, and metastasis[13] (Figure 1). It is believed that targeting TF signaling could be particularly important for the treatment of Triple-Negative Breast Cancer (TNBC) and disrupting TF/β1 interactions may help prevent recurrence and improve overall survival[14] (Figure 1).

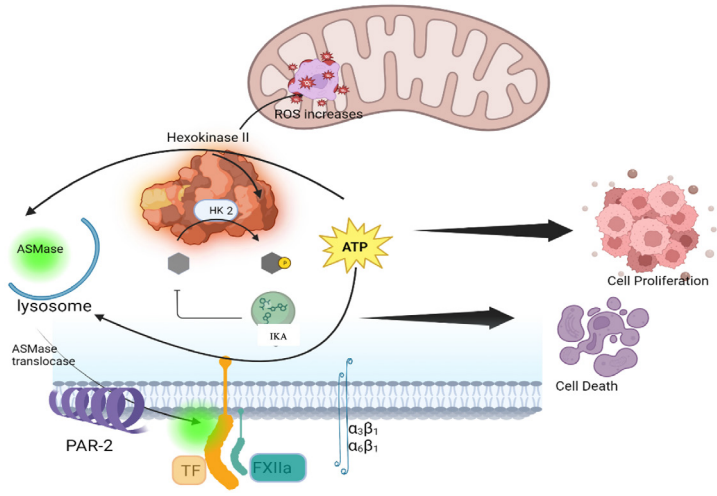

Figure 1. The Hexokinase II enzyme's role in the proliferation of neoplastic cells and its association with TF. HK-2 inhibition leads to cell death and inhibits ATP production. ATP activates tissue factor (TF), initiating its decryption and triggering sphingomyelin hydrolysis through acid sphingomyelinase. In breast cancer, TF, regulated by integrin mechanisms, plays a crucial role in the TF-VIIa-PAR2 signaling pathway, impacting the tumor microenvironment and metastasis.

ROS: Reactive Oxygen Species; PAR-2: Protease-Activated Receptor 2; ASmase: Acid sphingomyelinase

Cancer cells exhibit a distinctive metabolic phenotype wherein they preferentially employ aerobic glycolysis over mitochondrial oxidative phosphorylation for glucose metabolism, in contrast to the normative metabolic patterns observed in normal cells. The sustained elevation in lactate production by cancer cells under oxygen-rich conditions, a phenomenon recognized as aerobic glycolysis, was originally identified more than 75 years ago by Otto Warburg (Figure 2)[15-19]. Since cancer cells require energy to sustain cell growth and proliferation, the high glycolytic activity must provide sufficient ATP levels to meet the demands of rapidly proliferating tumor cells within a hypoxic microenvironment[20,21]. This condition affects various mechanisms in the body abnormally; one of these mechanisms is angiogenesis, which can be triggered directly or indirectly.

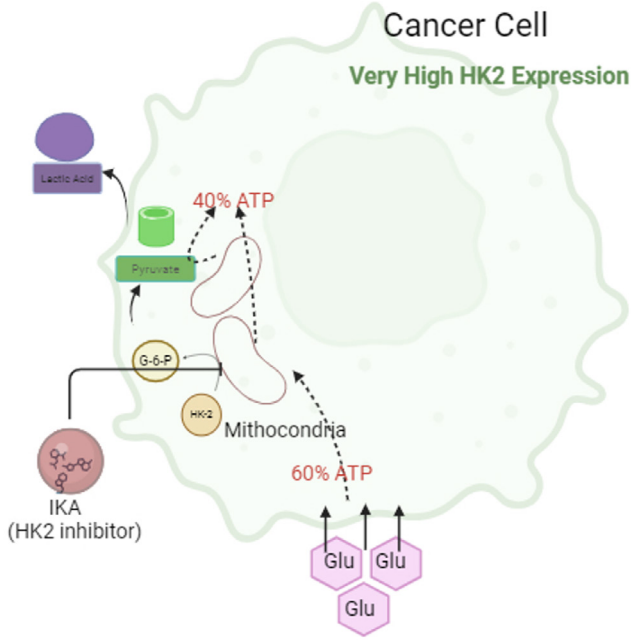

Figure 2. The mechanism by which IKA quickly and efficiently kills cancer cells through rapid energy depletion. While these percentages may vary significantly based on growth rates and cancer types, it's crucial to highlight that both glycolysis and mitochondrial ATP production are essential contributors to fueling cancer growth and facilitating metastasis. Malignant cells' energy source is ATP and about 60% of the ATP is produced by glycolysis and the other 40% by the mitochondria[22].

TF, the third protein of the coagulation system, is found as a transmembrane protein in all tissues. Due to its structural feature, TF possesses a distinct architecture and function compared to other coagulation proteins. Molecularly, it comprises three distinct domains, and it is also known as CD142 due to its signaling transmission effect. Present in the blood in micro-particles at concentrations ranging from 100 to 150 pg/mL, TF initiates the coagulation process by forming the TF/VIIa complex. In an environment containing ionized calcium and the TF/VIIa complex, citrated plasma coagulates within 2-15 seconds[23].

The deficiency of TF is not observed in vivo, given its presence in varying proportions as a structural and functional molecule in all tissues. This is attributed to its involvement in vascularization since the embryogenic period, and its absence has been reported to result in fatality[24-28].

TF serves as the primary precursor within the extrinsic coagulation cascade, exerting a notable influence on the advancement and metastatic phases across various cancer types[22]. Research has shown that TF is involved in cancer invasion, particularly through a unique pathway, independent of the coagulation pathway, via PARs, which mediate intracellular signaling. These findings demonstrate that TF is both an initiator of the coagulation pathway and deeply involved in tumor progression and tumor angiogenesis (Figure 3)[29-32].

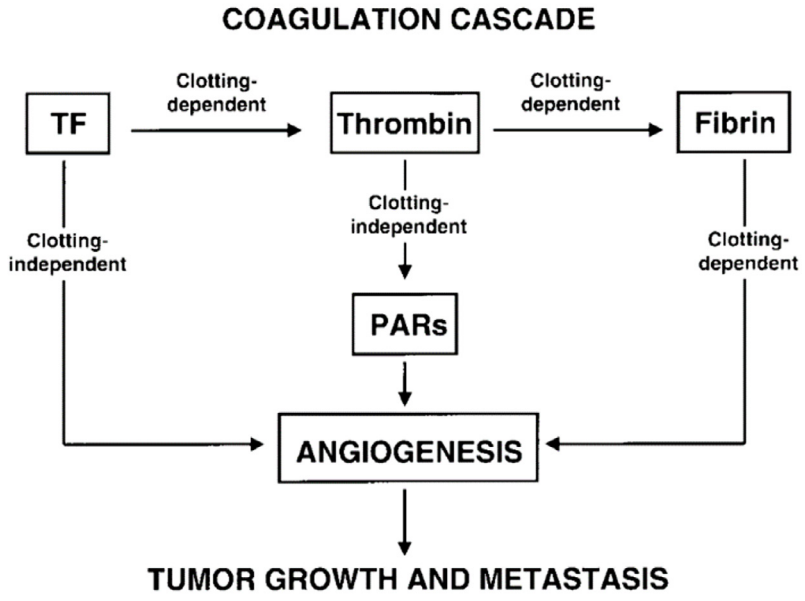

Figure 3. Diagram of the direct and indirect effects of tissue factor on angiogenesis[33-34]

Anticancer antibiotics are a class of chemicals that effectively fight against various types of cancer. These antibiotics exert their anticancer effects by interfering with various cellular processes involved in tumor growth and survival[27]. These groups of medicines are used to prevent and treat the spread of cancer by inhibiting DNA synthesis and repair through other mechanisms. Disrupting their structure by entering between DNA chains and/or causing stabilization of the microtubule, which prevents its depolymerization by binding to β-tubulin, are just some of these mechanisms[35]. Anticancer antibiotics can be classified according to their mechanism of action. These classes can be specified as; Aromatic Polyketides (Anthracyclines), Glycopeptides, Non-ribosomal Peptides, Mitosanes, Enediynes, Indolocarbazoles, Epothilones and Other Agents[36].

In the treatment of breast cancer, anticancer antibiotics are often used as part of chemotherapy protocols. These antibiotics act by preventing the growth and division of cancer cells or by causing the cancer cells to undergo apoptosis in different ways. Certain anticancer antibiotics used to treat breast cancer include anthracyclines (e.g., Doxorubicin), Mitomycin C, and Bleomycin[37,38].

Anthracycline derivatives cause DNA damage by increasing the formation of free radicals that damage breast cancer cells. Ikarugamycin is also an anthracycline derivative, and its hexokinase-2 inhibitory effect was discovered recently and showed therapeutic effect in pancreatic cancer[39,40].

The present study aimed to demonstrate the in vitro bioactivation of IKA, which had been hypothesized to be biologically active in breast cancer treatment manner, in MDA-MB-231 and MCF-7 cell lines. Additionally, the effect of TF and HK-2 inhibitor on cancer cell metabolism was investigated, and a comparison was made with the commonly used LDH-A inhibitor Sodium Oxamate in cancer studies and the chemotherapeutic agent Paclitaxel, widely employed in clinical settings.

METHODOLOGY

Chemicals and reagents

MTT (3-(4,5-dimethylthiazol-2-yl)-2,5-diphenyltetrazolium bromide) to determine bioactivity, hepes-buffered DMEM (Dulbecco's Modified Eagle Medium/High Glucose), fetal bovine serum (FBS), phosphate-buffered saline (PBS), penicillin-streptomycin (10,000 U/mL), L-glutamine, and ethanol for basic cell culture protocols. The Hexokinase 2 inhibitor Ikarugamycin (CAYMAN;15386), to compare therapeutic efficacy; Paclitaxel (Ptx) as a commonly used chemotherapeutic agent and Sodium Oxamate (NaOx), widely used in preclinical studies, (Figure 4) were also utilized.

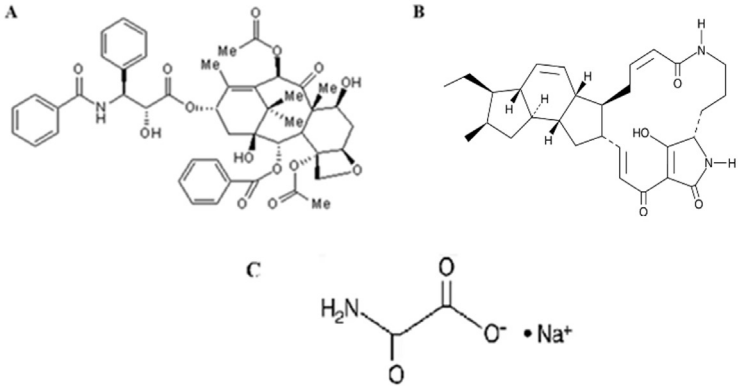

Figure 4. (A) Paclitaxel molecule(2α,4α,5β,7β,10β,13α)-4,10-Bis(acetyloxy)-13-{[(2R,3S)-3-(benzoylamino)-2-hydroxy-3-phenylpropanoyl]oxy}-1,7-dihydroxy-9-oxo-5,20-epoxytax-11-en-2-yl benzoate (B) Ikarugamycin molecule; (2R,3R,7Z,14S,19E)-3-ethyl-2,3,3aS,5aR,5bS,6,10,11,12,13,14,15,20aS,21,21aR,21bR-hexadecahydro-22-hydroxy-2-methyl-14,17-metheno-17H-as-indaceno[3,2-k][1,6]diazacycloheptadecine-9,16,18(1H)-trione (C) Sodium Oxamate molecule (Oxalic Acid monoamide, Oxamic Acid, CAS Number: 565-73-1) | Cayman Chemical)

Cell culture

The MDA-MB-231 and MCF-7 (ATCC) breast cancer cell lines were cultured in Dulbecco's Modified Eagle Medium/High Glucose (DMEM) supplemented with 10% (v/v) fetal bovine serum (FBS), 1% (v/v) penicillin-streptomycin, and 1% (v/v) L-glutamine. The cells were incubated at 37°C in a humidified incubator with 5% CO_2. Subsequently, upon reaching confluency, the cells were subcultured into T-25 cell culture flasks to maintain uniform growth conditions. Once a sufficient population was obtained, T-75 flasks were used for the experiments, and standardized cell passage techniques were employed by our team[41].

Cell viability assay

Cell seeding was conducted in a 96-well plate at a density of 1.0 x 10^4 cells per well, with each well containing 200 µL of the specified medium and incubated for 24 hours. To determine the IC_{50} values of IKA, a dose range varying from 0.1 to 1000 µM was applied to the cells, followed by incubation for the optimal incubation times (24 and 48 hours). After incubation, 5 mg/ml of MTT was added to each well according to the manufacturer's instructions and incubated for 3 hours[42]. Subsequent to the removal of the medium containing 3-(4,5-dimethylthiazol-2-yl)-2,5-diphenyltetrazolium bromide (MTT), 100 µL of dimethyl sulfoxide (DMSO) was introduced into each well, and a gentle agitation period of 5 minutes ensued to facilitate reaction completion. Ab-

sorbance readings at 570 nm were subsequently obtained using a plate reader (Synergy|HTX, BioTek, Agilent, USA). Each experiment was performed with 3 replicates. IC_{50} values were calculated by log[IC_{50}] using GraphPad Prism, and the experimental groups were formed accordingly: Control/ IKA (IC_{50})/ NaOx(IC_{50}) Paclitaxel (IC_{50}) (Table 1).

Table 1. Experimental Groups for both cell lines; MDA-MB-231 and MCF-7

	Group I MCF-7	**Group II MDA-MB-231**
Section A	Negative Control	Negative Control
Section B	HK-2 Inhibitor [IKA (IC_{50})]	HK-2 Inhibitor [IKA (IC_{50})]
Section C	LDH-A Inhibitor [NaOx(IC_{50})]	LDH-A Inhibitor [NaOx(IC_{50})]
Section D	Chemotherapeutic [Ptx(IC_{50})]	Chemotherapeutic [Ptx(IC_{50})]

Ptx: Paclitaxel; NaOx: Sodium Oxamate; $IC_{50:}$: the concentration of a particular drug that is needed to inhibit a given biological process to half of the maximum

Preparation of cell lysates

MCF-7 and MDA-MB-231 cell lines were collected by trypsinization and centrifuged at 1500 g for 5 minutes. The cell pellets were washed twice with cold PBS and then homogenized for 5 minutes with the addition of metal beads. Subsequently, a second centrifugation step was performed. The supernatants containing the cell lysates were collected and prepared for further experimentation[41,43,44].

TF activation - PT test / quick method

A total of 100 µL of plasma and 100 µL of cell lysate were incubated in a test tube at 37°C. After a 2-minute incubation, 100 µL of 0.025 M $CaCl_2$ was added to the mixture. The thromboplastic activities were observed, and the time at which the first appearance was noted[43-44]. The clotting time demonstrates an inverse relationship with tissue factor (TF) activity, hence, elongation of clotting time indicates a reduction in TF activity.

Morphological analysis of cells

MDA-MB-231 and MCF-7 cell lines were seeded at a density of 2 x 10^5 and 3 x 10^5 cells, respectively, in 6-well plates. After 24 hours, the cells were treated with the required drugs at predetermined doses and incubated for an additional 24 hours. The control groups were washed twice with PBS and observed under a light microscope for morphology and colonization status.

Statistical analysis

The study employed GraphPad Prism software for data analysis, with variables characterized by their standard deviation. A Student's t-test was employed for the comparison of means exhibiting a normal distribution. Two-way Analysis of Variance (ANOVA) was utilized to compare groups and elucidate differences among subgroups in variables demonstrating variations. P values<0.05 (*) were accepted as significant.

RESULTS and DISCUSSION

The inhibition of HK-2 is known to halt cell proliferation and glycolytic activity, leading to apoptosis in neoplastic cells[45,46]. IKA, which is used to treat bacterial infection primarily, has been found to exhibit in vitro bioactivation. The determined IC_{50} values for the MDA-MB-231 and MCF-7 breast cancer cell lines were 24.1 μM and 19.25 μM, respectively (Figure 5).

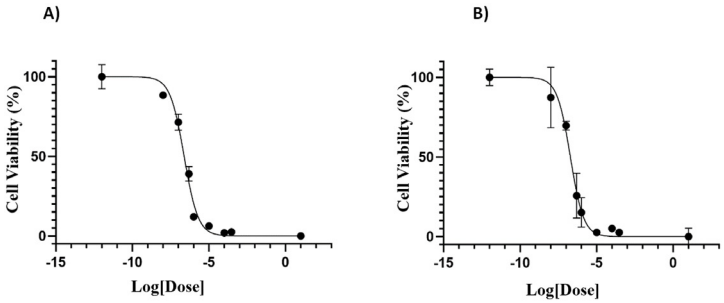

Figure 5. A) MDA-MB-231 cell viability of IKA application analyzed by MTT assay. B) MCF-7 cell viability of IKA application analyzed by MTT assay.

Table 2. Tissue Factor Activation by using Prothrombin Time (PT) Analysis

MCF-7	TF Activation (s)	MDA-MB-231	TF Activation (s)
Control	*51.11 ± 4.08	Control	66.50 ± 3.00
IKA (IC_{50})	*113.28 ± 9.53	IKA (IC_{50})	87.35 ± 6.45
NaOx (IC_{50})	*60.45 ± 5.27	NaOx (IC_{50})	70.37 ± 3.67
Ptx (IC_{50})	*98.52 ± 8.17	Ptx (IC_{50})	*91.00 ± 2.50

In the PT test conducted to determine tissue factor activation, it was found that the clot formation times were longer in both cell lines compared to the group treated with IKA, when compared to Paclitaxel, a commonly used clinical agent. Furthermore, while Paclitaxel exhibited more effective elongation in MCF-7, which is characterized by triple-positive breast carcinoma, IKA prolonged the clot formation

The data were evaluated using ANOVA and Student's t-test statistical analysis methods, and the graphs are represented as mean ± standard deviation and shown in Figure 6 (*p<0.05).

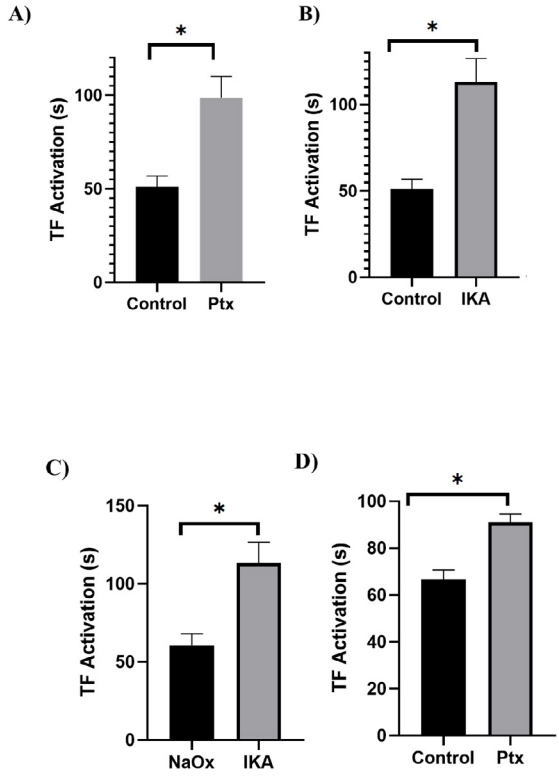

Figure 6. Comparison of MDA-MB-231 and MCF-7 cell lines' sections. A) Comparison of the control group and Ptx treatment in the MCF-7 breast cancer cell line (p<0.05) B) Comparison of the control group and IKA treatment in the MCF-7breast cancer cell line (p<0.05) C) Comparison of the NaOx and IKA treatment in the MCF-7 breast cancer cell line (p<0.05) D) Comparison of the control group and Ptx treatment in the MDA-MB-231 breast cancer cell line (p<0.05)

When all the data were individually examined, for the MDA-MB-231 cell line, except for Ptx, the other two drugs were not statistically significant when compared to the control group. The relationship between IKA and both the control group and NaOx, which is used in clinical treatments, was not found to be statistically significant. The MCF-7 cell line is a cell type with a higher chance of response to treatment and a higher survival rate compared to MDA-MB-231. When compared to the control group, all treatment groups were found to be statistically significant ($p<0.05$).

In the determined groups, predetermined doses of drug molecules were applied to MDA-MB-231 and MCF-7 cell lines. After the optimum incubation period of 24 hours, images were captured using a light microscope (ZEISS, Germany). The obtained images revealed not only a quantitative decrease in cell viability but also qualitative changes in their morphological structures. Additionally, the ability of cancer cells to proliferate by clustering/colonizing, which is a distinctive characteristic of cancer, was observed to be diminished (Figure 7).

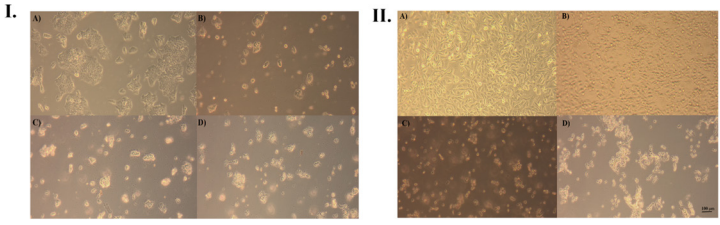

Figure 7. I) Light microscope images of MCF-7 cell line A. Control group B. Ptx (IC_{50}) group C. NaOx (IC_{50}) group D. IKA (IC_{50}) group II) Light microscope images of MDA-MB-231 cell line A. Control group B. Ptx (IC_{50}) group C. NaOx(IC_{50}) group D. IKA (IC_{50}) group (10x).

The inhibition mechanism of Hexokinase 2 (HK-2) was first noticed in cancer treatment in the 1950s[47], leading to research efforts in this area. However, the search for a more potent HK-2 molecule is ongoing, aiming to reduce undesirable effects and improve the patient's quality of life compared to current clinical agents. Sodium Oxamate, especially used in the treatment of breast cancer, ovarian cancer, and small-cell lung cancer, inhibits LDH-A, thereby halting the formation of lactate, the final product of glycolysis in cancer cells. It is also known that Taxol-resistant breast cancer cells can emerge in breast cancer patients. In this context, the unique molecule IKA suggests a potential advantage over Paclitaxel and Sodium Oxamate for cancer treatment[48].

The significance of invasive cancer cells communicating with the tumor microenvironment is that it enables them to overcome environmental challenges, establish themselves, and colonize. In many cases, glucocorticoids are used to treat complications associated with cancer. The progression of breast cancer begins with an increase in stress hormones and glucocorticoid levels, which subsequently activate consecutive glucocorticoid receptors, enhancing cancer colonization and reducing survival rates. This suggests the need for caution when treating cancer patients with glucocorticoid therapy. Beyond this, while cytotoxic chemotherapy has been shown to be effective in breast cancer treatment, it has also exhibited prometastatic effects. Paclitaxel and doxorubicin trigger tumor-derived extracellular vesicle production in chemoresistant breast cancer models. These vesicles facilitate tumor colonization in metastatic sites, particularly in the lungs. Therefore, caution is required when treating cancer patients with glucocorticoid therapy and certain chemotherapy drugs[49,50].

Differences in cell morphology were observed under a light microscope in MDA-MB-231 and MCF-7 cell groups consisting of control and treatment groups, without staining. As shown in Figure 7, pronounced cell retraction and detachment of cells from the cell culture base were observed in all treated cell groups. These changes, which were not observed in control cells and are characteristic of apoptotic cell death, became visible in all treatment groups 24 hours after treatment[51]. Morphological changes were more prominent in experimental groups created with IKA and Ptx drug treatment.

Apart from its role in the coagulation system, tissue factor (TF) plays a crucial role in embryogenesis, wound healing, inflammatory response, tumor growth, metastasis, and angiogenesis. TF is involved in various cellular functions on the surfaces of cells such as endothelial cells and monocytes. Therefore, TF is implicated in the pathophysiology of inflammation, atherogenesis, and carcinogenesis. Studies have shown the co-localization of TF and VEGF in tumor cells. Investigations suggest that abnormal vascular structure is associated with TF, and vascularization during the embryonic period is linked to TF[24-28].

Bozkaya et al. propose that these findings indicate the potential utility of TF and VEGF levels in predicting thromboembolic complications in atherosclerotic diabetic patients.TF and VEGF levels showed significant variations between diabetic and non-diabetic groups ($p<0.001$)[52]. The association between thrombosis and cancer was first noted in 1865 by Professor Armand Trousseau through his observations. Trousseau reported that a significant number of patients with idiopathic venous thromboembolism were subsequently diagnosed with cancer[33].

Another remarkable aspect of our study is that, while the individual effects of HK-2 and TF on tumoral formations were previously known in the cancer mechanism, their direct relationship has not been investigated in the literature before. In one of the studies where TF and HK-2 were examined together, histological analyses were conducted on tissues obtained from autopsies of patients who died due to acute myocardial infarction. The results indicated that the extent of plaque disruption and the expression of TF and HK-2 are crucial vascular factors in the onset of acute myocardial events[53].

Overall, our research sheds light on the potential advantages of IKA in cancer treatment when compared to both Paclitaxel and Sodium Oxamate, and it explores the previously unexplored direct relationship between TF and HK-2 in tumorigenesis, offering novel insights into the mechanisms of vascular factors in disease progression. To further investigate the mechanism of action of breast cancer treatment candidate molecule, IKA, advanced techniques will be employed. The continuation of positive results may lead to preclinical studies, opening the floodgates for in vivo experiments and clinical studies.

STATEMENTS OF ETHICS

This study does not require any ethical permission.

CONFLICT OF INTEREST STATEMENT

The authors declare that there is no conflict of interest regarding the publication and dissemination of the information provided herein.

AUTHOR CONTRIBUTIONS

All authors contributed to the design and implementation of the research, to the analysis of the results, and to the writing of the manuscript.

FUNDING SOURCES

The authors declare that there are no funding sources of interest regarding the publication.

ACKNOWLEDGMENTS

This article is based on the doctoral thesis prepared at Istanbul Medipol University, Institute of Health Sciences, Department of Biochemistry.

REFERENCES

1. Sung H, Ferlay J, Siegel RL, Laversanne M, Soerjomataram I, Jemal A, et. al. Global cancer statistics 2020: GLOBOCAN estimates of incidence and mortality worldwide for 36 cancers in 185 countries. CA Cancer J Clin, 2021;71(3):209-249. Doi: 10.3322/caac.21834

2. Hu Z. Tissue factor as a new target for CAR-NK cell immunotherapy of triple-negative breast cancer. Sci Rep, 2020;10(1):2815. Doi: 10.1038/s41598-020-59736-3

3. Arruebo M, Vilaboa N, Sáez-Gutierrez B, Lambea J, Tres A, Valladares M, et. al. Assessment of the evolution of cancer treatment therapies. Cancers, 2011;3(3):3279-3330. Doi: 10.3390/cancers3033279

4. Guo D, Meng Y, Jiang X, Lu Z. Hexokinases in cancer and other pathologies. Cell Insight, 2023;2(1):100077. Doi: 10.1016/j.cellin.2023.100077

5. Ciscato F, Ferrone L, Masgras I, Laquatra C, Rasola A. Hexokinase 2 in cancer: a prima donna playing multiple characters. Int J Mol Sci, 2021;22(9):4716. Doi: 10.3390/ijms22094716

6. Irwin DM, Tan H. Molecular evolution of the vertebrate hexokinase gene family: identification of a conserved fifth vertebrate hexokinase gene. CBPD, 2008;3(1):96-107. Doi: 10.1016/j.cbd.2007.11.002

7. Huang Y. Targeting glycolysis for cancer therapy using drug delivery systems. J Control Release, 2023;353:650-662. Doi: 10.1016/j.jconrel.2022.12.003

8. Mathupala SP, Ko YA, Pedersen PL. Hexokinase II: cancer's double-edged sword acting as both facilitator and gatekeeper of malignancy when bound to mitochondria. Oncogene, 2006;25(34):4777-4786. Doi: 10.1038/sj.onc.1209603

9. Patra KC, Wang Q, Bhaskar PT, Miller L, Wang Z, Wheaton W, et. al. Hexokinase 2 is required for tumor initiation and maintenance and its systemic deletion is therapeutic in mouse models of cancer. Cancer cell, 2013;24(2):213-228. Doi: 10.1016/j.ccr.2013.06.014

10. Yang T, Ren C, Qiao P, Han X, Wang L, Lv S, et. al. PIM2-mediated phosphorylation of hexokinase 2 is critical for tumor growth and paclitaxel resistance in breast cancer. Oncogene, 2018;37(45):5997-6009. Doi: 10.1038/s41388-018-0386-x

11. Wang J, Pendurthi UR, Rao LVM. Sphingomyelin encrypts tissue factor: ATP-induced activation of A-SMase leads to tissue factor decryption and microvesicle shedding. Blood Adv, 2017;1(13):849-862. Doi: 10.1182/bloodadvances.2016003947

12. Wang J, Pendurthi UR, Rao LVM. Acid sphingomyelinase plays a critical role in LPS- and cytokine-induced tissue factor procoagulant activity. Blood, 2019;134(7):645-655. Doi: 10.1182/blood.2019001400

13. Schaffner F, Ruf W. Tissue factor and PAR2 signaling in the tumor microenvironment. Arterioscler Thromb Vasc Biol, 2009;29(12):1999-2004. Doi: 10.1161/atvbaha.108.177428

14. Ünlü B, Kocatürk B, Rondon AM, Lewis CS, Swier N, Van den Akker RF, et. al. Integrin regulation by tissue factor promotes cancer stemness and metastatic dissemination in breast cancer. Oncogene, 2022;41(48):5176-5185. Doi: 10.1038/s41388-022-02511-7

15. Christofk HR, Vander Heiden MG, Harris MH, Ramanathan A, Gerszten RE, et. al. The M2 splice isoform of pyruvate kinase is important for cancer metabolism and tumour growth. Nature, 2008;452(7184):230-233. Doi: 10.1038/nature06734

16. Otto AM. Warburg effect(s)—a biographical sketch of Otto Warburg and his impacts on tumor metabolism. Cancer Metab, 2016;4(1):1-8. Doi: 10.1186/s40170-016-0145-9

17. Bononi G, Masoni S, Di Bussolo V, Tuccinardi T, Granchi C, Minutolo F. Historical perspective of tumor glycolysis: a century with Otto Warburg. Semin Cancer Biol, 2022;86:325-333. Doi: 10.1016/j.semcancer.2022.07.003

18. Koppenol WH. Bounds PL, Dang CV. Otto Warburg's contributions to current concepts of cancer metabolism. Nat Rev Cancer, 2011;11(5):325-337. Doi: 10.1038/nrc3038

19. Hamanaka RB, Chandel NS. Targeting glucose metabolism for cancer therapy. J Exp Med 2012;209(2):211-215. Doi: 10.1084/jem.20120162

20. Lis P, Dyląg M, Niedźwiecka K, Ko YH, Pedersen PL, Goffeau A, et. al. The HK2 dependent "Warburg effect" and mitochondrial oxidative phosphorylation in cancer: targets for effective therapy with 3-bromopyruvate. Molecules, 2016;21(12):1730. Doi: 10.3390/molecules21121730

21. Romero-Garcia S, Moreno-Altamirano MMB, Prado-Garcia H, Sánchez-García FJ. Lactate contribution to the tumor microenvironment: mechanisms, effects on immune cells and therapeutic relevance. Front Immunol, 2016;7:52. Doi: 10.3389/fimmu.2016.00052

22. Nakashima RA, Paggi MG, Pedersen PL. Contributions of glycolysis and oxidative phosphorylation to adenosine 5-triphosphate production in AS-30D hepatoma cells. Cancer Res, 1984;44:5702-5706.

23. Emekli N. Can tissue factor, a multifactorial molecule of the hemostasis, to be used as a biomarker for thrombosis, inflammation and cancer? Acta Pharm Sci, 2017;3:93-104. Doi: 10.23893/1307-2080.APS.05521

24. Carmeliet P, Mackman N, Moons L, Luther T, Gressens, P. Van Vlaenderen I, et. al. Role of tissue factor in embryonic blood vessel development. Nature, 1996;383:73-75. Doi: 10.1038/383073a0

25. Teomey JR, Kratzer KE, Lasky NM, Stanton JJ, Broze GJ. Targeted disruption of the murine tissue factor gene results in embryonic lethality. Blood, 1996;88:1583-1587. Doi: 10.1182/blood.V88.5.1583.1583

26. Rosen ED, Chan JCY, Idusogie E, Clotman F, Vlasuk G, Luther T, et. al. Mice lacking factor VII develop normally but suffer fatal perinatal bleeding. Nature, 1997;390:290-294. Doi: 10.1038/36862

27. Melis E, Moons L, De Mol M, Herbert JM, Mackman N, Collen D, et al. Targeted deletion of the cytosolic domain of tissue factor in mice does not affect development. Biochem Biophys Res Commun, 1997;286:580-586. Doi: 10.1006/bbrc.2001.5425

28. Mackman N. Role of tissue factor in hemostasis, thrombosis and vascular development. Arterioscler Thromb Vasc Biol, 2004;24:1015-1022. Doi: 10.1161/01.atv.0000130465.23430.74

29. Koizume S, Miyagi Y. Tissue factor in cancer-associated thromboembolism: possible mechanisms and clinical applications. Br J Cancer 127, 2022;2099-2107. Doi: 10.1038/s41416-022-01968-3

30. Schaffner F, Ruf W. Tissue factor and protease-activated receptor signaling in cancer. Semin Thromb Hemost, 2008;34(2):147-153. Doi: 10.1055/s-2008-1079254

31. Ueno T, Toi M, Koike MS, Nakamura S, Tominaga T. Tissue factor expression in breast cancer tissues: its correlation with prognosis and plasma concentration. Br J Cancer, 2000;83:164-170. Doi: 10.1054/bjoc.2000.1272

32. Wojtukiewicz MZ, Hempel D, Sierko E, Tucker SC, Honn KV. Protease-activated receptors (PARs) --biology and role in cancer invasion and metastasis. Cancer Metastasis Rev, 2015;34:775-796. Doi: 10.1007/s10555-015-9599-4

33. Rickles FR, Edwards RL. Activation of blood coagulation in cancer: Trousseau's syndrome revisited. Blood, 1983;62:14-31. Doi: 10.1182/blood.V62.1.14.14

34. Yarat A. Tissue factor and cancer. In: Book of the National Congress of Thrombosis, Hemostasis and Angiology. Istanbul: Tasarım Printing-Advertising Services; 2004. p. 197-203.

35. Shrestha G, St. Clair LL. Lichens: a promising source of antibiotic and anticancer drugs. Phytochem Rev, 2013;12:229-244. Doi: 10.1007/s11101-013-9283-7

36. Yu HL, Jiang SH, Bu XL, Wang JH, Weng JY, Yang XM, et. al. Structural diversity of anti-pancreatic cancer capsimycins identified in mangrove-derived *Streptomyces xiamenensis* 318 and post-modification via a novel cytochrome P450 monooxygenase. Sci Rep, 2017;7(1):40689. Doi: 10.1038/srep40689

37. Saeidnia S, Saeidnia S. Anticancer antibiotics. In: New Approaches to Natural Anticancer Drugs. Cham: Springer; 2015. p. 51-66.

38. Martin RC, Robbins K, Fagés JF, Romero FD, Rustein L, Tomalty D, et. al. Optimal outcomes for liver-dominant metastatic breast cancer with transarterial chemoembolization with drug-eluting beads loaded with doxorubicin. Breast Cancer Res Treat, 2012;132:753-763. Doi: 10.1007/s10549-011-1926-z

39. Li Z, Li Y, Wang X, Liang Y, Luo D, Han D, et. al. LINC01977 promotes breast cancer progression and chemoresistance to doxorubicin by targeting miR-212-3p/GOLM1 axis. Front Oncol, 2021;11:657094. Doi: 10.3389/fonc.2021.657094

40. Jiang SH, Don, FY, Da LT, Yang XM, Wang XX, Weng JY, et. al. Ikarugamycin inhibits pancreatic cancer cell glycolysis by targeting hexokinase 2. The FASEB J, 2020;34(3):3943-3955. Doi: 10.1096/fj.201901237R

41. Yavuz-Dokgöz E, Yigitbasi T. Pterostilben ve laktat dehidrogenaz inhibitörünün kanser hücre hatlarında tümör metabolizmasına etkisinin araştırılması. [Doctoral thesis]. Istanbul Medipol University; 2020. p. 50-55.

42. Van Meerloo J, Kaspers GJ, Cloos J. Cell sensitivity assays: the MTT assay. In: Cancer cell culture: methods and protocols. Totowa (NJ): Humana Press; 2011. p. 237-245.

43. Alturfan AA, Eralp L, Emekli N. Investigation of inflammatory and hemostatic parameters in female patients undergoing total knee arthroplasty surgery. Inflammation, 2008;31:414-421. Doi: 10.1007/s10753-008-9093-z

44. Alturfan A, Eralp L, Tözün R, Emekli N. Primer osteoartrit olgularında plazma ve sinovyal sıvı doku faktörü ve koagülasyon parametrelerinin incelenmesi. CMJ, 2010;32(1):34-39.

45. Wang K, Fan H, Chen Q, Ma G, Zhu M, Zhang X, et. al. Curcumin inhibits aerobic glycolysis and induces mitochondrial-mediated apoptosis through hexokinase II in human colorectal cancer cells *in vitro*. Anti-cancer drugs, 2015;26(1):15-24. Doi: 10.1097/CAD.0000000000000132

46. Dai W, Wang F, Lu J, Xia Y, He L, Chen K, et. al. By reducing hexokinase 2, resveratrol induces apoptosis in HCC cells addicted to aerobic glycolysis and inhibits tumor growth in mice. Oncotarget, 2015;6(15):13703. Doi: 10.18632%2Foncotarget.3800

47. McComb RB and Yushok WD. Properties of particulate hexokinase of the Krebs-2 ascites tumor. Biochim Biophys Acta, 1959;34:515-526. Doi: 10.1016/0006-3002(59)90304-X

48. Zhou M, Zhao Y, Ding Y, Liu H, Liu Z, Fodstad O, et.al. Warburg effect in chemosensitivity: targeting lactate dehydrogenase-a re-sensitizes taxol-resistant cancer cells to taxol. Mol Cancer, 2010;9(1):1-12. Doi: 10.1186/1476-4598-9-33

49. Fares J, Fares MY, Khachfe HH, Salhab HA, Fares Y. Molecular principles of metastasis: a hallmark of cancer revisited. Signal Transduct Target Ther, 2020;5(1):28. Doi: 10.1038/s41392-020-0134-x

50. Obradović MM, Hamelin B, Manevski N, Couto JP, Sethi A, Coissieux MM, et. al. Glucocorticoids promote breast cancer metastasis. Nature, 2019;567(7749):540-544. Doi: 10.1038/s41586-019-1019-4

51. Mgbonyebi OP, Russo J, Russo IH. Roscovitine induces cell death and morphological changes indicative of apoptosis in MDA-MB-231 breast cancer cells. Cancer Res, 1999;59(8):1903-1910.

52. Bozkaya TA, Ateş Ş, Üstündag ÜV, Çakıcı Ç, Keskin İ, Yiğit P, et. al. Tissue factor and vascular endothelial growth factor in detecting thromboembolic complication in diabetic atherosclerotic patients. Clin Med Insights Circ Respir Pulm Med, 2023:17:1-9. Doi: 10.1177/11795484231167737

53. Okuyama N, Matsuda S, Yamashita A, Moriguchi-Goto S, Sameshima N, Iwakiri T, et. al. Human coronary thrombus formation is associated with degree of plaque disruption and expression of tissue factor and hexokinase II. Circ J, 2015;79(11):2430-2438. Doi: 10.1253/circj.CJ-15-039

Acta Pharm. Sci. Vol 63:(1), 2025
Original article
DOI: 10.23893/1307-2080.APS6313

Determination of boron levels in tea samples: A preliminary study

Aslihan CIHAN[1,2], A. Begum OZEL KORLU[1], Burcin ALEV TUZUNER[3,4], Aysen YARAT[5*]

1 Marmara University, Institute of Health Sciences, Department of Biochemistry, Istanbul, Türkiye
2 İbrahim Çecen University, Faculty of Pharmacy, Department of Biochemistry, Agri, Türkiye
3 Istanbul Gelişim University, Faculty of Dentistry, Department of Basic Medical Sciences, Biochemistry, Istanbul, Türkiye
4 Istanbul Gelisim University, Life Sciences and Biomedical Engineering Application and Research Centre, Istanbul, Türkiye
5 Marmara University, Faculty of Dentistry, Department of Basic Medical Sciences, Biochemistry, Maltepe, Istanbul, Türkiye

ABSTRACT

The best sources of boron are fruits, vegetables, drinking tea and water. It is known that insufficient or toxic levels of boron intake may lead to disruptions in various metabolic pathways. Hence the increase of tea consumption in Türkiye more than other countries day by day, the boron intake from tea has become important too. This study aimed to determine the amount of boron in the most consumed teas in Türkiye and its health impact. Black bulk and bagged tea samples were used. All teas were pulverized to a certain size. Then, the teas were brewed under certain conditions and centrifuged. The boron content in pulverized and brewed tea samples was determined by the carminic acid method. The average boron level in dried tea samples was 10 ppm, while in brewed tea samples it was about 3.3 ppm. The boron levels transferred to the brewed tea sample decreased by approximately 3-4 times to around 30%. In conclusion, considering the daily upper limit level, our research supports the safety of tea consumption in terms of boron levels. It also helps fulfill our boron intake without surpassing the daily upper limit, thereby maintaining homeostasis and potentially helping with many health problems.

Keywords: boron, black tea, brewed tea, health, Türkiye

*Corresponding author: Aysen YARAT
E-mail: ayarat@marmara.edu.tr
ORCIDs:
Aslihan CIHAN: 0000-0003-1923-0108
Armagan Begum OZEL KORLU: 0000-0002-4197-3103
Burcin ALEV TUZUNER: 0000-0001-5122-4977
Aysen YARAT: 0000-0002-8258-6118
(Received 23 Feb 2024, Accepted 18 Apr 2024)

INTRODUCTION

Tea is obtained by processing the buds and the upper two leaves as much as possible of the green-leafed *Camellia sinensis* (L.), belonging to the Theaceae family, plant with various methods. It turns into a commercial beverage through fermentation[1]. Unfermented tea is green tea, semi-fermented tea is oolong tea, and fully fermented tea is black tea[2]. Another type of tea is white tea, which is produced by being protected from oxidation, but differently contains a high amount of bud leaves[3]. The most produced tea type worldwide is black tea, with a share of 78%[4]. During the fermentation step, polyphenol compounds found in fresh black tea leaves undergo various hydrolysis, oxidation, transformation and polymerization reactions and transform into theaflavins and thearubigens that give black tea its color[5,6]. Apart from polyphenol oxidase, which provides taste and color formation, the activities of many enzymes such as alcohol dehydrogenase enzyme, which provides the formation of some alcohols that contribute to aroma, transaminase enzyme, which provides the transformation of amino acids and the formation of terpenes, pectinase enzyme, which provides the breakdown of pectin substances, and peptidase enzyme, which provides the hydrolysis of proteins, play important roles in shaping the characteristic properties of black tea[7].

In Türkiye, tea is traditionally consumed widely at breakfast, after meals, in social environments, when hosting guests, during picnics, celebrations, evening conversations, and many other occasions. As a result, Türkiye surpasses other countries in terms of worldwide tea consumption. Consumption of tea bags and cup tea bags instead of bulk tea brewed in a teapot is becoming more common because it is more practical[8,9]. Although the teas in bulk tea and tea bags go through the same processes, they are different in terms of quality because they pass through different sieves just before packaging[10].

Tea content is quite complex, with more than 2000 chemical components, and even among the same type of tea, different content can be observed depending on soil structure, climate characteristics, and storage conditions[11]. The amount of water in the dry form of fresh tea leaves, which contain approximately 25% water when fresh, is approximately 5%. Other components mainly include phenolic compounds, flavonols, amino acids + proteins, caffeine, simple carbohydrates, polysaccharides, and minerals.

Boron is an essential element for plants as it plays an important role in the growth and development of plant cells, the synthesis of the cell wall and the continuity of its structure, the transport of necessary ions and various metabolites through membranes, and various enzymatic reactions[12]. Boric acid, which

can dissolve very well in the acidic soil where tea grows with the contribution of rain, is the main source of boron in tea. Thanks to its high membrane permeability, boric acid infiltrates the roots and reaches the uppermost leaves[13]. It is known that as the acidity of tea soil increases, the amount of boron absorbed by the roots increases. Boron fertilizers, which are known to have a positive effect on the growth of tea, and boron drugs used to prevent pest formation are unnatural boron sources of tea[14,15].

There is an increase in tea consumption in Türkiye compared to other countries, making the amount of boron taken with tea important. Therefore, this study aimed to determine the amount of boron in teas consumed most in Türkiye and its health impact.

METHODOLOGY

Chemicals

The chemicals used in this study were of analytical grade and were obtained from Merck (Darmstadt, Germany), Sigma-Aldrich (St. Louis, MO, USA) and Fluka (Buchs, Switzerland) companies.

Tea samples

The seventeen (six black bulk and eleven black bagged teas) frequently consumed teas were purchased from large markets with high sales circulation, and their packages were checked. The quantities to be used were separated and numbered. Then, the tea samples were ground into powder using a blender. They were labeled.

Modified carminic acid method

The modified carminic acid method was used to determine the boron concentration[16,17]. Carminic acid and concentrated sulfuric acid were used to prepare the carmine solution (0,4 mM). Boric acid was used to prepare boron standard solutions (1-10 ppm). All solutions were freshly prepared. In this method, the absorbance at 585 nm of the colored complex formed as a result of the reaction between boron and carminic acid in a sulfuric acid medium was measured. The boron concentration in the sample was determined using the boron standard curve. The lowest boron concentration that could be measured with this method was 0.25 ppm.

Boron determination in dry and brewed tea samples

A dry tea sample (0.125 g) was placed into porcelain crucibles. Due to the high volatility of boron at low pH values, sodium hydroxide (100 µL, 1 M) was added and the mixture was left to dry in an oven overnight at 85°C. The dried sample

was then burned in an ashing furnace at 550°C for 4 h. After cooling in a desiccator, the sample was acidified with hydrochloric acid (0.4 mL, 6 M). Then it was diluted with distilled water to 1 mL and centrifuged at 4000 rpm for 10 min. The supernatant was used for the carminic acid assay. Concentrated HCl (10 µL), concentrated H_2SO_4 (1 mL), and carmine solution (1 mL, 0,4 mM) were added to supernatant (0.2 mL) and to water blank (0.2 mL), respectively, and mixed. After incubation for 45 min at room temperature, the absorbance was measured at 585 nm wavelength in a spectrophotometer (Rayleigh-UV-1800). Measurements were repeated for two times.

To determine the amount of boron in brewed teas, each powdered tea sample was weighed 0.5 g and brewed with 50 mL of hot water for 20 minutes. After 20 minutes, the liquid portion was immediately separated from the tea and centrifuged at 4000 rpm for 10 minutes. Supernatants were aliquoted and stored in the deep freezer (at −20°C). The amount of boron in the supernatants was determined using the carminic acid method as described for dried tea samples in the paragraph above. However, this time a sample blank was used instead of a water blank. To prepare a sample blank, concentrated HCl (10 µL) and concentrated H_2SO_4 (2 mL) were added to the supernatant (0.2 mL). Carminic acid was not added.

Statistical analysis

The results were statistically evaluated using via GraphPad Prism 9.0. The values were expressed as means ± standard deviation. The Mann Whitney test was used for pairwise comparisons. A $p<0.05$ was considered statistically significant.

RESULTS and DISCUSSION

The main sources of boron in the human body include drinking water, tea, mineral water and food. Additionally, various industrial products such as antiseptics, preservatives, some drugs containing boron due to its plasticizer or flame retardant properties, cosmetic products, detergents, pesticides, adhesives, and carpets also contribute to boron intake. Results obtained from studies suggest that boron, as a dynamic trace element, affects a broad range of biological functions[18]. This emphasizes the necessity of determining boron levels in biological samples, particularly those relevant to human nutrition.

Although the metabolism of boron is not yet fully understood, it is thought to be absorbed entirely by the human body through the digestive system and can also be absorbed through the respiratory tract and skin contact.

Boron can accumulate in various organs and tissues of the human body at different rates. It is reported that boron, found at levels of 3-20 mg in the body, accumulates mostly in the heart (28 ppm), followed by the bones (4.3-17.9 ppm) and liver (2.3 ppm). Although daily boron intake varies by country, it is generally considered to be 1-3 mg[19,20].

In the present study, the average amount of boron in dried tea samples was found to be 10.21 and 13.06 ppm for black bulk tea and black bag tea, respectively. There was a significant difference between the boron amount ($p<0.05$) (Table 1). However, this significant difference may not be meaningful due to the use of black teas from different brands.

Table 1. Comparison of boron contents of black bulk and bagged teas

Boron (ppm)	Black bulk tea (n=6)	Black bagged tea (n=11)	p
Mean	10.21	13.06	<0.05 Mann Whitney test
Standard Deviation	0.80	3.66	

No significant difference was detected between the amount of boron in brewed black bulk and brewed bagged teas ($p>0.05$, Table 2)

Table 2. Comparison of boron contents of brewed black bulk and bagged teas

Brewed Tea Boron (ppm)	Black bulk tea (n=6)	Black bagged tea (n=11)	p
Mean	3.29	3.26	>0.05 Mann Whitney test
Standard Deviation	0.88	0.86	

The amount of boron in the brewed tea samples was about 3.3 ppm. The amount of boron transferred to the brewed tea sample decreased by approximately 3-4 times to around 30%.

In a study, boron concentrations have been determined in water-soluble and acid-soluble fractions in black teas and fruit teas available on the Polish Market using inductively coupled plasma-atomic emission spectrometry. The potential human health risk has been investigated. The mean total content of boron ranged from 8.31 to 18.40 mg/kg (ppm) in black teas. The degree of extraction of boron in black tea ranged from 8% to 27%. It has been concluded that it may not produce any health risks for human consumption, if other sources of metal contaminated food are not taken at the same time. The findings of Frankowska's

study were similar to this study[21]. The difference between this study and theirs was the method. They used the ICP method, while we used the spectrophotometric method (carminic acid method). However, the boron concentrations determined by ICP and by the carminic acid method were correlated with each other[16].

The boron level of black tea found in our study was similar to the boron concentration mentioned as between 3.10–57.8 ppm in a review of surveyed the elemental analysis of teas[22]. It was also similar to the boron concentration mentioned in another review article about micronutrients (B, Co, Cu, Fe, Mn, Mo, and Zn) content in made tea and tea infusion[23].

In the study examining the mineral nutrient composition of tea plants harvested at different shoot periods, changes in the composition of many elements, including boron, and their relationship with soil properties were examined. It was found that the boron content in tea leaves varied between 10.63-31.58 ppm[24]. Our results are consistent with the findings of this research.

In a study conducted in Türkiye, the boron concentrations in brewed teas (black tea, chamomile tea, apple tea, rosehip tea, sage tea, linden tea, and green tea produced by Lipton) have been determined using Optical Emission Spectroscopy. The boron content in the tea infusions after five minutes have been varied between 0.084 and 2.023 ppm[25]. This amount was lower than our results for brewed teas. The variation in infusion time, 20 minutes in our study and 5 minutes in theirs, could explain this difference.

Other factors that affect boron intake include age, gender, and metabolic rate. Considering these factors, the daily boron intake recommended by the European Food Safety Authority (EFSA) is as follows: 3 mg for ages 1-3; 4 mg for 4-6 years old; 5 mg for ages 7-10; 7 mg for ages 11-14; 9 mg for ages 15-17; and 10 mg for adults. According to the World Health Organization (WHO), although the safe dose range for adults was defined as 1-13 mg boron/day, this value has been revised to 28 mg boron/day for an adult weighing 70 kg. These calculations change over the years according to countries and organizations, and as a result, they have an impact on the limits imposed on the amount of boron in drinking water, tea and mineral water[26,27,28]. Assuming an individual consumes five glasses of tea (500 mL) daily, the average daily boron intake from bulk or brewed tea is 5.25 mg or 1.75 mg, respectively.

In conclusion, when considering the daily upper limit level, our research supports the safety of tea consumption in terms of boron levels. It also helps fulfill our boron intake requirements without surpassing the daily upper limit. Therefore, it has the potential to contribute to the maintenance of homeostasis and the prevention and treatment of many diseases.

STATEMENT OF ETHICS

This study does not require any ethical approval.

CONFLICT OF INTEREST STATEMENT

The authors declare no conflict of interest.

AUTHOR CONTRIBUTIONS

Design: AY, BAT. Acquisition of Data: AC, ABOK, BAT. Analysis of Data: AC, AY. Drafting of the Manuscript: AC, ABOK, BAT, AY. Critical Revision of the Manuscript: AC, ABOK, BAT, AY. Statistical Analysis: AY. Supervision: AY.

FUNDING SOURCES

No funding or other financial support was received.

ACKNOWLEDGMENTS

Not applicable.

REFERENCES

1. Öz G. Türk çayından üretilen farklı oksidasyon derecelerine sahip oolong çayların bazı fiziksel, kimyasal ve duyusal özelliklerinin belirlenmesi. [Master's Thesis]. Antalya: Akdeniz University; 2021.

2. Ağca CA. Anadolu kaynaklı Camellia sinensis (L.) O.Kuntze bitkisi üzerinde farmakognozik çalışmalar. [Doctoral Thesis]. Ankara; Ankara University; 2007.

3. Demirbaş M. Farklı işleme yöntemlerinin beyaz çay (Camellia sinensis L.) kalitesi üzerine etkisi. [Doctoral Thesis]. Erzurum: Atatürk University; 2020.

4. Akbulut A, Kara ŞM, Özcan A. Siyah, yeşil ve beyaz çayların kalite kriterleri, mineral içerikleri, antioksidan ve antimicrobial aktivite yönünden karşılaştırılması. Akademik Ziraat Dergisi, 2020;9(2):279-288. Doi: 10.29278/azd.720699

5. Acar S. Şanlıurfa'da tüketilen siyah çay çeşitlerinin ağır metal içeriklerinin saptanması. [Master's Thesis]. Sanliurfa: Harran University; 2019.

6. Lee LS, Kim YC, Park JD, Kim YB, Kim SH. Changes in major polyphenolic compounds of tea (*Camellia sinensis*) leaves during the production of black tea. Food Sci Biotechnol, 2016;25(6):1523-1527. Doi: 10.1007/s10068-016-0236-y

7. Balaban OT. Siyah çay üretiminde ayın bazı fizikokimyasal ve biyoaktif özelliklerinin araştırılması. [Master's Thesis]. Bayburt: Bayburt University; 2019.

8. Güneş S. Türk çay kültürü ve ürünleri. Milli Folklor Dergisi, 2012;12(93):234-251.

9. Mendi AF. Türkiye çay endüstrisi: sektörel ve ampirik bir çalışma. IJSSER, 2018; 4(2):252-274. Doi: 10.24289/ijsser.413420

10. Tufanoğlu E. Türkiye'de çay üretimi, tüketimi ve sorunları. [Master's Thesis]. Giresun: Giresun University; 2017.

11. Hajiboland R. Environmental and nutritional requirements for tea cultivation. Folia Hort, 2017; 29(2):199-220. Doi: 10.1515/fhort-2017-0019

12. Brdar-Jokanović M. Boron toxicity and deficiency in agricultural plants. Int J Mol Sci, 2020; 21(4):1424. Doi: 10.3390/ijms21041424

13. Hajiboland R, Bahrami-Rad S, Bastani S, Tolrà R, Poschenrieder C. Boron re-translocation in tea (*Camellia sinensis* (L.) O. Kuntze) plants. Acta Physiol Plant, 2013;35(8):2373-2381. Doi: 10.1007/s11738-013-1272-3

14. Balci M, Taban S. Effect of boron treatments on boron distribution and fresh leaf yield of the tea plant. Int J Agric Environ Food Sci, 2018;2(3):74-81. Doi: 10.31015/jaefs.18012

15. Baruah BK, Haque A, Das B, Medhi C, Misra AK. Boron in soil and water samples in some tea garden belt of Golaghat district, Assam. Adv Appl Sci Res, 2011; 2(4):298-305.

16. Kuru R, Yilmaz S, Tasli PN, Yarat A, Sahin F. Boron content of some foods consumed in Istanbul, Turkey. Biol Trace Elem Res, 2019; 187(1):1-8. Doi: 10.1007/s12011-018-1319-9

17. Hatcher JT, Wilcox LV. Colorimetric determination of boron using carmine. Anal Chem, 1950; 22(4):567-569. Doi: 10.1021/ac60040a017

18. Kuru R, Yarat A. Bor ve sağlığımıza olan etkilerine güncel bir bakış. Clin Exp Health Sci, 2017; 7(3):107-114.

19. Bakirdere S, Orenay-Boyacioglu S, Korkmaz M. Effect of boron on human health. The Open Miner Process J, 2010;3:54-59. Doi: 10.2174/1874841401003010054

20. Dinca L, Scorei R. Boron in human nutrition and its regulations use. J Nutr Ther, 2013;2:22-29. Doi: 10.6000/1929-5634.2013.02.01.3

21. Ziola-Frankowska A, Frankowski M, Novotny K, Kanicky V. Comparison of the level of boron concentrations in black teas with fruit teas available on the Polish market. The Scientific World J, 2014; 2014:898425. Doi: 10.1155/2014/898425

22. Szymczycha-Madeja A, Welna M, Pohl P. Elemental analysis of teas and their infusions by spectrometric methods. Trends Anal Chem, 2012; 35:165-181. Doi: 10.1016/j.trac.2011.12.005

23. Karak T, Kutu FR, Natha JR, Sonar I, Paul RK, Boruah RK, et al. Micronutrients (B, Co, Cu, Fe, Mn, Mo, and Zn) content in made tea (*Camellia sinensis* L.) and tea infusion with health prospect: a critical review. Crit Rev Food Sci Nutr, 2017;57(14):2996-3034. Doi: 10.1080/10408398.2015.1083534

24. Kaya H. Farklı sürgün dönemlerinde hasat edilen çay bitkisinin mineral besin komposizyonu. [Master's Thesis]. Samsun: Ondokuz Mayıs University; 2019.

25. Moroydor Derun E, Kipcak AS, Dere Ozdemir O. The determination of the boron amounts of teas that are sold in Turkey by using the ICP-OES technique. In: Proceedings of the World Congress on Engineering; 2010; London, UK. Vol III. Hong Kong: IAENG; 2010. p. 2277-2279.

26. Kuru R, Kurt Mutlu E, Cempel E, Belentepe Celik S, Yarat A. Evaluation of dietary boron in terms of health: a retrospective study. Clin Exp Health Sci, 2018; 8:296-300.

27. World Health Organization, International Atomic Energy Agency, Food and Agriculture Organization of the United Nations. Boron. In: Trace elements in human nutrition and health. Geneva: World Health Organization; 1996. Chapter 13.

28. Meacham S, Karakas S, Wallace A, Altun F. Boron in human health: evidence for dietary recommendations and public policies. The Open Miner Process J, 2010;3:36-53. Doi: 10.2174/1874841401003010036

Acta Pharm. Sci. Vol 63:(1), 2025
Original article
DOI: 10.23893/1307-2080.APS6314

The relationship between digital financial literacy and financial behaviors of pharmacy faculty students: A comprehensive evaluation through structural equation model

Mustafa ÖZYEŞİL[1*], Havane TEMBELO[2]

1 Istanbul Beykent University, International Trade and Finance (Eng) Department, Istanbul, Türkiye

2 Ministry of Health of the Republic of Türkiye, Istanbul Provincial Health Directorate, Training and Registration Unit, Istanbul, Türkiye

ABSTRACT

This study aims to assess the relationship between financial literacy levels and digital financial skills among pharmacy faculty students. Conducted with students from pharmacy faculties in Istanbul, the research utilizes a dataset comprising factors like demographic characteristics, financial conditions, and digital financial literacy levels. The analysis, employing Structural Equation Modeling, elucidates the connections between financial literacy and digital financial skills. Significant correlations have been identified between young adults' financial behaviors and digital financial attitudes. This research contributes to the broader understanding of financial literacy, particularly underscoring the interplay between traditional financial literacy and digital financial literacy. The findings reveal notable correlations and contradictions with existing literature in the domain of financial literacy, as related to digital financial literacy and pharmacy students' financial behaviors. The multifaceted nature of financial literacy, especially in the context of intertwining traditional and digital aspects, has been expanded upon in this study.

Keywords: financial literacy, digital financial literacy, pharmacy student, behavior

*Corresponding author: Mustafa ÖZYEŞİL
E-mail: mustafaozyesil@beykent.edu.tr
ORCIDs:
Mustafa ÖZYEŞİL: 0000-0002-4442-7087
Havane TEMBELO: 0000-0003-3394-4166
(Received 20 Feb 2024, Accepted 24 Apr 2024)

INTRODUCTION

In today's world, making financial decisions and increasing financial well-being have significant impacts on individuals' lives. Young adults are at a critical stage in gaining financial independence and achieving future financial goals. Financial literacy is an important tool for individuals to make informed and effective financial decisions during this process. However, the level of financial literacy among young adults and its relationship with digital financial skills are still not fully understood.

Financial literacy includes more than one dimension; the focus is on the knowledge itself as well as the ability to acquire and use knowledge[1]. Digital literacy can be defined as using the digital technologies that come into our lives and are presented to us.

The competence to use the mentioned technologies together with the knowledge to find, create, evaluate and communicate, the use of effective technological possibilities, therefore requires both cognitive knowledge and technical skills as prerequisites for the use of technology[2]. While the Organization for Economic Co-operation and Development (OECD, 2018) defines this concept in various ways, various aspects of digital financial literacy include information about digital financial products and services, awareness of digital financial risks, and consumer rights and enforcement procedures. The multiplicity and importance of these definitions show the depth of the concept. Since all concepts require knowledge and conceptual literacy is required to use them effectively. Due to the prevalence and impact of financial know-how use, the financial services sector is trying to expand its existing financial literacy programs by taking advantage of the opportunities. Global economic investments increased rapidly in this area from 2017 to 2018. The approximate amount of investment in this field has increased from 12 billion US dollars to over 50 billion US dollars. There is a constant expansion of the scope mentioned in the studies conducted by Collins and Urban[3]. Financial know-how will become more responsible for individuals' economic well-being over time. Increasing these opportunities also has an increasing effect on perceived financial well-being. Financial well-being can be defined as: the conditions a person can face are the ability to meet their financial obligations and have a positive financial forecast for the future[3]. In this context, financial literacy and digital financial literacy, which are associated with financial well-being, are increasingly the subject of comprehensive research.

Although it has many different definitions, financial literacy is, in summary, considered as having some basic financial information and the ability to use this information to be successful in making the right financial decisions[4]. Today, the rapid development of communication technologies has caused financial instruments to enter our lives from many different points. People who have a certain level of financial literacy can utilize these opportunities more efficiently in terms of profitability and efficiency in economic activities. Today, at the level of financial literacy they have, it is essential to carry out financial transactions using complex and unconventional information that considers the developing and changing environmental conditions other than classical knowledge and practices. The concept of financial literacy has gained new dimensions with digitalization, and studies have shown that people are more successful as a result of having sufficient knowledge when applying financial information transactions[5]. When the literature is reviewed about the concept of financial literacy and digital financial literacy, it is stated that the concept of finance and digitalization is basically shaped around three elements: fintech, financial behavior in digital media and behavioral interventions. Fintech, one of these elements, in its most general definition, is the combination of technology and finance in order to provide financial services faster, better and easier. In other words, with the technology, financial services can be made more user friendly, and consumers can access financial services in new and different ways. The rapid increase in mobile applications and the widespread use of the internet are among the factors that have created Fintech in recent times. That's why consumers now expect to access fast, user-friendly and entertaining financial services that they can easily access from any point. In order to meet all these expectations, competition and studies in this field are increasing day by day in our country as well as in the whole world. Although the Turkish fintech field is a competitive environment, it is also an environmental system where new working and collaboration opportunities are found. An example of this is the implementation of the digital wallet project in Türkiye in 2012, with all banks and leading e-commerce companies working together[6]. In addition, some applications are put into effect in order to gain financial literacy skills and the necessary awareness in this sense. Applications located at the intersection of financial literacy and technology skills can help children and young people to acquire this awareness and parents who aim to teach children and young people savings and money management and saving. While the mentioned applications are being implemented one by one by banks or entrepreneurs, the opportunities offered by digital environments are used very efficiently in the context of creating a more conscious consumer base compared to others[7].

Today, it is possible for individuals to access digital communication and information resources, identify, manage and evaluate the resources through the technologies used for communication purposes and the application tools developed accordingly. In addition, information needs to be analyzed, synthesized and integrated with existing and new information. Apart from this, the phenomenon defined as the awareness, attitude and ability to use digital tools and digital environments appropriately in order to create new information, create expression in media channels and communicate with others, constitutes the broad framework of digital literacy[8]. When we evaluate the concept of digital literacy together with financial literacy, we see that individuals under the age of 18 have knowledge of money, budget, finance, etc. It is thought that it is necessary to develop the ability to use digital tools and related environments for virtual environment transactions by gaining the awareness of being able to act cautiously on issues. In this context, the concept of financial literacy emerges with its evolving dimension into digital processes and is offered with different models and applications[8].

The main aim of the study is to assess students' levels of financial literacy and digital financial skills, identify their strengths and weaknesses in these areas, and develop recommendations for financial literacy education programs. The methodology of the analysis focuses on revealing the relationships between financial literacy and digital financial skills using confirmatory factor analysis.

METHODOLOGY

This study was conducted to understand the level of financial literacy and its relationship with digital financial skills among students in pharmacy faculties at universities in Istanbul. The study focuses on providing an in-depth analysis of the demographic characteristics, financial situations, digital financial literacy levels, and financial behaviors of pharmacy students. In this context, the dataset used in the analysis includes demographic and financial characteristics of participants such as gender, age, type of university, class, credit card usage, and internet banking habits.

The flow of the study initially examines the demographic characteristics of the participants, followed by addressing their financial situations and spending habits. Subsequently, confirmatory factor analysis is conducted to measure financial literacy and digital financial literacy levels. The results have helped us understand the relationships between financial behaviors and digital financial attitudes of pharmacy faculty students.

In the analysis part of the study, the data set was evaluated through Structural Equation Model. The research model was created and after the consistency of the fit indices was determined, the relationships between the sub-dimensions of financial knowledge, financial attitude, financial behavior, digital financial attitude and digital financial behavior suggested by the model were analyzed.

Research type

This study is a comprehensive evaluation exploring the relationship between financial literacy levels and digital financial skills among pharmacy students. It adopts a correlational research design to analyze the interplay between financial behaviors and digital financial attitudes, using the Structural Equation Model for detailed analysis.

Data collection technique

The methodology employed involves an online survey to gather data. The survey is designed on a five-point Likert scale, with options ranging from "Strongly Disagree" to "Strongly Agree." It aims to assess participants' demographic information, financial situation, digital financial literacy, and financial behavior. The survey incorporates the Financial Literacy and Digitalization Scale developed by Kaya and Kılıç[9].

Research universe

The research universe encompasses pharmacy faculty students from various universities in Istanbul. The study provides a detailed analysis of these students' demographic characteristics, financial situations, and levels of digital financial literacy. The study delves into factors such as gender, age, university type, grade, credit card usage, and internet banking habits, offering insight into the diverse backgrounds of the participants.

Dataset and sample structure

The sample size of the study is 600 participants, predominantly female, and primarily aged 21 and under. The participants are students from different age groups, genders, university types, and academic years within pharmacy faculties. The study includes a detailed demographic distribution of participants, covering aspects such as household income levels and monthly expenses, further enhancing the understanding of the study's population.

The participants of this study are a sample of 600 students from the faculty of pharmacy of universities in Istanbul. Participants were selected from different age groups, genders, university types and grades. The data collection process

was carried out through online surveys. The survey form was prepared in a five-point Likert type as “Strongly Disagree” (1), “Disagree” (2), “Undecided” (3), “Agree” (4) and “Strongly Agree” (5). The survey forms were specifically designed to assess participants’ demographic information, financial situation, digital financial literacy, and financial behavior. Kaya and Kılıç developed the financial literacy and digitalization scale and in this research this scale was used[9].

The collected data were analyzed using statistical techniques such as descriptive statistics, correlation analyses, independent samples t-test, and analysis of variance (ANOVA). SPSS and R statistical software were used for statistical analysis. Data analysis was carried out in two stages. First, the validity of the scales was evaluated using confirmatory factor analysis. Then, the obtained data was analyzed using statistical methods. Correlation analysis was used to examine the relationships between financial knowledge, attitudes and behavior and digital financial attitudes and behavior.

RESULTS and DISCUSSION

From a total population of 1,000 people, 600 people were reached and all of them completed the survey. There is no missing data. The survey form included variables determined to measure the digital financial literacy level of the participants. These dimensions include Financial Knowledge, Financial Attitude, Financial Behavior, Digital Financial Attitude, Digital Financial Behavior.

When the distribution of participants by gender is examined, the rate of women is 82.7% and the rate of men is 17.3%. The rate of those between the ages of 18 and 21 is approximately 73%, and the rate of those over 21 is 27%. When the distribution by university type is examined, the rate of those studying at a public university is 24.5% and the rate of those studying at a foundation university is 75.5%. The rate of first graders is 36%, the rate of second graders is 30.8%, the rate of third graders is 10.8%, the rate of fourth graders is 14.8%, and the rate of fifth graders is 7.5%. 57.7% of the participants use credit cards. It was observed that 92.5% of the participants used internet banking. Table 1 shows the demographic characteristics and distribution of the sample group.

Table 1. Demographic distribution table

		n	%
Gender	Female	496	82.7
	Male	104	17.3
	Total	600	100.0
Age	18	122	20.3
	19	92	15.3
	20	149	24.8
	21	75	12.5
	21+	162	27.0
	Total	600	100.0
University Type	Public	147	24.5
	Private	453	75.5
	Total	600	100.0
Grade	1	216	36.0
	2	185	30.8
	3	65	10.8
	4	89	14.8
	5	45	7.5
	Total	600	100.0
Credit Card Usage	Yes	346	57.7
	No	254	42.3
	Total	600	100.0
Internet Banking Usage	Yes	555	92.5
	No	45	7.5
	Total	600	100.0

When the family monthly income distribution is examined, the rate of those whose income is less than 12,000 Turkish Lira (TL) is 13.7%, 12,000-16,999 TL is 19.8%, 17,000-21,999 TL is 16.7%, and the rate of those whose income is 22,000-26,999 TL is 9.2%. The rate of those with 27,000-31,999 TL is 9.3%, with 32,000-36,999 TL is 7.3%, with 37,000-41,999 TL is 7.2%, with 42,000-46,999 TL is 3%, with 47,000-51,999 TL is 2.8%, with income of 52,000 TL and above is 11%. The rate of those who spend 3,000-4,999 TL is 64%, 5,000-6,999 TL is 13.3%, 7,000-8,999 TL is 4.3%, 9,000-10,999 TL is 6%, 11,000 TL and more is 12.3%. When the distribution of sources where participants follow financial developments is examined, it is seen that the internet takes the lead. 94.7 % of the participants use the internet, 2.2% use

TV, and the remaining 0.7% use books, magazines, newspapers, etc. While using other resources, the rate of those using other resources is 2.5%. It is seen that the family ranks first with 64.8% in the distribution of resources acquired financial behavior towards spending money. It is followed by the social environment in second place with 16.7% and the school in third place with 6%. The rate of other sources is 11.2%. Table 2 shows the distribution of income levels of the sample group.

Table 2. Distribution table by income status

		n	%
Household Income	Less than 12,000 TL	82	13.7
	12,000-16,999 TL	119	19.8
	17,000-21,999 TL	100	16.7
	22,000-26,999 TL	55	9.2
	27,000-31,999 TL	56	9.3
	32,000-36,999 TL	44	7.3
	37,000-41,999 TL	43	7.2
	42,000-46,999 TL	18	3.0
	47,000-51,999 TL	17	2.8
	52,000 TL and above	66	11.0
	Total	600	100.0
Monthly Expenses	3,000-4,999 TL	384	64.0
	5,000-6,999 TL	80	13.3
	7,000-8,999 TL	26	4.3
	9,000-10,999 TL	36	6.0
	11,000 TL and above	74	12.3
	Total	600	100.0
What is the financial terminal where you follow financial developments?	Internet	568	94.7
	TV	13	2.2
	Book, Journal, Magazine etc.	4	0.7
	Other	15	2.5
	Total	600	100.0
What is the source from which you acquired the financial behavior of spending money?	Family	389	64.8
	Social Environment	100	16.7
	School	36	6.0
	Journal, Book etc.	8	1.3
	Other	67	11.2
	Total	600	100.0

Structural equation model

It was examined with Structural Equation Model to determine the validity of the financial literacy and digitalization scale. The ratio of chi-square statistics to degrees of freedom obtained for model fit indices, root mean square error of approximation (RMSEA), Tucker-Lewis index (TLI) value and comparative fit index values were examined[10]. A model's comparative fit index (CFI) and Tucker-Lewis index (TLI) values of 0.90 or above mean that it has a good fit. The fit indices calculated for the scales are given in the table below. When the model fit indices were examined, it was seen that the model had a good fit. Table 3 reflects the fit indices of the model used in the research.

Table 3. Model fit indices table

Acceptable Fit Indices	Calculated Fit Indices
$\chi 2$/sd. <5	3.268
GFI>0.90	0.932
AGFI>0.90	0.921
CFI>0.90	0.901
TLI>0.90	0.927
RMSEA<0.08	0.079
RMR<0.08	0.076

The model fit indices in Table 3 are based on widely accepted standard threshold values in structural equation modeling[11,12,13]. Values greater than 0.95 for the Comparative Fit Index (CFI) and Tucker-Lewis Index (TLI) as indicative of a good fit, and values less than 0.06 for the Root Mean Square Error of Approximation (RMSEA) as indicative of a close fit[11,12]. Provide more detailed recommendations for these indices, and[13] offers a comprehensive overview of model fit assessment in SEM, including a discussion of various fit indices and their acceptable thresholds. Table 4 of coefficients of the research model is given below.

Table 4. Model coefficients table

			Coefficients	Std. Coefficients	S.E.	C.R.	P
s5	<---	Financial Knowledge	1	0.626			
s4	<---	Financial Knowledge	1.24	0.752	0.087	14.323	<0.001
s3	<---	Financial Knowledge	1.449	0.73	0.103	14.038	<0.001
s2	<---	Financial Knowledge	1.41	0.763	0.097	14.461	<0.001
s1	<---	Financial Knowledge	1.165	0.698	0.086	13.604	<0.001
s14	<---	Financial Attitude	1	0.679			
s13	<---	Financial Attitude	0.806	0.71	0.052	15.522	<0.001
s11	<---	Financial Attitude	0.999	0.715	0,064	15,62	<0.001
s10	<---	Financial Attitude	1.105	0.7	0.072	15.328	<0.001
s9	<---	Financial Attitude	0.984	0.739	0.061	16.072	<0.001
s8	<---	Financial Attitude	0.839	0.655	0.058	14.437	<0.001
s7	<---	Financial Attitude	0.958	0.606	0.071	13.453	<0.001
s6	<---	Financial Attitude	0.881	0.579	0.068	12.891	<0.001
s20	<---	Financial Behavior	1	0.484			
s19	<---	Financial Behavior	1.591	0.601	0.16	9.952	<0.001
s18	<---	Financial Behavior	1.69	0.614	0.168	10.07	<0.001
s17	<---	Financial Behavior	1.592	0.774	0.142	11.18	<0.001
s16	<---	Financial Behavior	1.397	0.549	0.148	9.466	<0.001
s15	<---	Financial Behavior	1.312	0.621	0.13	10.125	<0.001
s29	<---	Digital Financial Attitude	1	0.544			

s30	<---	Digital Financial Attitude	0.962	0.505	0.101	9.513	<0.001
s33	<---	Digital Financial Attitude	1.284	0.804	0.104	12.38	<0.001
s34	<---	Digital Financial Attitude	1.034	0.488	0.111	9.277	<0.001
s35	<---	Digital Financial Attitude	1.182	0.644	0.106	11.154	<0.001
s22	<---	Digital Financial Behavior	1	0.355			
s23	<---	Digital Financial Behavior	1.19	0.677	0.153	7.788	<0.001
s24	<---	Digital Financial Behavior	1.187	0.664	0.153	7.746	<0.001
s32	<---	Digital Financial Behavior	1.131	0.705	0.144	7.864	<0.001

When the coefficients of the items in the model were examined, it was seen that all of them were significant. When the levels of the coefficients were examined, it was seen that all item sub-dimension correlations were high, so no items needed to be removed from the model. Figure 1 provides a graphical representation of the research model.

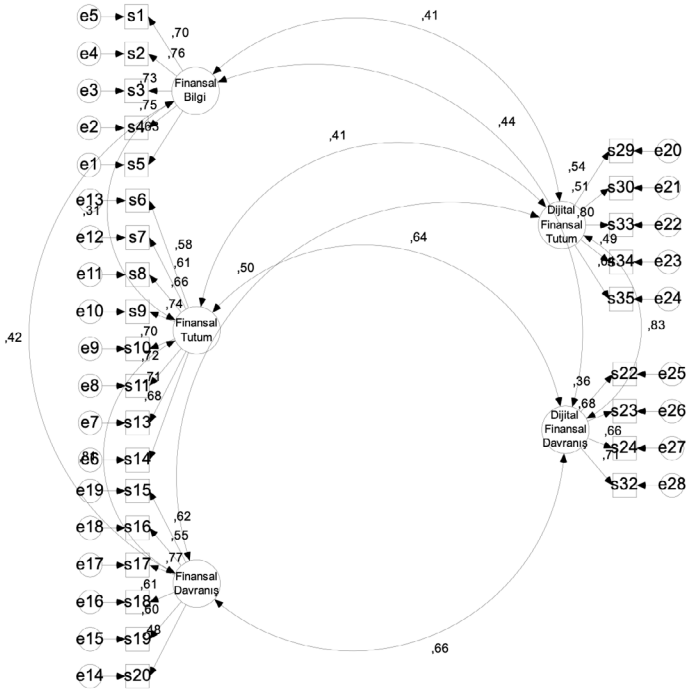

Figure 1. Research model

Relationships between sub-dimensions

The relationships between the sub-dimensions of the scale were examined by correlation analysis. Table 5 gives the analysis table of the sub-dimensions of the research scales.

Table 5. Scale sub-dimension analysis table

		Financial Knowledge	Financial Attitude	Financial Behavior	Digital Financial Attitude	Digital Financial Behavior
Financial Knowledge	r	1	.291**	.358**	.327**	.352**
	p		.000	.000	.000	.000
Financial Attitude	r	.291**	1	.669**	.293**	.485**
	p	.000		.000	.000	.000
Financial Behavior	r	.358**	.669**	1	.397**	.501**
	p	.000	.000		.000	.000
Digital Financial Attitude	r	.327**	.293**	.397**	1	.540**
	p	.000	.000	.000		.000
Digital Financial Behavior	r	.352**	.485**	.501**	.540**	1
	p	.000	.000	.000	.000	

According to the table, the financial knowledge sub-dimension has a positive significant relationship with financial attitude at the level of 29.1%, with the financial behavior sub-dimension at 35.8 %, with digital financial attitude at 32.7%, and with digital financial behavior at 35.2 % ($p<0.05$).

The financial attitude sub-dimension has a positive significant relationship with the financial behavior sub-dimension at 66.9%, with digital financial attitude at 29.3%, and with digital financial behavior at 48.5% ($p<0.05$). The financial behavior sub-dimension has a positive significant relationship with digital financial attitude at 39.7% and digital financial behavior at 50.1% ($p<0.05$). There is a 54% positive significant relationship between digital financial attitude and digital financial behavior ($p<0.05$).

The findings of this research, conducted to understand the relationship between digital financial literacy and the financial behaviors of pharmacy faculty students, have revealed several significant correlations and contrasts with existing literature in the field of financial literacy. This research has extended the understanding of financial literacy's multifaceted nature, particularly highlighting the intertwining of traditional financial literacy with digital financial literacy, as previously noted by Zait and Berata[1] and Aydın and Artar[5]. Alexander et al. emphasized increasing importance of digitalization in financial education, and the observed proficiency in digital financial literacy among those

with higher traditional financial literacy levels not only corroborates these studies but also underscores this importance[2].

Collins and Urban suggested that the predominance of female participants in this study sheds light on gender differences in financial literacy, aligning with the growing awareness of gender-specific needs in financial literacy programs[3]. This gender-based perspective in financial literacy is relatively underexplored in the literature, indicating a pivotal area for future investigation. Deloitte and Kızıloğlu identified that the extensive use of digital platforms for financial transactions and literacy among the study participants mirrors the shifting trends towards fintech and digital financial platforms[6,7]. This shift highlights the evolving landscape of financial literacy, where digital platforms are becoming central to financial education and behavior.

Contrasting with the findings of Klapper and Lusardi who reported a non-proportional relationship between financial literacy rates and economic development in the United States, this study suggests a more direct correlation between financial literacy and socioeconomic factors within the context of Istanbul's pharmacy students[14]. This variance could be attributed to the distinct demographic and regional characteristics of this study, thereby indicating the influence of local contexts on financial literacy. The impact of digital literacy on financial decision-making, emphasized by Kakinuma as a contributor to quality of life, is further highlighted in this study with specific focus on its influence on financial behaviors and attitudes[15]. It is suggested that the role of digital literacy in financial decision-making is context-dependent and multifaceted, thus requiring further exploration.

These findings underscore the necessity for financial literacy programs to incorporate digital literacy elements, echoing the suggestions made by Kaya and Kılıç[9]. The distinct gender differences in financial literacy underscore the importance of developing tailored educational approaches. It is acknowledged that this study's focus on a specific demographic—pharmacy students in Istanbul—limits its generalizability. Therefore, future research should consider exploring the impact of digital financial literacy across diverse age groups and socioeconomic backgrounds, thus broadening the understanding of financial literacy in various contexts.

This study has significantly enhanced the understanding of financial literacy, particularly by exploring the intersection of digital and traditional financial literacy among pharmacy faculty students. A unique focus on this specific demographic has been provided, underscoring how financial behaviors and lit-

eracy skills are shaped within specialized academic contexts. The investigation into gender-based differences in financial literacy is a notable aspect of this research, highlighting the need for gender-specific approaches in financial education – a relatively new consideration in the literature. Moreover, the research has contributed localized insights into the impact of socioeconomic factors on financial literacy in the context of Istanbul, diverging from broader geographic studies and adding depth to the understanding of these influences. The adoption of digital platforms in financial transactions and education, aligning with the global trend towards digitalization, has been comprehensively addressed, emphasizing the integration of digital literacy in financial education. Methodologically, the employment of Structural Equation Modeling has provided robust analysis, enhancing the research's credibility and offering a methodological blueprint for future studies in the field. Additionally, practical implications for the design and implementation of financial literacy programs have been derived, particularly emphasizing the inclusion of digital literacy elements and addressing gender-specific needs. In essence, this study not only aligns with but also advances the current literature on financial literacy by providing new insights into the digital era's dynamics and the nuanced role of gender in financial education, thereby shaping the future direction of financial literacy programs.

This study was conducted to understand the demographic characteristics, financial situations, digital financial literacy and financial behaviors of students studying at the Faculty of Pharmacy in Istanbul. The analysis results show that the participants have various characteristics according to demographic factors such as gender, age, university type, grade, credit card usage and internet banking habits. When we look at the gender distribution, it is seen that the participation rate of women in the research is higher than that of men. This situation suggests that it may be useful to examine financial literacy education and programs in relation to gender-based needs. In addition, it was determined that the majority of the participants had the habit of using internet banking and followed financial developments on the internet. This highlights the importance of efforts by financial institutions to provide more information on digital platforms and to increase students' digital financial literacy.

Confirmatory factor analysis results showed that there were strong and significant relationships between financial knowledge, attitude and behavior and digital financial attitude and behavior. People who are proficient in financial literacy are also more conscious about digital financial literacy. It is important that financial literacy programs include not only basic financial knowledge but

also digital financial literacy. This is necessary so that students can make more informed financial decisions. Consequently, understanding the factors that influence students' financial behavior is important to improve individuals' financial well-being. This study provides important information that can guide the design and implementation of financial literacy education programs. Future research should evaluate more specific strategies and approaches to improve students' financial literacy levels, including different dimensions.

The findings of this study point to various practices in the development and implementation of financial literacy programs. In particular, organizations that offer financial literacy education should update their programs to ensure integrity that including digital financial literacy topics. Additionally, it is possible to make financial literacy programs more effective by developing educational materials and strategies appropriate to gender-based needs.

Since this study was conducted in a certain time period and on a certain sample group, its general validity is limited. In addition, its limitations include the fact that it is based on participants' statements, is not based on objective data, and contains a subjective evaluation. Future research may increase the generalizability of the results by conducting larger and more diverse sample groups.

This study provided a basic understanding of the financial behavior of pharmacy school students. Future research should aim to evaluate the impact of financial literacy programs on a long-term basis and understand the differences between different demographic groups. Additionally, studies that examine the need for digital financial literacy in more detail can better direct developments in the field of financial literacy.

STATEMENT OF ETHICS

Ethical committee approval was received from the Ethics Committee of Yeni Yüzyıl University (Approval No: 2024/01-1167, Date: 09.01.2024).

CONFLICT OF INTEREST STATEMENT

The authors declare no conflict of interest.

AUTHOR CONTRIBUTIONS

All authors contributed to the work equally throughout.

FUNDING SOURCES

This work was not supported or funded by any company or institution.

ACKNOWLEDGMENTS

The authors would like to express their gratitude to the Istanbul Provincial Health Directorate for their support and assistance throughout this study. Additionally, we thank the students from the participating pharmacy faculties for their time and contributions to the survey. This research was made possible through the collaborative efforts and valuable feedback of colleagues and experts in the field of digital financial literacy and education.

REFERENCES

1. Zait A, Bereta P. Financial literacy conceptual definition and proposed approach for a measurement instrument. J Account Manag, 2015;4(3):37-42.

2. Alexander B, Adams S, Cummins M. Digital literacy an NMC horizon project strategic brief. New York: The New Media Consortium; 2016. p. 16.

3. Collins JM, Urban C. Measuring financial well-being over the lifecourse. Eur J Financ, 2019;341-359. Doi: 10.1080/1351847X.2019.1682631

4. Baramki N. A research on college students financial literacy level: Hacettepe University sample. [Doctoral thesis]. Ankara: Hacettepe University; 2015.

5. Aydın Ö, Artar OK. The relationship between financial literacy and finance education: a research for university students of Sütlüce region. J Int Trade, 2021;7(2):22-29.

6. Deloitte Fintech ecosystem in Turkey. Accessed December 14, 2023. Available from: https://www2.deloitte.com/tr/tr/pages/finance/articles/fintech-ecosystem-in-turkey.html

7. Kızıloğlu SK. Dijital iletişim bağlamında finansal okuryazarlık: çocuklara ve ebeveynlere yönelik dijital uygulamalar ve yeni nesil harçlık modelleri. RumeliDE Dil Edeb Çalışmaları Derg, 2023;Ö13:922-935. Doi: 10.29000/rumelide.1379245

8. Martin A. A European framework for digital literacy. Nord J Digit, 2006;1(2):151-161. Doi: 10.18261/ISSN1891-943X-2006-02-06

9. Kaya IU, Kılıç MB. Finansal okuryazarlık ve dijitalleşme: ölçek geliştirme üzerine bir çalışma. İktisadi İdari ve Siyasal Araştırmalar Derg, 2021;6(15):296-315. Doi: 10.25204/iktisad.901135

10. Tucker LR, Lewis C. A reliability coefficient for maximum likelihood factor analysis. Psychometrika, 1973;38:1-10. Doi: 10.1007/BF02291170

11. Hu LT, Bentler PM. Cutoff criteria for fit indexes in covariance structure analysis: conventional criteria versus new alternatives. Struct Equ Model Multidiscip J, 1999;6(1):1-55. Doi: 10.1080/10705519909540118

12. Schermelleh-Engel K, Moosbrugger H, Müller H. Evaluating the fit of structural equation models: tests of significance and descriptive goodness-of-fit measures. Methods Psychol Res Online, 2003;8(2):23-74.

13. Kline RB. Principles and practice of structural equation modeling. New York: The Guilford Press; 2011.

14. Klapper L, Lusardi A. Financial literacy and financial resilience around the world. Financ Manag, 2020;49(3):589-614. Doi: 10.1111/fima.12283

15. Kakinuma Y. Financial literacy and quality of life: a moderated mediation approach of fintech adoption and leisure. Int J Soc Econ, 2022;1713-1726. Doi: 10.1108/IJSE-10-2021-0633

Acta Pharm. Sci. Vol 63:(1), 2025
Original article
DOI: 10.23893/1307-2080.APS6315

Protective benefits of quercetin and lipoic acid on methotrexate-induced oxidative stress in rat spleen

Ayşe AKDOĞAN[1], Nihal Şehkar OKTAY[2*]

1 Institute of Health Sciences, Marmara University, Istanbul, Türkiye
2 Department of Biochemistry, Faculty of Dentistry, Marmara University, Istanbul, Türkiye

ABSTRACT

The study aims to examine the effect of Methotrexate (MTX) treatment on rat spleen and investigate the antioxidant properties of quercetin (Que) and lipoic acid (LA) on MTX. Rats were divided into groups as Controls, MTX-given group, MTX+Que-given group, and MTX+LA-given group. At the end of the experiment, total protein, glutathione (GSH), lipid peroxidation (LPO), nitric oxide (NO), and total sialic acid (SA) levels, also superoxide dismutase (SOD), and catalase activities were determined in spleen homogenates. MTX increased oxidant parameters and both Que and LA effectively decreased LPO, SA, and NO levels. Administration of MTX increased GSH levels and decreased SOD activity, besides Que normalized GSH level and SOD activity, LA decreased GSH activity. Que and LA may be effective in recovering MTX-induced toxicity by decreasing oxidative stress and can be useful in normalizing the damage situation in rat spleen.

Keywords: methotrexate, oxidative stress, quercetin, lipoic acid, spleen

INTRODUCTION

Methotrexate (MTX) (4-amino-N10-methyl-pteroylglutamic acid), a weak bicarboxylic organic acid, acts as an anticancer agent and immunosuppressant[1,2].

*Corresponding author: Nihal Şehkar OKTAY
E-mail: nihal.oktay@marmara.edu.tr ; nsehkar@yahoo.com
ORCIDs:
Ayşe AKDOĞAN: 0009-0001-7580-0956
Nihal Şehkar OKTAY: 0000-0002-2878-288X
(Received 27 Feb 2024, Accepted 8 May 2024)

It was developed based on its structural similarity to folic acid and its capacity to inhibit folate-dependent enzymes[3]. After its initial use in the treatment of acute leukemia, MTX has also been used to treat various types of cancer, as well as autoimmune and inflammatory diseases[1,3].

The primary pharmacological mechanism of MTX is to competitively inhibit dihydrofolate reductase, an intracellular enzyme that reduces folic acid to tetrahydrofolate cofactors[4]. MTX has 100x greater affinity to dihydrofolate reductase than folic acid, which effects the conversion of folic acid to tetrahydrofolate which is required for DNA synthesis[5]. Inhibition of purine and pyrimidine thymidylate synthesis by MTX leads to deoxynucleotide pool imbalance, decreased folate, purine, and thymine deficiency in actively proliferating cells such as tumor cells, leading to blockage of DNA and RNA synthesis, and eventually cell death[4,5].

MTX has a toxic effect on the body since either monoglutamate, the natural form of the drug, or polyglutamate are inhibitors of several enzymes. The polyglutamated forms are stored in the cells and kept in the body for weeks, resulting in a decrease in folate levels and both drug forms are not specific to malignant cells[3,5]. The toxicity caused by MTX may vary depending on the dose and duration of use according to the disease and patient profile[6]. These side effects may be life-threatening such as a decrease in the immune system, dysfunction of blood cells, various liver complications and organ involvement. The exact way in which MTX causes toxicity in the body is not completely known. However, it is mainly linked to the generation of oxidative stress in organs such as the kidney, liver, and heart[7]. This is caused by an increase in reactive oxygen species (ROS), which leads to high levels of neutrophil infiltration and release of pro-inflammatory cytokines[8].

Quercetin (Que) is a potent antioxidant belonging to the flavonol subclass of flavonoids. It is not synthesized in the body but is taken from various vegetables and fruits through diet and the best-known source of Que is onion[9,10]. Que is known to have anti-oxidative effects as well as anti-inflammatory, antidiabetic, anti-proliferative, anti-viral, and anti-carcinogenic properties[11-13]. By possessing hydroxyl groups within its structure, Que has lipophilic properties, and it demonstrates an exceptional ability to cross the blood-brain barrier easily and therefore it has been reported to protect from neurodegenerative diseases[10]. Que shows a strong antioxidant property and can scavenge many ROS due to the presence of the phenolic hydroxyl group and the double bonds in its structure[9,14]. These hydroxyl groups in its structure act as active hydrogen donors and reduce free radicals. Thus, Que makes them stable and prevents

unsaturated fatty acid oxidation[14,15]. Que also protects the organism from oxidative damage by taking an active role in maintaining the oxidant/antioxidant balance[9,14].

Lipoic acid (LA, 1,2-dithiolane-3-pentanoic acid) is a natural dithiol compound synthesized enzymatically in mitochondria[16,17]. LA is a crucial cofactor for the mitochondrial enzymes, therefore it is critical in mitochondrial energy metabolism[16,18]. Unlike other antioxidants, LA is soluble in both water and fat, so it can act anywhere in the body[19]. In addition, its small size and high lipophilicity allow it to easily cross biological membranes[6].

The spleen is the largest of the lymphoid tissue organs. It is the center for the destruction of red blood cells and platelets. It also filters out old blood cells that are coated with antibodies or incorrectly produced. It plays an active role in the immune system by filtering out foreign bodies such as bacteria as well as abnormal erythrocytes. It is also the organ where red blood cells are stored[20,21].

There are limited studies focused on the oxidative effects of MTX on spleen tissue. Thus, we aimed to examine the protective benefits of Que and LA on MTX-induced oxidative stress in the spleen tissue of rats.

METHODOLOGY

Experimental groups

This study was approved by the Marmara University Animal Experiments Local Ethics Committee (MÜHDEK) (Protocol No: 01.2023mar). In the study, Wistar albino rats (2 months old, 200-250 gr.), taken from Istanbul University Aziz Sancar Experimental Medicine Research Institute, were used. The animals were housed in cages at room temperature with a maximum of 4 rats. They were fed ad libitum and consumed standard rat feed and tap water. MTX (50 mg/5 ml) was obtained from Koçak Farma Pharmaceuticals and Chemicals Industry Inc., Türkiye. Lipoic acid (catalog number: 1077-28-7) and quercetin (catalog number: 117-39-5) were obtained from Sigma-Aldrich Chemical Company (St. Louis, MO, USA). Experimental groups were created as follows:

Control group (n=6): 0.1 cc/100 g saline i.p. was administered to each rat for 5 days.

MTX-given group (n=6): Given 20 mg/kg MTX i.p. on day 1st, followed by 0.1 cc/100 g saline i.p. for 5 days.

MTX + Que- given group (n=6): Given 20mg/kg MTX i.p. on day 1st, followed by 50mg/kg Que i.p. dissolved in 0.1 cc/100 g saline for 5 days.

MTX + LA-given group (n=6): Given 20 mg/kg MTX i.p. on day 1st, followed by 50 mg/kg LA i.p. dissolved in 0.1 cc/100 g saline for 5 days.

Administration dose, timing, and experimental protocol were determined based on previous studies[22,23]. On the 6th day, anesthesia of the animals was performed by intraperitoneal injection of sodium pentothal (50 mg/kg). After euthanasia by taking cardiac blood, spleen tissues were taken and homogenized with saline solution (0.9% g NaCl). Total protein[24], lipid peroxidation (LPO)[25], nitric oxide (NO)[26], total sialic acid (SA)[27], glutathione (GSH)[28] levels, and superoxide dismutase (SOD)[29], and catalase (CAT)[30] activities were determined in 10% (w/v) homogenates prepared from spleen tissue.

Statistical analysis

Graph-Pad Prism 9.0 (GraphPad Software, San Diego, CA, USA) software was used for statistical analysis. The one-way ANOVA method and Tukey's test were used for the comparison of more than two group averages and the interpretation of the differences between them. The t-test was used for the comparison of two groups. $P<0.05$ was accepted as significant.

RESULTS and DISCUSSION

The study focused on examining the effects of Que and LA on MTX-induced oxidative stress on rat spleen tissue. Since the spleen plays an important role in regulating blood cells in the body, when it is damaged, the immune system is also affected. Despite its widespread use in the treatment of cancer, autoimmune, and inflammatory diseases, MTX is known to have toxic effects, but studies on its effect on the spleen tissue are limited. Due to mice, one of the frequently preferred experimental animals, synthesize folic acid in their intestines[31], they were not suitable for the present study.

Oxidant parameters; LPO, NO, and SA levels results are shown in Figure 1.

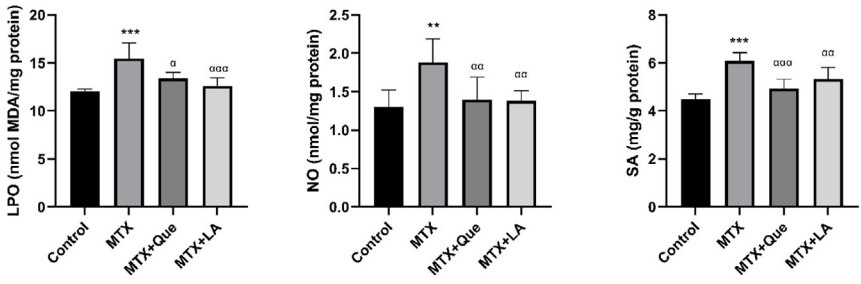

Figure 1. Levels of LPO, NO, and SA in spleen tissue. Values are given as mean±standard deviation, Control: Control group; MTX: Methotrexate-given group; MTX-Que: Methotrexate and Quercetin-given group; MTX-LA: Methotrexate and Lipoic acid-given group; LPO: Lipid Peroxidation; MDA: Malondialdehyde; NO: Nitric Oxide; SA: Sialic Acid. **p<0,01, ***p<0.001 significantly different from Control group; $^{\alpha}$p<0.05, $^{\alpha\alpha}$p<0.01, $^{\alpha\alpha\alpha}$p<0.001 significantly different from MTX group.

LPO levels of the spleen tissues increased significantly in the MTX group compared to the controls (p<0.001) and also decreased significantly in the MTX+ Que and MTX+LA groups compared to the MTX-given group (p<0.05, p<0.001, respectively). Splenic NO level increased significantly in the MTX-given group compared to the controls (p<0.01), while significant decreases were observed in the MTX+Que and MTX+LA groups compared to the MTX-given group (p<0.001, p<0.01, respectively). A significant increase in the SA level of the spleen tissue was detected in the MTX group compared to the controls (p<0.001), while significant decreases were observed in the MTX+ Que and MTX+LA groups compared to the MTX-given group (p<0.001, p<0.01, respectively).

Antioxidant parameters; GSH level, SOD, and CAT activities results are shown in Figure 2.

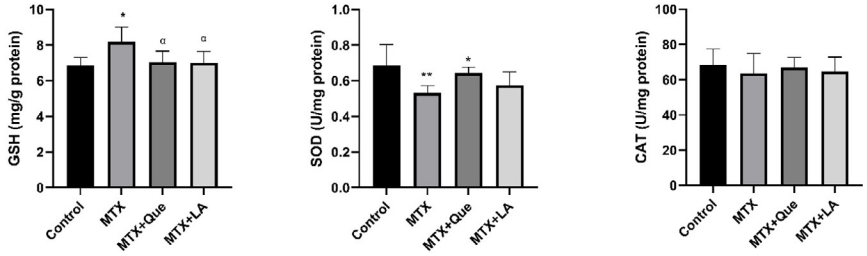

Figure 2. Level of GSH, activities of CAT and SOD in spleen tissue. Values are given as mean±standard deviation, Control: Control group; MTX: Methotrexate-given group; MTX-Que: Methotrexate and Quercetin-given group; MTX-LA: Methotrexate and Lipoic acid-given group; GSH: Glutathione; CAT: Catalase; SOD: Superoxide Dismutase, *p<0,05, **p<0,01 significantly different from Control group; [a]p<0.05 significantly different from MTX group.

GSH level of the spleen tissue increased significantly in the MTX-given group compared to the controls (p<0.05) and decreased significantly in the MTX+Que and MTX+LA groups compared to the MTX-given group (p<0.05). SOD activity decreased significantly in the MTX group compared to the controls (p<0.01). Administration of Que significantly increased SOD activity compared to the MTX-given group (p<0.05). Although there was a slight increase in the MTX-LA group, the result was insignificant.

No significant change was observed in the CAT activity of the groups.

Although MTX is preferred in the treatment of various cancers and autoimmune diseases, serious side effects up to organ involvement may be observed in patients due to long-term and high dose use[32]. In addition, while MTX-polyglutamate forms accumulate in intracellular stores with MTX use, folate stores decrease. These MTX-polyglutamate can act for weeks even if MTX administration is stopped, which increases the toxic effect of the drug[32,33]. The main reason for the side effects of MTX is that it can harm healthy cells as well as cancerous ones. MTX can also cause oxidative damage in the surrounding tissues and organs because the antioxidant system is unable to eliminate the reactive species that increase during treatment. The oxidative stress may cause involvement or loss of function in various organs such as the spleen.

Que reacts directly with radicals and neutralizes them. It also shows antioxidant properties by inhibiting LPO by breaking down lipid peroxyl radicals and chelating metals[15]. In many studies on animals and cells, it has been documented that Que induces GSH synthesis, increases CAT and SOD activities, and decreases MDA content[9,14,34]. Likewise, external supplementation with LA acts as a potent antioxidant and can reduce oxidative stress both in vitro and in-vivo[35].

It has been reported that LA protects DNA, membrane lipids, and intracellular proteins from oxidative damage[33]. In addition to its antioxidant capacity, LA has been proven to participate in the regeneration of oxidized forms of other endogenous antioxidant agents such as vitamin E, C, and GSH, which are depleted especially during oxidative stress[17,35].

In our study, significant increases were found in oxidant parameters consisting of LPO, NO, and SA in the spleen tissue of MTX-given rats compared to the controls. Besides, administration of Que and/or LA to the MTX-given group was effective in reducing and/or normalizing these parameters. In studies conducted with serum and different tissues of animals treated with MTX, it has been proven that the MDA level, which is an indicator of LPO, is increased[33,36]. In parallel with the results of our study, Soliman et al.[7] reported that the administration of MTX increased LPO levels in the spleen tissue. Also, in previous studies with different tissues, decreased MDA levels were found with the administration of Que[15] and LA in MTX-given groups[17].

NO is one of the nitrogen-derived reactive species in the organism. Previous studies showed that MTX administration increased NO levels in rat spinal cord[37], serum[36], liver[38,39], heart[40], and kidney[41]. Excessively produced NO in the cell can react with superoxide radicals and cause nitration of proteins and the formation of peroxynitrite radicals. In addition, the production of NO in the organism leads to rapid depletion of GSH, which is an antioxidant in the cell[38]. In our study, MTX increased NO levels in spleen tissue. Besides, we found that the NO level in spleen tissue was significantly reduced by the antioxidant effects of Que and LA compared to the MTX-given group. Thus, we can suggest that Que and LA may be effective in preventing NO-induced oxidative damage in spleen tissue.

SA, found at the terminal end of many glycoconjugates in all biological membranes, is an acetylated derivative of neuronic acid[40]. SA is also a marker of oxidative stress and a more accurate indicator of inflammation since it shows little variability between individuals[42]. In our study, a significant increase was observed in the SA level of the MTX group compared to the controls. Consistent with the literature, SA levels decreased significantly with the treatment of Que and LA compared to the MTX group[43]. Increased SA levels following MTX treatment may be a response of spleen tissue to protect itself against oxidative damage.

In previous studies, GSH levels were examined in various tissues of animals treated with MTX, and decreases were found compared to the control group. Besides, treatment with antioxidants, such as LA and Que, leads to an increase in GSH level[6,7,15]. However, in our study, GSH levels increased significantly in the spleen tissue of MTX-given rats. We suggest that this increase is due to

the activation of the antioxidant defense mechanism in the spleen, which is an important part of the immune system and develops an immune response to radical formation. Besides this, we found that GSH levels in the MTX+Que and MTX+LA groups decreased significantly compared to the MTX group and approached the control levels. Based on our experimental design, we believe that starting antioxidant treatment following the MTX administration on the first day and continuing the treatment for five days resulted in mild MTX-induced oxidative damage in the spleen. Additionally, the use of Que and LA may help protection of spleen tissue against oxidative damage by increasing GSH levels.

Considering the animal trials in which MTX treatment was applied, a decrease in SOD activity was found[17,39], and a significant elevation was observed with the administration of Que[34,43] and LA[6,35]. Following these studies, we found a decrease in SOD activity in the spleen tissue of the MTX group. The inhibition of cellular NADPH by as a result of MTX-induced oxidative stress may cause a decrease in SOD activity. Although a significant increase was observed with Que treatment, LA did not change SOD activity. In some previous studies CAT activity, an antioxidant enzyme in various tissues, decreased with MTX administration, while an increase was observed after Que and LA treatment[35,44-46]. In the present study, no difference was found in the CAT activity of the groups; this may be a result of the animals developing an immune response to a single dose of 20 mg/kg MTX administration and tolerating the oxidative damage caused by MTX. In the literature, SOD and CAT activities have been found to decrease with MTX administration, but there are also studies with different results. In the study conducted by Armağan et al. increased levels of liver SOD and CAT activities were detected and the administration of LA decreased SOD and CAT activities slightly compared to the controls[47]. Besides, in kidney tissue, SOD activity level was observed to decrease compared to the control group, while CAT activity level was observed to increase compared to the controls, but these results were insignificant. Uzar et al. administered MTX to rats at a dose of 20 mg/kg and found that cerebellum SOD and CAT activities were significantly increased in the MTX-treated group compared to the control group[37]. Additionally, Devrim et al. applied MTX to 60 mg/m^2 body surface area to rats for 7 weeks and detected a non-significant increase in SOD and CAT activities in kidney tissue compared to the control group[48]. However, Soylu Karapınar et al. measured a significant decrease in CAT activity of the rat ovarian tissue after MTX administration compared to the controls, but after LA treatment there was a slight increase in the MTX+LA group compared to the MTX-given group[49].

The current study showed that MTX-induced oxidative stress causes tissue toxicity and damages spleen tissue. Que and LA were able to restore the oxidative state by fixing the damage. Que and LA protected the antioxidant system by regulating GSH levels and SOD enzymes, both of which were useful in decreasing oxidant parameters.

STATEMENT OF ETHICS

Ethics approval is not required in this study, as no human and experimental animal samples are involved.

CONFLICT OF INTEREST STATEMENT

Declared none.

AUTHOR CONTRIBUTIONS

Concept: A.A., Ş.O., Design: Ş.O., Data Collection and Processing: A.A., Ş.O., Analysis or Interpretation: A.A., Ş.O., Literature Search: A.A., Ş.O.

FUNDING SOURCES

This work was supported by Marmara University BAPKO with the project numbered TYL-2023-10990.

ACKNOWLEDGMENTS

Declared none.

REFERENCES

1. Karami F, Ranjbar S, Ghasemi Y, Negahdaripour M. Analytical methodologies for determination of methotrexate and its metabolites in pharmaceutical, biological and environmental samples. J Pharm Anal, 2019;9(6):373-391. Doi: 10.1016/j.jpha.2019.06.001

2. Koźmiński P, Halik PK, Chesori R, Gniazdowska E. Overview of dual-acting drug methotrexate in different neurological diseases, autoimmune pathologies and cancers. Int J Mol Sci, 2020;21(10). Doi: 10.3390/ijms21103483

3. Cronstein BN, Aune TM. Methotrexate and its mechanisms of action in inflammatory arthritis. Nat Rev Rheumatol, 2020;16(3):145-154. Doi: 10.1038/s41584-020-0373-9

4. Rubino FM. Separation methods for methotrexate, its structural analogues and metabolites. J Chromatogr B Biomed Appl, 2001;764(2001):217-254. Doi: 10.1016/S0378-4347(01)00402-9

5. Neuman MG, Cameron RG, Haber JA, Katz GG, Malkiewicz IM, Shear NH. Inducers of cytochrome P450 2E1 enhance methotrexate-induced hepatocytotoxicity. Clin Biochem, 1999;32(7):519-536. Doi: 10.1016/s0009-9120(99)00052-1

6. Tabassum H, Parvez S, Pasha ST, Banerjee BD, Raisuddin S. Protective effect of lipoic acid against methotrexate-induced oxidative stress in liver mitochondria. Food Chem Toxicol, 2010;48(7):1973-1979. Doi: 10.1016/j.fct.2010.04.047

7. Soliman MM, Al-Osaimi SH, Hassanmohamed E, Aldhahrani A, Alkhedaide A, Althobaiti, F, et al. Protective impacts of Moringa oleifera leaf extract against methotrexate-induced oxidative stress and apoptosis on mouse spleen. J Evid Based Complementary Altern Med, 2020;6738474. Doi: 10.1155/2020/6738474

8. Mercantepe T, Tümkaya L, Mercantepe F. Effects of infliximab against methotrexate toxicity in splenic tissue via the regulation of CD3, CD68, and C200R in rats. Cells Tissues Organs, 2019;206(6):308-316. Doi: 10.1159/000500905

9. Deepika, Maurya PK. Health benefits of quercetin in age-related diseases. Molecules, 2022;27(8):1-14. Doi: 10.3390/molecules27082498

10. Li Y, Yao J, Han C, Yang J, Chaudhry MT, Wang S, et al. Quercetin, inflammation and immunity. Nutrients, 2016;8(3):1-14. Doi: 10.3390/nu8030167

11. Alizadeh SR, Ebrahimzadeh MA. Quercetin derivatives: drug design, development, and biological activities, a review. Eur J Med Chem, 2022;229:114068. Doi: 10.1016/j.ejmech.2021.114068

12. Di Petrillo A, Orrù G, Fais A, Fantini MC. Quercetin and its derivates as antiviral potentials: a comprehensive review. Phytother Res, 2022;36(1):266–278. Doi: 10.1002/ptr.7309

13. Reyes-Farias M, Carrasco-Pozo C. The anti-cancer effect of quercetin: molecular implications in cancer metabolism. Int J Mol Sci, 2019;20(13):1-19. Doi: 10.3390/ijms20133177

14. Batiha GE, Beshbishy AM, Ikram M, Mulla ZS, El-Hack MEA, Taha AE, et al. The pharmacological activity, biochemical properties, and pharmacokinetics of the major natural polyphenolic flavonoid: quercetin. Foods, 2020;9(3):374. Doi: 10.3390/foods9030374

15. Yuksel Y, Yuksel R, Yagmurca M, Haltas H, Erdamar H, Toktas M, et al. Effects of quercetin on methotrexate-induced nephrotoxicity in rats. Hum Exp Toxicol, 2017;36(1):51-61. Doi: 10.1177/0960327116637414

16. Shay KP, Moreau RF, Smith EJ, Smith AR, Hagen TM. Alpha-lipoic acid as a dietary supplement: Molecular mechanisms and therapeutic potential. Biochim Biophys Acta, 2009;1790(10):1149-1160. Doi: 10.1016/j.bbagen.2009.07.026

17. Somi MH, Hajipour B, Abad GD, Hemmati MR, Ghabili K, Khodadadi A, et al. Protective role of lipoic acid on methotrexate induced intestinal damage in rabbit model. Indian J Gastroenterol, 2011;30(1):38-40. Doi: 10.1007/s12664-011-0090-z

18. Packer L, Witt EH, Tritschler HJ. Alpha-lipoic acid as a biological antioxidant. Free Radic Biol Med, 1995;19(2):227-250. Doi: 10.1016/0891-5849(95)00017-r

19. Arpag H, Gül M, Aydemir Y, Atilla N, Yiğitcan B, Cakir T, et al. Protective effects of alpha-lipoic acid on methotrexate-induced oxidative lung injury in rats. J Invest Surg, 2018;31(2):107-113. Doi: 10.1080/08941939.2017.1296513

20. Sills RH. Splenic function: physiology and splenic hypofunction. Crit Rev Oncol/Hematol, 1987;7(1):1-36. Doi: 10.1016/s1040-8428(87)80012-4

21. Ulusoy M, Acar M, Zararsız İ. Lenfatik sistem ve klinik önemi. KTD, 2014;15(3):365-370. Doi: https://dergipark.org.tr/tr/pub/kocatepetip/issue/17401/182196

22. Aslankoc R, Ozmen O, Ellidag HY. Ameliorating effects of agomelatine on testicular and epididymal damage induced by methotrexate in rats. J Biochem Mol Toxicol, 2020;34(3):e22445. Doi: 10.1002/jbt.22445

23. Bae EH, Lee J, Ma SK, Kim IJ, Frøkiaer J, Nielsen S, et al. **α**-Lipoic acid prevents cisplatin-induced acute kidney injury in rats. Nephrol Dial Transplant, 2009; 24(9):2692-2700. Doi: 10.1093/ndt/gfp176

24. Lowry OH, Rosebrough NJ, Farr AL, Randall RJ. Protein measurement with the Folin phenol reagent. Biol Chem, 1951;193(1):265-275.

25. Ledwozyw A, Michalak J, Stepień A, Kadziołka A. The relationship between plasma triglycerides, cholesterol, total lipids and lipid peroxidation products during human atherosclerosis. Clin Chim Acta, 1986;155(3):275-283. Doi: 10.1016/0009-8981(86)90247-0

26. Miranda KM, Espey MG, Wink DA. A rapid, simple spectrophotometric method for simultaneous detection of nitrate and nitrite. Nitric Oxide, 2001;5(1):62-71. Doi: 10.1006/niox.2000.0319

27. Warren L. The thiobarbituric acid assay of sialic acids. J Biol Chem, 1959;234:1971-1975.

28. Beutler E. Reduced Glutathione (GSH). In: Bergmeyen HV, editor. Red blood cell metabolism: a manual of biochemical methods. 2nd ed. New York: Grune and Stratton; 1975. p. 112-114.

29. Mylroie AA, Collins H, Umbles C, Kyle J. Erythrocyte superoxide dismutase activity and other parameters of copper status in rats ingesting lead acetate. Toxicol Appl Pharmacol, 1986;82(3):512-520. Doi: 10.1016/0041-008x(86)90286-3

30. Aebi H. Catalase. In: Bergmeyer HU, editor. Methods of enzymatic analysis. Weinheim/New York: Verlag Chemie/Academic Press Inc.; 1974. p. 673-680.

31. Custer RP, Freeman-Narrod M, Narrod SA. Hepatotoxicity in Wistar rats following chronic methotrexate administration: a model of human reaction. J Natl Cancer, 1977;58(4):1011-1017. Doi: 10.1093/jnci/58.4.1011

32. Lucas, CJ, Dimmitt SB, Martin JH. Optimising low-dose methotrexate for rheumatoid arthritis — a review. Br J Clin Pharmacol, 2019;85(10):2228-2234. Doi: 10.1111/bcp.14057

33. Çakır T, Baştürk A, Polat C, Aslaner A, Durgut H, Şehirli AÖ, et al. Does alfa lipoic acid prevent liver from methotrexate induced oxidative injury in rats? Acta Cir Bras, 2015;30(4):247-254. Doi: 10.1590/S0102-865020150040000003

34. Li B, Yang M, Liu JW, Yin GT. Protective mechanism of quercetin on acute myocardial infarction in rats. Genet Mol Res, 2016;15(1):15017117. Doi: 10.4238/gmr.15017117

35. Pınar N, Çakırca G, Özgür T, Kaplan M. The protective effects of alpha lipoic acid on methotrexate induced testis injury in rats. Biomed Pharmacother, 2018;97:1486-1492. Doi: 10.1016/j.biopha.2017.11.078

36. Ahmad A, Alkharfy KM, Bin Jardan YA, Shahid M, Ansari MA, Alqahtani S, et al. Sinapic acid mitigates methotrexate-induced hepatic injuries in rats through modulation of Nrf-2/HO-1 signaling. Environ Toxicol, 2021;36(7):1261-1268. Doi: 10.1002/tox.23123

37. Uzar E, Sahin O, Koyuncuoglu HR, Uz E, Bas O, Kilbas S, et al. The activity of adenosine deaminase and the level of nitric oxide in spinal cord of methotrexate administered rats: protective effect of caffeic acid phenethyl ester. Toxicology, 2006;218(2-3):125-133. Doi: 10.1016/j.tox.2005.10.014

38. Elsawy H, Algefare AI, Alfwuaires M, Khalil M, Elmenshawy OM, Sedky A, et al. Naringin alleviates methotrexate-induced liver injury in male albino rats and enhances its antitumor efficacy in HepG2 cells. Biosci Rep, 2020;40(6):BSR20193686.

39. Mehrzadi S, Fatemi I, Esmaeilizadeh M, Ghaznavi H, Kalantar H, Goudarzi M. Hepatoprotective effect of berberine against methotrexate induced liver toxicity in rats. Biomed Pharmacother, 2018;97:233-239. Doi: 10.1016/j.biopha.2017.10.113

40. Oktay S, Calışkan S. Potential therapeutic effect of lipoic acid on methotrexate-induced oxidative stress in rat heart. Eur J Biol, 2023;82(2):306-310. Doi: 10.26650/EurJBiol.2023.1306497

41. Uz E, Oktem F, Yilmaz HR, Uzar E, Ozguner F. The activities of purine-catabolizing enzymes and the level of nitric oxide in rat kidneys subjected to methotrexate: protective effect of caffeic acid phenethyl ester. Mol Cell Biochem, 2005;277(1-2):165-170. Doi: 10.1007/s11010-005-5875-x

42. Rajappa M, Shanmugam R, Munisamy M, Chandrashekar L, Rajendiran KS, Thappa DM. Effect of antipsoriatic therapy on oxidative stress index and sialic acid levels in patients with psoriasis. Int. J. Dermatol, 2016;55(8):e422-e430. Doi: 10.1111/ijd.13196

43. Ak E, Muhan A, Calışkan S, Oktay S. Comparison of the protective effect of alpha lipoic acid and quercetin in methotrexate- induced lung damage. Bagcilar Med Bull, 2023;8(1):82-87. Doi: 10.4274/BMB.galenos.2023.2023-01-011

44. Cellat M, Kutlu T. Effects of esculetin on the methotrexate induced liver and kidney damage in rats. Fırat University Veterinary Journal of Health Sciences, 2021;35(3):151-157.

45. Oktem F, Yilmaz HR, Ozguner F, Olgar S, Ayata A, Uzare E, et al. Methotrexate-induced renal oxidative stress in rats: the role of a novel antioxidant caffeic acid phenethyl ester. Toxicol Ind Healh, 2006;22(6):241-247. Doi: 10.1191/0748233706th2650a

46. Erboga M, Aktas C, Erboga ZF, Donmez YB, Gurel A. Quercetin ameliorates methotrexate-induced renal damage, apoptosis and oxidative stress in rats. Ren Fail, 2015;37(9):1492-1497. Doi: 10.3109/0886022X.2015.1074521

47. Armagan I, Bayram D, Candan IA, Yigit A, Celik E, Armagan HH, et al. Effects of pentoxifylline and alpha lipoic acid on methotrexate-induced damage in liver and kidney of rats. Environ Toxicol Phar, 2015;39(3):1122-1131. Doi: 10.1016/j.etap.2015.04.003

48. Devrim E, Cetin R, Kılıcoglu B, Erguder BI, Avcı A, Durak I. Methotrexate causes oxidative stress in rat kidney tissues. Ren Fail, 2005;27(6):771-773. Doi: 10.1080/08860220500244823

49. Soylu Karapinar O, Pinar N, Ozcan O, Ozgur T, Dolapcıoglu K. Protective effect of alpha-lipoic acid in methotrexate-induced ovarian oxidative injury and decreased ovarian reserve in rats. Gynecol Endocrinol, 2017;33(8):653-659. Doi: 10.1080/09513590.2017.1306847